School of Agriculture, Engineering and Science

UNIVERSITY OF
KWAZULU-NATAL

INYUVESI
YAKWAZULU-NATALI

Critical Tracking and Stress Analysis of Transnet Engineering Trailers

Yuvraj Dwarika - 206507859

In fulfilment of the MSc-Eng. Degree in Mechanical Engineering

May 2017

Examiner's Copy

Supervisor: Dr. Clinton Bemont

PREFACE

The research contained in this *Critical Tracking and Stress Analysis of Transnet Engineering Trailers* was completed by the candidate whilst based in the Discipline of Mechanical Engineering, School of Agriculture, Engineering and Science, University of KwaZulu-Natal, Howard College, South Africa. The research was financially supported by Transnet Engineering.

The contents of this work has not been submitted in any form to another university and, except where the work of others is acknowledged in the text, the results reported are derived from investigations undertaken by the candidate.

As the candidate's Supervisor I agree to the submission of this thesis;

_____

Signed: Dr. C Bemont

Date: ……

DECLARATION- PLAGIARISM:

I, **Yuvraj Dwarika** declare that:

(i) The research reported in this dissertation, except where otherwise indicated, is my original work.

(ii) This dissertation has not been submitted for any degree or examination at any other university.

(iii) This dissertation does not contain other persons' data, pictures, graphs or other information, unless specifically acknowledged.

(iv) This dissertation does not contain other persons' writing, unless specifically acknowledged:

a) Where other written sources have been quoted, their words have been re-written but the general information attributed to them has been referenced.

b) Where exact words are used, the writing is placed inside quotation marks, and referenced.

(v) Where I have reproduced a publication of which I am the author, co-author or editor, I have indicated in detail which part of the publication was written by myself alone and have fully referenced the publication.

(vi) This dissertation does not contain text, graphics or tables copied and pasted from the Internet, unless specifically acknowledged.

Signed: ……..

Date: ……..

Place: …….

ACKNOWLEDGEMENTS

I extend sincere gratitude to my supervisor Dr Clinton Bemont, whose guidance and assistance enabled me to complete this dissertation. I also wish to thank the following people:

The Transnet Engineering staff;
Mr. Collin Moopanar for giving me approval to undertake this project.
Mr. Kavithasen Govender and Mr. Theo Govender, for assistance and engineering expertise with ANSYS software.
Mr. Pieter Hugo, who offered guidance and expertise with ANSYS software and validating the project.

Transnet Engineering mechanical design office for the supply and use of the existing trailer computer drawn models and assistance with the associated software.

The managerial and operational staff at Transnet Port Terminal and Transnet National Port Authority, without whose use of vehicles and equipment the project would have never been completed. I am extremely grateful for them allowing me to use their assets especially since they are a busy operational organisation.

Esteq Test and Measurement, for specifications and supply of equipment, training and technical support throughout the project.

I also thank God for the strength, gift of mental capacity to get through this, and everlasting graciousness over me.

Abstract

Transnet Engineering (TE) produces specialised trailers that are not commercially available. The design of the trailers is based on experience plus knowledge of original equipment manufacturer (OEM) designed and operational trailers. Since trailers are a new specialised product to TE no design data is available and for safety and reliability the trailer is "over"- designed. The risk of any part failing during operation is however minimised, if the trailer is soundly designed throughout, rather than focusing on critical areas and optimising the structure.

Since no trailer analysis has previously been undertaken in Transnet, the design had to be monitored and validated with the aim to reduce material costs and tare weight by approximately 10%. The aim of this project was to undertake and improve a theoretical simulation analysis and implement a practical system to measure and capture critical data on bath-tub and multi-purpose trailers. This would allow a better understanding of the loading characteristics of the trailers in the port environment and validate the existing design with the data acquired from practical field testing. Based on the theoretical simulations and data acquired during field testing, an efficient design is proposed that will save on material and labour thus reducing the net tare weight. A reduction in tare weight will allow for better tractive power from the hauler and improve the life span of the parts such as the brakes, tyres and bearings.

Worldwide knowledge regarding this project is limited; OEMs and tertiary institutions have undertaken similar projects but only for highway trailers and related topics. The current open market does not offer a study which meets this project's needs; by adapting this practice to other aspects of the mechanical design, the product can be optimised for its application.

Contents

List of Figures:

List of Tables:

List of Acronyms and Abbreviations:

ADR- European agreement concerning the international carriage of dangerous goods by road, Economic Commission for Europe Committee on Inland Transport.
Bogie- Suspension unit of the trailer
BTT- Bath-tub trailer
CAD- Computer Aided Design
COM- Centre of mass
FEA- Finite Element Analysis
FEM- Finite Element Method
g- Acceleration constant due to gravity
Goose neck – the section of the centre beam that connects/transitions the front and centre of the trailer
Hauler- Port Terminal tractor/truck
Inter Quartile- is the spread of the middle 50% of the data values.
Kp- Kingpin
Lower Quartile- is the median of the lower half of the data set.
MPT- Multi-purpose trailer
NRCS- National Regulator for Compulsory Specifications
NRTA- National Road Traffic Act
OEM- Original equipment manufacturer
SABS- South African Bureau of Standards
SANS- South African National Standards
Skid plate- Wear plate that is mounted where the trailer slides onto the hauler's fifth wheel when coupling.
STD- Standard Deviation
TE-Transnet Engineering
TNPA- Transnet National Port Authority
TPT- Transnet Port Terminal
Upper Quartile- is the median of the upper half of the data set.
VDI - Verein Deutscher Ingenieure

1. Introduction

1.1 Background of port trailers

In Transnet's Port environment trailers are used to transport 20 and 40 foot shipping containers and 20, 25 and 40 ton skips. The trailers most suitable for these tasks are skeletal and flatbed trailers.

A skeletal trailer consists of a chassis but does not have a body, and is designed to carry shipping containers. These trailers are fairly common and widely used in the commercial trucking industry. The TE bath-tub trailer (BTT) was designed with this as its primary function [1].

A flatbed trailer consists of a chassis fitted with a platform body. Equipment or transported items are carried on the deck and secured by roping and sheeting. Twist locks are fitted to each corner which means that they can also carry shipping containers. Certain flatbed trailers have a modified extended centre beam called a trombone which allows the trailer to carry abnormally large and heavy loads which would overhang on a standard trailer structure. TE's multi-purpose trailer (MPT) is a flatbed capable of transporting different types of skips and two different types of shipping containers [1].

Once a trailer type is selected the sub-components of the trailer, namely the chassis, suspension, axles, tyres and wheels need to be designed or selected.

The chassis is the fundamental platform on which the vehicle is designed to withstand static and dynamic trailer loads, and usually consists of two high strength longitudinal centre beams with a series of cross-members. The chassis must also be designed to accommodate axle sets, a braking system, and a coupling device to the hauler, along with any other required elements such as a greasing system, compressor and fuel tank [1].

The number of axles required is dependent on the carrying capacity of the overall vehicle, i.e. the trailer plus the hauler. The fifth wheel (coupling device of the hauler for securing the towed trailer) and axle sets of a hauler will limit the carrying capability. This is relative to the load that can be placed at the rear axle sets of a trailer [1].

Another important factor is the length and width of the trailer. Whilst it must be able to support the products it needs to transport, it must have a usable turn radius in its operation environment and be able to be manoeuvred on the roads it must navigate, without damaging itself and its hauling vehicle or the environment [1].

The trailer's suspension system absorbs impacts caused by travelling over irregular surfaces, and is determined by its application and operational requirements. The sensitivity and durability of the goods transported will also influence the suspension selection. Fragile cargo may require rubber or air suspension, while more robust cargo can accept parabolic or leaf spring suspension systems. Variable controlled ride height is a requirement for certain applications in which case air suspension would be the obvious choice. Taper leaf springs with dampers and anti-roll bars are the most common suspension choice. This arrangement replaces the older multi-leaf springs which were prone to friction wear and damage [1].

1.2.1 Bath-tub trailer – background and purpose

This was the first trailer built by TE for Transnet Port Terminals (TPT). It is a skeletal trailer primarily used for transporting two 20 foot shipping containers or a single 40 foot container for loading and unloading between the port and docked ships. The skeletal framework can also be used to support other items such as engines, forklifts and general products. These trailers were previously built by an outsourced supplier for TPT, but since most of them had completed their life cycles, and TPT's business had expanded, a great demand existed. Transnet is now attempting where possible to source work and product manufacture inter-divisionally, which means TE had an opportunity to propose the BTT to TPT. The trailer shown in Figure 1.1 is utilised in Durban and Port Elizabeth port terminals.

Figure 1.1: Example of a TE BTT

1.2.2 Multi-purpose trailer – background and purpose

MPT were the second trailers produced and are shown in Figure 1.2. They are flatbed trailers primarily used for transporting two 40 ton skips which hold a commodity of choice loaded at the port and transported to the docked ship. The flatbed framework can also be used to support other items, such as shipping containers since the addition of twist locks allows it to be loaded with either two 20 foot containers or a single 40 foot container. These trailers were the first of their kind manufactured in South Africa for its ports, and were a significant achievement.

Figure 1.2: TE MPT with un-laden TE 20 ton skips

1.3 Design parameters

1.3.1 Transnet requirements

The design is based on TPT's requirements for the trailers which are outlined in Chapters 1.2.1 and 1.2.2. The trailers also needed to be designed and manufactured to be homologated with the National Road Traffics Act (NRTA).

TE had the advantage, that the trailers previously supplied to TPT were scrutinised to minimise problematic areas and components which meant that TE could improve on these designs. The improvements were not only based on maintenance records and visual root cause analysis, but personnel (hauler driver and assistant, crane operators and drivers, fleet owners and maintenance mechanics) who used the trailers were also asked to give input to make the new trailer more user-friendly. Significantly, the product was thus designed to satisfy TPT since they were the customer.

1.3.2 Dimensional and total mass constraints

The dimensional parameters for each trailer had to be set. Using NRTA TRH11-dimensional, mass limitations and other requirements for abnormal load vehicles, the overall length, overall width, and laden mass classes for the trailers were specified as shown in Table 1.1 [2].

Trailer	Maximum Width limit (m)	Maximum Length limit (m)	Maximum Mass limit (t)
BTT	Class D1 – 2.75	Class D1 - 27	Class M3 - 80
MPT	Class D1 – 2.75	Class D1 - 27	Class M5 - 125

Table 1.1: Trailer classification [2]

These parameters were pre-determined using the base design criteria of previously supplied trailers. The fact that each trailer payload capacity needed to be 60.96 tons for the BTT and 88.4 tons for the

MPT (from Table 4.1), also meant that an overall limit of 80 tons and 125 tons respectively was reasonable for the gross mass of each trailer [2].

The trailer was to have no overhang or load projection, in other words nothing loaded or structurally part of the trailer could externally exceed the primary structure of the trailer. This was in keeping with the regulations. The wheelbase (kingpin to centre point of axles) for semi-trailers was not to exceed 10 m based on Regulation 225 [2]. The loading forces of the trailer could then be calculated to select the bogie/axle wheel sets and the kingpin. The masses in Table 1.2 were used for the calculation of the loading forces in Chapter 4.

Trailer	Trailer structure body mass (kg)	Mass of bogie and wheels (kg)	Total tare mass (kg)
BTT	6 710	3 490	10 200
MPT	9 110	4 350	13 460

Table 1.2: BTT and MPT masses used for theoretical analysis

1.3.3 Kingpin and axle loading

The selection of the kingpin used to couple to the fifth wheel is shown in Chapters 4.4 and 4.7 and is based on the horizontal shear calculation. The kingpin had to comply with the rules set out in the Compulsory Vehicle Specifications provided by the National Regulator for Compulsory Specifications (NRCS). JOST kingpins were selected since they are made by a leading manufacturer and easily accessible by TE. The KZ1516 and KZ1016 kingpins illustrated in Figure 1.3 are employed in the BTT and MPT respectively [3].

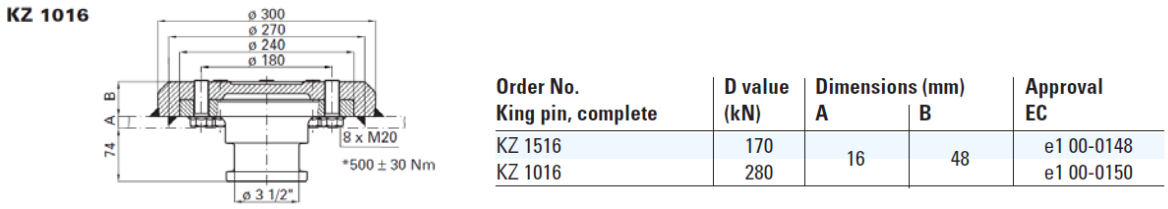

Order No. King pin, complete	D value (kN)	Dimensions (mm) A	Dimensions (mm) B	Approval EC
KZ 1516	170	16	48	e1 00-0148
KZ 1016	280			e1 00-0150

Figure 1.3: Kingpin model and specifications [3]

To select the bogie/axle combination, Regulation 240 stipulates that each axle mass loads shall not exceed the limits, as shown in Table 1.3.

Axle type	Mass limit on axles with four wheels (kg)
Two unit (tandem)	18 000
Three unit (tridem)	24 000

Table 1.3: Axle types and mass limits per axle [2]

In Chapters 4.4, 4.7, 4.10.2.2 and 4.10.3.2, when the reaction forces on the bogie are calculated and validated, Table 1.3 provides values that the axles must comply to. The BTT or the two unit axle type, was granted exemption from the Director General of the Department of Transport because the rated axle loads were higher than recommended in Table 1.3. Specialised consideration is also given to refuse removing vehicles, breakdown vehicles and buses which exceed the laden values in Table 1.3 to 20 400 kg [2]. Regulation 240 restricts the mass load on axles in accordance with the restricted carrying capacity on public roads [2], although the trailers manufactured for TPT are only meant to operate within the designated private port terminal at a fully laden speed of no more than 30 km/hr.

All bogies not only have to meet the load characteristics but also be able to brake to the required standard in SABS 1447-2 [4]. A Freuhauf Heavy Duty Tandem Bogie was used for the BTT [5]. This is a double axle suspension system with four wheels per axle, a drum braking system and leaf spring suspension. For the MPT trailer, a GO suspension and axles, Jumbo Tridem, CS-601/U/11BLD/PORT was used [6]. This is a triple axle suspension system with four wheels per axle, a drum braking system and leaf spring suspension. Each bogie is capable of a maximum load of 22 670 kg per axle [5], [6]. Both bogies were fitted with a Knorr-Bremse pneumatic braking system which complied with SANS 1447-2 [4].

1.3.4 Auxiliary and associated components

All the other components had to comply with standards for fitment to the trailer and had to be specified in compliance summary of evidence for the homologation submission:

Item Description	Test Standard or Equivalent if not SANS
Lights and retro-reflective devices	SABS 1046 [7] SABS 1376-3 [8]
Brakes and braking equipment	SABS 1447-2 [4]
Rear warning sign (chevron)	SABS 1329-3 [9]
Kingpin and mounting plate	EC e100-0148 as per JOST specification [3]
Rear underrun protection device	SANS 1055 [10]
Wheel flaps	SANS 1496 [11]
Pneumatic braking connections	SABS 1447-2 [4]
Vehicle identification number	SANS 3779 [12]
Trailer dimensions	NRTA Act no.93 of 1996 [13]
Axle unit suspension	NRTA Act no.93 of 1996 [13]
Data plates	Compulsory Vehicle Standards [13]
Tyres	Compulsory Vehicle Standards for Pneumatic Tyres [13]

Table 1.4: Components and relevant standard for homologation

The items in Table 1.4 cannot be manufactured within TE and were therefore outsourced and integrated into the design. This area required extensive research as TE did not have a specialist in this area, but through the help of NRTA, NRCS, SANS/SABS and approved suppliers, the trailers were manufactured in accordance with the stipulations. Table 1.4 also provides examples of the various accessories on the trailer which increase the sprung mass and later used in Chapter 4 for the FEA of each trailer.

1.4. Research Question

This study set out to answer the following question:

> Can a trailer design be verified and then improved by experimentally analysing structural loading in relation to vehicle road conditions and speed?

This aim was to better understand the characteristics of trailers in the port environment so that an improved trailer can be designed. Experimentally measuring stress distribution and the effects of road conditions and speed, will enable verification of existing trailers and allows for future designs to be better optimised by strengthening them in critical areas, and by reducing over-design in others. It was expected that the impact of poor road conditions and increased speed would be revealed. This would also allow the improved specification and selection of sub-systems such as the bogie suspension, braking system and tyres.

1.5 Report Layout:

a) Chapter 2 surveys the literature relevant to the topic.
b) Chapter 3 presents the research methodology and the approach for executing the project.
c) Chapter 4 describes the project via analytical calculations for the trailer main centre beams and for setting up and performing of the FEA models. The results of the calculations and simulations are compared.
d) Chapter 5 discusses the field testing of the trailers, the equipment and generated data, and includes a validation of the FEA models.
e) Chapter 6 utilises the information from Chapter 4 and Chapter 5 to design and analyse the re-modelled trailers.
f) Chapter 7 gives an overview, conclusion and future recommendations.

2. Literature Review

Semi-trailer design and manufacturing has formed an active industry for the past 96 years. Progress in engineering results in constantly developing methods which enable efficient and lighter steel structures as well as simpler fastening methods while maintaining structural integrity [14].

This dissertation is specifically focused on studying the operating conditions validating a finite element analysis (FEA) model and improving the design of custom built trailers manufactured by TE. The factors which played a role in validating the models with test data were:

a) Improving the engineering design through reducing material and overall tare mass of the trailer.
b) Predicting and verifying vertical, longitudinal and lateral accelerations for the trailers in a low speed port environment application of 30 km/hr.
c) Enabling continuous improvement in trailer design for future manufacturers.

2.1 Theoretical and analytical methods for trailer design

The trailer chassis is made up of a variety of steel structural members. Sound engineering knowledge and analysis is required to achieve optimal construction of the steel member placements and thicknesses of the materials. The present study was aimed at designing a trailer with emphasis on the strength of the structure. In trailer design the centre beams are always designed to save mass efficiently, and the supporting structural side members for the deck of the trailer are designed to effectively be used in the loading areas.

Research carried out on semi-trailer designs has mainly focused on the main beam design of the structure. Robert Lowdon‘s (2007) [15] detailed semi-trailer main beam design was based on various static load conditions and commercial design legislation. Lowdon‘s in-depth theoretical design analysis was geared towards finding various stresses and common thicknesses of material which would satisfy all the listed specifications, and was undertaken in a well-structured manner. The centre beams were symmetrically designed, and the predefined material properties made it quite simple to select a safety factor against the calculated stresses. A practical validation for the design was undertaken by strain-gauging the prototype at maximum stress points which were found in the FEA [15].

The Australian National Code of Practice, Heavy Vehicle Modifications, Chassis Frame Section H illustrates the force analysis over the length of a chassis with the aid of a diagram. Also explained in this standard [16] are fabrication practices for reinforcing structural members, critical joining and fastening methods. It provides methods for constructing a chassis using standard size steel structural

members with correct methods for reinforcing them. The calculations are well laid out and provide an easy manner to assess the structural members for validity of use.

A team of engineers (2013) [17] from the Vishwakarma Institute of Technology in Pune, India published a journal paper entitled Analytical Optimisation of Chassis frame for 40ft Dual-Axle Flatbed Trailer Design. The objective was to design a new optimised chassis frame with a tare mass of up to 10% lower than the conventional trailer chassis for road goods transport industry in India. The approach was to assume different thicknesses of materials for sections of the trailer subjected to different loads, and then to calculate the shear stresses and possibility of reducing these areas based on the tensile strength of the materials. The weld size calculation was also optimised for the centre beams based on material thicknesses. The middle and side structural members were calculated using C channel sections based on bending moment, bending stress, and shape factor (Section of Modulus). The entire paper illustrated that an analytical method can be used to completely optimise a chassis frame. Although a finite element analysis simulation is necessary to validate the design, the main part of design can still be completed using mechanical design calculations.

Ricardo, Antonio and Luis Otto of the State University of Campinas, Brazil, developed a new underride device. The aim of this project was to develop a rear bumper in such a way that when a motor vehicle rear-ends a truck the device will compress to the upper deck of the trailer and only allow the front of the vehicle to be damaged. The idea was primarily to decrease injuries and fatal accidents caused by motor vehicle drivers who crash into the rear of trucks or trailers [18].The rear underrun devices on South African vehicles comply with SANS1055. This standard gives the bumper minimum and maximum height and width dimensions to comply with, and the device is tested at with a load range from 12.5-50% of the gross vehicle mass (GVM), but may not exceed 25-100kN. To meet these requirements, a bumper has to be designed according to its GVM, or a standard design can cover a whole fleet of different trailers or trucks. The problem with this is that if the strongest underrun devices are used, they would also be the most expensive to manufacture because of their material requirements. The new device put forward by the State University of Campinas shows that a standardised bumper can be used for all heavy vehicles with the safety of the motorist in mind. The South African standard is based on the loading capacity of the vehicle and therefore becomes a safety device for the cargo of heavy vehicles. The university's design is much more cost effective and saves materials [18].

Although the use of CAD/FEA packages can provide rapid solutions and improvements to previous designs, analytical design analysis provides a good basis for assessment and proper understanding of the designs, and is likely to also enable better utilisation of the simulation tools.

2.2. Finite element software simulation methods

Engineering software is a powerful tool when designing any product. Besides the many computations that can be done in a short period of time, design optimisation can be implemented much more efficiently and accurately, provided the information is correct.

A presentation of Finite Element Modelling with ANSYS by Tommaso, Gregoire and Alberto (2011) [19] from the Zurich Centre of Structure Technologies provides a good overview of the subject. The use of a finite element method (FEM) is explained and compared to that of analytical solutions as well as how a FEM translates partial differential equations into a set of linear algebraic equations. Geometry (shell or solid), element type, material properties, mesh definition, boundary conditions, analysis, and post processing is done in sequential order, and the differences and importance for each stage is explained in detail for all necessary functions.

The Basics of FEA Procedure by R. B. Agarwal (2015) [20] explains various concepts in FEA, and focuses on the spring element concept. A spring element is not very useful in the analysis of real engineering bodies; however it represents an ideal structural form for an FEA. A structure is generally divided into several hundred elements, which generate a very large number of equations that can be solved with computational iterations. Spring elements do not require discretisation (division into smaller elements) and follow basic mechanical behaviours set out in Hooke's law. The theory behind the spring element is explained with various governing equations behind the computer modelling approach, plus cases such as boundary conditions with known values. This literature is relevant to the present study as the spring element and boundary conditions were used to model the suspension on the trailer and from the hauler. Since the suspension stiffness can be a defined value from the manufacture, a spring was considered to be an ideal simulation tool to model stiffness.

A study titled Design and Analysis of Dump Body on Three Wheeled Auto Vehicle was performed by a team of engineers (2015) [21] from KL University, Vijayawada, India. The dump body which was analysed and simulated using ANSYS, is similar to a skip rather than a trailer. Nevertheless this report provided a well laid out methodology for boundary conditions and their translations in the various x, y and z directions which were used as examples in the present study.

Mohammed and Raghavendra (2015) [22] in an Optimisation Study on Trailer Arm Chassis by Finite Element Method, focused on the design and optimisation of a trailer arm chassis. The study also shows different types of simulations and the material properties used for FEM. Static analysis techniques are commonly used for automotive chassis structure design and carried out to find the characteristics of a chassis in a static condition so that stresses can be determined at the initial loading

condition. The trailer chassis was designed using modelling software, analysed by using FEA, optimised by using varying thicknesses, shapes and materials. This static analysis methodology, boundary conditions and loading of the trailer presented a suitable method for the TE trailer FEA.

Mehdi, Iraj, Vinko and Amir (2014) [23] published a study called Stress and Dynamic Analysis of Optimized Trailer Chassis. The optimisation begins with a detailed analytical load configuration on the components which act on the chassis. The different mass and positions provide an accurate calculation of the reaction forces acting on the chassis. The static FEA for the chassis was performed using ANSYS software. To achieve accurate results for the FEM, an adequate choice of both the finite elements size plus definition was done. The Augmented Lagrangian Method was chosen as it allows for manually setting the contact stiffness parameters, and allowing a better approximation of the interactions occurring within the contact areas of the welded structures. The chassis was modelled by taking advantage of symmetry and the use of shell elements. The mesh was biased towards the joints where the most deformation occurs. This approach was used for setting up and meshing the TE trailers.

Walter, Jun and Vagner (2005) [24], in their Structural Dynamics of the Chassis of a Light Trailer present a commercial loading trailer of 350 kg which was subjected to field testing and FEMs. The main goal of their study was to identify critical points on the trailer chassis joints and to reinforce them to improve performance and reliability. Experimental testing was undertaken to determine road profiles which could be used in the simulation software. In the FEA setup, half elliptical trailer springs and tyres were modelled as linear springs with boundary conditions for various simulations using MSC Nastran software. Rigidity values were assigned to the respective spring components which allowed for fine-tuning of the trailer performance. Other tyre and suspension types based on their respective stiffness's could be used for simulation and improvement. Critical points of the trailer were modelled for improvement using ANSYS software based on a global-local technique.

Moaaz and Ghazaly (2014) [25] of Beni-Suef University, Egypt and South Valley University, Egypt respectively show a truck chassis simulated in ANSYS, of an actual production model. The main aim of the report was to highlight vehicle structural design and optimisation using ANSYS software. The results were compared to the FEA and the difference in magnitude was discussed for loading cases. Concentration of stresses on matting and hinged components were highlighted, and where thicknesses could not be changed, repositioning of the structural member was performed. The tare weight was reduced using FEA and CAD design. A stress analysis was undertaken to predict the weak points for fatigue analysis, and to predict the life of the chassis for future research.

David, Joao and Antonio (2009) [26] from the University of Lisbon, Portugal set up a structural optimisation system using ANSYS and Matlab software in such a way that a semi-trailer could be designed based on performance and industrial cost. Using an algorithm tool in Matlab and the ANSYS finite element code, the constraints, load cases, structural mass, design parameters performance criteria, and production cost for the chassis can be defined. The models based on these factors are carefully analysed and compared for different material thicknesses and profiles used in the construction. This optimisation process allowed a mass reduction of 17% and a material cost reduction of 19% for the investigated trailer.

Patel, Bhatt and Patel (2013) [27] presented a report in which the analytical results for a truck chassis (ladder frame design) were compared to that of FEM using ANSYS. The results were accurate to validate the calculations. The report also makes reference to J.P Vidosic and usable safety factors which is 1.25-2.5 for this type of application [28].

Kurdi and Rahman (2010) [29], engineers from Malaysia, published FEA simulation of a chassis with loading from the road roughness and static loading. The results are validated with actual data and the report concludes that static loading is superior to cyclic loading for design purposes. Although more research is recommended for cyclic loading failure scenarios, the data will be used for fatigue life prediction in the interim. This was important for the present study as the static FEA analysis was only assessed.

Datar, Bindu and Dandekar (2012) [30], a team of engineers simulated load data from a road surface that had continuous irregular indentations of up to 50mm. A custom trailer frame was modelled, and I beams and C channels were compared for primary material for a 40 ton load. A durability analysis was performed using a 3g vertical acceleration. While the study was intended to custom design a preliminary design model based on custom conditions, the actual data was also compared. TE mechanical design/structural engineers use the ADR specification as a reference, and investigating actual field conditions allows for design validation and recommendations to be made for the application.

Grzegorz, Hubert, Marek and Maciej (2011) [31] used a FEM to design the centre beams of a custom extendable 18m trailer. The trailer was intended to carry abnormally large cargo with a maximum load capacity of 40 tons, and to be extendable by up to 5 m. A tubular chassis arrangement was used to cater for the adjustable length needed in a telescopic extendable configuration. The design was optimised using FEA software by modifying the initial high stress points to be acceptable, and the final trailer was designed with a maximum load capacity of 58 tons and a trailer mass of 12.5 tons.

The trailer was manufactured and there has never been a load bearing failure according to the manufacturer.

Hein and Ton published a report on the Design of a Multi-Functional Semi-Trailer using structural sandwich panels [32]. The design was for a cooling unit type trailer and it explained the difference between current trailers and chassis-less designs. The composite sandwich panel design was to use lightweight non-metallic materials for the panels and structural rigid metallic materials for the core to provide strength and rigidity. The trailer box would be the chassis and provide enough strength for the kingpin and suspension to be mounted directly onto the floor of the unit. A cost analysis was done at all stages of the FEA design which clearly showed the sandwich panel design to be the most economical option.

Roslan, Mohd and Ojo (2008) [33] published a stress analysis study to validate the fatigue study and life prediction of a semi-trailer chassis. This trailer would be in one of the highest classes based on its Gross Vehicle Weight Rating according to United States Government Regulations. The static analysis was done on an FEA package and highlighted deformation and critical high stressed areas which could fail. The study was undertaken to establish boundary conditions, loading points and an evaluation of the structure by calculating the deformation in the high stress region of the trailer's length plus the Von-Mises stress distribution to find high localised points that could be subject to failure. The safety factor use in this design was at the highest Von-Mises stress point found in the FEA; it was therefore not pre-determined but rather made in the process of the design. This approach will be taken into consideration for use in the various FEAs of the present study.

The studies presented in Chapter 2.2 use the Von-Mises stress criteria to evaluate FEA models. Design and structural engineers make this choice because Von-Mises is a specific measure of stress in multiple planes. It also shows when a particular material will start to yield plastically instead of elastically, to show failure, and is therefore suitable for ductile materials such as mild steel used in trailer designs [34]. Maximum principal and maximum shear stress are also used for the evaluation of stress in ductile materials. However Von-Mises stress correlates these stresses best and is the primary theory to use to exhibit yielding. The Cosmos companion presentation [35] illustrates comparisons of stress types that show the consistency of Von-Mises stress to exhibit concentrated stresses and yielding [35].

In gear application studies using FEA, Von-Mises stress plots are used to validate analytical surface, contact and bending stresses. The Von-Mises stress was found to be within a range of 0.41-2.89 MPa in the study conducted by Govind, Yogesh and Dipak, for Stress Analysis of Helical Gear by Finite Element Method [36]**.** Achari, Chaitanya and Prabhu [37] in their study of a Comparison of Bending

Stress and Contact Stress of a Helical Gear as Calculated by AGMA Standards and FEA, provide results within 0.4-3.1% [37]. The Von-Mises stress criteria is therefore ideal for mild steel trailers since it is sufficient to evaluate maximum principal, maximum shear, surface, contact and bending stresses.

FEA performed on structures have a tendency to illustrate high localised stresses that occur predominantly at right angles and right angled mating structural members. Examples of localised stresses are found and explained in [25], [35], ANSYS, FEA Best Practices presentation [39], Paul Kurowski's (1994) [40] engineering article; Avoiding Pitfalls in FEA [40], Simon L. Cowling's (2008) [41] dissertation on Design Optimisation of a Cane Haulage Vehicle [41] and Patrick Safarian's FEA Validation Requirements and Methods presentation [42]. Cowling from the University of KwaZulu-Natal compiled the dissertation; Design Optimisation of a Cane Haulage Vehicle, which uses analytical methods and FEA for the design of a specific application trailer [41]. The centre beam FEA provides high localised stresses shown in the Von-Mises stress plots mainly due to spring constraints in the region where the spring elements attach to the centre beam [41]. These results have been accepted as localised, and deemed to not significantly influence the results of the overall design.

In the studies under Chapter 2.2 fatigue analysis is a method used to assess localised stressed areas and in Chapter 2.3 they are monitored using data acquisition methods. Although fatigue analysis is not part of the present work it will be taken into account using Cowling's research [41]. In Chapter 2.2 of Cowling's study it provides an overview of design methodologies with various dynamic safety factors which have been sourced from well-known trailer OEMs and trailer designer engineers. Static load case is multiplied by the dynamic design factor resulting in a design incorporating dynamic effects. Dynamic design factors (DDF) ranging from 1.2 to 3.0 [41] are commonly used and incorporated in the design for the static vertical FEA. It is incorporated using the proportional relationship from the basic formula [42];

$$\sigma = (DDF)\frac{m*a}{A} \quad (1)$$

Where σ is the stress from force, m is mass, a is acceleration and A is area [42].

2.3. Data acquisition testing methods

Data acquisition testing of commercial vehicles is a relatively new field, and has primarily been studied by vehicle manufacturers. It has sparked the interest of tertiary institutions since hauling by road has become a booming worldwide industry. In South Africa individual companies and manufacturers who have studied vehicles in detail do not make their findings easily accessible, this is

likely to maintain their intellectual property, and thereby their position in the application industry. The main focus in testing is to optimise vehicle models by using CAD and FEA software with measured test data; by doing this all the assumptions made at the design phase can be validated, and static and dynamic results allow for the improvement of existing vehicles.

A presentation by Patrick Safarian, shows an array of examples where FEA modelling and type tests were done to validate a model. Although the examples are not industry specific, the presentation gives the main reasons why FEA should be used as a tool to aid the final design phase, and the analytical methods and assumptions of the FEA must be shown to be sufficiently accurate or conservative before they are applied to comply with regulations [43].

An investigation was initiated when a manufacturer discovered a problematic situation where the kingpin would change position and not allow successful coupling. The aim of the project [44] was to develop an FEA model of the coupling components and to show that excessive speeds can damage the kingpin. Parameters were set up and tested to validate the theory and it was shown that a damping system and controlled speed would eliminate the component problems [44]. Similarly the TE hauler-trailers are limited at a speed which cannot be exceeded when laden to prevent damage to the hauler and to the trailer components.

Keil, Attanayake, Ikonomov and Hathaway (2012) [45] of Western Michigan University, Kalamazoo, USA used a methodological approach to reverse engineer a truck. The core of the report focused on data acquisition equipment, road surface variations, and validation of the flexible cargo holding body of a Wabash 53-foot trailer. Comparison and testing were done at controlled speeds. The data recorded from the test track was tested in an ADAMS CAD/FEA environment. The overall comparison was deemed satisfactory and the exact match between the FEA and field data results was found to be possible due to the high complexity of the model.

Ebrahim, Alimohamed, Morteza and Hekmat (2010) [46] from the Razi University of Kermanshah Iran presented a study of the design, fabrication and testing of a hay bale trailer which has a drag-chain bed for unloading bales from the trailer to the ground. It also has a hydraulic ram in order to lower the deck. Solid Works was used to model the trailer to accommodate for the number of bales, while the load used was calculated from the mean weight of the bales, and used as the loading condition in the FEA with ANSYS software. The trailer was analysed with no load, medium load, and fully laden on uneven and flat farm roads. The results, even in farmland conditions, showed that load variations on the trailer were not significant. Road conditions at Transnet ports also affect the trailer structure depending on the load.

A team of engineers; Pauwelussen, Visscher, Merts and Kural (2014) at HAN University of Applied Sciences together with the assistance of several trailer manufacturers are pursuing a project in which realistic fatigue assessment can be done in trailers without reducing their life cycles with the aim of creating a reduced weight trailer for better fuel efficiency. The report is titled An Integrated Testing and Model based Design Approach for Semi-Trailer Weight Reduction [47]. The welding analysis of the trailers was done using FEM and thereafter the steel structural members that depict high stress areas were replicated into a test specimen and fatigue loaded onto a fatigue machine. This procedure determines the life cycle of the joint, and the trailer can be subjected to routine maintenance correction at this point, or a re-evaluation of operability. Aluminium and unique shell fabrication methods were also investigated to help reduce fatigue loading. The emerging data validates the FEM in practice and therefore allows the loading conditions to be adjusted accordingly by users.

The team also used field test data to explore the trailer's critical handling aspects; braking, forces on the kingpin and axles, torque on the axle system, slip angles of the body, air spring suspension forces, and yaw accelerations. Vertical and horizontal accelerations are being taken at these points to determine exactly how each component behaves relative to the others on the same vehicle. This allows for better design practices since critical areas can be identified, and weight distribution can be better understood for vehicle stability and handling dynamics [47], [48].

Actual vehicle dynamics have been researched in-depth at the University of Michigan Transport Research Institute (UMTRI). Vehicle braking, turning, rollover, and handling characteristics have been studied. Much of the research undertaken in the heavy articulated vehicle field is based on principles and practices originally developed at UMTRI [49]. In the basic mechanics of a motor vehicle, the tyre and its movements (driving, steering or rolling) exercise the most significant impact on the vehicle's capability. Slip angle and slip ratio together with cornering force and braking/driving force determines the travel of the tyre and hence of the vehicle [49]. UMTRI also presents a detailed overview of the close range of lateral acceleration loading values for rollover threshold of heavy vehicles. The rollover threshold is determined dependent on the density and centre of mass of the cargo. High density, low centre of mass loads have a higher rollover threshold (0.4-0.5g) compare to those with a higher centre of mass (0.17-0.31g). Tankers and logging truck trailers have a threshold that ranges from 0.23-0.31g. UMTRI further states that rollover of a heavy commercial vehicle is an either/or situation, and rollover accidents are commonly owed to the experience of a driver and their vehicle, if it is not an emergency/unavoidable accident. The Transnet trailers operate at low speeds and are therefore not subjected to extreme handling conditions of the type encountered on highways. Also the containers and skips encountered in the ports have a higher centre of mass compared to general cargo.

3. Research methodology

The aim of this project was to perform an analysis of TE trailers with a view to closely match them to their expected tasks, while improving their overall design, user efficiency and capital cost thereby increasing profitability. In addition the aim was to reduce fuel expended, operational costs and environmental impact. The work flow set out to satisfactorily analyse the trailers can be found below.

The successive process between design phases for better optimisation have been defined as:

1. Assess the existing loading of the trailers analytically, and determine if a better optimised redesign is viable, focusing on the centre beams.
2. Build FEA models of the existing trailers to ascertain whether the existing trailers are correctly designed to meet the prescribed loading conditions and specifications. To validate calculated reaction forces from 1 with FEA models of each trailer using ANSYS. This validation would provide an independent CAD/FEA method to be compared such that the existing trailers' models are then a basis for executing a modified analyses and redesign.
3. Validate FEA model results and inputs with actual operating conditions using a custom data acquisition system. This would allow a validation to be made of the simulation analysis using the field data.
4. Field testing of the trailers aims to also compare acceleration data against the specification values used in 2.
5. Comparison and validation of all above results will then aid the redesign of new trailers.
6. The new trailers will be redesigned for prototyping based on the project as it would comply to all NRTA, NRCS, SANS/SABS homologation requirements which were completed for the existing trailers.

3.1 Chapter Outline

Chapter 4 - Theoretical and FEA analysis

Chapter 4 starts by analytically assessing the theoretical forces acting over the length of the existing trailers. This is required to determine whether the centre beams can be better optimised for the redesign of the trailers whilst complying with safety factors. The force loading and beam analysis are calculated and discussed for each trailer. This is vital to show that an engineering approach can provide initial optimisation of the trailer prior to FEA. For the FEA of each trailer type, the loading specifications and acceleration values that were used are presented. Then the ANSYS trailer model setup is separately presented including material properties. The sub-chapters show each directional load case to highlight the peaks of individual accelerations on the trailer. The individual vertical load case shows a comparison of the reaction forces that were determined in the theoretical analysis. A combined loading case of vertical, lateral and longitudinal accelerations conducted for each trailer is described to show the resultant stresses. Finally, the results are scrutinised and discussed.

Chapter 5 - Field testing

In Chapter 5 the strain/stress data is collected so as to validate the FEA model. Instances are selected where a load case in the field can be compared to FEA results to correlate data. This is done to determine whether the TE ANSYS trailer models are a good representation of reality that can be used in the future redesign. The equipment and software used is presented with explanations as to why it was selected for the applications. Each trailer is separately analysed and the sensor location is explained and illustrated in relation to the structure of the trailer. Field testing of the trailers aims to also compare acceleration data against the specification values used in the initial FEA. This chapter offers a critical discussion and it allows for a potential new set of acceleration values to be determined for future trailer design.

Chapter 6 - Trailer optimisation

Chapter 6 utilises loading based on minimum relevant specifications, as validated by the field test data, to design improved trailers. This allows for the total tare mass to be reduced and the trailer structure to be better optimised where necessary.

Chapters 7 to 9

The closing Chapters 7, 8 and 9 give an analysis and overview of the entire project via the Discussion, Conclusion, and Recommendations. These chapters combine an in-depth analysis of the main project findings.

4. Analysis and results of the BTT and MPT

4.1. Centre main beams overview

The most critical structural member in any truck trailer is its pair of centre beams. In this chapter an analysis of the beams is carried out. The first constraints of the beam are contained in the NRTA Act no.93 of 1996 [13] as shown in Chapter 1.3. The dimensions and various specifications, such as trailer length and axle location used with these beams, are discussed in Chapter 4.2. The different loading scenarios must be then considered to determine the structural requirements of the beams for the existing trailers. These scenarios were also used for the redesigned trailers, because the payload, kingpin and bogie locations of the redesigned trailers must be identical to those of the existing trailers including the regulatory requirements for homologation purposes discussed in Chapter 1.3.

The dimensions and material specification of the beams are generally based on local supply per industry norms with the exception of the web height of the beam; this is typically not constant on trailers and depends on their loading conditions. The beams generally have a varying web height along the length of the beam. Based on the stress data of the loading scenarios, the required height is calculated, and an overall design is confirmed by using the worst case scenarios. The model then undergoes an FEA to investigate the stresses which are checked against the material yield strength for structural adequacy.

4.2 Loading design analysis

4.2.1 Kingpin set back

The kingpin set back distance is measured from the front-most point of the trailer to the centre of the kingpin. The setback for each of the trailers is shown in Table 4.1. This distance allows sufficient space between the trailer front and hauler so that the maximum allowable turning radius is possible.

4.2.2 Landing legs

The position of the landing legs is not regulated but has to be a sufficient distance from the centre of the kingpin, so that when the hauler turns it can clear the rear end of the hauler. The landing legs need to be installed as close to the kingpin as possible as they take the load when the trailer is uncoupled from the hauler. They also provide sufficient height off the ground such that the hauler fifth wheel can couple to the trailer easily with no interference. On both TE trailers the legs were mounted near the goose neck transition of the centre beams.

4.2.3 Axle spread

The axle spread for the trailers is 1360 mm. This is a commonly used industry value and suitable spread for maintaining an acceptable clearance between the tyres. Larger wheel spreads allow for shorter unsupported lengths, which allow for the centre beams to be decreased in size resulting in a lighter trailer. Manoeuvrability and tyre wear is however negatively affected.

4.2.4 Trailer wheel base

The trailer wheel base is adjusted or pre-set on the hauler to ensure that it is within the specified limits. Table 4.1 summarises Chapter 4.2.

Design Specification	BTT	MPT
Trailer length	13 m	13 m
Kingpin set back	750 mm	500 mm
Axle spread	1360 mm	1360 mm
Load capacity	60 960 kg	88 400 kg

Table 4.1: Design parameters of trailers

Figures 4.1 and 4.2 highlight the main structural members and sub-components.

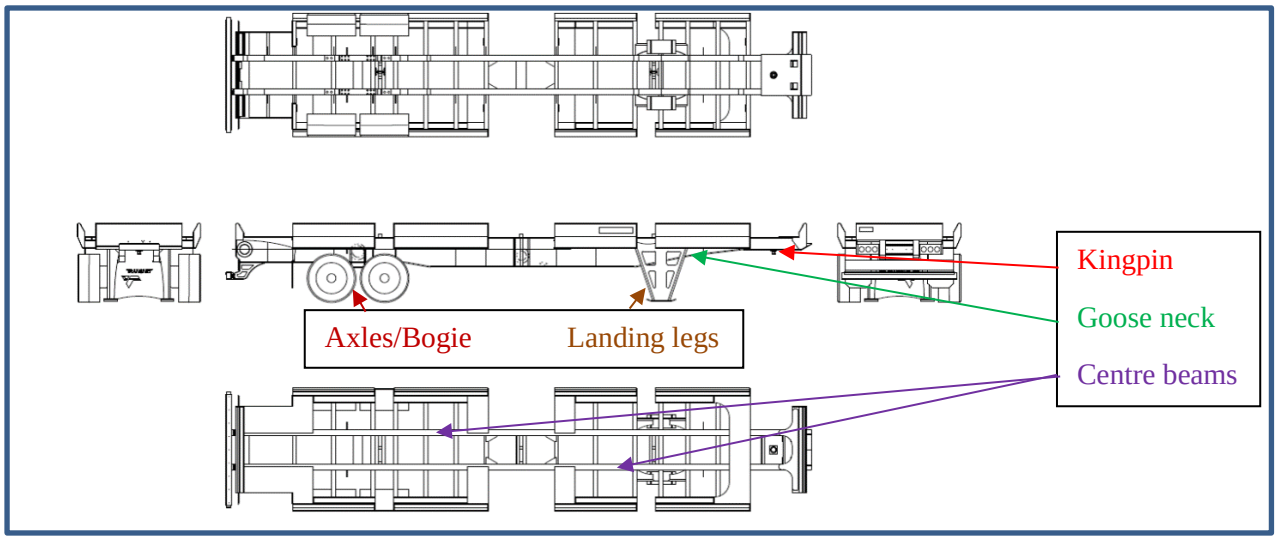

Figure 4.1: General assembly drawing of TE BTT

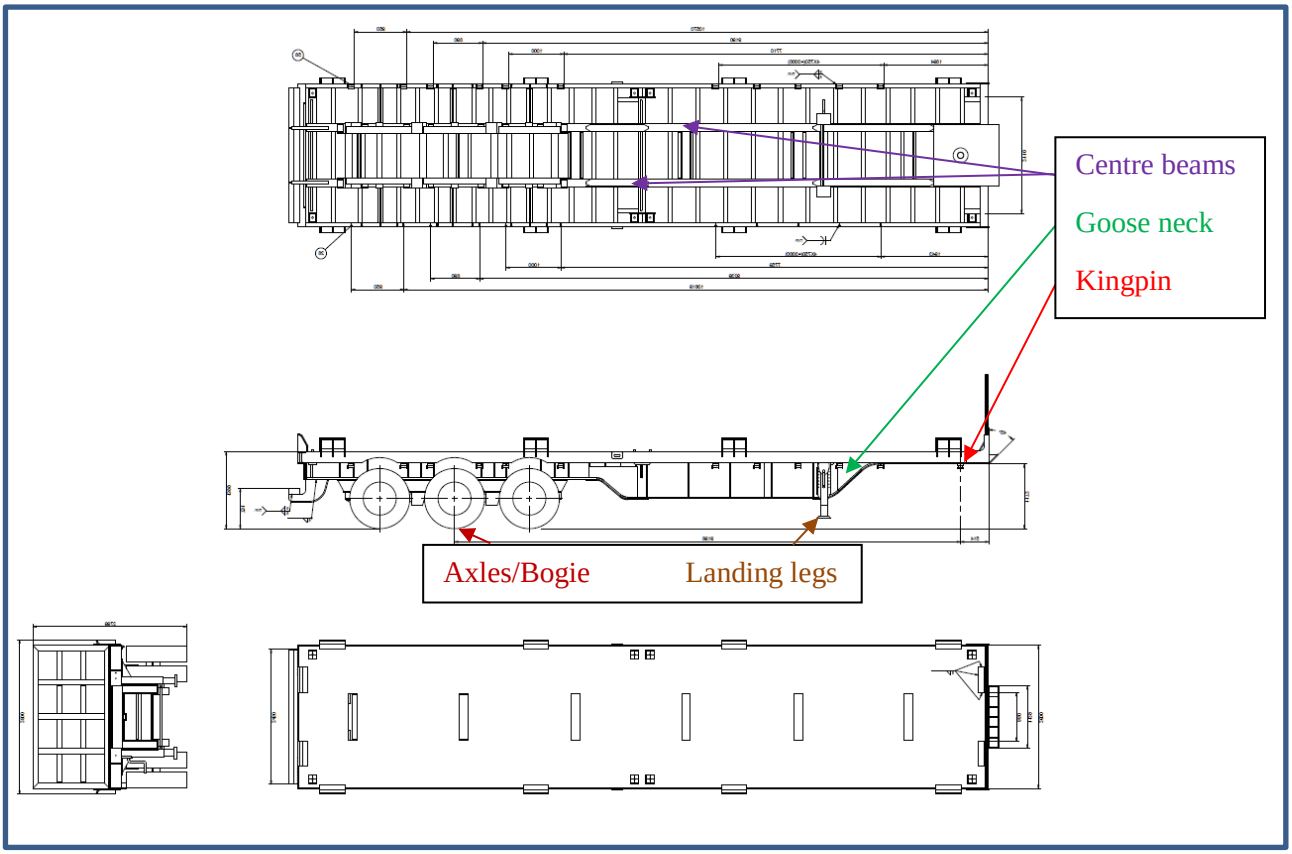

Figure 4.2: General assembly drawing of TE MPT

4.3 Trailer loading overview

4.3.1 Axles

The maximum load allowed on each axle is 22 670 kg. The BTT therefore has a maximum allowable bogie load of 45 340 kg (2 single axles) and MPT of 68 010 kg (3 single axles).

4.3.2 Scenario

The trailers are designed to carry either skips and/or containers with the following gross mass details:

Item description	BTT quantity	MPT quantity	Gross Mass (kg)
TE 20 ton skip	N/A	3	65 400
TE 25 ton skip	N/A	2	57 200
TE 40 ton skip	N/A	2	88 400
20 foot shipping container	2	2	60 960
40 foot shipping container	1	1	30 480

Table 4.2: Load scenarios of the trailers [50]

4.4 BTT main beams reaction loads

The different ways in which the trailer could be loaded had to be established in order to design the centre pair of main beams. Table 4.2 has already described the hauled products which, along with knowledge of their position, allowed the reaction loads to be calculated to determine the vertical forces on the kingpin and bogie. Figure 4.3 (which is not a scaled representation), shows the various masses (from Tables 1.2 and 4.2) and critical forces. These allow a calculation to be made of the peak loading which the BTT would experience.

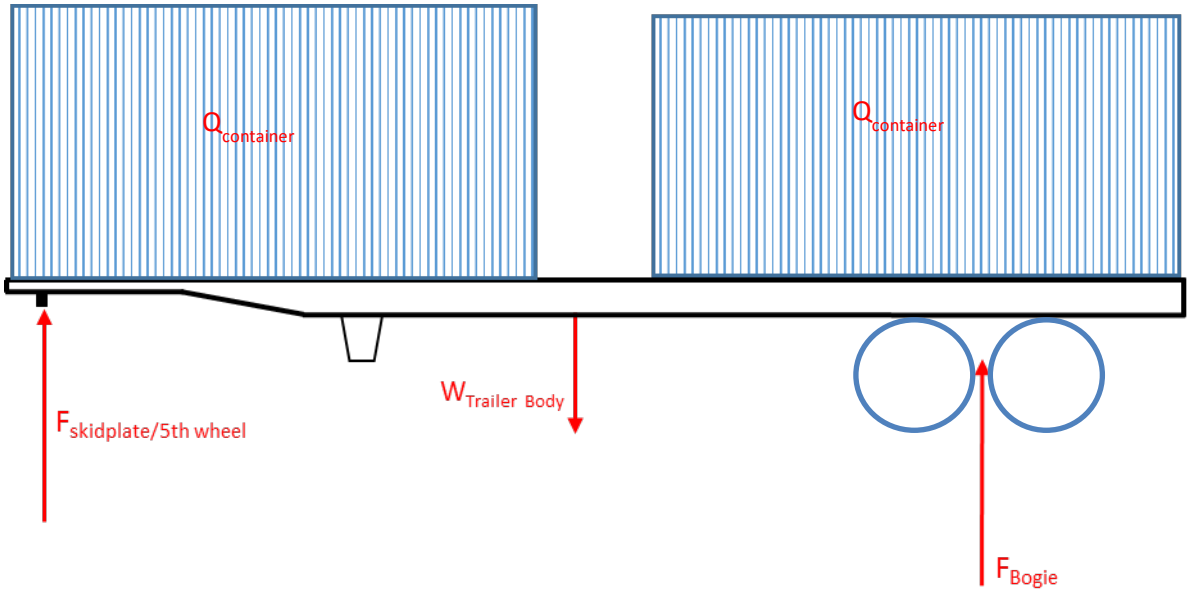

Figure 4.3: Force load diagram for BTT

The weight distribution of the containers is assumed as uniformly distributed for the BTT. The container has structural members which are closely spaced between each other within its main outer rectangle base, which sits on the trailer's skeletal frame. The 6.058 m container has a mass distribution $Q_{container}$ of 5031.4 kg/m (30 480 kg/6.058 m) [50]. Using the method of superposition the following could be derived (distances/dimensional prefixes are shown in Figure 4.4 which is not a scaled representation):

$$Taking\ moments \sum M_{king\ pin} = 0$$

$$(Q_{container}\ x\ 6.058)\left(-K + \frac{6.058}{2}\right) + (Q_{container}\ x\ 6.058)\left(A - E + \frac{6.058}{2}\right) + (W_{trailer\ body}\ x\ C) - (F_{bogie}\ x\ A) = 0$$

$$F_{bogie} = \frac{(Q_{container}\ x\ 6.058)\left(-K + \frac{6.058}{2}\right) + (Q_{container}\ x\ 6.058)\left(A - E + \frac{6.058}{2}\right) + (W_{trailer\ body}\ x\ C)}{A} \quad (2)$$

$$Taking\ moments\ \sum M_{bogie} = 0$$

$$(Q_{container}\ x\ 6.058)\left(A + K - \frac{6.058}{2}\right) + (Q_{container}\ x\ 6.058)\left(E - \frac{6.058}{2}\right) - \left(F_{kingpin}\ x\ A\right) + \left(W_{trailer\ body}\ x\ (A - C)\right) = 0$$

$$F\ kingpin = \frac{(Q_{container}\ x\ 6.058)\left(A+K-\frac{6.058}{2}\right)+(Q_{container}\ x\ 6.058)\left(E-\frac{6.058}{2}\right)+\left(W_{trailer\ body}\ x\ (A-C)\right)}{(A)} \quad (3)$$

These equations offered an opportunity to set up a Microsoft Excel calculator for the trailers in order to compute the various forces based on the masses, distances and loads for the structure. This allowed an easy to use interface.

The 'D-value' of the kingpin is defined as the theoretical reference value for the horizontal force between the towing vehicle and the trailer [51]. The D-value was also calculated to make sure the correct kingpin could be selected [51]. The vertical reaction force for the kingpin must not exceed 32 000 kg as this is the safe working load for a TE hauler's fifth wheel. Equation 4 is an industry standard formula for the calculation of the D-value and is widely used by OEMs of fifth wheels and kingpins for rating coupling equipment. The 0.6 coefficient used in the equation takes into account acceleration, braking and load movement of the cargo which is experienced by the coupling equipment.

$$D = g\ x\ \frac{(0.6\ x\ T\ x\ R)}{(T + R - U)} \quad (4)$$

Where:

g = acceleration due to gravity 9.81 m/s^2

U= vertical load of fifth wheel

R = total weight of the laden trailer

T = weight of hauler

The existing BTT reaction loads were calculated to determine the vertical forces on the kingpin and the bogie which are later on used in Chapter 4.10.2 to validate the reaction forces of the FEA model.

2 x 20 ft Containers								
Distance								
L	12.25	m						
A	9.4	m						
B	2.85	m						
C	5.75	m						
K	0.75	m						
E	3.208	m						
Total trailer mass	10 200	kg						
Trailer body mass	6710	kg						
20 ft Gross mass	30 480	kg						
Total Payload	60960	kg						
Gravity	9.81	m/s2						
Hauler mass	5000	kg						
Forces			ACTUAL		ALLOWABLE		DESIGN CHECK	
5th Wheel Load	257825.01	N	26.28	Tonnes	32	Tonnes	OK	
Bogie Load	407211.62	N	41.51	Tonnes	45.4	Tonnes	OK	
Axle 1	203605.81	N	20.75	Tonnes	22.7	Tonnes	OK	
Axle 2	203605.81	N	20.75	Tonnes	22.7	Tonnes	OK	
GCW	670036.63	N	68.30	Tonnes	82.4	Tonnes	OK	
King Pin Calculation			ACTUAL		ALLOWABLE		DESIGN CHECK	
D value	167891.0529	N	167.89	kN	170	kN	OK	

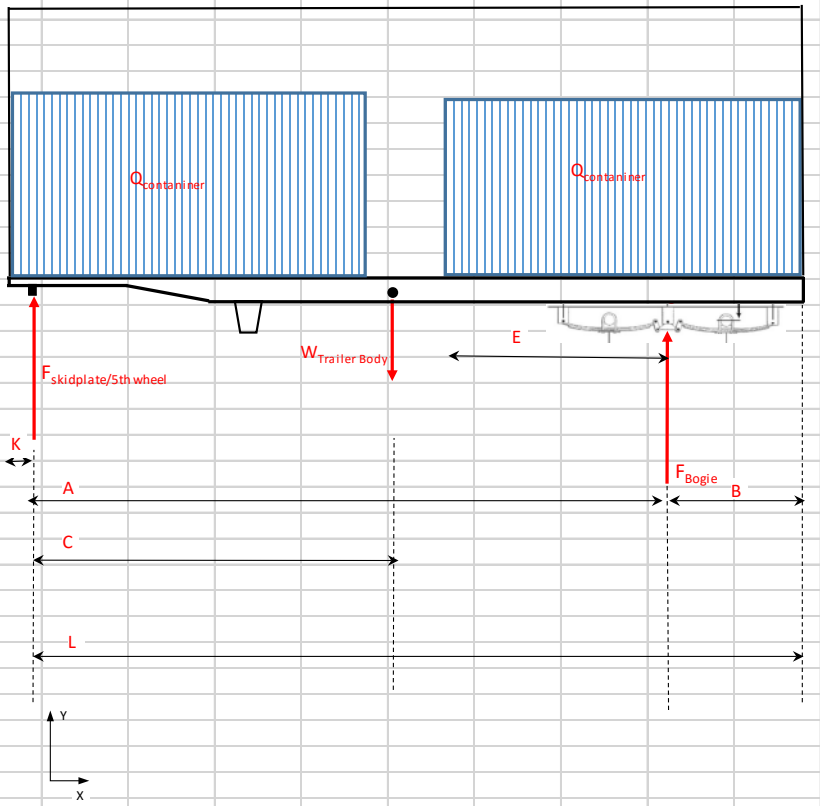

Figure 4.4: Microsoft Excel spreadsheet used to determine loading scenario of 2 x 20 foot containers on the BTT

4.5 BTT shear forces and bending moments

Shear forces and bending moments calculated for the existing trailers length could be used to calculate the required centre beam web and flange dimensions for the various sections along the redesigned trailer's length. The relevant payload, kingpin and bogie locations of the redesigned trailer must be identical to those of the existing trailers including the regulatory requirements for homologation purposes discussed in Chapter 1.3. Using Figure 4.4 and omitting the trailer body mass for the centre beam design, the reaction loads were calculated. Figure 4.5 is derived from the data in Table 4.3.

Dimension	Distance x (m)	Shear force (N)
Start of container 1/trailer	0	0
Kingpin	0.75	-37 018.53
	0.75	195 246.73
End of container 1	6.058	-66 745.74
Start of container 2	6.942	-66 745.74
Bogie	10.15	-225 762.85
	10.15	141 183.41
End of container 2/trailer	13	0

Table 4.3: Shear force values over the length of the BTT under peak design load

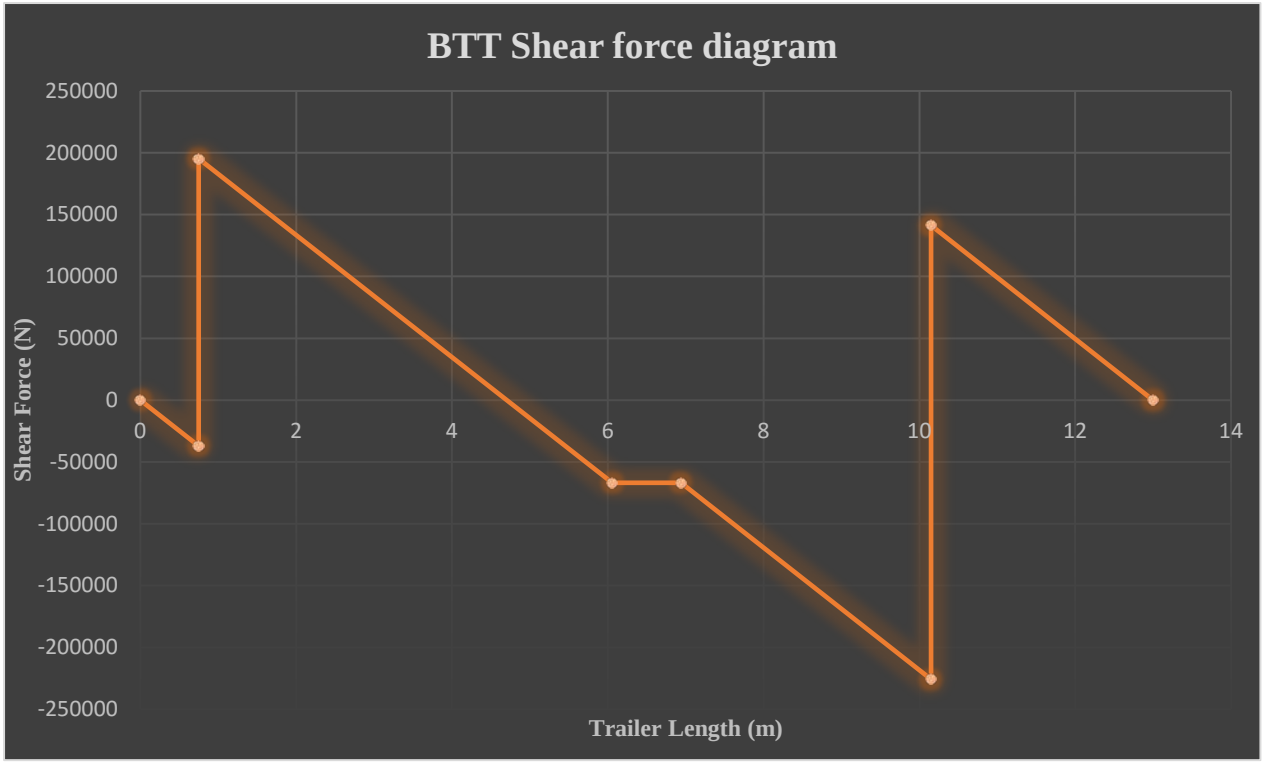

Figure 4.5: Shear force graph for BTT under peak load

The bending moment was required to ensure that the centre beams would resist the bending stresses experienced by the trailer. Figure 4.6 is derived from the data in Table 4.4.

Dimension	Distance x (m)	Bending moment (Nm)
Start of container 1/trailer	0	0
Kingpin	0.75	-13 881.95
Maximum moment	4.71	372 289.04
End of container 1	6.058	327 159.68
Start of container 2	6.942	268 289.93
Bogie	10.15	-201 186.37
End of container 2/trailer	13	0

Table 4.4: Bending moment values over the length of the BTT under peak design load

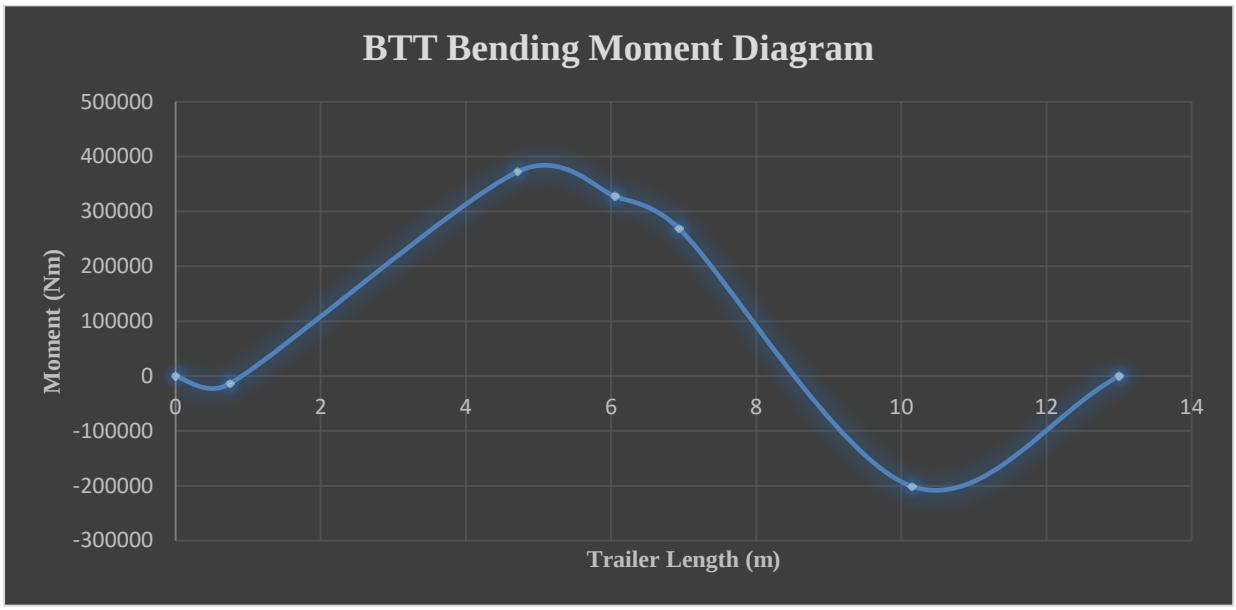

Figure 4.6: Bending moment graph for BTT under peak load

Appendix A provides the relevant equations for Chapter 4.5.

4.6 Flange and web design of BTT

The specifications for a flange beam was used for the trailer's pair of main centre beams. This is commonly used by semi-trailer manufacturers since the shape is the most efficient for supporting loading of this nature. The variables of the beam are the flange width, flange thickness, web height, and web thickness. These are illustrated in Figure 4.7.

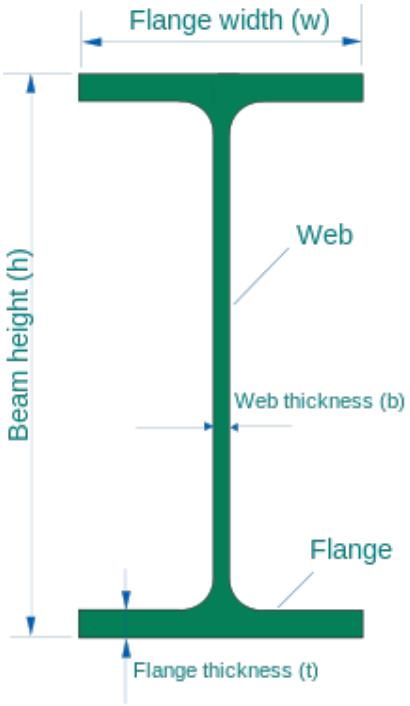

Figure 4.7: Centre beam parameters [52]

The existing BTT centre beams were constructed from Macsteel's 300WA mild steel [55] which has a yield strength of 300 MPa. This manufacturer's carbon steel is easily available in South Africa and is relatively easy to weld and form for applications such as this. The dimensions were a 130 mm flange, with a thickness of 20 mm, and a web thickness of 8 mm. Web thickness typically starts from 4 mm. This dimension was used for the initial preliminary redesign with a view to reduce the centre beam dimension from the existing 8 mm. The web height variation was also considered and depended on the varying load on the beams along the trailer span. Macsteel's S355 mild steel was used for the redesign of the centre beams which superseded the discontinued 300WA. S355 has a yield strength of 355 MPa [55].

To calculate the shear stresses experienced by the beam the following equation [42] was used:

$$\mathrm{T}_{beam} = \frac{VQ}{It_{web}} \qquad (5)$$

Where V is the shear force, Q is the first moment of area about the neutral axis, I is the moment of inertia of the cross section and t_{web} is the thickness of the web.

To calculate the bending stress experienced by the centre beam the following equation [42] was used:

$$\sigma = \frac{My}{I} \tag{6}$$

where: M: bending moment

y: centroid distance to neutral axis

I: moment of inertia of the cross section

A 130 mm flange, with a thickness of 12 mm was preselected as this is commonly available in industry. Using the results per centre beam calculated in Chapter 4.5 (total divided by 2), the stresses were calculated, using the existing web height. The data from Tables 4.3 and 4.5 with eq.(5) was used to generate Figure 4.8 which shows a comparison of the existing centre beam shear stresses and the redesigned centre beam shear stresses with their respective material's yield stress.

Shear force	Start of trailer to Kingpin	Kingpin to end of Container 1	End of Container 1 to Start of Container 2	Start of Container 2 to Bogie	Bogie to end of Container 2/Trailer
Critical length (m)	0- 0.75	0.75-6.058	6.058-6.942	6.942-10.15	10.15-13
Existing web height (mm)	240	240-630	630	630-530	530

Table 4.5: Shear force sections of the main beam over the length of the BTT

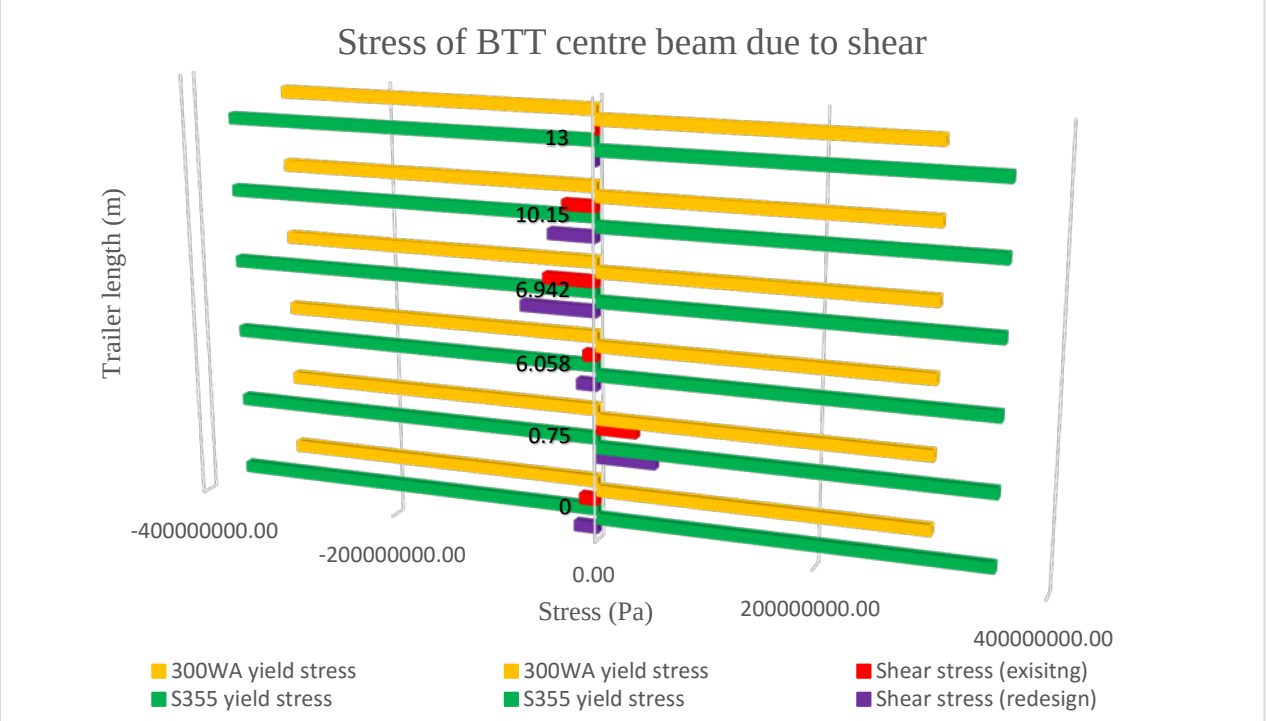

Figure 4.8: Stress of BTT centre beam due to shear

Using the bending moments per centre beam from Table 4.4 (total divided by 2) and the preselected centre beam dimensions substituted into eq.(6), the maximum bending stress for the existing and redesigned centre beam was calculated as shown in Figure 4.9 with their respective material's yield stress.

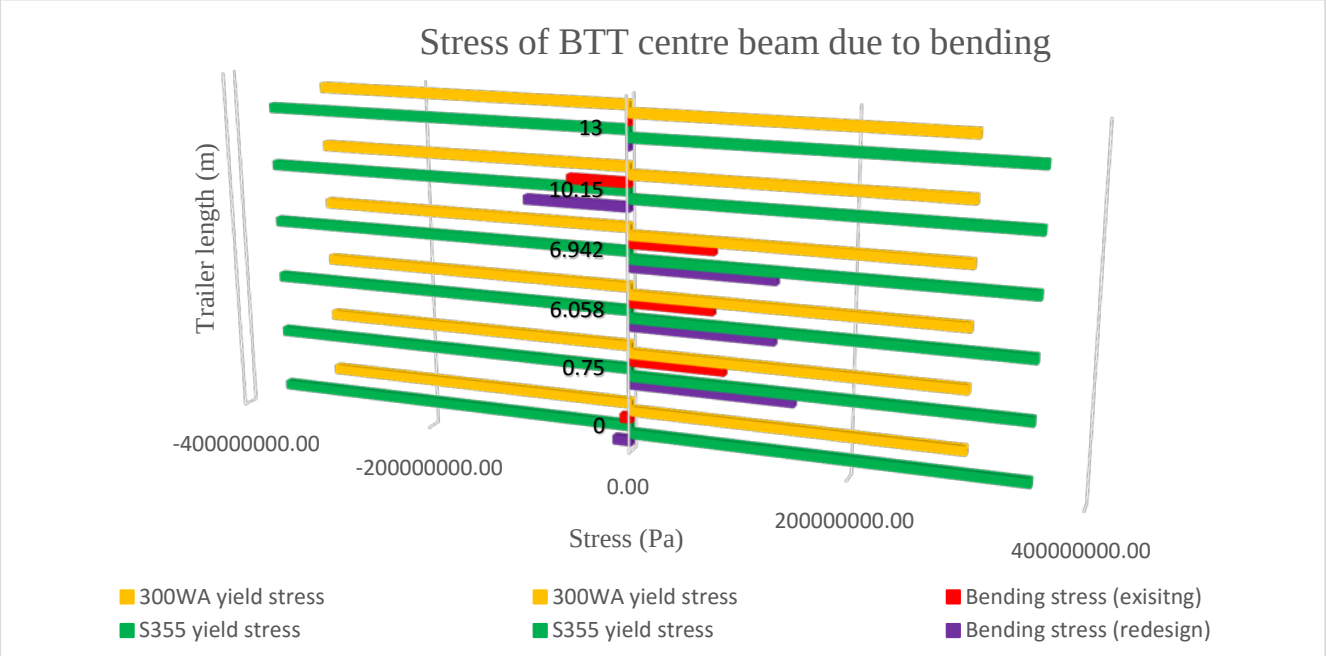

Figure 4.9: Stress of BTT centre beam due to bending

Using Figures 4.8 and 4.9, acceptable safety factors (SF) with a minimum range from 2.36 was complied with [28] along the length of the trailer for the redesigned centre beams. Due to the nature of the kingpin and bogie, a constraint was placed on the allowable height of the centre beam because these dimensions had to be pre-determined. For coupling purposes, 240 mm (minimum height required for front end of the trailer for coupling to vehicles), and 530 mm for the bogie end of the trailer, in order to be as parallel as possible to the centre axis of the axles. Therefore the critical sections of the trailer based on the shear and bending stresses with their corresponding graphs have been defined as shown in Table 4.6 [15].

Critical length (m)	0- 0.75	0.75-6.058	6.058-6.942	6.942-10.15	10.15-13
Recommended web height (mm) using 4 mm web thickness	240	240-630	630	630-530	530

Table 4.6: Recommendations for new main centre beam for BTT

The necessary data for the shear and bending analysis (Figure 4.8 and 4.9) are given in Appendix C. The dimension reduction calculated for the centre beams in this chapter will be used as the basis of the redesigned BTT later shown in Chapter 6.1.2.

4.7 MPT main beams reaction loads

The analysis carried out in Chapters 4.4 to 4.6 for the BTT was also conducted for the MPT. Figure 4.10 (which is not a scaled representation), shows the various masses and critical forces that will allow for a calculation of the loading peaks that the MPT trailer would experience.

The mass distribution of the skips is calculated as point loads because of the 330 mm sectioned floor channels at the front, middle and rear which seat onto the trailer's top plate. The skip is designed with a concave structural shape with the front and side walls leading to the floor. This is a requirement for off-loading the skip efficiently into the ship's hull with a single motion. In addition no commodity will stick in the corners which could occur with a conventional floor with perpendicular side walls. The geometry concentrates the load to the middle floor channel with the front and rear providing support for stability. The commodity is heap loaded into the skip.

Dimension V in Figure 4.10 results from the supporting side guards of the trailer which allow the skip to only be loaded in this rearward position because of the side guards. Hence Skip 2's centre of mass appears and is off centre to the bogie.

The vertical reaction force for the kingpin must not exceed 32 000 kg as this is a safe working load for a TE hauler's fifth wheel. A calculator using Microsoft Excel was created. Using force balance and superposition the analysis in Figure 4.10 was derived to determine the reaction vertical forces on the kingpin and bogie, and are later on used in Chapter 4.10.3 to validate the reaction forces of the FEA model.

90 TON MULTI-PURPOSE KING PIN & BOGIE LOADING

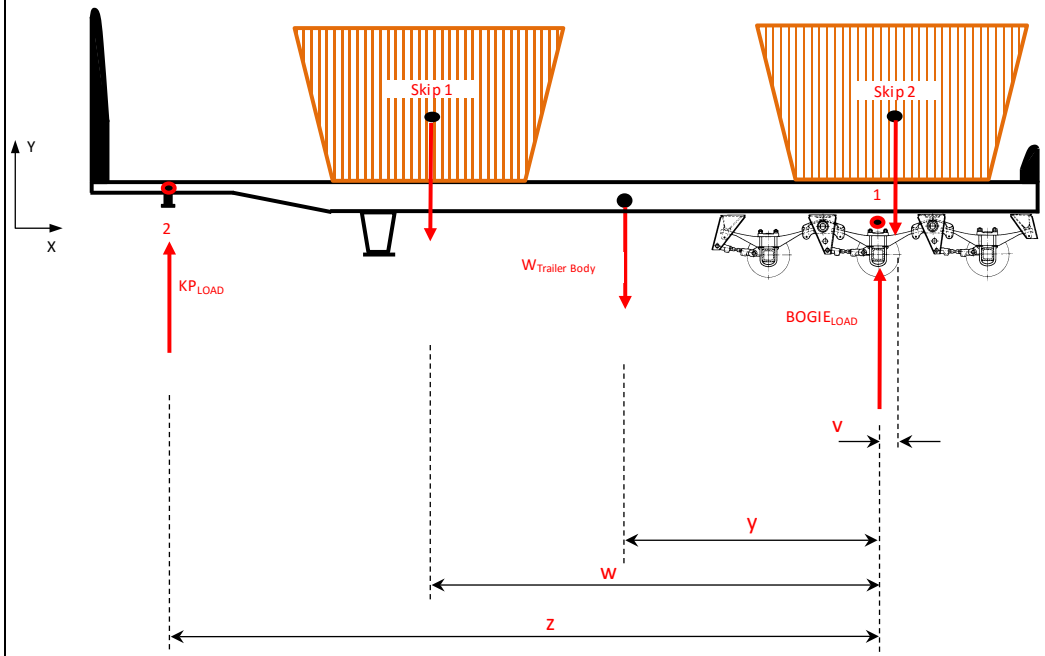

King Pin Type

KZ1016	280 kN	X
KZ1516	170 kN	

Hauler Weight		5000 kg	
T =	34982 kg		T - Max Permissible total mass of hauler (kg)
R =	103460 kg		R - Max permissible mass of semi-trailer (kg)
U =	29982 kg		U - Max Permissble imposed load on king pin(kg)
g =	9.81 m/s^2		
D =	196 kN		D = g x (0.6 x T x R)/(T + R - U)

Option 2: Two (2) x 40ton Skips

U/KP_{LOAD}	32000	kg	v	0.619	m
Trailer Body	9110	kg	w	6.200	m
PAYLOAD	44200	kg	y	3.200	m
$BOGIE_{LOAD}$	68010	kg	z	9.200	m

TAKING MOMENTS ABOUT POINT 1 (BOGIE)

UNLADEN

KP_{Actual} 3168.7 OK

LADEN

KP_{Actual} 29981.8 OK

TAKING MOMENTS ABOUT POINT 2 (KING PIN)

UNLADEN

$BOGIE_{Actual}$ 5941.3 OK

LADEN

$BOGIE_{Actual}$ 67528.2 OK

Σ $LOADING_{Actual}$ < $LOADING_{Allowable}$

KP_{Actual} + $Bogie_{Actual}$ < $KP_{Allowable}$ + $Bogie_{Allowable}$

97510 < 100010 OK

Figure 4.10: Microsoft Excel spreadsheet used to determine MPT kingpin and bogie loading

4.8 MPT shear forces and bending moments

Shear forces and bending moments calculated for the existing trailers length could be used to calculate the required centre beam web and flange dimensions for the various sections along the redesigned trailer's length. The relevant payload, kingpin and bogie locations of the redesigned trailer must be identical to those of the existing trailers including the regulatory requirements for homologation purposes discussed in Chapter 1.3. Using Figure 4.10 and omitting the trailer body mass for the centre beam design, the reaction loads were calculated. Figure 4.11 is derived from the data in Table 4.7.

Dimension	Distance x (m)	Shear force (N)
Start of trailer	0	0
Kingpin	0.5	0
	0.5	263 036.17
Skip 1	3.5	263 036.17
	3.5	-170 565.83
Bogie	9.7	-170 565.83
	9.7	433 602
Skip 2	10.319	433 602
	10.319	0
End of trailer	13	0

Table 4.7: Shear force values over the length of the MPT under peak design load

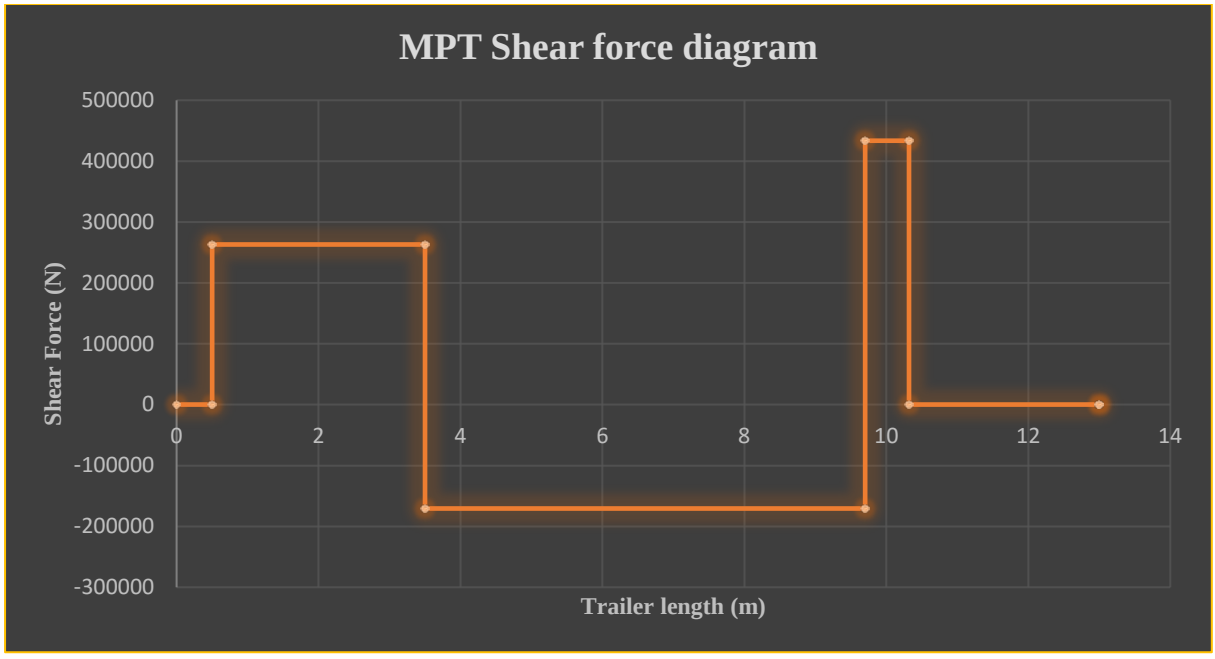

Figure 4.11: Shear force graph of the MPT under peak load

The bending moment was required to ensure that the centre beams would resist the bending stresses experienced by the trailer. Figure 4.12 is derived from the data in Table 4.8.

Dimension	Distance x (m)	Shear force (N)
Start of trailer	0	0
Kingpin	0.5	0
Skip 1	3.5	789 108.51
Bogie	9.7	-268 399.64
Skip 2	10.319	0
End of trailer	13	0

Table 4.8: Bending moment values over the length of the MPT under peak design load

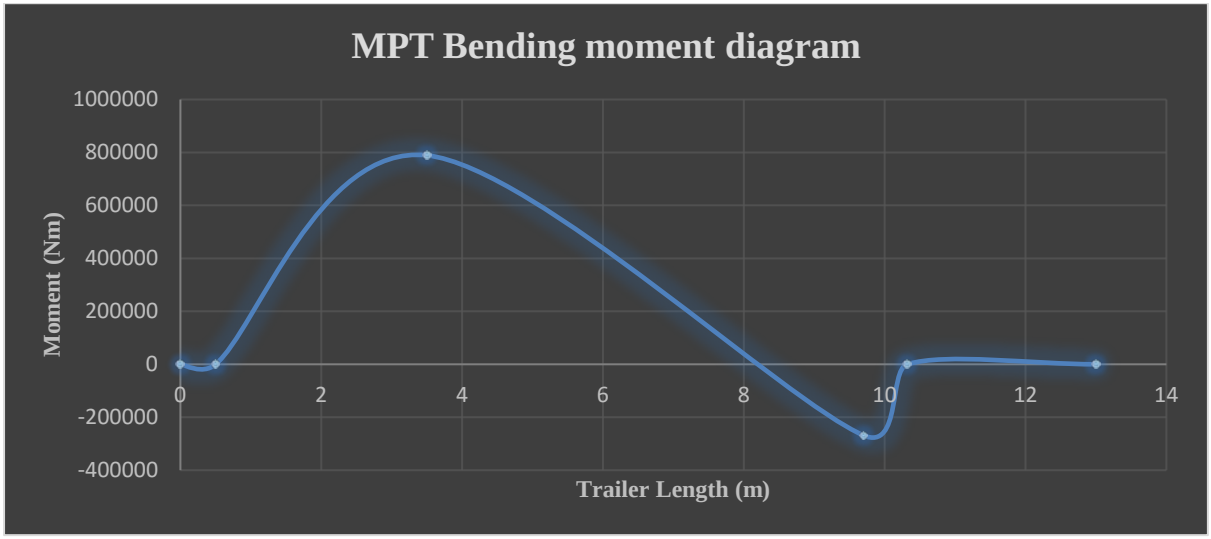

Figure 4.12: Bending moment graph for MPT under peak load

Appendix B provides the relevant equations for Chapter 4.8.

4.9 Flange and web design of MPT

Macsteel's S355 [55] steel was used for the existing MPT centre beam construction and for the purpose of the redesign. Equations (5) and (6) were used to calculate the stresses associated in the beam. A 150 mm flange, with a thickness of 20 mm was preselected for the redesign as used in the existing trailers. Using the results per centre beam calculated in Chapter 4.8 (total divided by 2) plus different thicknesses commonly available for the web, the stresses were calculated using the existing web height. The existing web thickness used was 16 mm so available material increments below that were used, namely 14mm. The initial preliminary redesign for the centre beams provided a very little decrease when the web thickness was only changed whilst using the existing web heights for the various sections of the MPT's length as shown in Table 4.9.

Shear force	Start of trailer to Kingpin to Skip 1	Skip 1 to Bogie	Bogie to Skip 2 to End of trailer
Critical area (m)	0-3.5	3.5-9.7	9.7-13
Existing web height (mm)	180-450	450-800	800-450

Table 4.9: Shear force sections of the main beam over the length of the MPT

Therefore the height of the web was minimised along the length of the centre beam. Due to the nature of the kingpin and bogie, a constraint was placed on the allowable heights of the centre beam because these dimensions had to be pre-determined for coupling purposes. 180 mm height was needed for the kingpin, and 600 mm for the bogie end of the trailer; in order to be as parallel as possible to the centre axis of the axles. Using a 14 mm web thickness, the web height dimensions were decreased in increments since a decrease was found to be viable. Figures 4.13 and 4.14 illustrate the stresses for the redesigned centre beams against the existing centre beams.

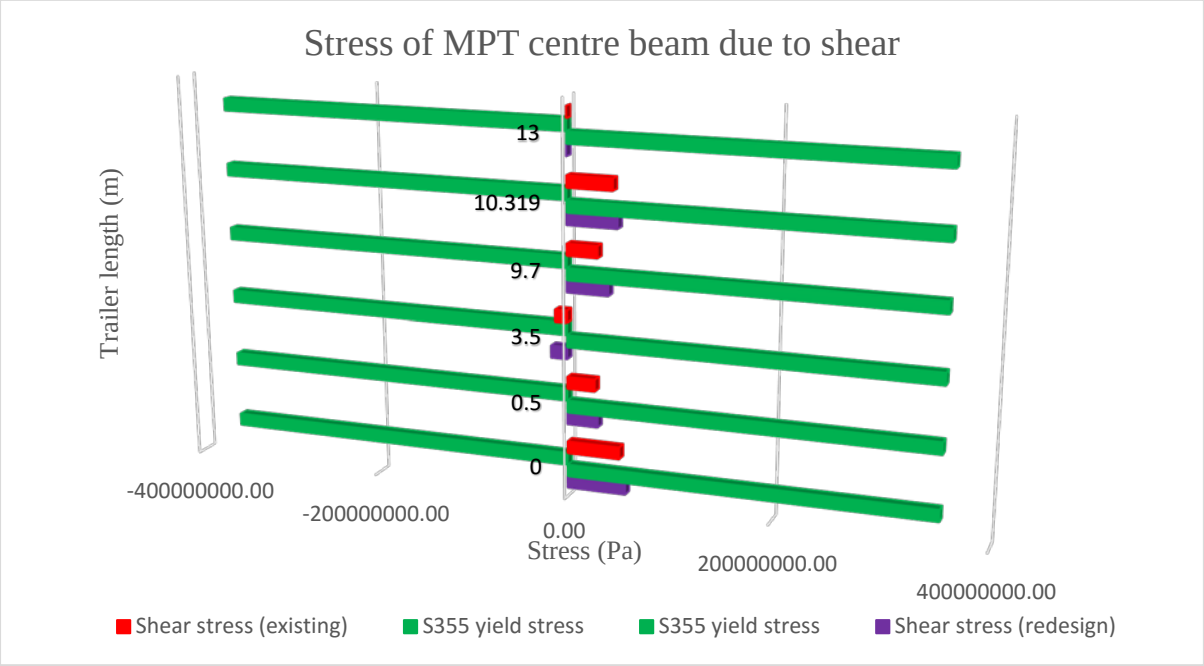

Figure 4.13: Stress of MPT centre beam due to shear

Using the bending moments from Table 4.8 per beam (total divided by 2) and the centre beam dimensions (found in Table 4.9) substituted into eq.(6), the maximum bending stress per centre beam was calculated as shown in Figure 4.14.

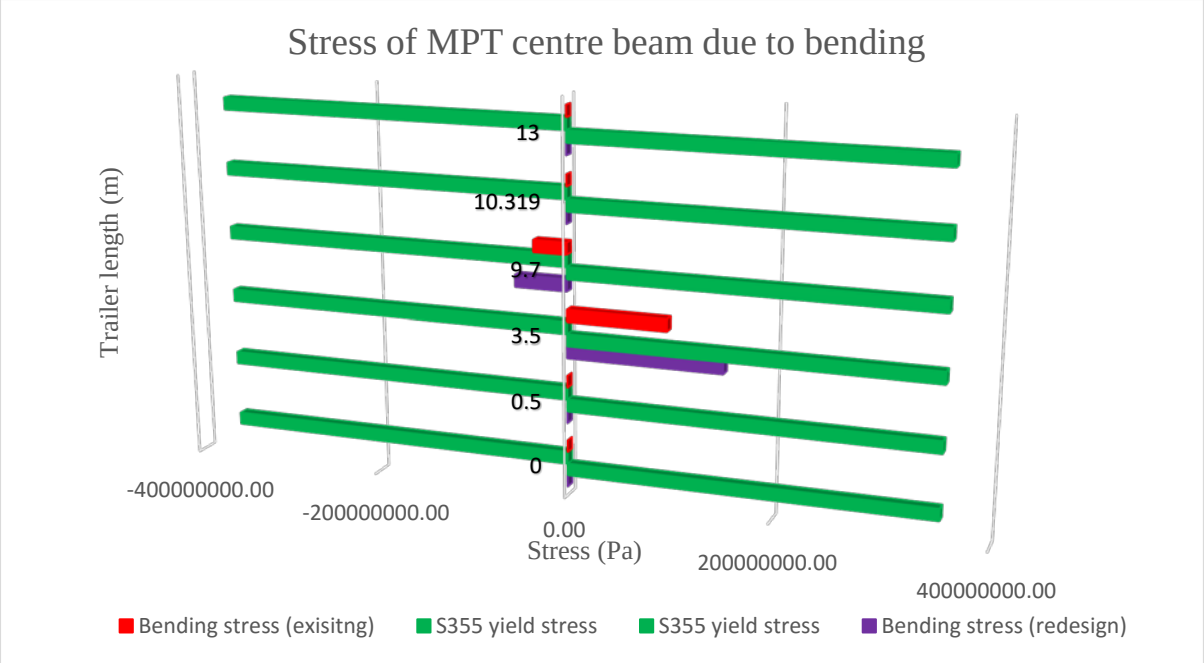

Figure 4.14: Stress of MPT centre beam due to bending

An acceptable minimum safety factor (SF) of 2.33 was complied with [28] for the redesigned centre beam using the calculations for Figures 4.13 and 4.14. Therefore the critical sections of the trailer based on the shear force and bending stresses with their corresponding graphs are defined as shown in Table 4.10.

Critical length (m)	0-3.5	3.5-9.7	9.7-13
Existing web height (mm)	180-450	450-800	800-450
Recommended web height (mm) using 14 mm web thickness	180-450	450-600	600-450

Table 4.10: Recommendations for new main centre beam for MPT

The necessary data for the shear and bending analysis performed in Chapter 4.9 are given in Appendix C. The dimension reduction calculated for the centre beams in this chapter will be used as the basis of the redesigned MPT later shown in Chapter 6.1.3.

4.10 Finite element analysis of original BTT and MPT

4.10.1 Introduction and loading accelerations

The design process of the trailer requires that an FEA analysis be done to ensure structural integrity, and to determine that loading takes place within safe limits of the material specifications. The FEA of the existing trailers is necessary to meet the requirements of the research methodology as shown in Chapter 3. ANSYS Mechanical software was used for the linear static analysis.

The reference loading conditions used for the vertical, longitudinal and lateral accelerations are based on the specifications found in ADR- European Agreement Concerning the International Carriage of Dangerous Goods by Road, Verein Deutscher Ingenieure (VDI) Guideline 2700 part 2: Securing of Loads on Road Vehicles and UMTRI Research Review of Heavy Commercial Vehicles [49], [53], [54].

The ADR standard specify conditions of 2g vertical, 2g longitudinal and 1g lateral accelerations [53] for the design of trailers operating on highway conditions at speeds of up to 120 km/hr. On the port environment a fully laden trailer will never exceed a maximum operating speed of 30 km/hr., which is quarter the maximum speed in the ADR standard.

Cowling used 1g vertical acceleration with a 2.75 safety factor applied to the mass load for the vertical FEA load case, 0.897g longitudinal acceleration; determined by applying a safety factor of 2 to the minimum brake performance of trailers exceeding 35km/hr and 0.3g lateral acceleration for the design of a 40 ton cane haulage trailer for highway speeds [41].

TE's mechanical design office currently uses 2g vertical, 0.5g longitudinal and 0.25g lateral accelerations to assess current trailers in internal assessment reports such as PD_PEP_NAT_RE_003. Initially 2g vertical, 0.7g longitudinal and 0.3g lateral accelerations were used to assess trailers in internal assessment reports such as PD_PEP_NAT_RE_001 and PD_PEP_NAT_RE_002.

UMTRI research review on the Rollover of Heavy Commercial Vehicles recommend 0.25g lateral acceleration for heavy loads as the trailer rollover threshold for reasons previously discussed in Chapter 2.3 of the literature review, and recommend 0.5g for longitudinal acceleration [49].

VDI Guideline 2700 Part 2: Securing of Loads on Road Vehicles, uses 0.8g for longitudinal acceleration [54].

SABS 1447 Part 2: Low Speed Trailers, provides a corresponding force for brake performance of 0.23g for the maximum design mass of the trailer up to 40 km/hr. [4].

Taking into consideration the various acceleration loading conditions presented it was decided to perform the FEA to the accelerations as laid out in Table 4.11 [49], [53], [54].

Acceleration Type	**Project analysis (g)**
Vertical	2
Longitudinal	0.8
Lateral	0.25
Combined vertical, longitudinal and lateral	2, 0.8 and 0.25

Table 4.11: Acceleration (g) values for directional loading

A longitudinal acceleration of 0.5g could have been used based on the above presented standards/specifications or 0.46g by applying a safety factor of 2 [41] to the trailer brake performance value of 0.23g [4], but a more conservative longitudinal acceleration of 0.8g [54] was chosen for the FEA. In the port cargo operational environment there are no speed humps, severe gradients, or obstacles to be negotiated, since other commodity handling machines such as wharf cranes, rubber tyre gantry cranes, straddle carriers and various container handlers and wheel loaders also operate in this environment. Due to the nature of these other heavy vehicles, it is an absolute requirement to keep the roads well maintained.

The accelerations in Table 4.11 were individually used for the FEA loading cases on both the BTT and MPT trailers in Chapters 4.10.2 and 4.10.3 respectively. A combined loading case incorporating accelerations in all directions was also carried out to examine the resultant stress on both trailer models. Individual acceleration load cases allow the stress extremities to be determined, and these can be negated where a combined loading case cancels stresses in opposing directions, potentially resulting in a lower peak stress than the individual case.

4.10.2 BTT analysis

4.10.2.1 General finite element model

Linear static analyses were conducted using the model of the trailer as shown in Chapter 2.2 [20], [21], [29]. The main part of the CAD trailer's geometry was mid-surfaced before applying translations and connections between structural members for correct structural bonding. The model was automatically meshed (Figure 4.15) using ANSYS, predominantly with quadrilateral shell elements since the stresses of concern needed to be as accurate as possible [19], [23]. The suspension system spring effects caused by the leaf springs were approximated in the analyses by means of rigid body connections; 1D bar for the axles and spring elements as shown in Figures 4.17 and 4.18 respectively. Multi-point rigid body constraints as shown in Figure 4.19 were used to transfer the forces caused by the payload and the trailer's own weight through the suspension. To simulate the effects of the hauler suspension on the trailer when the trailer is coupled to the fifth wheel, a spring element was used to emulate this effect [20], [22], [23], [24]. Spring constants as per manufacturers specifications were used for the trailer and hauler suspension. The model setup from CAD to FEA including the process described in Chapter 4.10.2.1 is further elaborated on in Chapter 7.

A solid kingpin was used in the analysis, due to the solid representation having a better distribution and dissipation of the load when compared to the surface representation [19]. The containers mass was applied by means of point mass loads from its centre of mass, and distributed on the surfaces of the trailer that come into contact with the floor of the container as shown in Figure 4.16 and 4.20.

The material properties for the analyses of the existing trailer are shown in Table 4.12. All stress comparisons were done by looking at the equivalent Von-Mises stress criteria.

Material	**Yield stress (σ_y)**	**Ultimate tensile stress (σ_{uts})**	**Poisson's ratio (γ)**	**Young's modulus (E)**	**Density (ρ)**
300WA Structural steel	300 MPa	450 MPa	0.3	209 GPa	7850 kg/m^3

Table 4.12: Material properties for BTT [55]

The stress legends in the different FEA load case comparisons have been adjusted to show the localised stresses as the maximum. The global coordinates in the comparisons correspond to X denoting longitudinal, Y denoting vertical and Z denoting lateral directions.

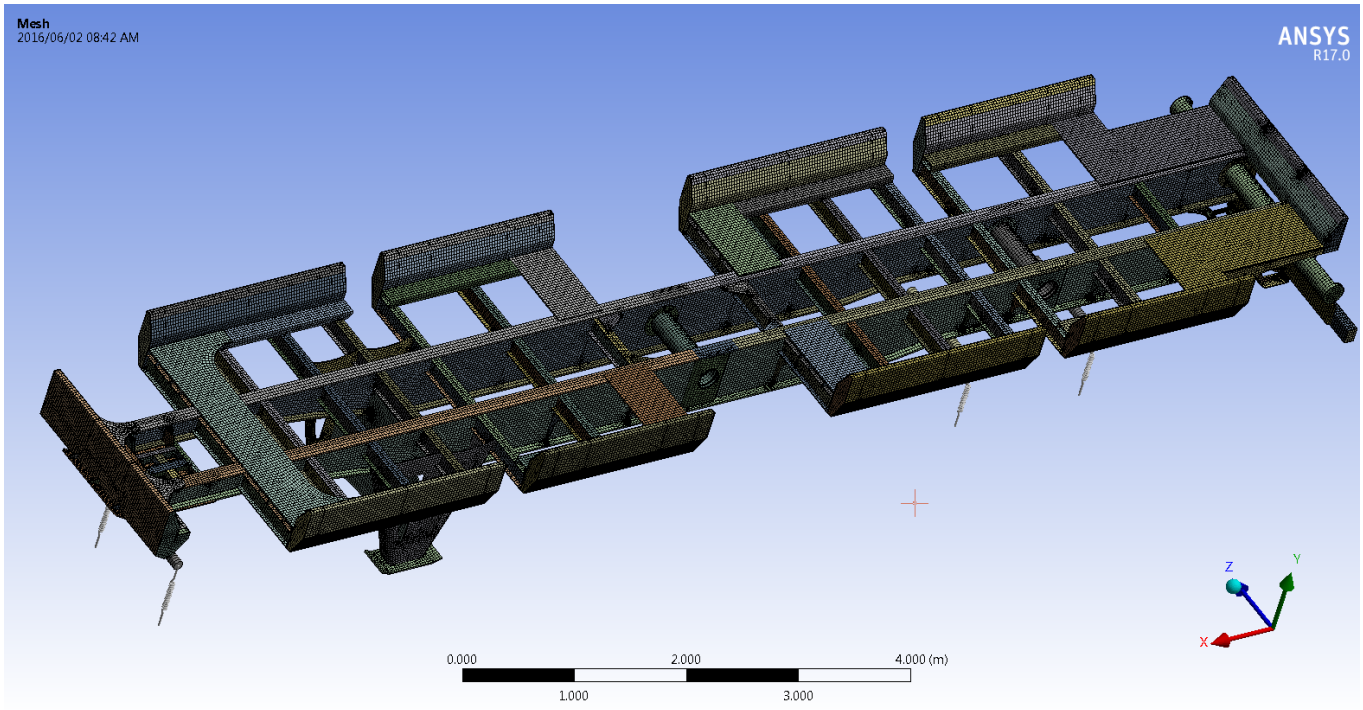

Figure 4.15: Schematic of the trailer with the applied mesh

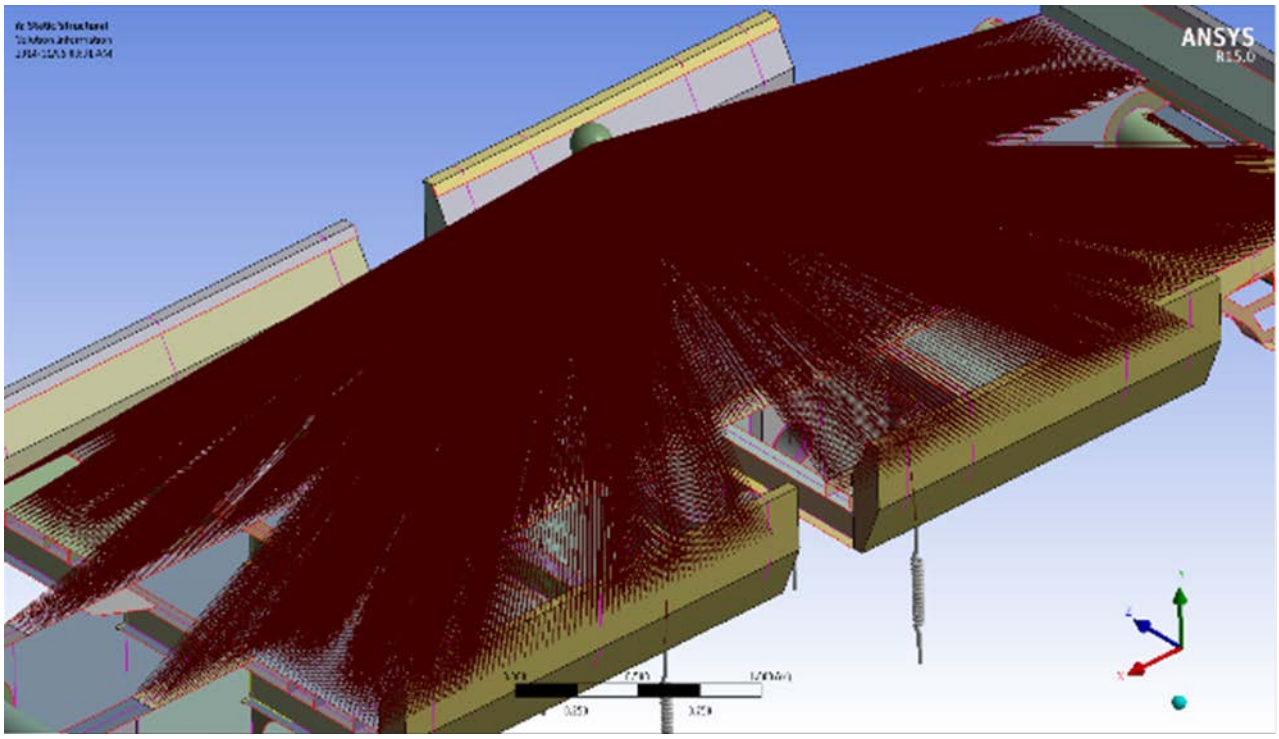

Figure 4.16: View of the 20 foot shipping container load applied to the trailer surfaces

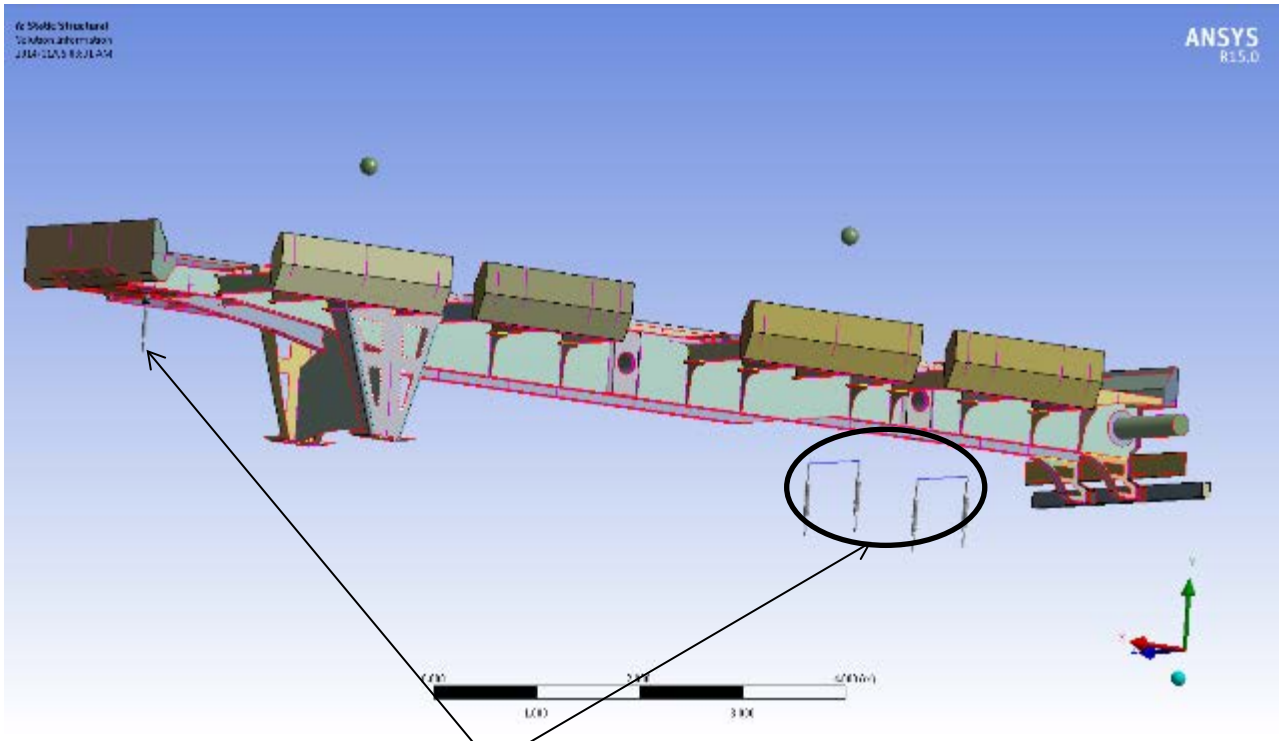

Figure 4.17: Spring elements for simulating the suspension

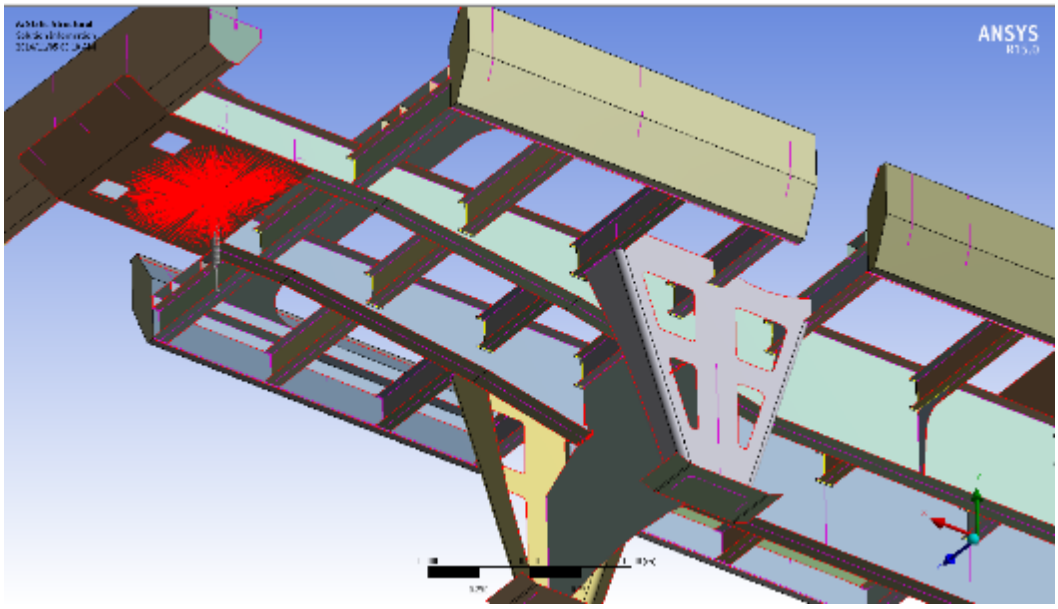

Figure 4.18: Applying of the spring elements using multi-point constraints to the relevant geometry on front end of the trailer

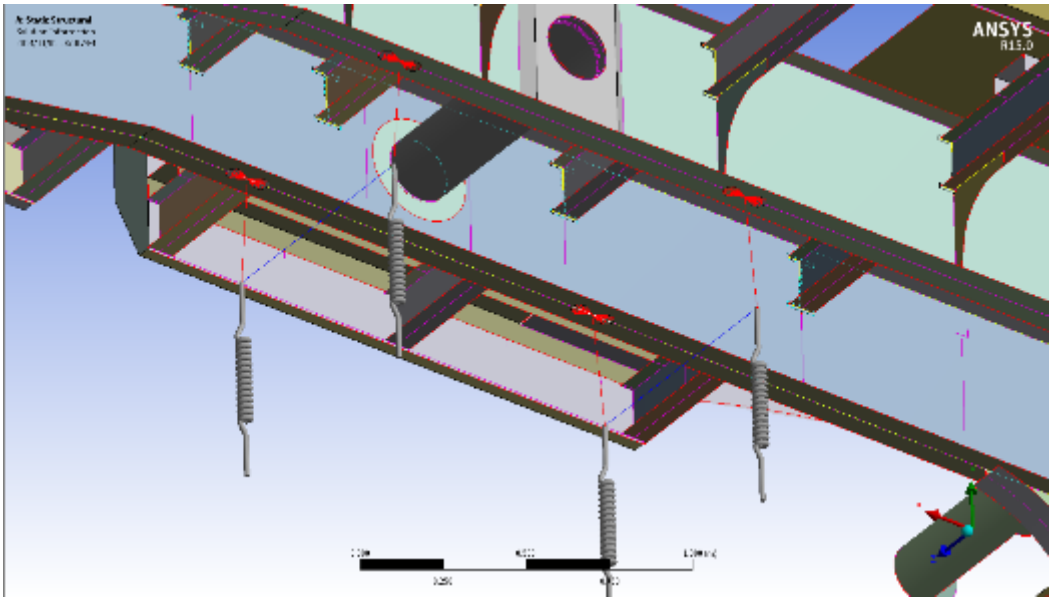

Figure 4.19: Applying of the spring elements using multi-point constraints at rear end of the trailer

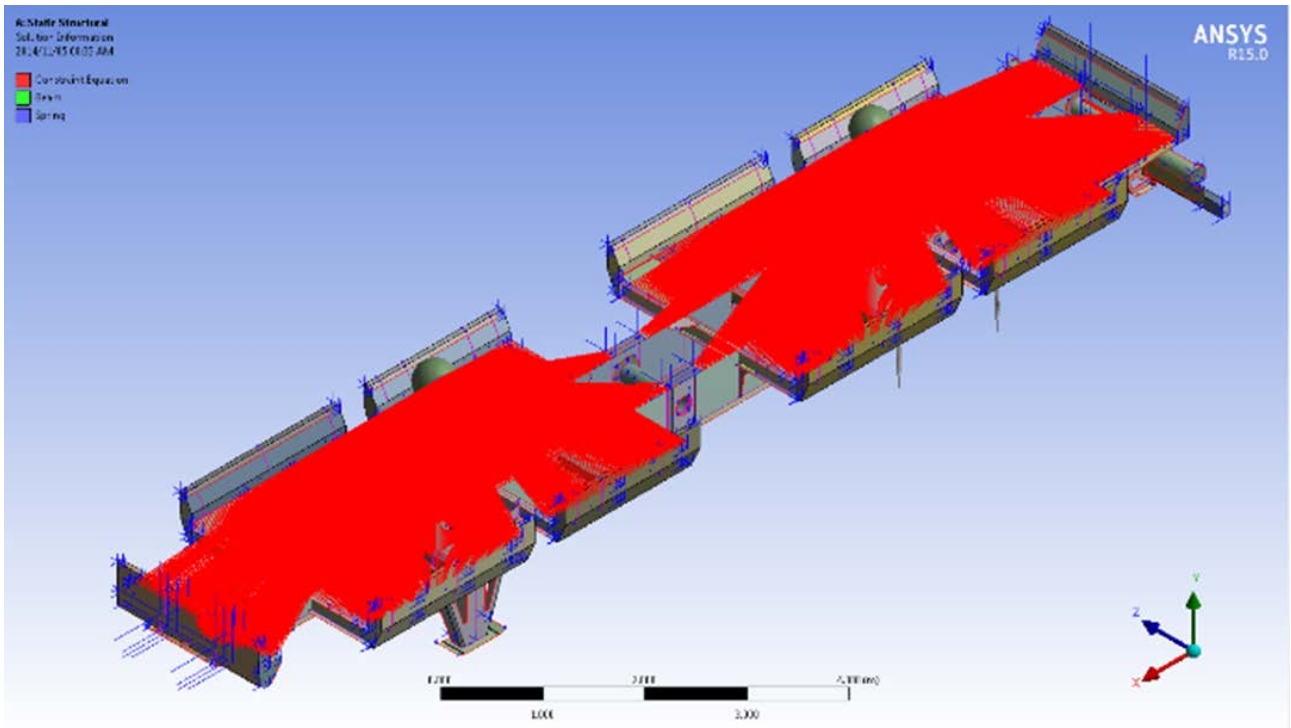

Figure 4.20: Full representation of the trailer with the 2 x 20 foot container distributed loads applied with rigid bodies and meshing elements and constraints highlighted

4.10.2.2 BTT - 2g vertical downward acceleration

The loaded trailer must be able to withstand a load of 60.96 tons in total from the two 20 foot shipping containers which have a tare mass sum and a payload of 30.48 ton each [50]. The loading accelerations selected as per Chapter 4.10.1 were used to check that the Von-Mises stresses would not exceed the yield stress of the material.

The 2g caseloads are tabulated below:

Force	Magnitude	Location
Gravity	19.62 m/s^2 (2 x g)	Entire model
Container loads	30.48 tons per container	On surface areas of the container which are in contact with the trailer

Table 4.13: Vertical loads and values

The caseload constraints are tabulated below:

Constraint	Location
Translation X	On kingpin
Translation Y	On bottom of springs
Translation Z	On kingpin and suspension

Table 4.14: Load constraints

Figures 4.21 to 4.26 show that the model complied with the design criteria with a peak allowable stress of 253 MPa except for the localised stresses in Figure 4.23. Stress only occurs on a few elements at the localised points. The region where spring elements attach to the centre beams, and right angled connections between mating members, has a tendency to produce high stress regions [25], [38], [39], [40], [41].

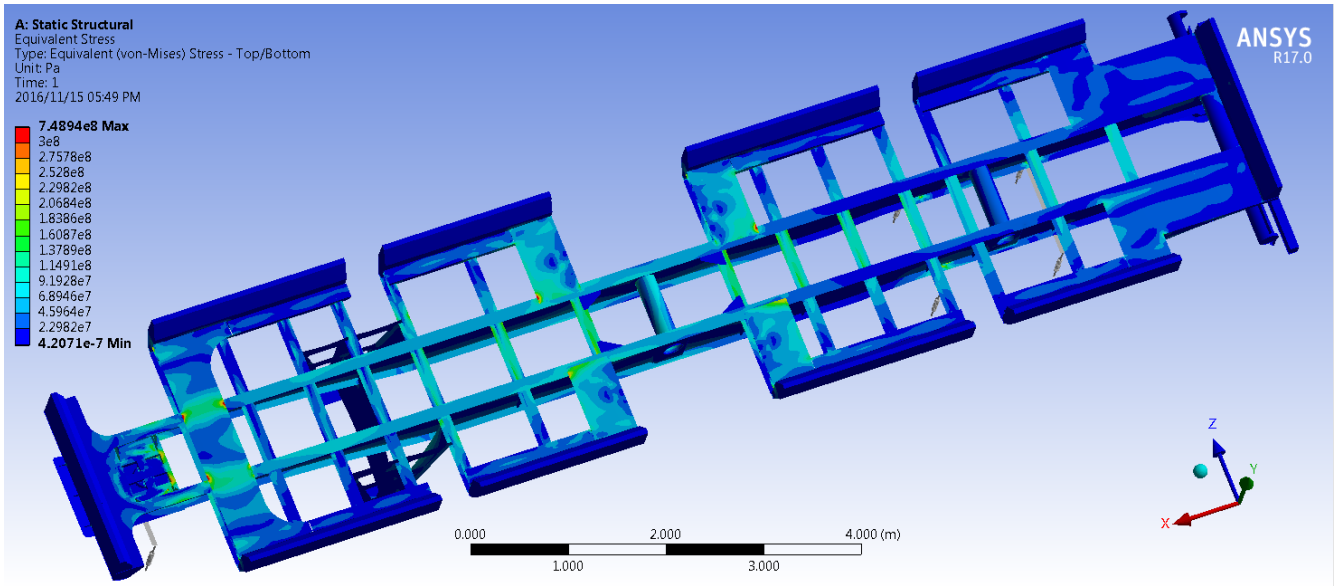

Figure 4.21: Stress plot - top view (Von-Mises)

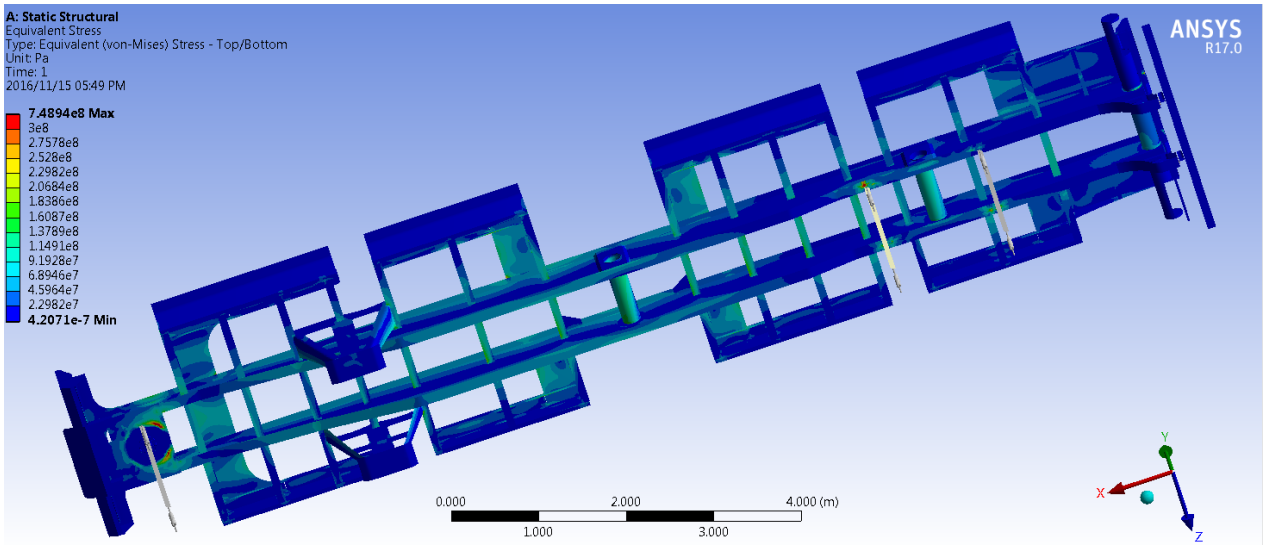

Figure 4.22: Underframe Stress plot - top view (Von-Mises)

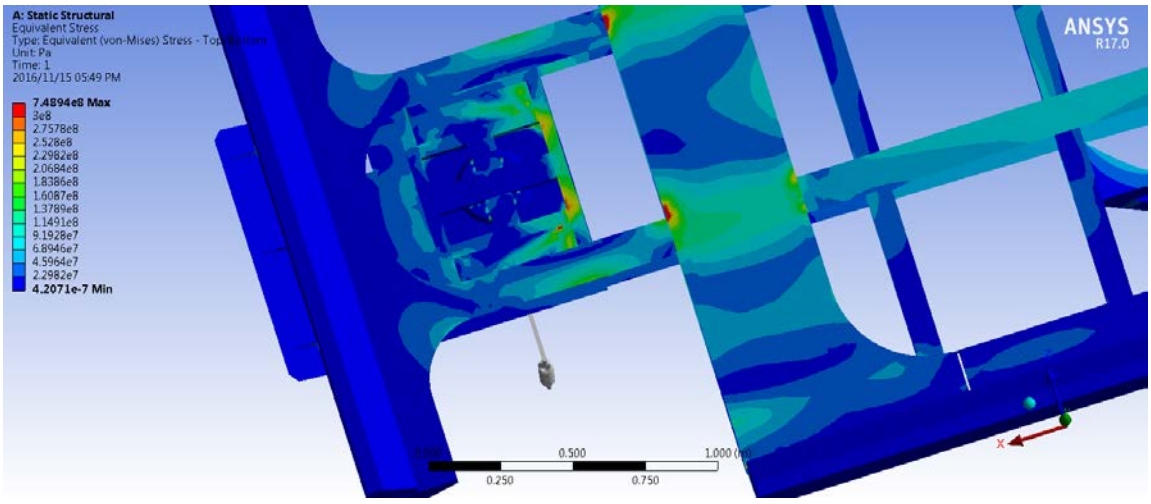

Figure 4.23: Localised stresses (>300 MPa) found near the kingpin

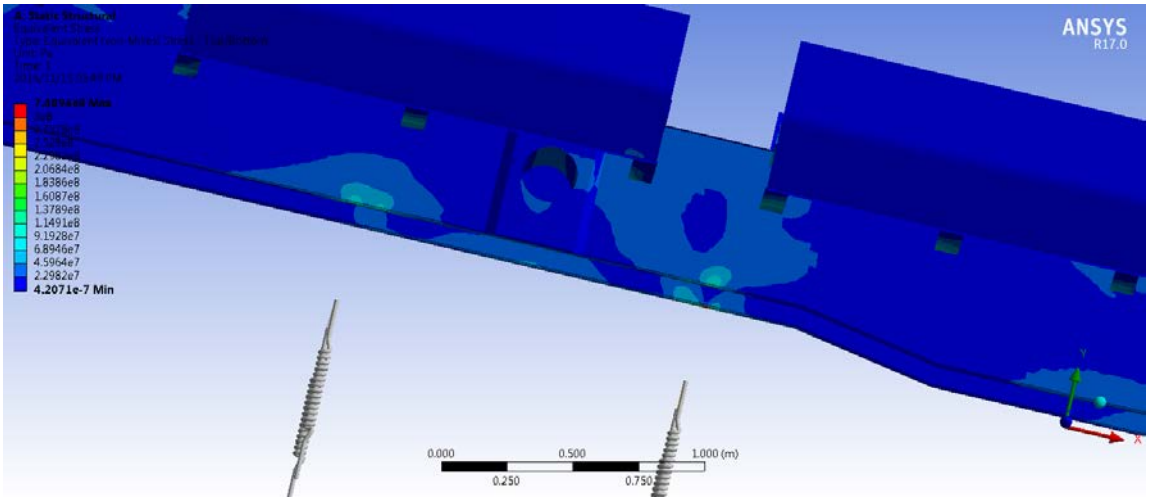

Figure 4.24: Close up Stress plot – bogie/suspension mounting (Von-Mises)

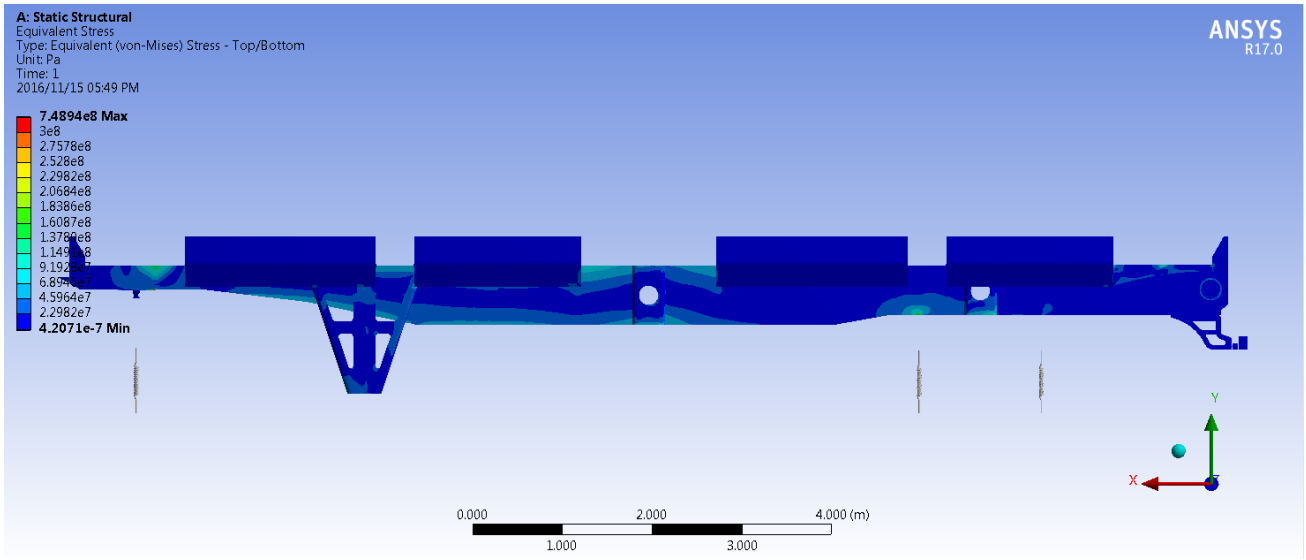

Figure 4.25: Stress plot of main centre beam (Von-Mises)

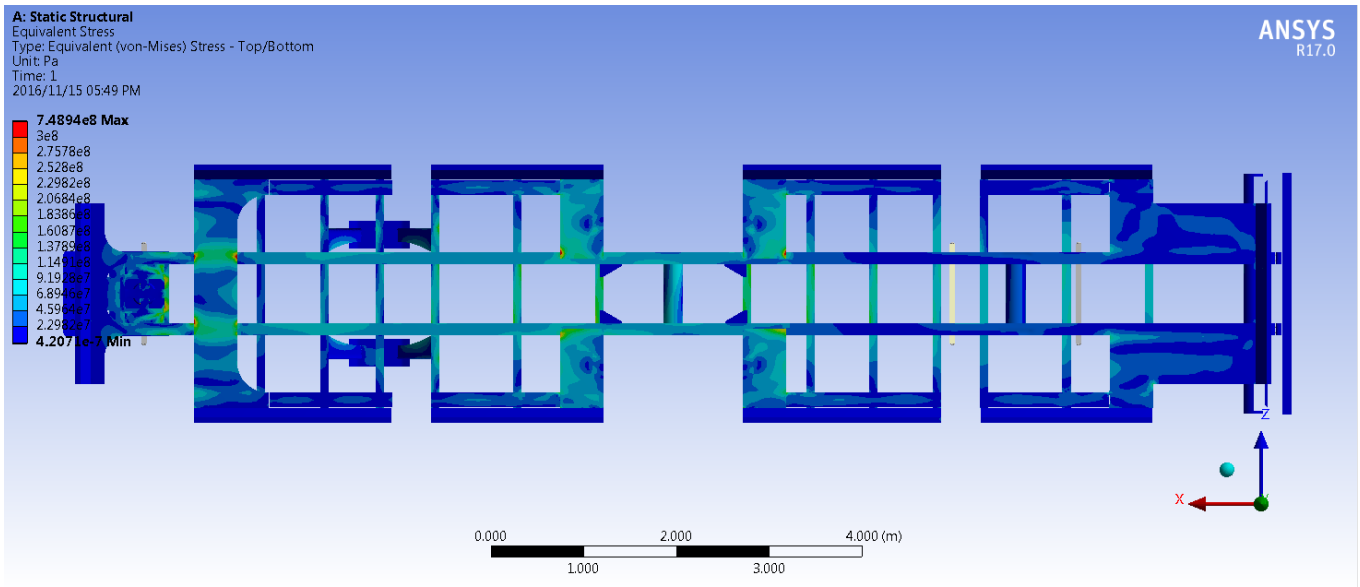

Figure 4.26: Stress plot of top of trailer (Von-Mises)

The suspension and fifth wheel loads obtained from the simulation were compared to the theoretical values obtained by the analytical methods shown in Figure 4.4 which were multiplied by two. This was done to validate the load transfer that occurred in the simulation. The tabulated results show the comparison:

Load	Simulation load result (N)	Theoretical load result (N)	Difference (%)
Fifth Wheel	519 000	515 650.02	0.65
Bogie (Suspension)	800 270	814 423.24	1.74

Table 4.15: Loads obtained from the 2g vertical downward acceleration simulation

Table 4.16 shows the load distribution over the two axles.

Axle position	Load (N)
Rear	395 190
Front	405 080

Table 4.16: Load distribution over the axles

The difference between the simulated and theoretical load results in Table 4.15 is due to the mass of the trailer. In the FEA solution the trailer mass was 6379 kg, whereas the tare mass of the trailer, used in the force reaction calculation was 6710 kg. The FEA only uses the critical structure and does not take into account the sprung (non-structural) and un-sprung accessories and components that make up the total tare mass, this is commonly the case in FEA design [22], [23], [24], [25], [26], [33]. The un-sprung components incorporated into the FEA are given in Chapter 4.10.2.1. The items in Table 4.17 were accurately quantified based on supplier information and components that were weighed. Since welding, paint and the accessories of the trailer cannot be quantified accurately, the remainder mass (tare mass subtract the quantified components) was used.

Description of item	Mass type	Mass (kg)	Percentage of item mass to total mass (%)
Structural mass from FEA	Sprung	6 379	62.54
Rims and tyres	Un-sprung	1 640	16.08
Axles and suspension	Un-sprung	1 850	18.14
Greasing system	Sprung	20	0.20
Braking system	Sprung	20	0.20
Welding, paint and accessories	Sprung	291	2.85
Tare/Total mass	Sprung and un-sprung	10 200	100

Table 4.17: Subcomponent masses of the BTT

The greasing system, braking system, welding, paint and accessories masses shown in Table 4.18 increased the sprung structural mass of the FEA trailer model. The greasing system, braking system, welding, paint and accessories were incorporated into the FEA. The masses were small in relation to the structure of the trailer but the details of these components increase the model accuracy as shown in Table 4.18 [22], [23], [24], [25], [26], [33].

Load	Simulation load result (N)	Theoretical load result (N)	Difference (%)
Fifth wheel	520 980	515 650.02	1.02
Bogie (Suspension)	804 470	814 423.24	1.22

Table 4.18: Load comparison using structural mass from FEA with accessories and relevant components

4.10.2.3 BTT – 0.8g longitudinal acceleration and 1g vertical acceleration

The structure must sustain a 0.8g longitudinal and 1g vertical acceleration together with the applied loads. The resulting Von-Mises stress should not exceed the yield stress of the material.

The 0.8g + 1g caseloads are tabulated below:

Force	Magnitude	Location
Gravity (vertical)	-9.81 m/s^2 (g)	Entire model
Container loads	30.48 tons per container	On surface areas of the container which are in contact with the trailer
Longitudinal acceleration	7.848 m/s^2 (0.8 x g)	Entire model

Table 4.19: Vertical and longitudinal loads and values

The caseload constraints are tabulated below:

Constraint	Location
Translation X	On kingpin
Translation Y	On bottom of springs
Translation Z	On kingpin and suspension

Table 4.20: Load constraints

The analysis results complied with the design criteria as shown in Figure 4.27 to 4.31. The stresses were found to be below the yield stress with a peak allowable stress of 208 MPa. The stresses exceeded the 300 MPa yield stress however failure would not occur due to the highly localised nature of the stresses where spring elements attach to the centre beams, and right angled connections between mating members, has a tendency to produce high stress regions [25], [38], [39], [40], [41].

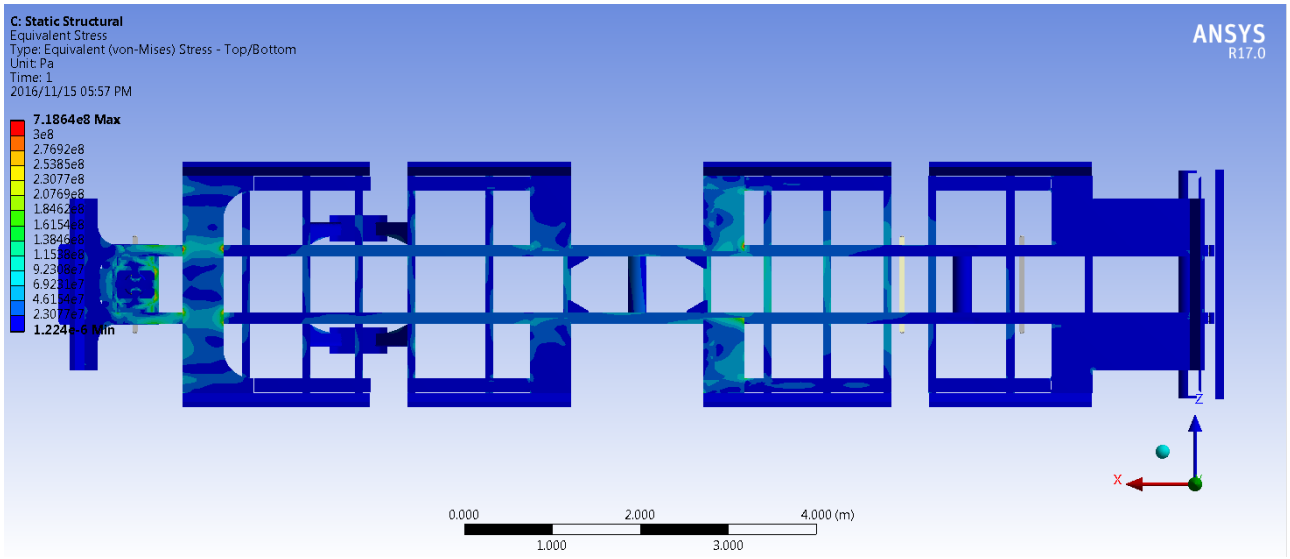

Figure 4.27: Stress plot - top view (Von-Mises)

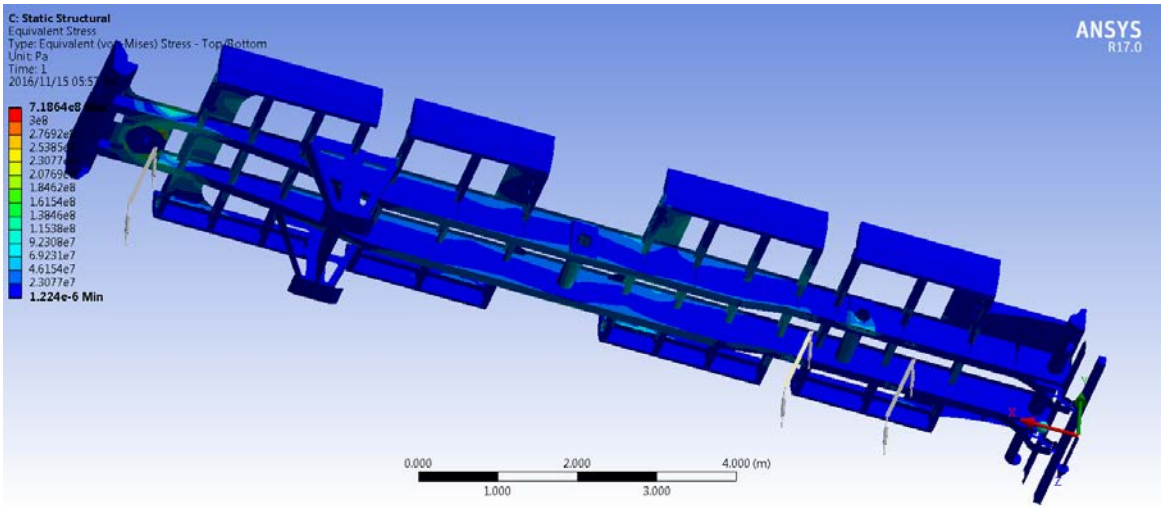

Figure 4.28: Underframe Stress plot (Von-Mises)

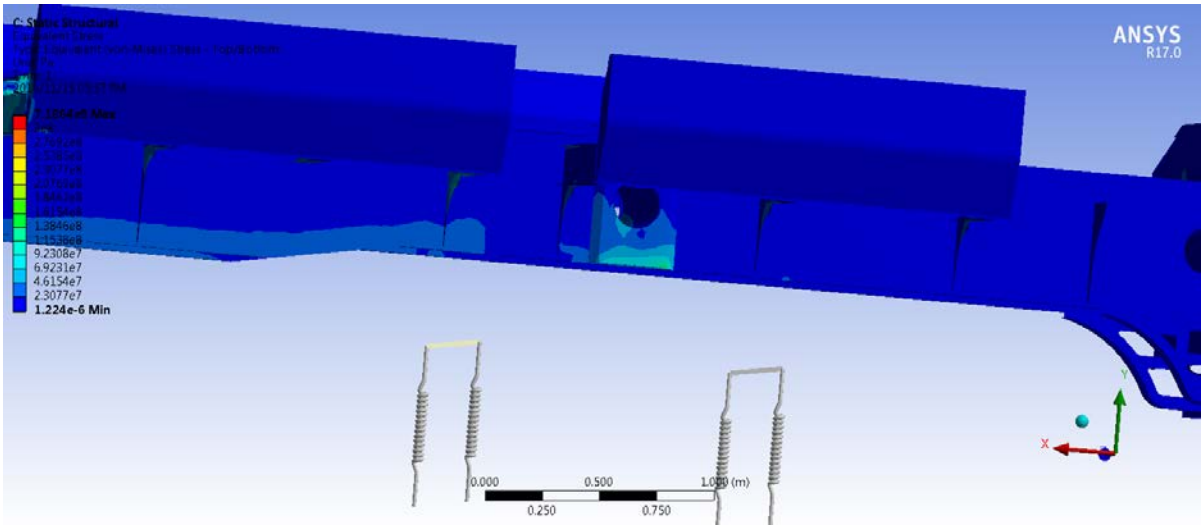

Figure 4.29: Close up Stress plot – bogie/suspension mounting (Von-Mises)

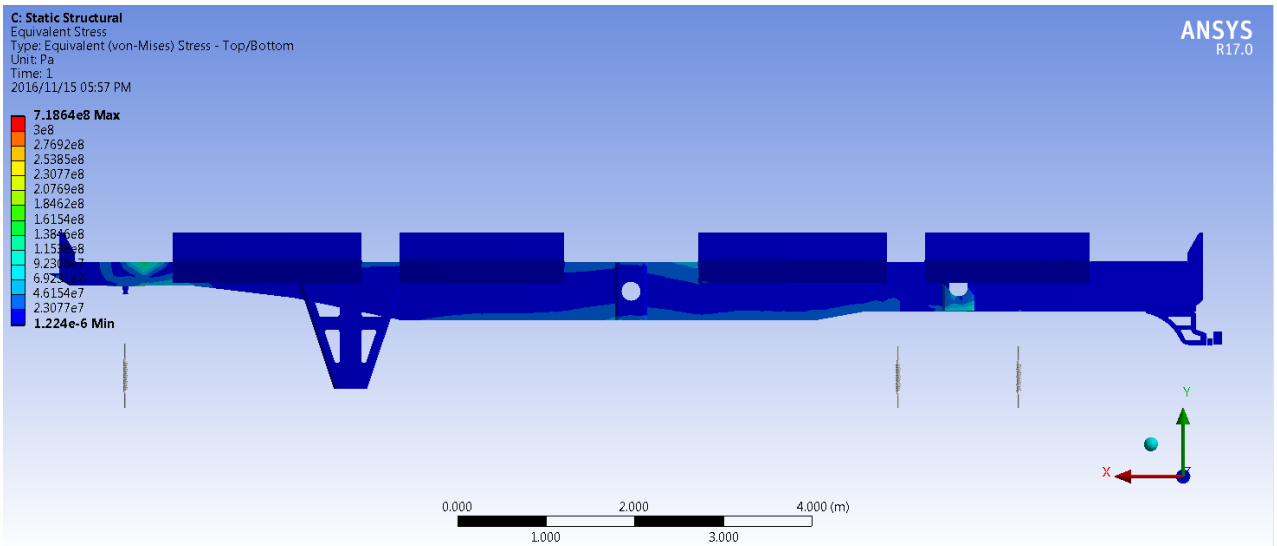

Figure 4.30: Stress plot of main centre beam (Von-Mises)

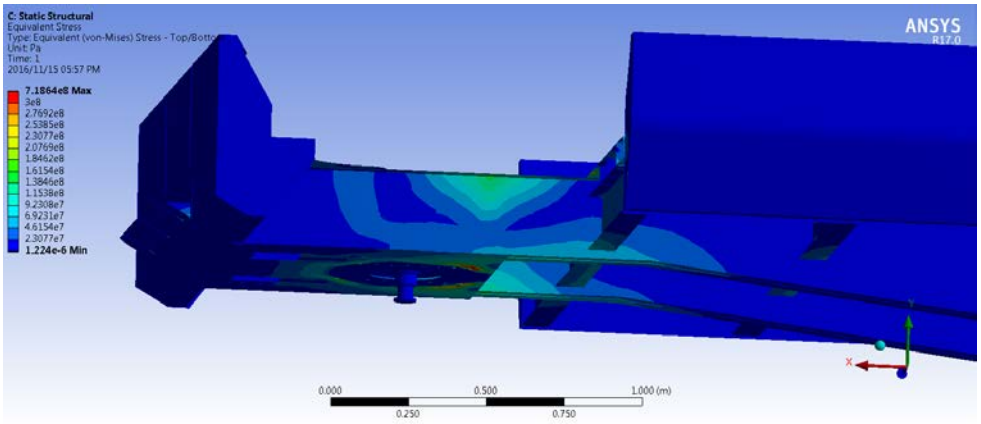

Figure 4.31: Close up Stress plot – kingpin (Von-Mises)

4.10.2.4 BTT – 0.25g lateral acceleration and 1g vertical acceleration

The trailer structure must sustain a 0.25g lateral and 1g vertical acceleration together with the applied loads. The resulting Von-Mises stress should not exceed the yield stress of the material.

The 0.25g + 1g caseloads are tabulated below:

Force	Magnitude	Location
Gravity (vertical)	-9.81 m/s^2 (g)	Entire model
Container loads	30.48 tons per container	On surface areas of the container which are in contact with the trailer
Lateral acceleration	2.4525 m/s^2 (0.25 x g)	Entire model

Table 4.21: Vertical and lateral loads and values

The caseload constraints are tabulated below:

Constraint	Location
Translation X	On kingpin
Translation Y	On bottom of springs
Translation Z	On kingpin and suspension

Table 4.22: Load constraints

The analysis complied with the design criteria as shown in Figure 4.32 to 4.36. The stresses were found to be below the yield stress with a peak allowable stress of 208 MPa except for the highly localised stress points [25], [38], [39], [40], [41]. In reality the hauler suspension provides support and movement to the front of the trailer which prevents excessive twisting of the underframe, yielding much lower stresses. The bogie and tyres of the trailer also provide roll to compensate for excessive lateral forces and therefore would not be fixed as in the FEA model, yielding much lower stresses.

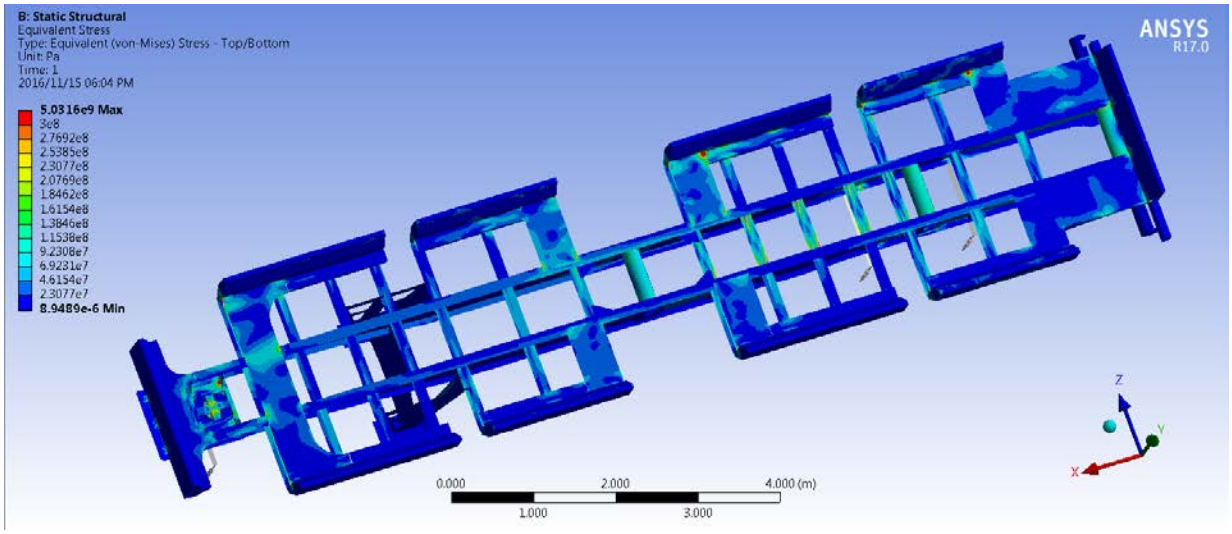

Figure 4.32: Stress plot - top view (Von-Mises)

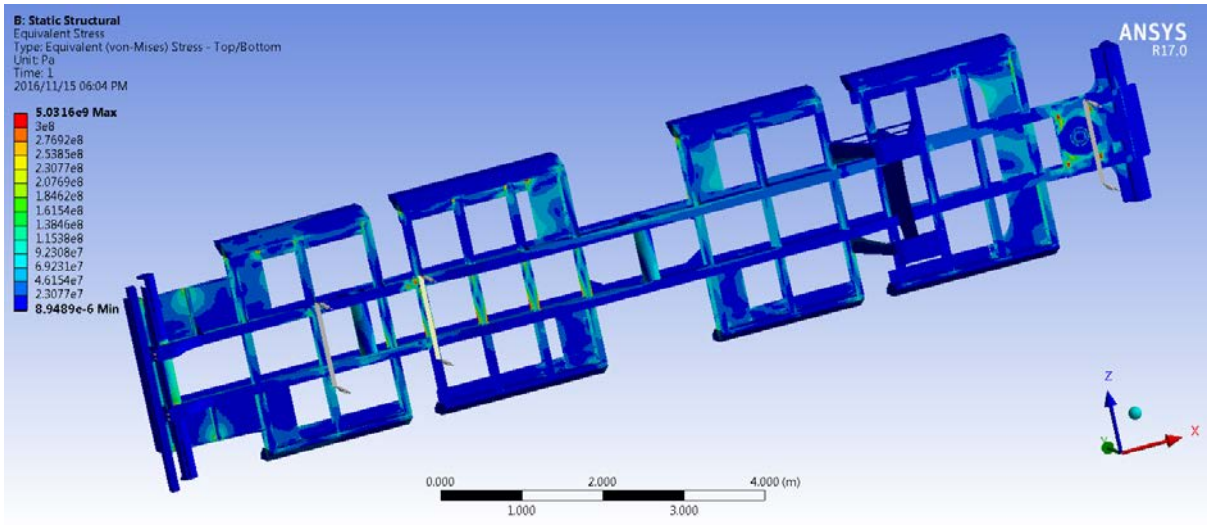

Figure 4.33: Underframe Stress plot - top view (Von-Mises)

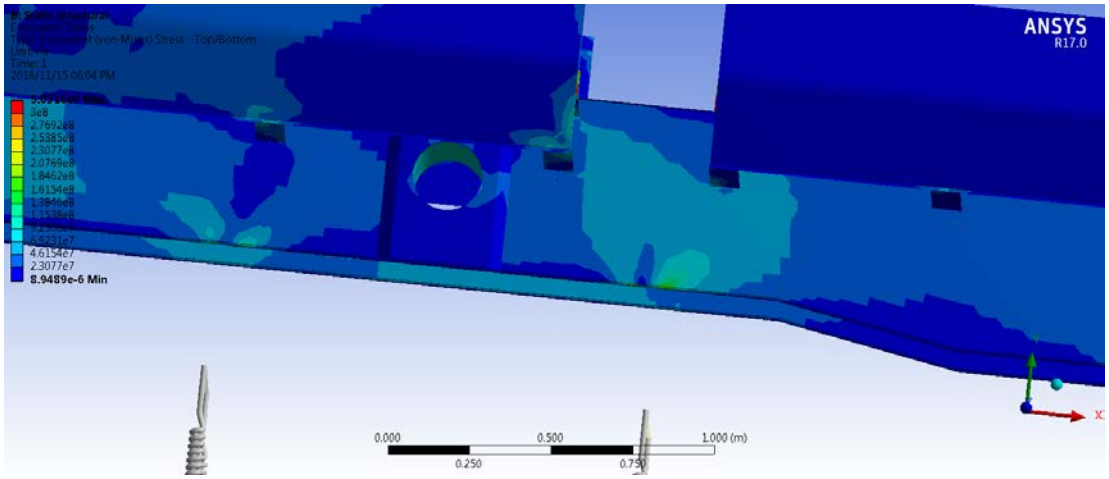

Figure 4.34: Close up Stress plot – bogie/suspension mounting (Von-Mises)

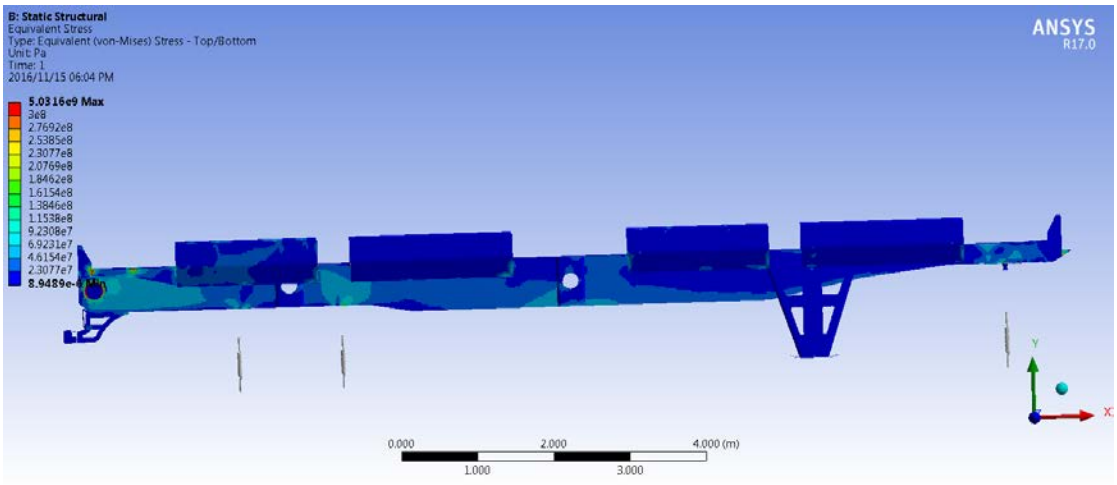

Figure 4.35: Stress plot of main centre beam (Von-Mises)

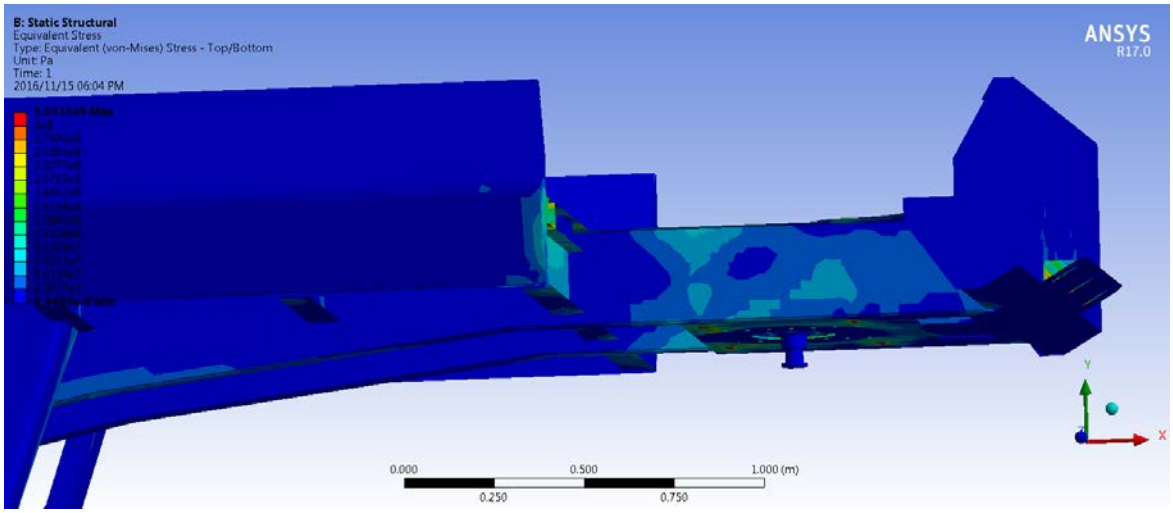

Figure 4.36: Close up Stress plot – kingpin (Von-Mises)

4.10.2.5 BTT – 2g vertical and 0.8g longitudinal and 0.25g lateral acceleration

The trailer structure must sustain a 2g vertical acceleration, 0.8g longitudinal and 0.25g lateral acceleration together with the applied loads. This loading scenario allows the total combined cases to be analysed on the structure at once. The resulting Von-Mises stress should not exceed the yield stress of the material.

The 2g + 0.8g + 0.25g caseloads are tabulated below:

Force	Magnitude	Location
Gravity(vertical)	-19.62 m/s^2 (2 x g)	Entire model
Container loads	30.48 tons per container	On surface areas of the container which are in contact with the trailer
Longitudinal acceleration	7.848 m/s^2 (0.8 x g)	Entire model
Lateral acceleration	2.4525 m/s^2 (0.25 x g)	Entire model

Table 4.23: Vertical, longitudinal and lateral loads and values

The load case constraints are tabulated below:

Constraint	Location
Translation X	On kingpin
Translation Y	On bottom of springs
Translation Z	On kingpin and suspension

Table 4.24: Load constraints

The analysis complied with the design criteria and the stresses as shown in Figures 4.37 to 4.43 were found to be below the yield stress with a peak allowable stress of 254 MPa, except for highly localised stress points shown on the top plates [25], [38], [39], [40], [41]. Certain areas that depict stressed areas that were not found in Chapters 4.10.2.2 to 4.10.2.4 are due to combined loading acting on that structural member, however these stresses were below the peak allowable stress of 254 MPa.

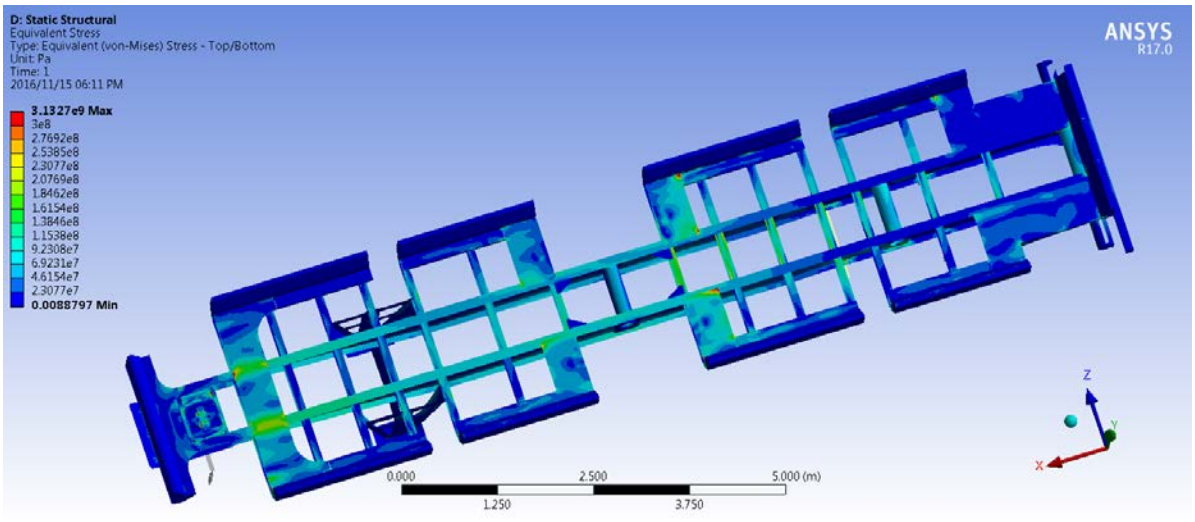

Figure 4.37: Stress plot - top view (Von-Mises)

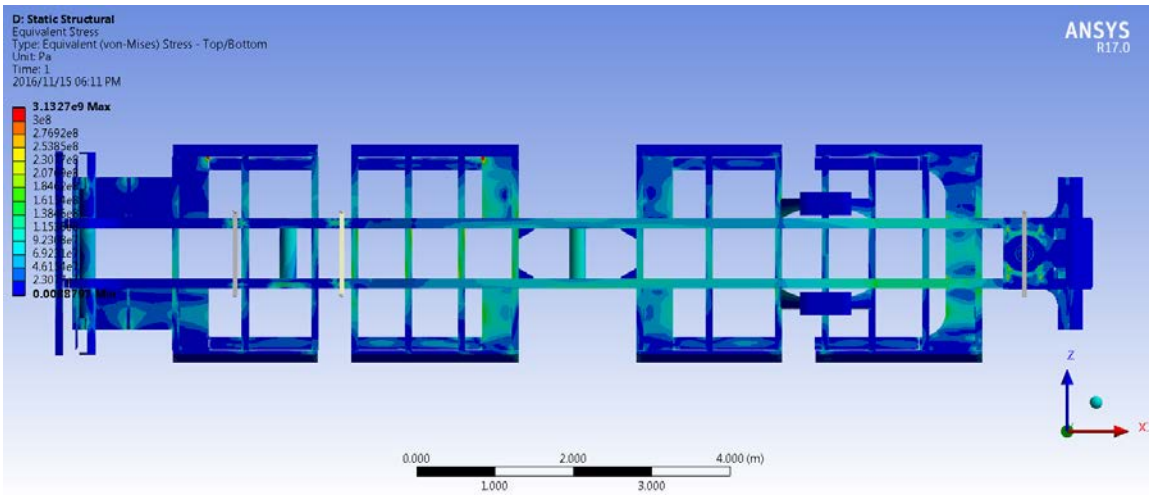

Figure 4.38: Underframe stress plot (Von-Mises)

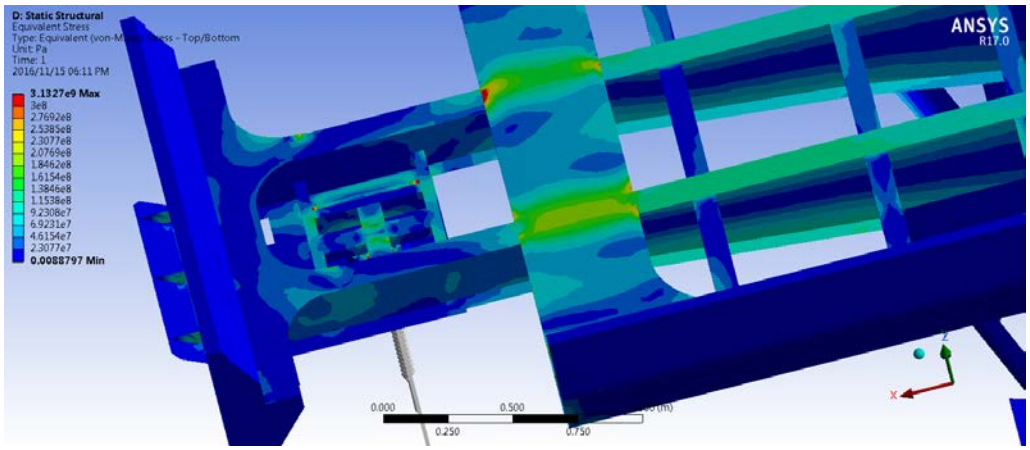

Figure 4.39: Localised stresses (>300 MPa) found near the kingpin

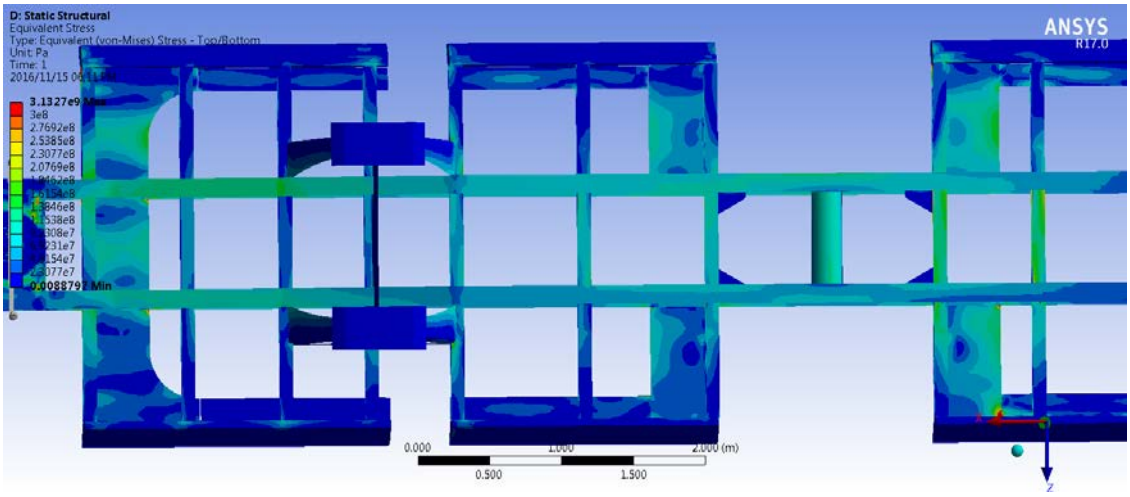

Figure 4.40: Underframe stress plot (Von-Mises)

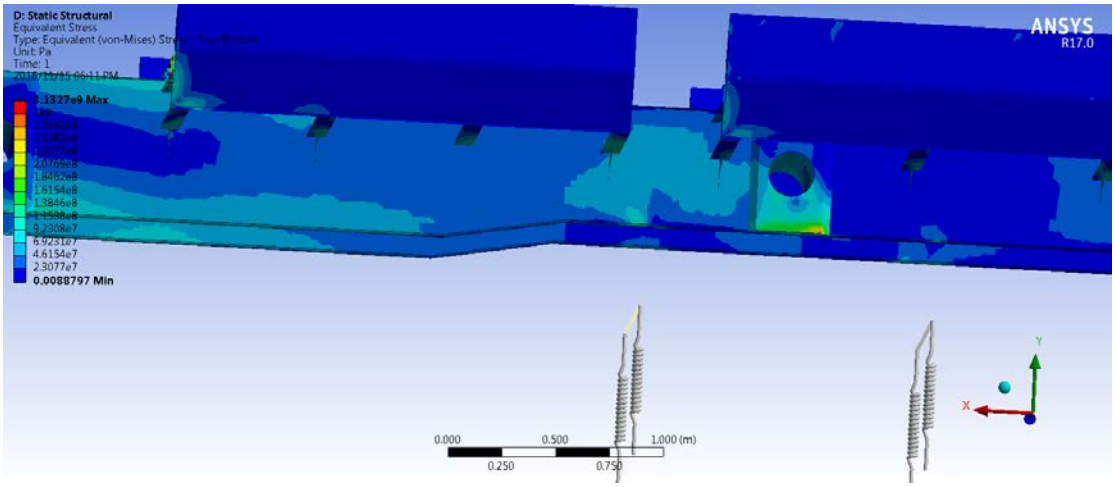

Figure 4.41: Bogie end stress plot (Von-Mises)

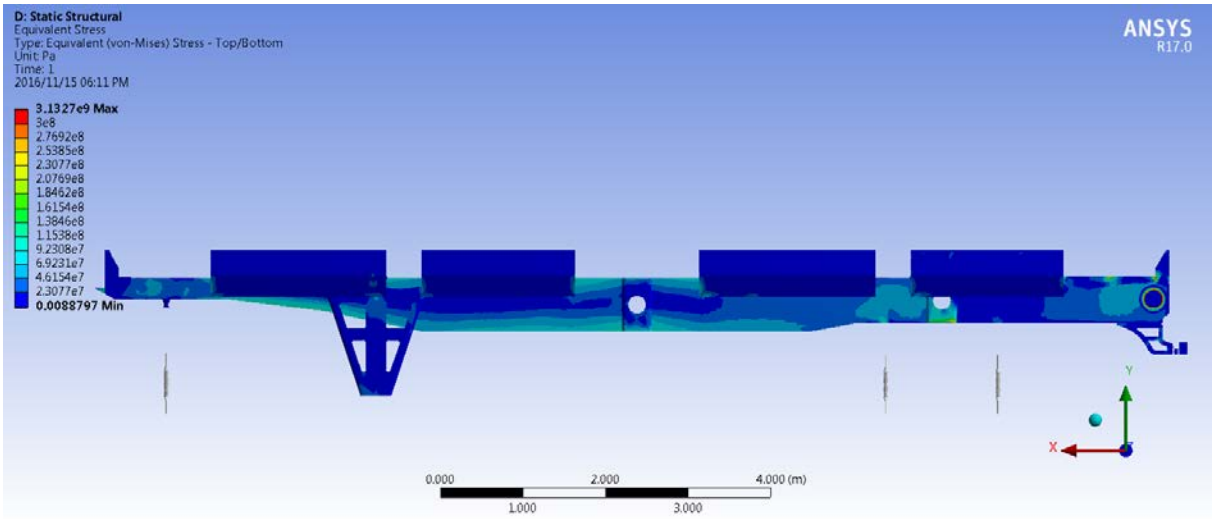

Figure 4.42: Stress plot of main centre beam (Von-Mises)

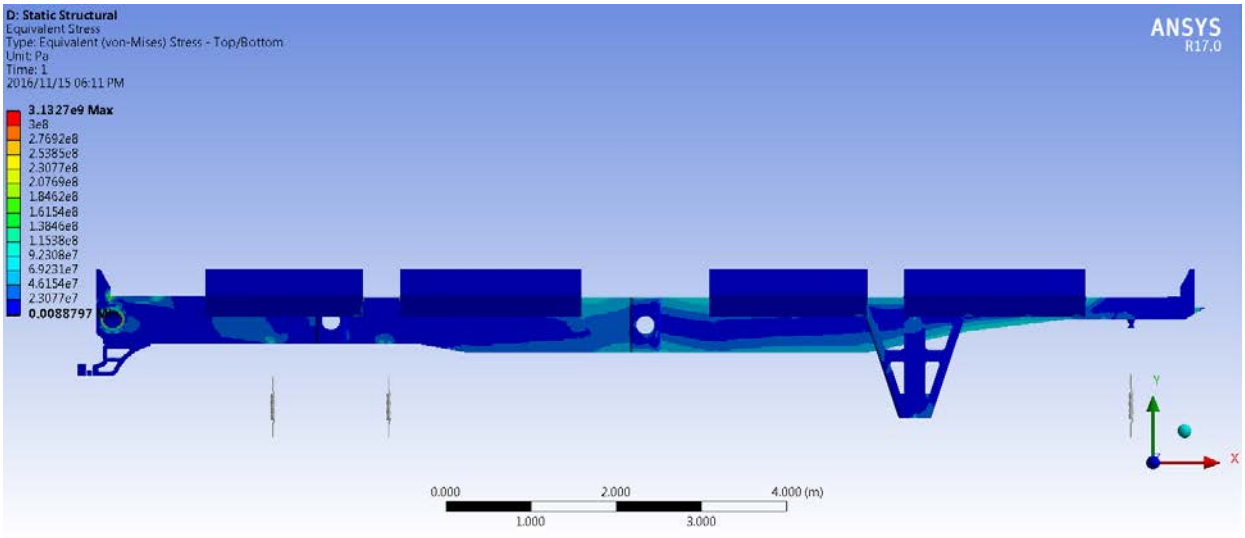

Figure 4.43: Stress plot of main centre beam (Von-Mises)

4.10.3 MPT analysis

4.10.3.1 General finite element model

Linear static analyses were conducted using the model of the trailer as with the BTT in Chapter 4.10.2.1 [20], [21], [29]. The main part of the CAD trailer geometry was mid-surfaced before applying translations and connections between structural members for correct structural bonding. The loading accelerations which were used are given in Chapter 4.10.1. The model was automatically meshed as shown in Figure 4.44 using ANSYS, predominantly with quadrilateral shell elements since the stresses of concern needed to be as accurate as possible [19], [23]. The front headboard of the trailer was modelled as a mass element across the front of the trailer as this is a safety structure and does not bear load from the commodity handling equipment. The suspension system spring effects caused by the leaf springs were approximated in the analyses by means of rigid body connections, and 1D bar and spring elements as shown in Figures 4.44 and 4.45 respectively. The rigid body multi-point constraints as shown in Figure 4.46 were used to transfer forces due to payload and the trailer's weight through the suspension. To simulate the effects of the hauler suspension on the trailer when coupled to the fifth wheel, a spring element was used to emulate this effect as shown in Figure 4.45 [22], [23], [24]. Spring constants as per manufacturers specifications were used for the trailer and hauler suspension. The model setup from CAD to FEA including the process described in Chapter 4.10.3.1 is further elaborated on in Chapter 7.

A solid kingpin was used in the analysis for reasons previously explained in Chapter 4.10.2.1, and shown in Figure 4.47 [19], [23]. The skip mass was applied by means of point mass loads from its centre of mass distributed on the surfaces of the trailer that comes into contact with the floor of the skip. The skip is designed so that three channel sections make up the floor which is in contact with the trailer as shown in Figure 4.48. The point mass load applied in the FEA as shown in Figure 4.48 offers the ideal situation.

The material properties for the analyses of the existing trailer are shown in Table 4.25. All stress comparisons were done by looking at the equivalent Von-Mises stress criteria.

Material	**Yield stress (σ_y)**	**Ultimate tensile stress (σ_{uts})**	**Poisson's ratio (γ)**	**Young's modulus (E)**	**Density (ρ)**
S355 Structural steel	355 MPa	470-630 MPa	0.3	209 GPa	7850 kg/m^3

Table 4.25: Steel properties of the MPT [55]

The stress legends in the different FEA load case comparisons have been adjusted to show localised stresses as the maximum. The global coordinates in the comparisons correspond to X denoting longitudinal, Y denoting vertical and Z denoting lateral directions.

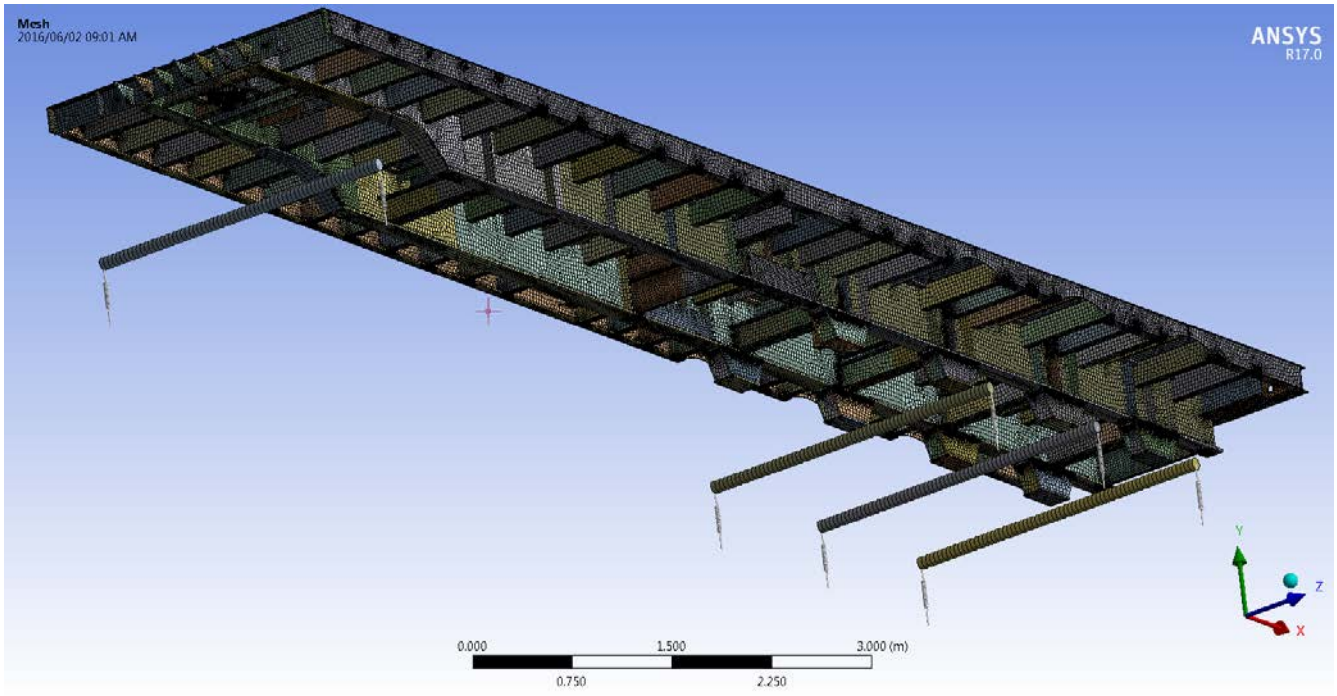

Figure 4.44: Schematic of the trailer with the applied mesh, 1D bar and spring elements

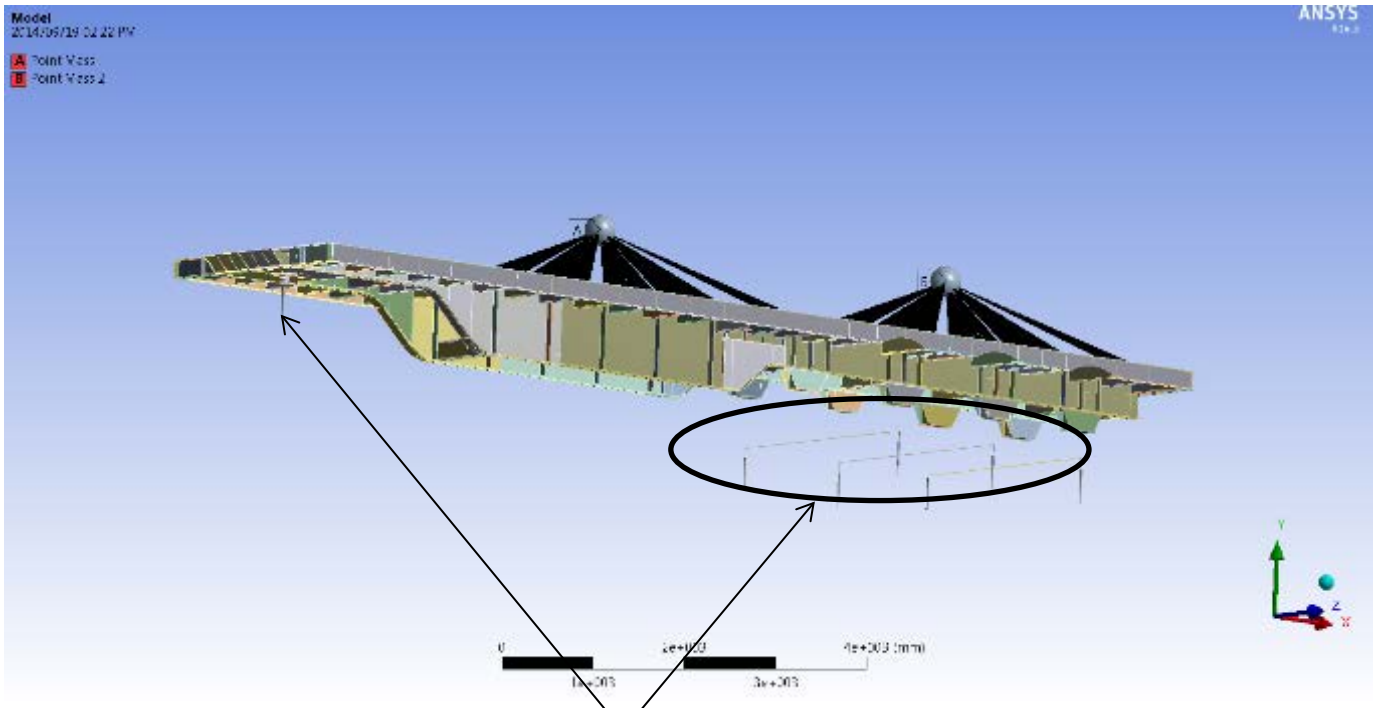

Figure 4.45: Spring elements included for simulating the suspension

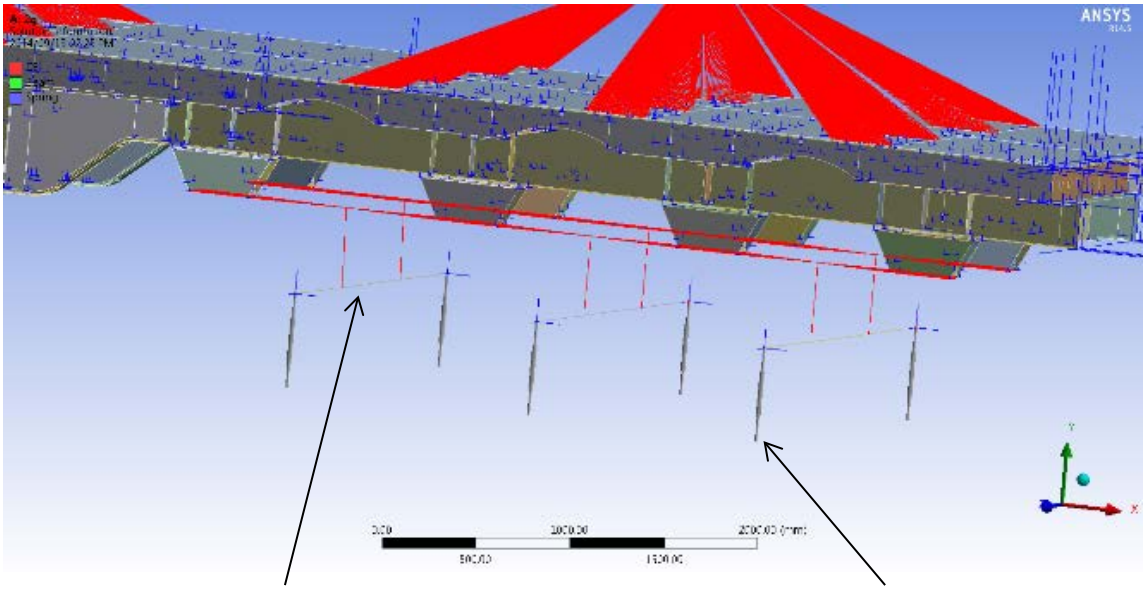

Figure 4.46: Translation Z constraint applied to the suspension and translation Y constraint applied to the bottom of the springs

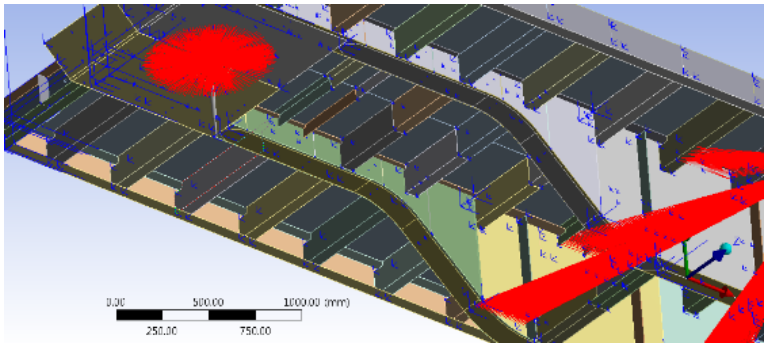

Figure 4.47: Translation X and Z constraint applied to the kingpin representing the connection to the hauler

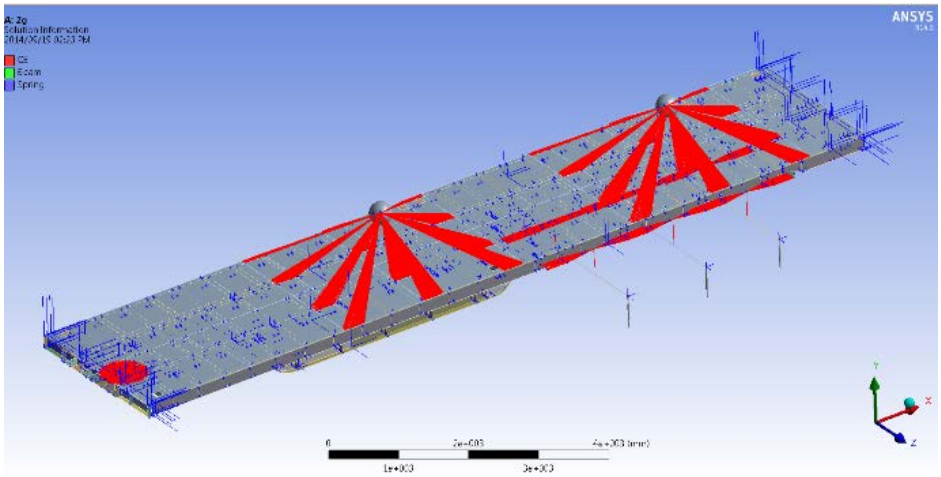

Figure 4.48: General representation of the trailer with the 2 x 44.2 ton skip loads applied, with meshing elements and constraints highlighted

4.10.3.2 MPT - 2g Vertical downward acceleration

The loaded trailer must be able to withstand a load of 88.4 tons in total from the two 40 ton skips which have a tare mass sum and a payload of 44.2 ton each. The loading accelerations selected as per Chapter 4.10.1 were used to check that the Von-Mises stresses would not exceed the yield stress of the material.

The 2g caseloads are tabulated below:

Force	Magnitude	Location
Gravity	19.62 m/s^2 (2 x g)	Entire model
Skip loads	44.2 tons per skip	On surface areas of the skip which are in contact with the trailer

Table 4.26: Vertical load cases and values

The caseload constraints are tabulated below:

Constraint	Location
Translation X	On kingpin
Translation Y	On bottom of springs
Translation Z	On kingpin and suspension

Table 4.27: Load constraints

Figures 4.49 to 4.53 show the analysis complied with the design criteria with a peak allowable stress of 266 MPa. The high stress regions at the suspension pedestals are localised due to modelling approximations. The region where spring elements attach to the centre beams, and right angled connections between mating members, has a tendency to produce high stress regions [25], [38], [39], [40], [41].

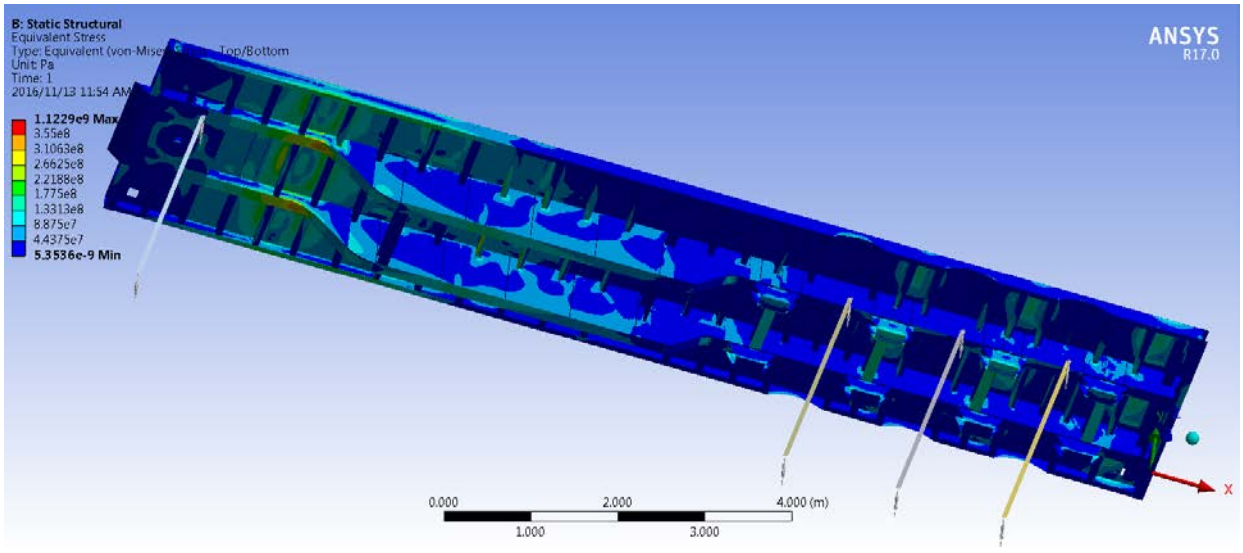

Figure 4.49: Underframe stress plot (Von-Mises)

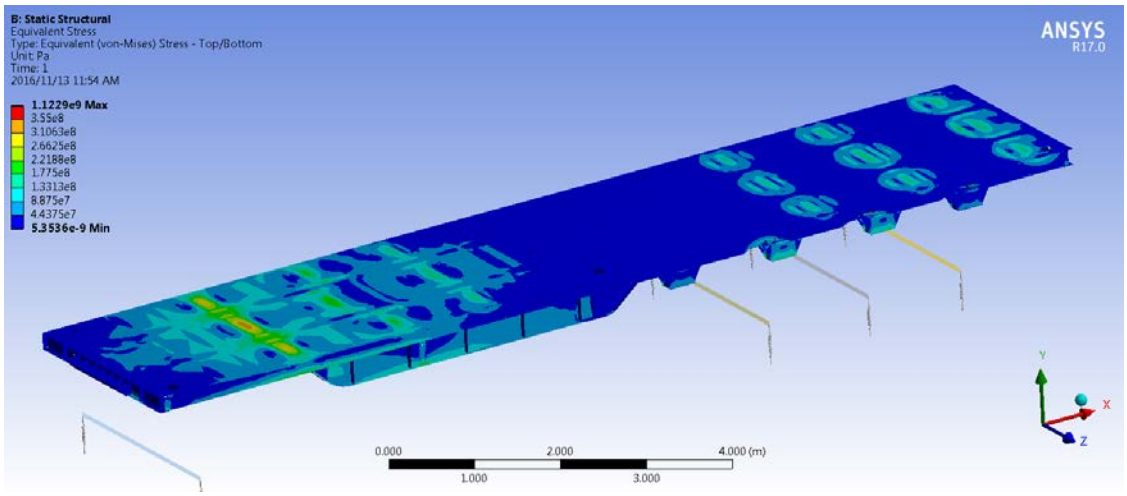

Figure 4.50: Stress plot - top view (Von-Mises)

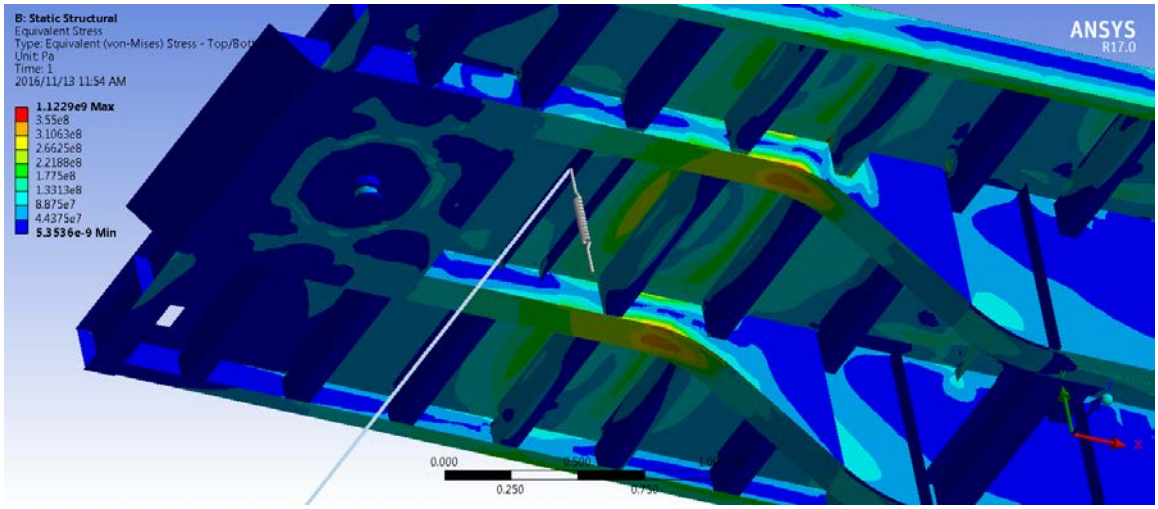

Figure 4.51: Stress plot on the bend of the goose neck

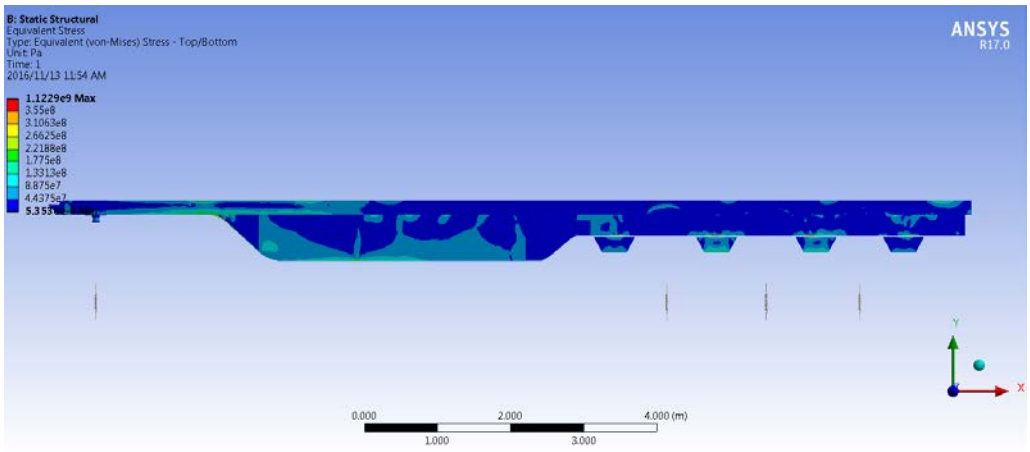

Figure 4.52: Stress plot of main centre beam (Von-Mises)

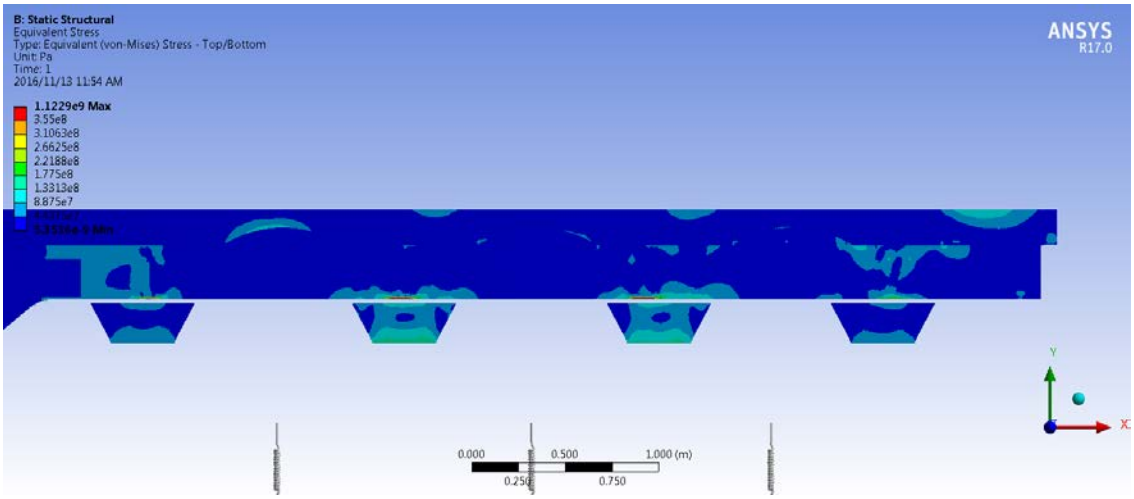

Figure 4.53: High stress region (>355 MPa) found on the connection points of the main beam to the suspension pedestals

The suspension and fifth wheel load values obtained from the simulation when subjected to a 2g vertical acceleration were compared to the theoretical values obtained by analytical methods from Figure 4.10 multiplied by 2g. This was done to validate the load transfer that occurred in the simulation. The tabulated results below show the comparisons:

Load	Simulation load result (N)	Theoretical load result (N)	Difference (%)
Fifth wheel	565 210	588 242.92	3.92
Bogie (Suspension)	1 294 840	1 324 903.28	2.27

Table 4.28: Loads obtained from the 2g vertical downward acceleration simulation

The loads on each of the axles from the 2g vertical downward acceleration simulation were:

Axle position	Load (N)
Rear	429 870
Middle	432 810
Front	432 160

Table 4.29: Load distribution on axles

The differences between the simulated and theoretical load results in Table 4.28 are mainly due to the mass of the trailer. In the FEA solution the trailer mass was 8750 kg, whereas the tare mass of the trailer, used in the force reaction calculation was 9110 kg. The FEA only uses the critical structure and does not take into account the sprung (non-structural) and un-sprung accessories and components that make up the total tare mass, this is commonly the case in FEA design [22], [23], [24], [25], [26], [33]. The un-sprung components are incorporated into the FEA as shown in Chapter 4.10.3.1. The items in Table 4.30 were accurately quantified based on supplier information and weighing the components. Since welding, paint and the accessories of the trailer cannot be quantified accurately the remainder mass (tare mass subtract the quantified components) was used.

Description of item	Mass type	Mass (kg)	Percentage of item mass to total mass (%)
Structural mass from FEA	Sprung	8 750	65.01
Rims and tyres	Un-sprung	2 460	18.28
Axles and suspension	Un-sprung	1 890	14.04
Greasing system	Sprung	20	0.15
Braking system	Sprung	20	0.15
Welding, paint and accessories	Sprung	320	2.38
Tare/Total mass	Sprung and un-sprung	13 460	100

Table 4.30: Subcomponent masses of the MPT

The greasing system, braking system, welding, paint and accessories masses shown in Table 4.30 increased the sprung structural mass of the FEA trailer model. The greasing system, braking system, welding, paint and accessories were incorporated into the FEA. The masses were small in relation to the structure of the trailer but the details of these components increase the model accuracy as shown in Table 4.31 [22], [23], [24], [25], [26], [33].

Load	Simulation load result (N)	Theoretical load result (N)	Difference (%)
Fifth wheel	567 680	588 242.92	3.50
Bogie (suspension)	1 299 420	1 324 903.28	1.92

Table 4.31: Load comparison using structural mass from FEA with accessories and relevant components

4.10.3.3 MPT – 0.8g longitudinal acceleration and 1g vertical acceleration

In this analysis the fully loaded trailer structure should sustain a 0.8g longitudinal and 1g vertical acceleration together with the applied loads. The resulting Von-Mises stress should not exceed the yield stress of the material.

The 0.8g + 1g caseloads are tabulated below:

Force	Magnitude	Location
Gravity(vertical)	-9.81 m/s^2 (g)	Entire model
Skip loads	44.2 tons per skip	On surface areas of the skip which are in contact with the trailer
Longitudinal acceleration	7.848 m/s^2 (0.8 x g)	Entire model

Table 4.32: Vertical and longitudinal loads and values

The caseload constraints are tabulated below:

Constraint	Location
Translation X	On kingpin
Translation Y	On bottom of springs
Translation Z	On kingpin and suspension

Table 4.33: Load constraints

The analysis complied with the design criteria and the stresses were found to be below the yield stress as shown in Figures 4.54 to 4.56. Although the peak stress displayed in the stress legend is below the yield stress, it is localised to a single element [25], [38], [39], [40], [41].

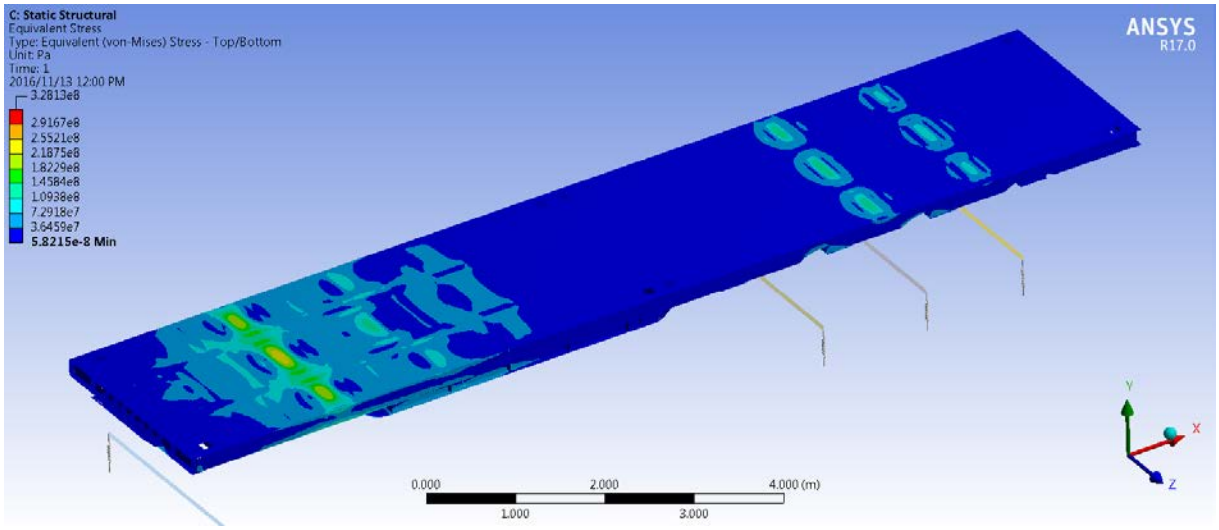

Figure 4.54: Stress plot - top view (Von-Mises)

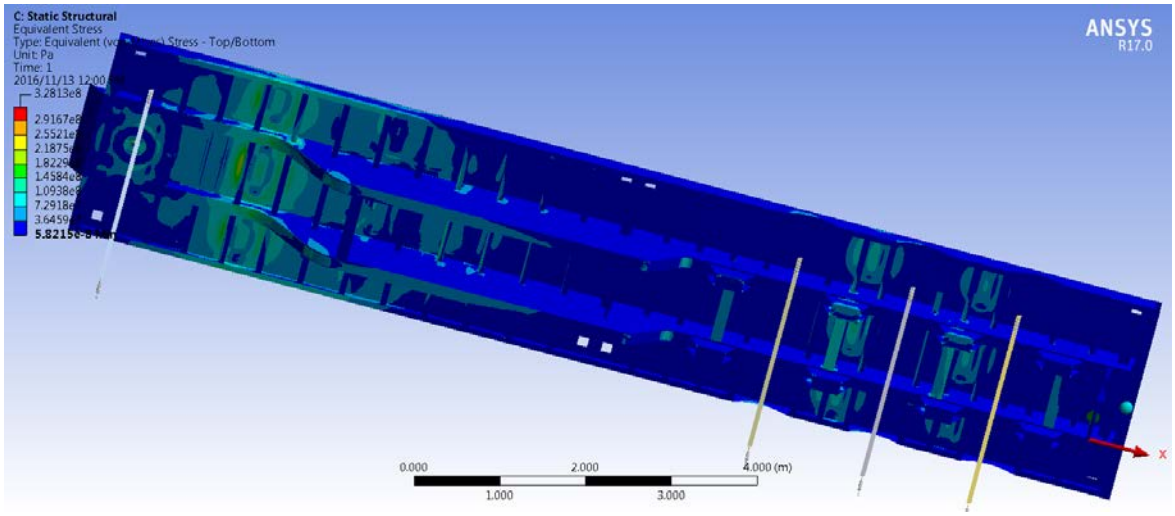

Figure 4.55: Underframe stress plot (Von-Mises)

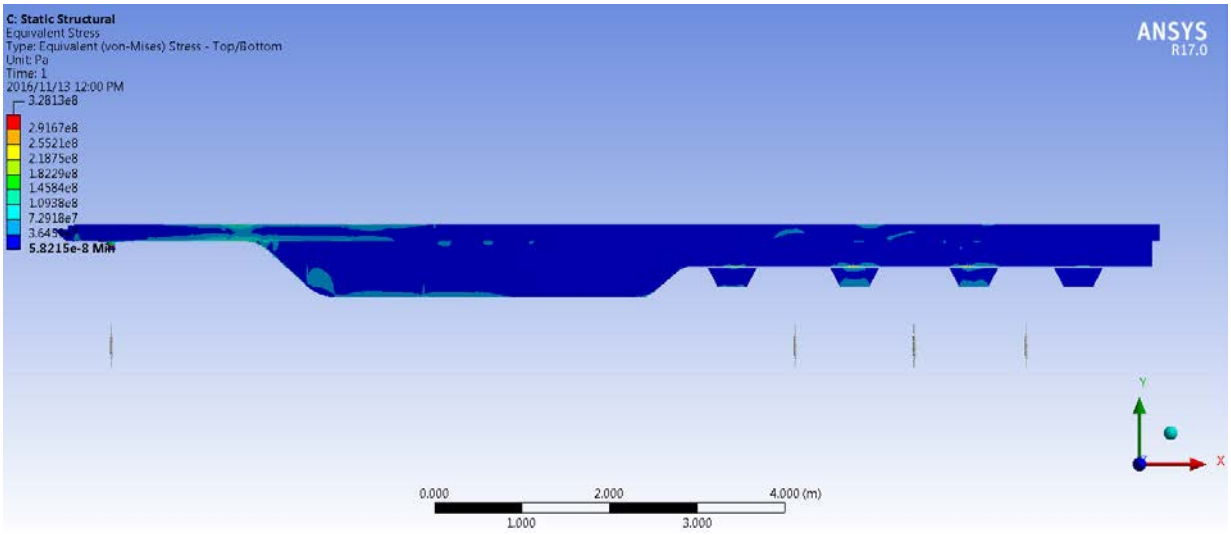

Figure 4.56: Stress plot of main centre beam (Von-Mises)

4.10.3.4 MPT – 0.25g lateral acceleration and 1g vertical acceleration

The fully loaded trailer structure must sustain a 0.25g lateral and 1g vertical acceleration together with the applied loads. The resulting Von-Mises stress should not exceed the yield stress of the material.

The 0.25g + 1g caseloads are tabulated below:

Force	Magnitude	Location
Gravity (vertical)	-9.81 m/s^2 (g)	Entire model
Skip loads	44.2 tons per skip	On surface areas of the skip which are in contact with the trailer
Lateral acceleration	2.4525 m/s^2 (0.25 x g)	Entire model

Table 4.34: Vertical and lateral loads and values

The caseload constraints are tabulated below:

Constraint	Location
Translation X	On kingpin
Translation Y	On bottom of springs
Translation Z	On kingpin and suspension

Table 4.35: Load constraints

The analysis complied with the design criteria and the stresses were found to be below the yield stress as shown in Figures 4.57 to 4.59. Although the peak stress displayed in the stress legend is below the yield stress, it is localised to a single element [25], [38], [39], [40], [41].

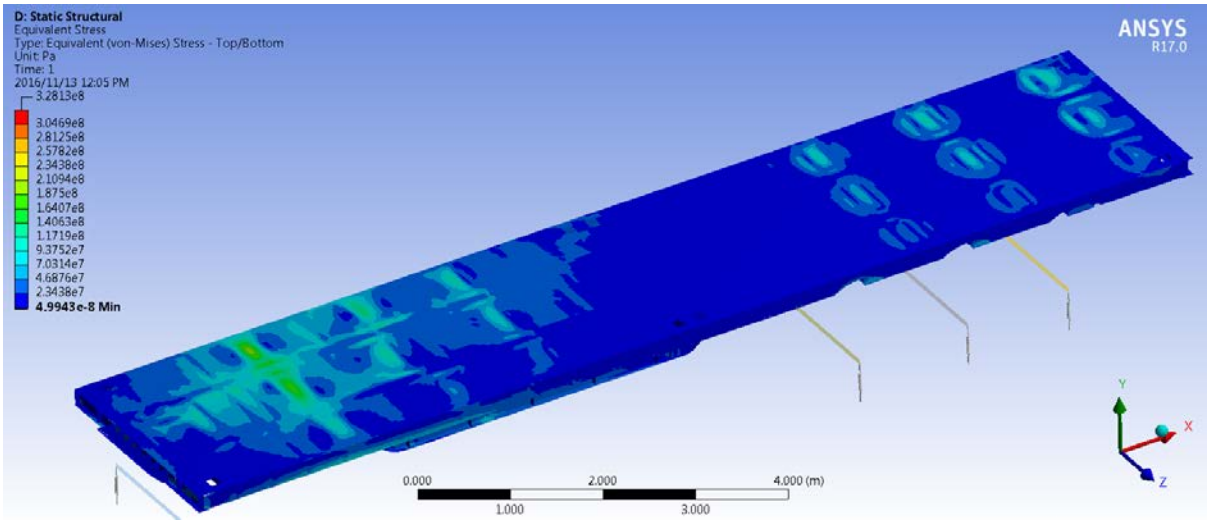

Figure 4.57: Stress plot - top view (Von-Mises)

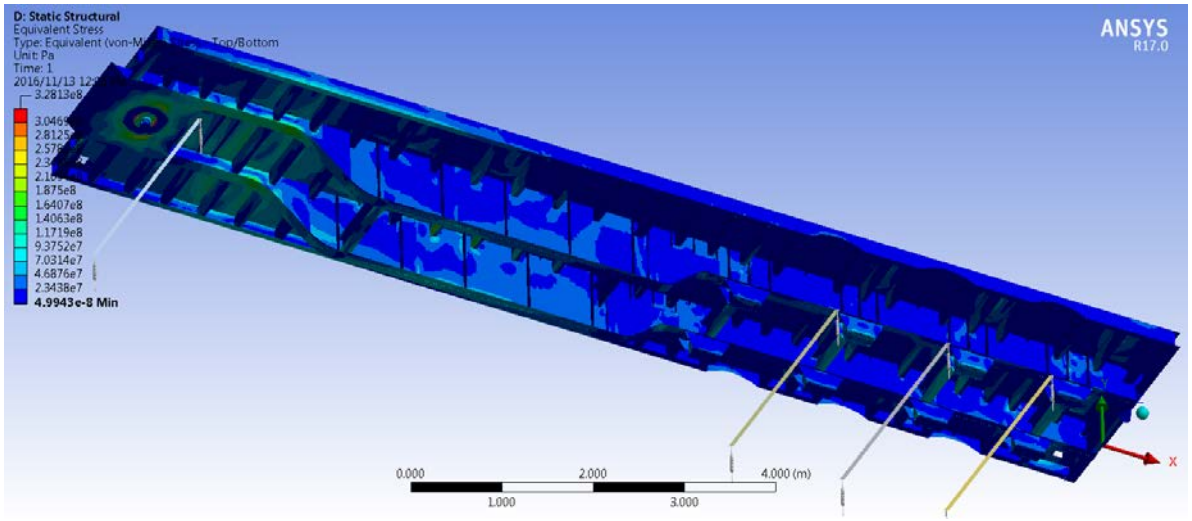

Figure 4.58: Underframe stress plot (Von-Mises)

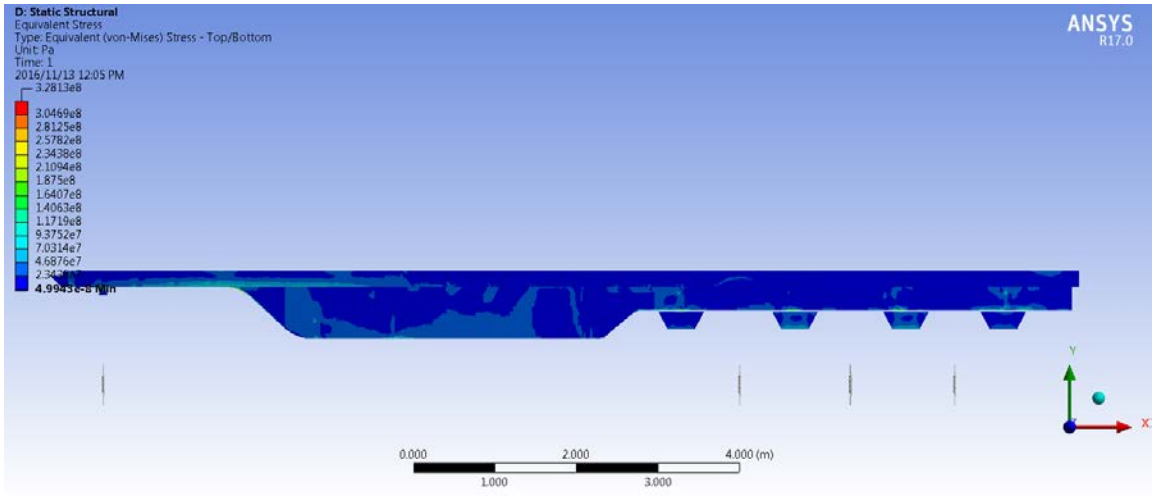

Figure 4.59: Stress plot of main centre beam (Von-Mises)

4.10.3.5 MPT – 2g vertical and 0.8g longitudinal and 0.25g lateral acceleration

The fully loaded trailer structure must sustain a 2g vertical acceleration, 0.8g longitudinal and 0.25g lateral acceleration together with the applied loads. This loading scenario allows the total combined cases to be analysed on the structure at once. The resulting Von-Mises stress should not exceed the yield stress of the material.

The 2g + 0.8g + 0.25g caseloads are tabulated below:

Force	Magnitude	Location
Gravity(vertical)	-19.62 m/s^2 (2 x g)	Entire model
Skip loads	44.2 tons per skip	On surface areas of the skip which are in contact with the trailer
Longitudinal acceleration	7.848 m/s^2 (0.8 x g)	Entire model
Lateral acceleration	2.4525 m/s^2 (0.25 x g)	Entire model

Table 4.36: Vertical, longitudinal and lateral loads and values

The load case constraints are tabulated below:

Constraint	Location
Translation X	On kingpin
Translation Y	On bottom of springs
Translation Z	On kingpin and suspension

Table 4.37: Load constraints

The analysis complied with the design criteria with a peak allowable stress of 218 MPa as shown in Figures 4.60 to 4.68. The high stress regions (Figures 4.60, 4.62, 4.63 and 4.68) are localised, and considered to be the result of modelling approximations previously explained in Chapter 4.10.3.2. In reality the hauler suspension provides support and movement to the front of the trailer which prevents excessive twisting of the underframe, yielding much lower stresses. The bogie and tyres of the trailer also provide roll to compensate for excessive lateral forces and therefore would not be fixed as in the FEA model, yielding much lower stresses.

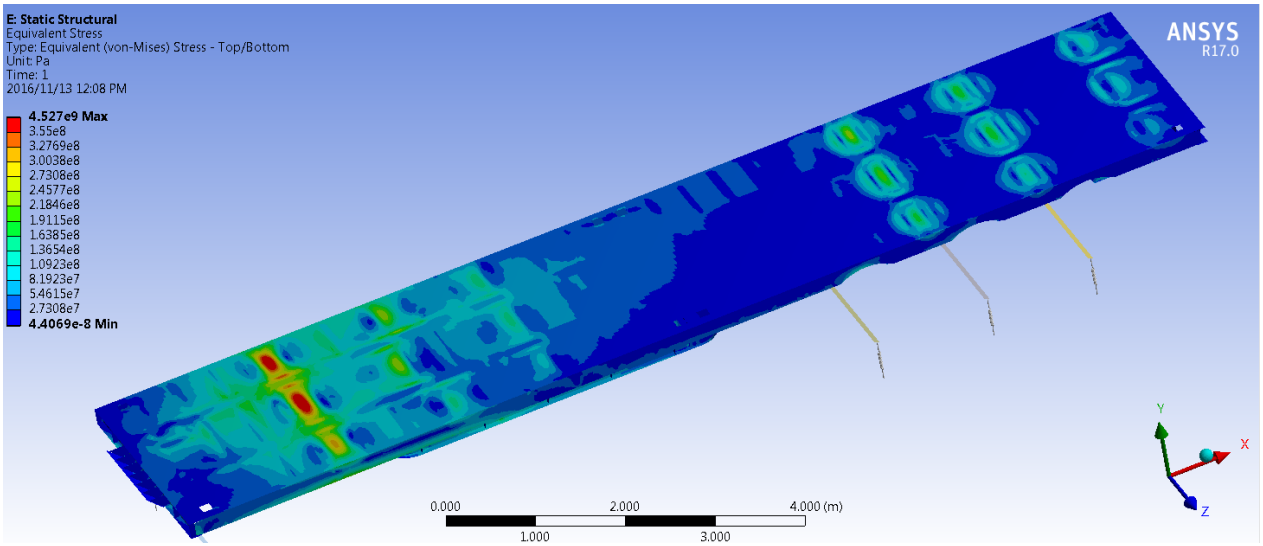

Figure 4.60: Stress plot - top view (Von-Mises)

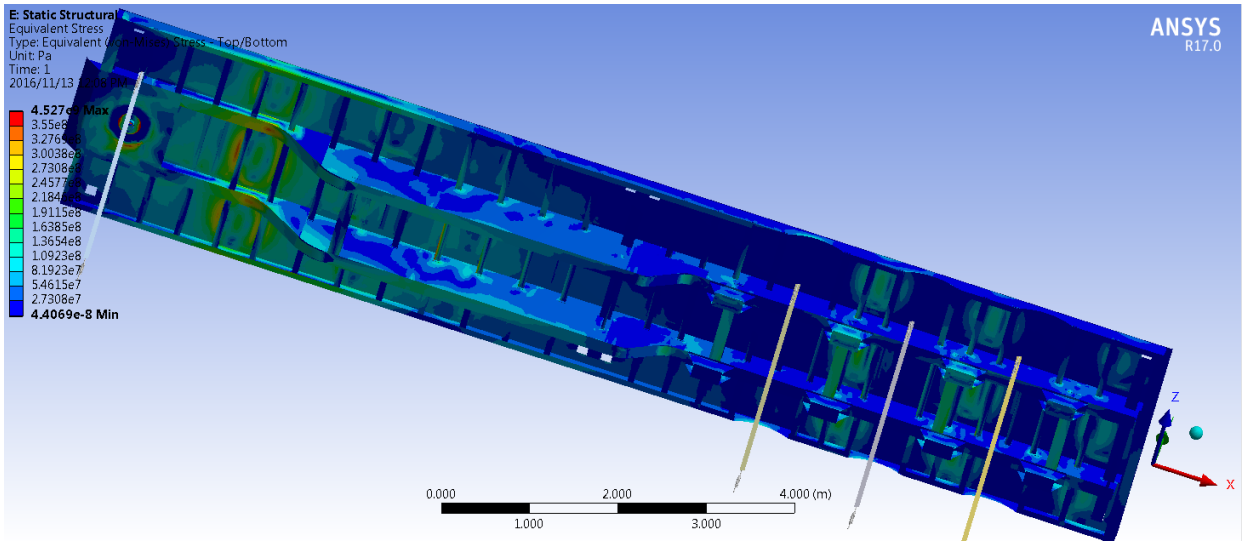

Figure 4.61: Underframe stress plot (Von-Mises)

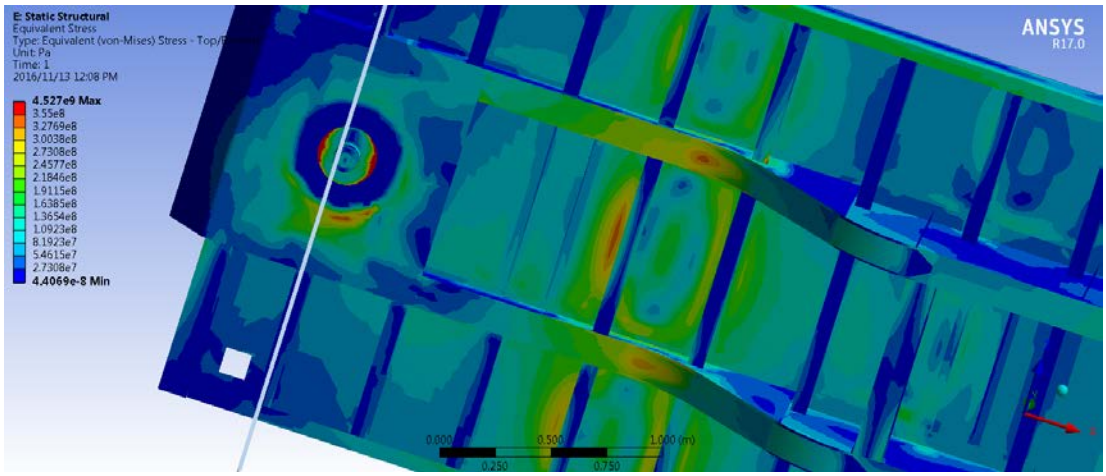

Figure 4.62: High stress region (>355 MPa) found near the kingpin

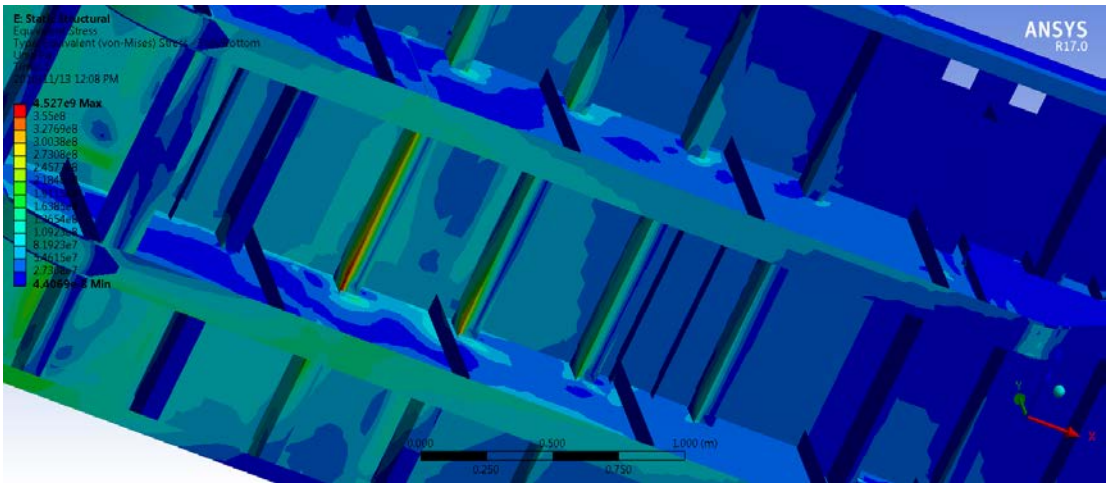

Figure 4.63: High stress region (>355 MPa) found on the structural cross member number 10 (using front structural beam as 1)

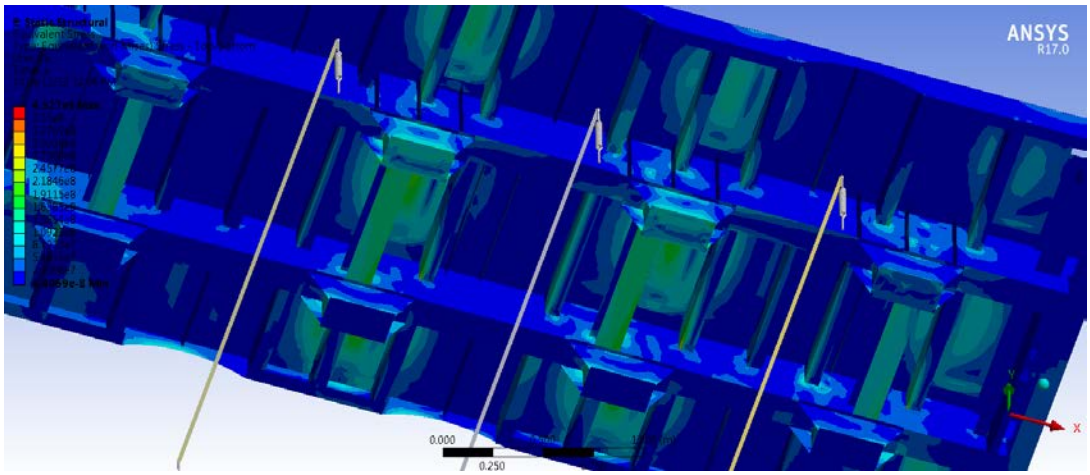

Figure 4.64: Underframe of bogie end stress plot (Von-Mises)

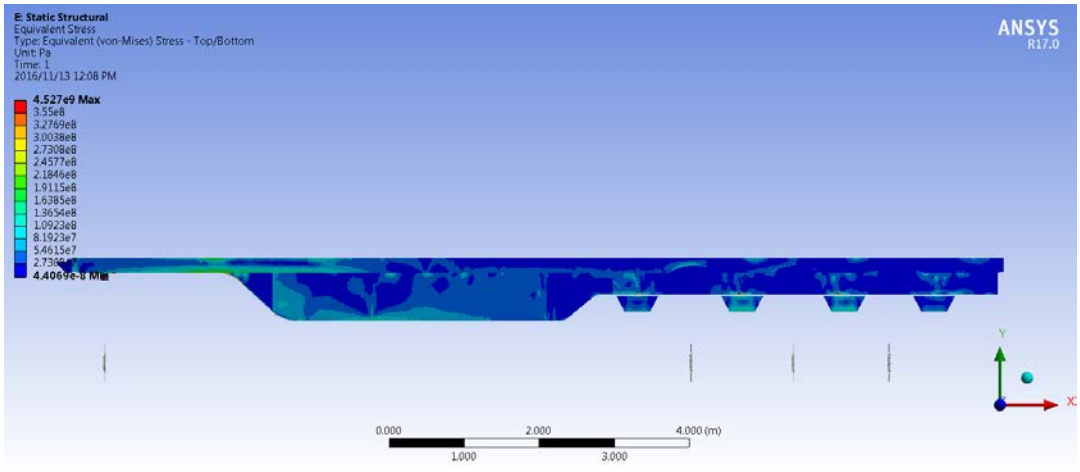

Figure 4.65: Stress plot of main centre beam (Von-Mises)

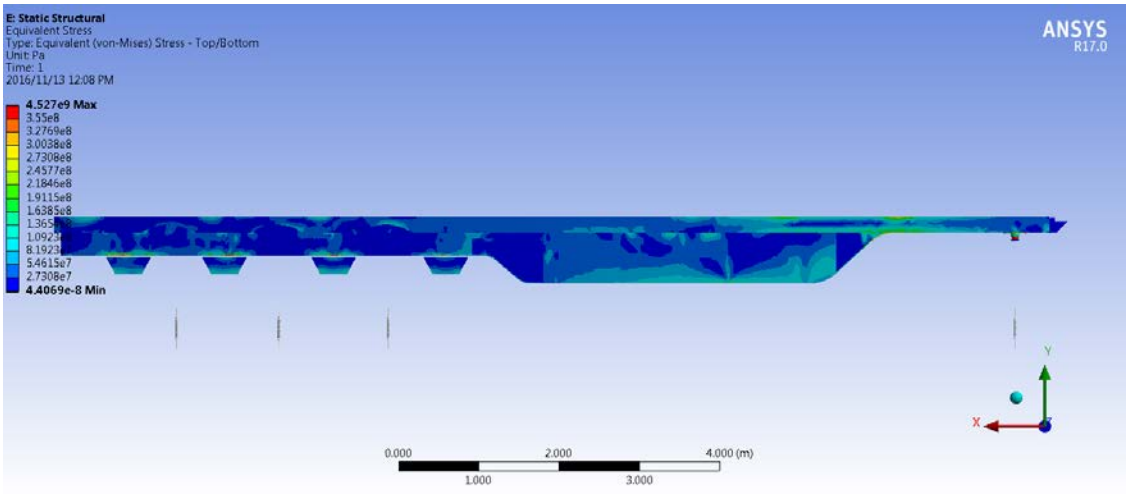

Figure 4.66: Stress plot of main centre beam (Von-Mises)

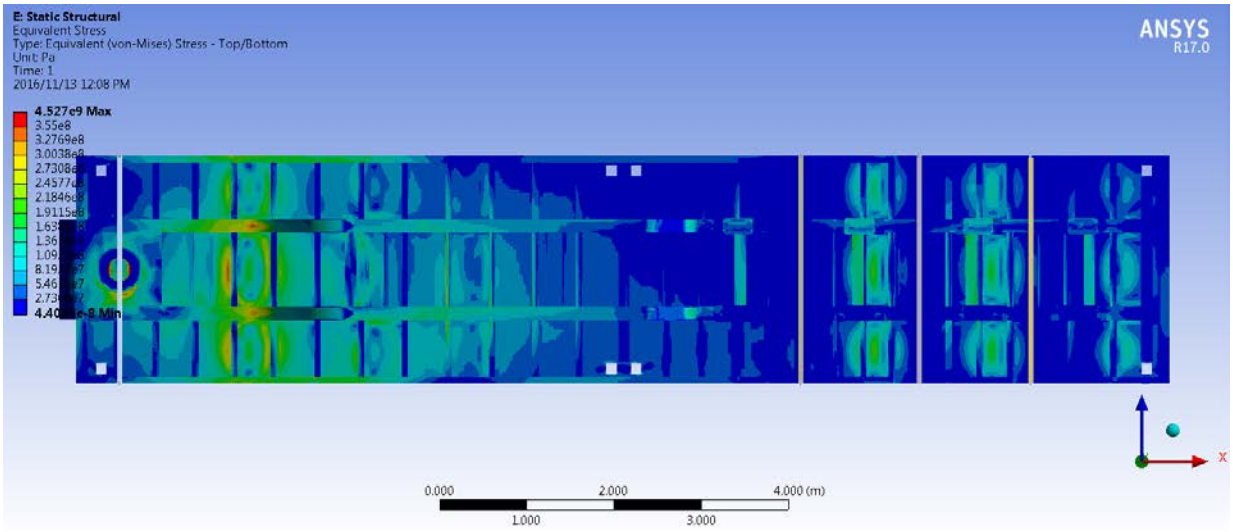

Figure 4.67: Stress plot of main centre beam bottom flange (Von-Mises)

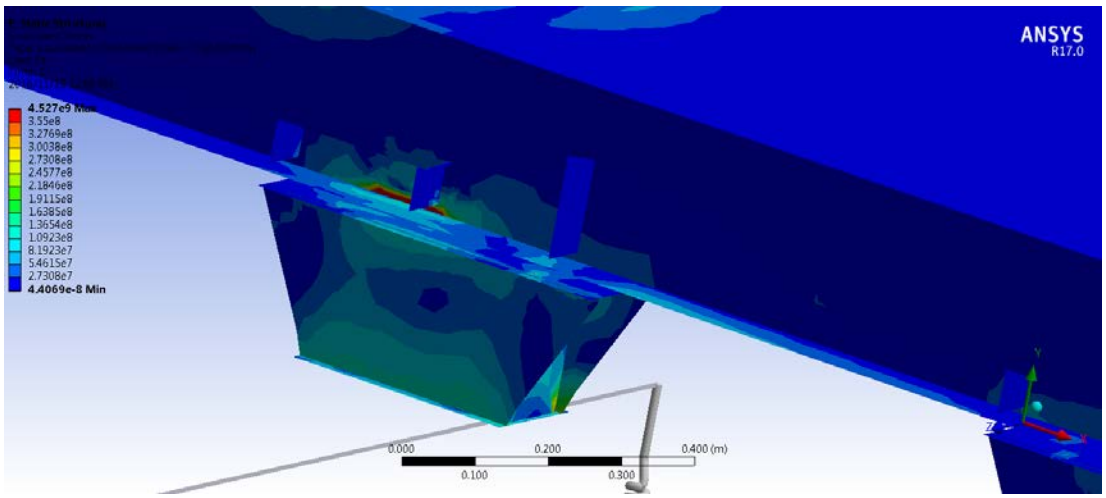

Figure 4.68: High stress region (>355 MPa) found on the connection points of the main beam to the suspension pedestals

5. Field Testing of Trailers

5.1. Introduction

Field testing of the trailers in Transnet Port conditions was performed to precisely determine the actual forces the trailers experience compared to the values in Chapter 4.10.1. This allowed a unique set of data to be obtained that could be used for simulating and designing trailers specifically for the Transnet Port environments, data not previously available. Stresses on the trailer were monitored as closely as possible to the loads in the high stress regions (kingpin, goose neck and bogie) in the FEA solutions in Chapter 4, and in other locations considered critical, to see whether the corresponding stresses are high or localised as a result of modelling properties. Using the data acquired from the field tests, allows for a set of more realistic parameters to be applied to the models, resulting in the simulation and design of a better trailer.

5.2. Test and measurement equipment

Once the FEA solutions were completed, they gave an indication of the number of parameters that required measurement, as well as their ranges. Based on this information, a specification was composed with the help of ESTEQ Test and Measurement to supply a data acquisition system for the project.

5.2.1 Data acquisition hardware specification

The system consisted entirely of HBM QuantumX equipment. This test and measurement equipment is robust and highly efficient for setup purposes while providing accuracy and reliability in the measurement of data. The product is used for testing heavy duty vehicles and has a proven track record in industrial environments. The system for the field testing consisted of the components shown in Table 5.1.

Component Name	Component Description	Component Purpose
HBM QuantumX CX22W	Portable data recorder that collects, evaluates, and saves captured measurement data directly	This is needed for the nature of the hauler and trailers actual operation in the port
HBM QuantumX MX1601	16 channel universal amplifier for standard signals	This amplifier is required for the accelerometers that were placed on the various points of the trailer
HBM QuantumX MX1615B	16 channel strain gauge bridge amplifier for stress analysis; enabling connection for sensors or strain gauges in full, half, or quarter-bridge configurations	This amplifier is used for various strain gauges on the trailer where critical high stress regions are noted from the FEA

Table 5.1: HBM hardware overview

The above three components form the core of the system and were custom built into a robust case with a direct current (DC) power supply of 24V (which is the operational voltage of the components), courtesy of two 12V batteries in series. This DC supply however, is insufficient for the entire operation of the system, but acts as a "buffer'' between the components, when the vehicle starts or shuts down in case power is momentarily lost. The primary source of power was 24V DC supplied by the hauler batteries.

5.2.2 Data acquisition sensors specification

The sensors required for the trailer data measurement were classified into three main categories: acceleration (g), strain, and speed. Stress and acceleration assisted in validating FEA results and the speed assisted in validating the g values used in Chapter 4.10 for the FEA simulations. Table 5.2 provides an overview.

The accelerometers and GPS sensor were easily chosen as standard equipment for use with HBM QuantumX components. The strain gauges were a combination of linear and rosette gauges because of the application requirements and the amplifier channels available. The main difference between the gauges is that a linear gauge measures micro-strain in one direction and requires other properties of the steel in order to compute a stress using a function/computational channel which has to be created using the application software. While a rosette gauge measures micro-strain in three different angularly spaced measuring grids and can compute principal stress automatically by pre-entering

relevant gauge information and steel properties. The limiting factor of the rosettes is that three channels are required per rosette (one per grid) and an amplifier has only sixteen channels, which would limit the number of measuring points compared to a linear gauge using a single channel. To resolve this both types of gauges were purchased and depending on the structural member being measured, expected stresses and inspection of the FEA models, a suitable gauge choice was made.

Component Name	Component Description	Component Purpose
HBM Strain Gauges (K-LY4 and K-RY8) with connection cable	Linear strain gauges and 3-measuring grid rosettes with connecting cables (no soldering required)	The strain gauges were connected at the critical stress points along the trailer's structural members; kingpin, goose neck and the bogie
Dytran 7523A3 accelerometer	Triaxial DC accelerometer, 15g range and 93 mV/g sensitivity	The accelerometers are required to take the acceleration readings in the X, Y and Z directions
GARMIN GPS 18x 5Hz	High-sensitivity, 12-parallel-channel, magnetic base for easy mounting, RS 232 and USB interfaces	The GPS module was required to track the speed of the trailer in operation as well as to capture route information

Table 5.2: Sensors overview

Clamps and connectors were used and insulated throughout and consequently kept the system robust and secure for field testing conditions.

Figure 5.1: HBM QuantumX data acquisition hardware custom built into Pelican Hard case

5.2.3 Data acquisition and interpretation software

The software used with the HBM QuantumX was the recommended Catman AP and Easy. The software has a user friendly interface and allows for quick on-site set-up, reliable acquisition, visualisation, and post analysis. For post analysis of the data nCode Glyphworks, software was also used. The preloaded database has instant and assignable sensor identification, custom visualisation, and start/stop tools for data excitation and acquisition. The built-in mathematical and analysis functions helped to convert the micro-strain measured from the strain gauges into stress using the steel properties. Data is always auto-saved when using the software, so if a hardware component fails whilst active, the data is saved without user interaction until the system is powered on again. The entire system was procured and training was done with ESTEQ for various aspects such as strain gauge fitment, hardware troubleshooting, and software features.

5.3. Testing of the BTT

5.3.1 Preparation of the trailer and test

To initiate the testing, arrangements had to be made with TPT's Durban Pier 2 maintenance workshop's staff by briefing them on the project and the requirements. Trailer T72 and hauler H143 were made available for the test.

First the sensors had to be installed, so the trailer paint was stripped and cleaned at various points for strain gauge fitment. Esteq Test and Measurement provided knowledge for the placement of the strain gauge type at the various points on the trailer. The strain gauges and accelerometers were fitted at the locations described in Table 5.3 and shown in Figures 5.2 to 5.5.

Location on Trailer	Sensor
Kingpin (Kp)	Rosette strain gauge and accelerometer
Goose neck on each side beam	Rosette strain gauge at either alternate bend
Centre of mass (COM) of trailer	Accelerometer
Bogie	Linear strain gauges on web and flange for each axle end. Accelerometer

Table 5.3: Sensor allocation to critical areas of the trailer

Figure 5.2: Rosette gauge installed at top of kingpin support

Figure 5.3: Rosette gauges installed on the goose neck at the bend points on the main side beams

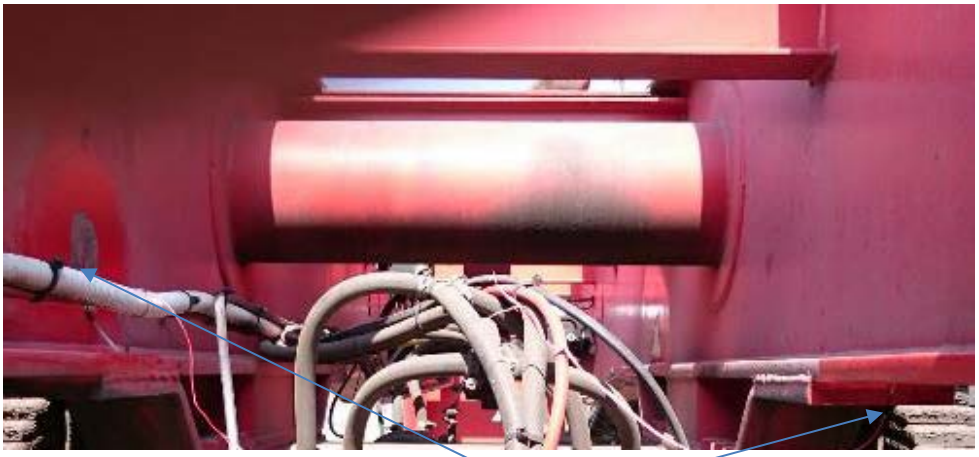

Figure 5.4: Linear gauges mounted on the web and flange of the front and rear axle

The accelerometers were also mounted at the kingpin, centre of mass and bogie, and all cabling harnesses were trunked through the trailer and then checked as shown in Figure 5.5.

Figure 5.5: All circuits checked before setup onto hauler

Once the trailer was ready, it was necessary to arrange a hauler with a well experienced driver and assistant as well as implement a cargo operation in the port to move two fully laden 20 foot shipping containers. Once this was arranged, the QuantumX equipment was installed in the hauler and the test was initiated in the operational environment (Figure 5.6).

Figure 5.6: The hauler and trailer loaded and ready for testing

5.3.2 Field test conditions

The data acquisition was initiated from the instant the trailer was coupled and in motion, to capture the relevant acceleration, speed, micro-strain and stress measurements since an un-laden trailer may react more dynamically to road conditions. Durban Pier 2 road conditions are not ideal; lack of maintenance has resulted in severely uneven road surfaces. These surfaces mainly occur to and from the fuelling station and the workshops. In the area of cargo operations the road surfaces are even and well maintained, this is beneficial for loaded trailers.

All scenarios were of interest, as there was a possibility that the un-laden trailer might yield significant data depending on the speed travelled and the extent of dynamic movement on the worst road surfaces, as compared to it being laden on a more ideal road surfaces; there is little background knowledge in this regard for truck trailers. When the hauler and trailer were ready to leave the workshop, the activity routes in Table 5.4 were followed.

Route	Description of Route
1	Workshop to cargo operations (un-laden)
2	Cargo operations to loading area of trailer (un-laden)
3	Loading area at cargo operations to fuelling station (fully laden)
4	Fuelling station to operational routes (fully laden) and off-loading at cargo operations and return trip to workshop (un-laden)

Table 5.4: Route overview at Durban Pier 2

Routes 1, 2 and 4 are essentially the same; it was only at cargo operations that the driver noted low fuel of the hauler. Multiple repeat routes in operations were needed for more data acquisition hence refuelling was necessary. Generally vehicles are fuelled before going into cargo operations and operational routes.

On operational routes were the trailer was laden, sectors were driven repeatedly on with more severe turning, acceleration and emergency braking to try and attain all possible outcomes that might occur.

5.3.3 Field test data

5.3.3.1 Acceleration test data

The acceleration was first analysed. The sample rate used was 150Hz. Tables 5.5 to 5.8 provide an overview of the data collected for each of the routes. The data was filtered to omit periods when the vehicle was stationary and idling with no effective readings. This was done to provide more effective spectrum of results, and to provide a more accurate minimum (min), maximum (max), mean, standard deviation (STD) and quartile values to aid collective accuracy. At no point did the hauler and trailer exceed the 30 km/hr limit, this was verified using the GPS speed results. X, Y and Z denote accelerations experienced in the lateral, longitudinal and vertical directions respectively.

Route 1	g Values								
Name	**Kp x**	**Kp y**	**Kp z**	**COM x**	**COM y**	**COM z**	**Bogie x**	**Bogie y**	**Bogie z**
Samples	*43939*	*43939*	*43939*	*44051*	*44051*	*44051*	*44253*	*44253*	*44523*
Min	-0.180	-0.417	-0.620	-0.196	-0.319	-0.433	-0.8973	-0.897	-0.670
Max	0.222	0.421	0.714	0.233	0.536	0.594	0.8385	0.839	0.806
Mean	0.004	0.009	-0.002	0.009	0.010	-0.007	0.0121	-0.002	-0.004
STD	0.029	0.052	0.042	0.030	0.053	0.060	0.065	0.037	0.093
Lower quartile	0.012	0.015	0.018	0.006	0.008	0.025	0.011	0.019	0.027
Inter quartile	0.030	0.049	0.032	0.029	0.038	0.034	0.047	0.035	0.043
Upper quartile	0.019	0.033	0.014	0.023	0.030	0.009	0.036	0.016	0.016

Table 5.5: Acceleration values from the workshop to cargo operations

Route 2	g Values								
Name	**Kp x**	**Kp y**	**Kp z**	**COM x**	**COM y**	**COM z**	**Bogie x**	**Bogie y**	**Bogie z**
Samples	*40242*	*40242*	*40242*	*40378*	*40378*	*40378*	*38306*	*38306*	*38306*
Min	-0.327	-0.481	-0.829	-0.316	-0.584	-1.026	-0.838	-0.519	-1.454
Max	0.375	0.748	0.998	0.542	0.806	1.609	0.926	0.563	2.960
Mean	0.014	0.033	-0.011	0.036	0.043	-0.034	0.036	0.023	-0.018
STD	0.040	0.072	0.101	0.042	0.084	0.014	0.092	0.057	0.225
Lower quartile	0.009	0.006	0.050	0.013	-0.0005	-0.089	-0.011	-0.007	-0.104
Inter quartile	0.046	0.076	0.077	0.047	0.083	0.108	0.09	0.059	0.166
Upper quartile	0.037	0.071	0.027	0.059	0.082	0.019	0.081	0.052	0.062

Table 5.6: Acceleration values from cargo operations to loading area of trailer

Route 3	g Values								
Name	**Kp x**	**Kp y**	**Kp z**	**COM x**	**COM y**	**COM z**	**Bogie x**	**Bogie y**	**Bogie z**
Samples	*72780*	*72780*	*72780*	*71984*	*71984*	*71984*	*70429*	*70429*	*70429*
Min	-0.136	-0.172	-0.235	-0.131	-0.197	-0.484	-0.162	-0.204	-0.351
Max	0.199	0.278	0.202	0.197	0.258	0.394	0.191	0.230	0.313
Mean	0.033	0.055	-0.021	0.046	0.070	-0.051	0.049	0.050	-0.032
STD	0.032	0.034	0.074	0.031	0.030	0.053	0.045	0.041	0.058
Lower quartile	0.013	0.036	-0.048	0.027	0.054	-0.071	0.027	0.026	-0.054
Inter quartile	0.041	0.037	0.054	0.041	0.034	0.038	0.045	0.048	0.043
Upper quartile	0.054	0.073	0.006	0.067	0.087	-0.032	0.072	0.074	-0.012

Table 5.7: Acceleration values from loading area at cargo operations to fuelling station

Route 4	g Values								
Name	**Kp x**	**Kp y**	**Kp z**	**COM x**	**COM y**	**COM z**	**Bogie x**	**Bogie y**	**Bogie z**
Samples	*158152*	*158152*	*158152*	*157676*	*157676*	*157676*	*156486*	*156486*	*156486*
Min	-0.278	-0.324	-0.743	-0.297	-0.403	-0.499	-0.256	-0.661	-0.785
Max	0.259	0.452	0.930	0.266	0.424	1.078	0.302	0.925	0.767
Mean	0.038	0.070	-0.025	-0.007	-0.012	-0.011	0.060	0.065	-0.041
STD	0.044	0.043	0.112	0.041	0.034	0.074	0.071	0.061	0.090
Lower quartile	0.016	0.049	-0.067	-0.026	-0.030	-0.036	0.031	0.032	-0.074
Inter quartile	0.047	0.042	0.082	0.041	0.036	0.050	0.057	0.061	0.065
Upper quartile	0.064	0.092	0.015	0.015	0.006	0.014	0.088	0.093	-0.010

Table 5.8: Acceleration values from fuelling station to operational routes and offloading at cargo operations and return trip to workshop

The data in Tables 5.5 to 5.8 was arranged in a manner to enable easy assessment of the results and compare the various values at the three positions measured on the trailer. It was expected that the acceleration values of the kingpin and bogie would have greater emphasis on the extremities since the end points of the trailer are more responsive due to the dynamics involved. The centre of mass

provides an amalgamation of the other results, particularly when evaluating the mean values. When the results were compared certain extremities in the data were noted to be of concern, for example in Route 2 (Figure 5.7) Bogie z had a maximum reading of 2.96g (Figure 5.8). These peaks which lasted approximately 0.02 seconds are considered to be due to the bouncing of the un-laden trailer.

In Table 5.6, Bogie z experienced a peak of 2.96g, COM z experienced a peak of 1.609g, and Kp z a peak of 0.998g. The relative level of these accelerations validate translation of the load through the trailer, as the acceleration from the bogie is conveyed through the centre of mass which then causes the kingpin to react as it is the only pivot point to the fifth wheel. The timing of the different peak readings also validate this in the correct sequential order as shown in Figure 5.8.

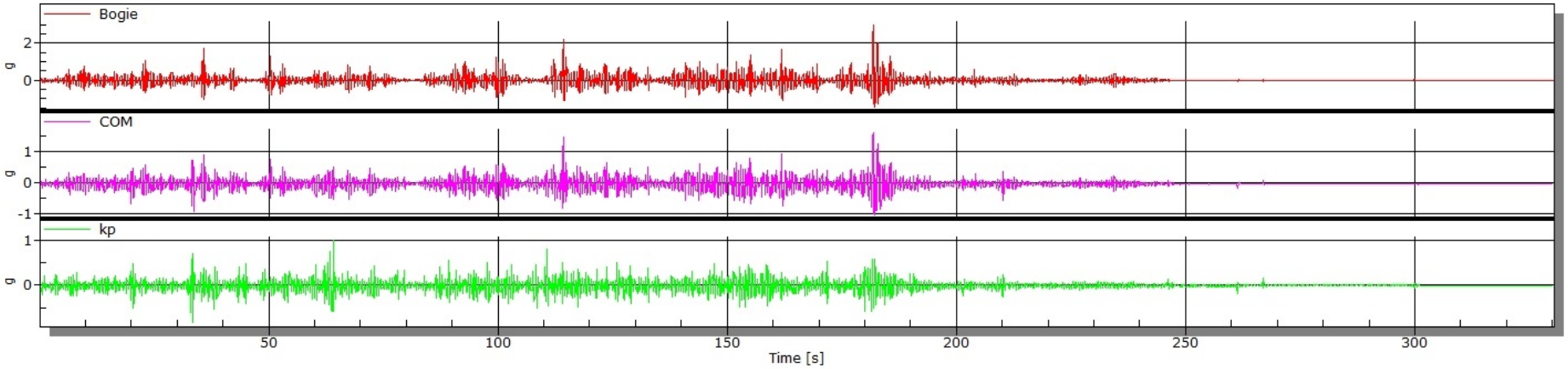

Figure 5.7: Z direction acceleration (g) values for Route 2 (Unfiltered). Data after approximately 250s were omitted in the tabulated results of Route 2.

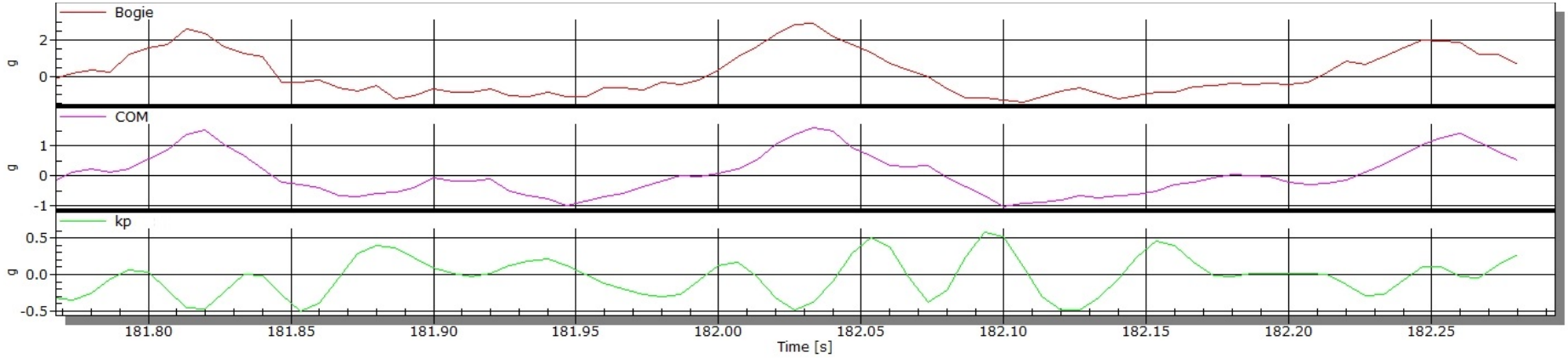

Figure 5.8: Z direction acceleration (g) maximum values for Route 2

On Route 3 where the shipping containers were loaded onto the trailer (Figures 5.9, 5.10, 5.11 and 5.12), the g values were significantly lower compared to the un-laden Route 2 road surface dynamic loads. In watching the loading of the containers from the straddle carrier, it might be thought that the greatest vertical acceleration experienced by the trailer would likely be during the loading, however data showed that the dynamic conditions induced equal or larger accelerations. However the trailer was un-laden when the acceleration peaks occurred which is favourable for the structure as the trailer will then only be reacting to its own mass under these large g forces thus not resulting in large absolute loads.

Figure 5.9: Loading of second container at rear of the BTT

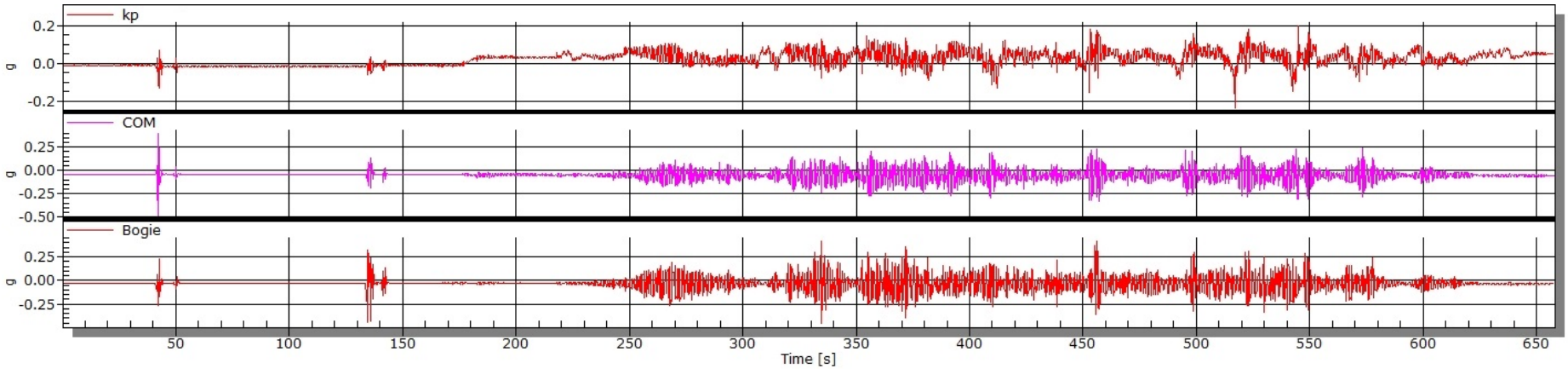

Figure 5.10: Z direction acceleration (g) test data for Route 3 (Unfiltered; to show loading spikes whilst stationary)

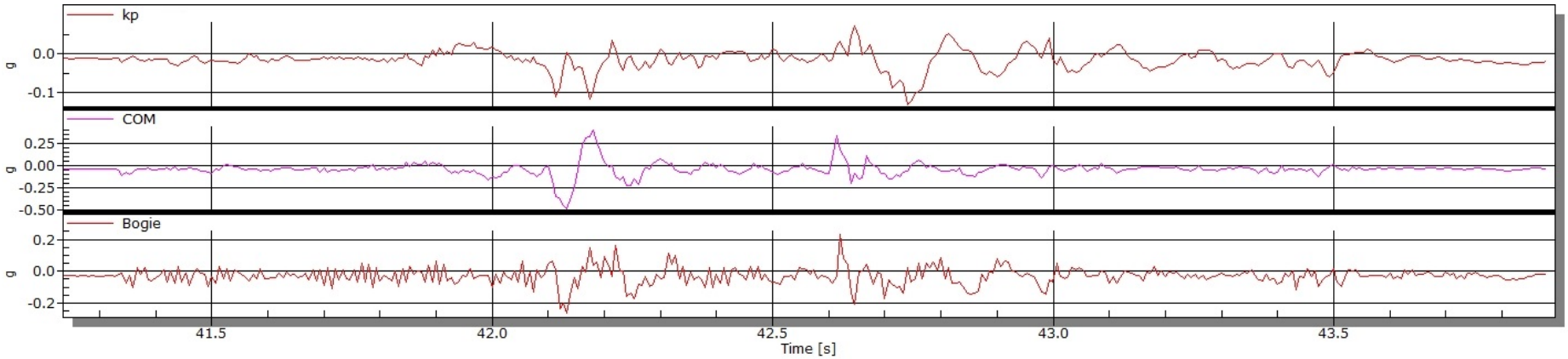

Figure 5.11: Z direction acceleration (g) test data for loading of first container at front of the trailer

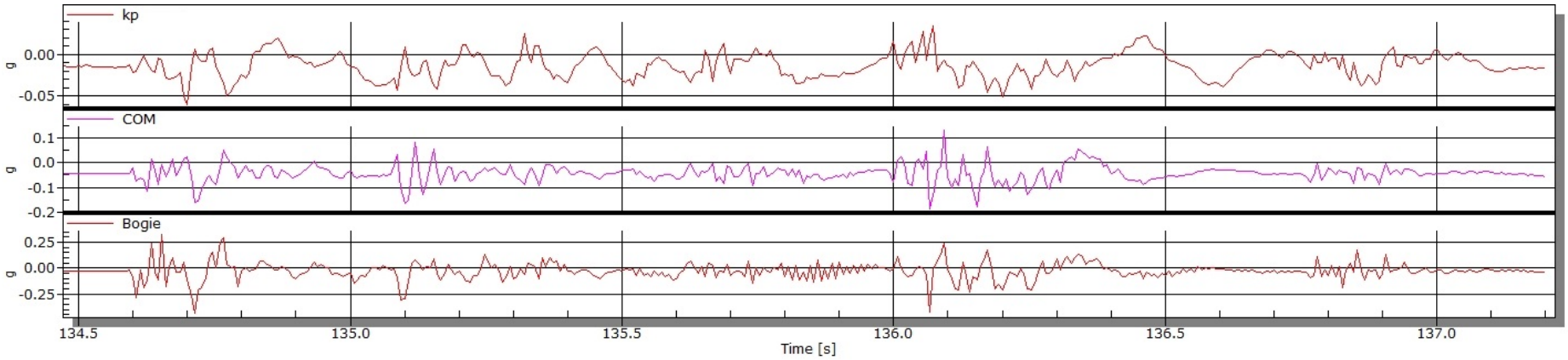

Figure 5.12: Z direction acceleration (g) test data for loading of second container at rear of the trailer

Route 4 acceleration results of the laden trailer is seen in Figure 5.13. The trailer was then off loaded at approxiamately 500 seconds and then returned to the workshop. Peak accelerations are illustrated in Figure 5.14. These values are one part of the results used to determine the new set of acceleration loading results for the FEA model as shown in Chapter 5.3.4.

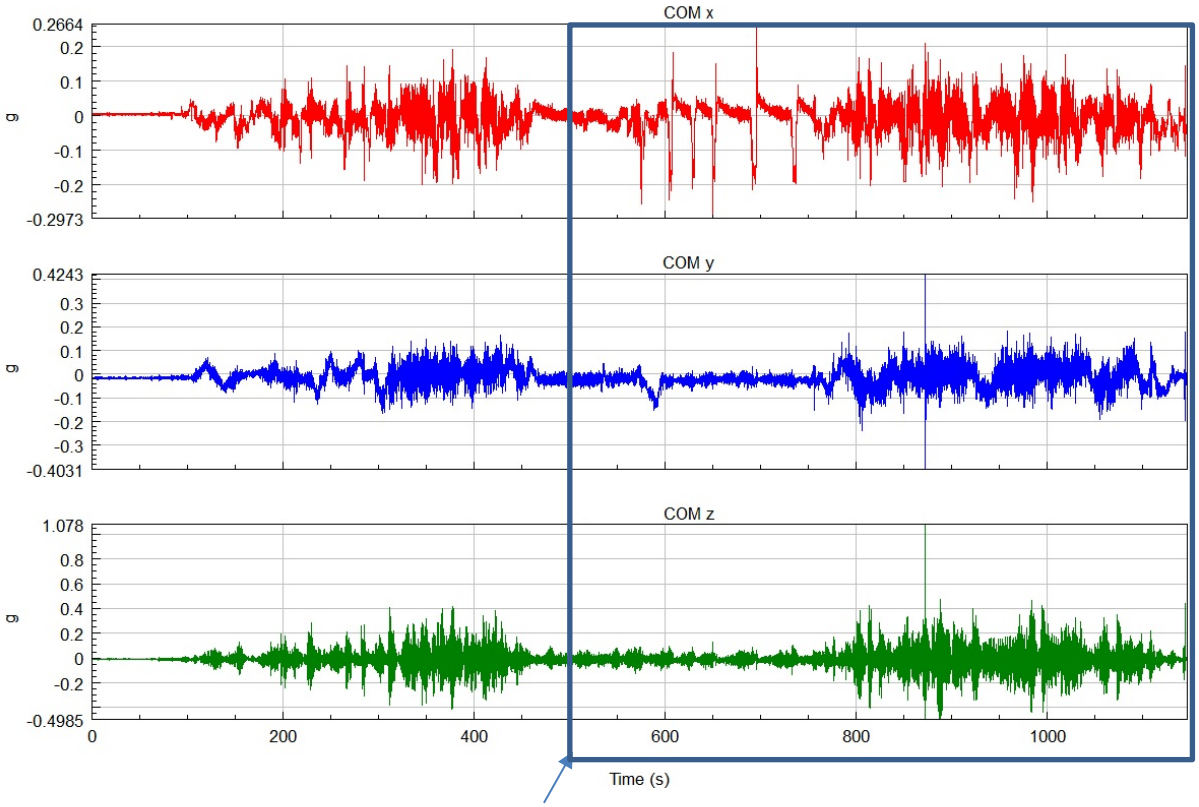

Figure 5.13: Filtered (laden and un-laden) COM acceleration values (g) for Route 4

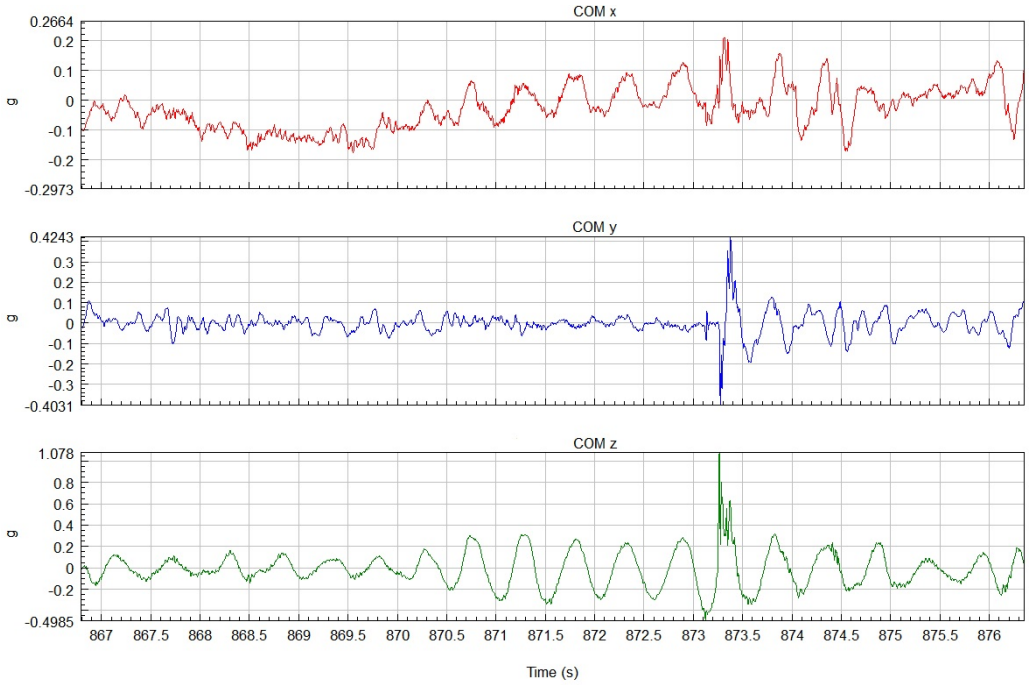

Figure 5.14: Route 4 COM maximum acceleration values (un-laden)

5.3.3.2 Strain gauge test data

The strain gauges were placed along the length of the trailer as shown in Table 5.9, where the data could be captured and compared to that obtained from the FEA.

Structural member on Trailer	Gauge type and location
Kingpin	Rosette strain gauge and accelerometer
Goose Neck 1	Rosette strain gauge at goose neck bend closest to kingpin
Goose Neck 2	Rosette strain gauge at goose neck bend closest to landing legs
Bogie Rear 1 and Rear 2	Linear strain gauge on flange and web respectively for rear axle
Bogie Front 1 and Front 2	Linear strain gauge on web and flange respectively for front axle

Table 5.9: BTT strain gauge placements

Route 1	**Stress in MPa**						
Name	**Bogie Rear 1**	**Bogie Rear 2**	**Bogie Front 1**	**Bogie Front 2**	**Kingpin**	**Goose Neck 1**	**Goose Neck 2**
Samples	*69811*	*69811*	*69811*	*69811*	*69811*	*69811*	*69811*
Min	-24.06	-21.06	-15.42	-17.42	0.18	0.07	0.02
Max	150.48	9.67	6.72	15.03	44.43	19.23	16.3
Mean	21.20	-8.35	-3.88	2.68	29.60	3.55	3.14
STD	12.68	6.21	3.85	3.17	11.80	2.70	2.74
Lower quartile	15.33	-13.72	-6.14	0.67	30.14	2.20	1.45
Inter quartile	9.12	10.83	4.59	3.97	6.60	2.18	2.44
Upper quartile	24.45	-2.89	-1.55	4.64	36.74	4.34	3.89

Table 5.10: Stress values from the workshop to cargo operations

Route 2	Stress in MPa						
Name	**Bogie Rear 1**	**Bogie Rear 2**	**Bogie Front 1**	**Bogie Front 2**	**Kingpin**	**Goose Neck 1**	**Goose Neck 2**
Samples	*49567*	*49567*	*49567*	*49567*	*49440*	*49567*	*49567*
Min	-89.67	-20.10	-13.42	-35.82	0.44	0.08	0.31
Max	148.79	8.95	11.59	16.83	166.26	23.06	22.85
Mean	-56.78	6.99	-0.23	-9.20	20.25	5.93	5.50
STD	22.73	3.69	4.14	4.61	8.78	4.88	3.07
Lower quartile	-71.57	-8.84	-3.78	-11.64	14.19	1.88	3.47
Inter quartile	19.88	4.50	6.66	5.11	12.41	6.98	3.63
Upper quartile	-51.69	-4.34	2.88	-6.53	26.60	8.86	7.10

Table 5.11: Stress values from cargo operations to loading area of trailer

Route 3	Stress in MPa						
Name	**Bogie Rear 1**	**Bogie Rear 2**	**Bogie Front 1**	**Bogie Front 2**	**Kingpin**	**Goose Neck 1**	**Goose Neck 2**
Samples	*98781*	*98781*	*98781*	*98781*	*95528*	*98781*	*98781*
Min	-48.04	-8.95	-24.59	-39.06	4.56	-8.61	1.257
Max	52.39	32.31	6.47	6.13	75.96	94.01	128.47
Mean	-17.38	2.36	-11.83	15.75	48.31	47.86	47.56
STD	12.40	4.13	5.89	4.75	12.57	21.50	16.56
Lower quartile	-27.41	0.19	-17.08	19.92	39.09	49.27	34.65
Inter quartile	23.50	4.22	10.22	11.41	19.95	27.80	35.52
Upper quartile	-3.91	4.41	-6.86	6.33	59.05	60.41	71.24

Table 5.12: Stress values from loading area at cargo operations to fuelling station

Route 4	Stress in MPa						
Name	**Bogie Rear 1**	**Bogie Rear 2**	**Bogie Front 1**	**Bogie Front 2**	**Kingpin**	**Goose Neck 1**	**Goose Neck 2**
Samples	*171994*	*171994*	*171994*	*171994*	*172017*	*171316*	*171316*
Min	-19.20	-11.58	-6.64	-26.38	25.1	-37.83	-77.17
Max	187.90	33.88	45.09	49.94	81.05	98.06	59.06
Mean	16.08	3.66	22.36	21.37	56.96	19.35	10.35
STD	10.79	4.61	8.50	9.75	9.539	10.47	10.38
Lower quartile	8.82	1.00	17.73	15.36	49.50	35.52	3.52
Inter quartile	12.59	4.28	10.06	11.27	14.61	10.08	10.09
Upper quartile	21.41	5.28	27.80	26.63	64.12	48.59	6.58

Table 5.13: Stress values from fuelling station to operational routes and offloading at cargo operations and return trip to workshop

The stress data was compiled in Tables 5.10 to 5.13 in a similar manner to the acceleration data. Certain tabulated values were extremely high (as shown in Figure 5.15) and beyond the possible stress range because strain gauge channels occasionally experienced sudden disturbances or noise. Electrostatic and magnetic noise from reciprocating or rotating machines, electric motors, starters, generators, relays and transformers of the hauler systems and the straddle carrier, were all origins of the noise experienced at the kingpin and goose neck areas, this is a known problem [56].

The tabulated data which was extremely high and beyond the possible stress range was thus filtered which caused the total range to be narrowed, however the filtered data still contained stress values exposed to noise and disturbances which are within an acceptable stress range but higher than what would be experienced in ideal conditions. The data captured for the kingpin over a period of five minutes is shown in Figure 5.15. The peak disturbances were extreme and considered illegitimate [56], and were therefore filtered out after consulting with Esteq Test and Measurement. These disturbances were mostly recorded by the strain gauges exposed at the front of the trailer nearest to the hauler and its electrical sub-systems.

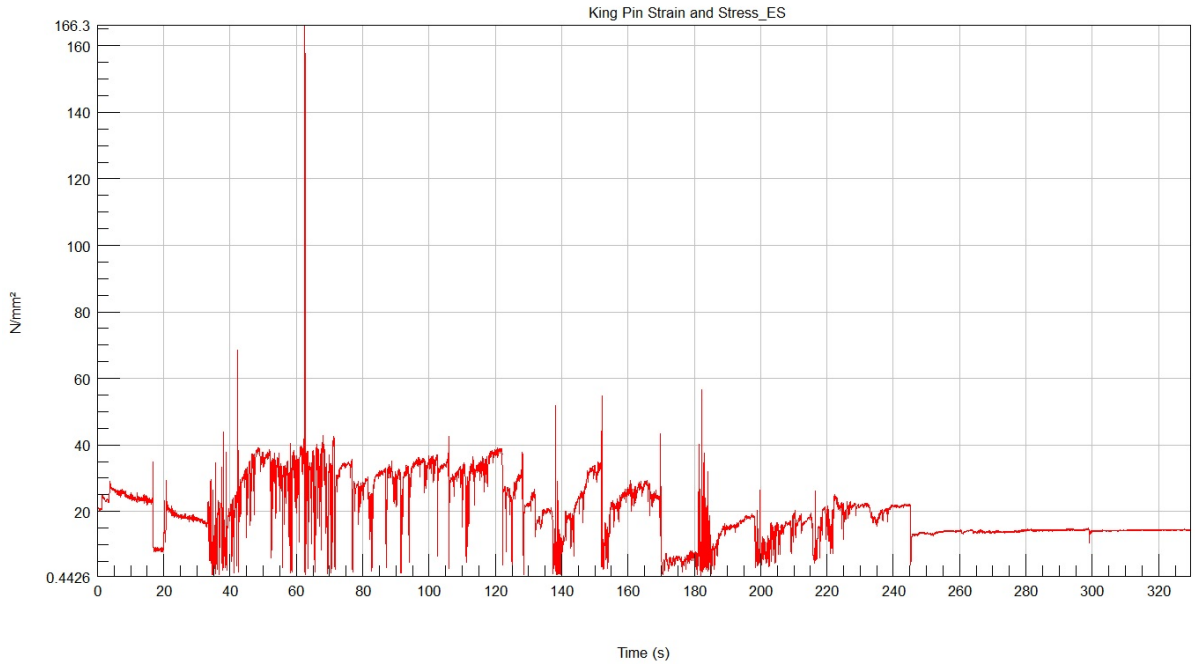

Figure 5.15: Kingpin data for Route 2

The Goose Neck 2 channel also experienced similar noise, but this happened at the end of the data acquisition period when other vehicles were in the vicinity for off-loading the trailer as shown in Figure 5.16.

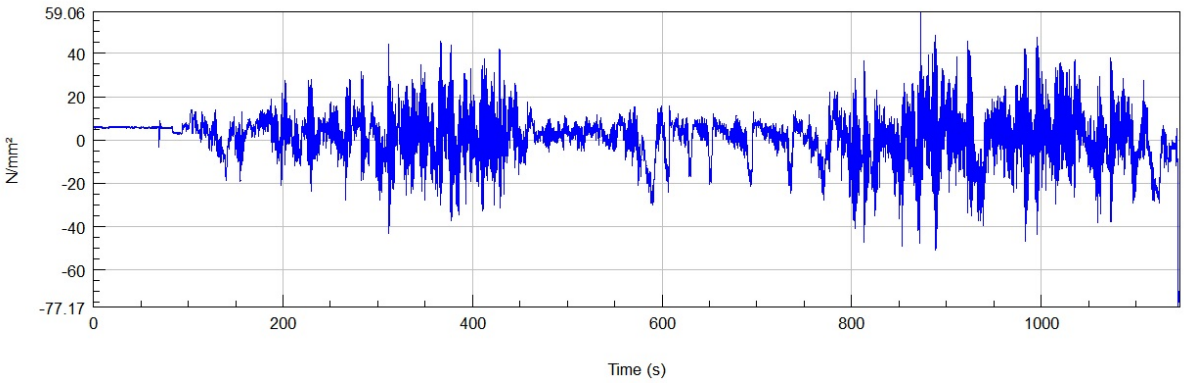

Figure 5.16: Goose Neck 2 (stress vs. time) data filtered for Route 4

Unfortunately the bogie channels showed an internal amplifier error when the stress was computed because the gauges did not zero when the trailer was un-laden. However by subtracting this error from the data the correct data was attained. Bogie Rear 1 upon investigation had an intermittent cable connection which caused incorrect data acquisition which can be seen by the overall increase in values compared to the other bogie strain gauges in a similar position on the other centre beam (Table

5.10 to 5.13). Although this data is not a true representation, a valid comparison could still completed in Chapter 5.3.4 by using the symmetry of the trailer.

The BTT FEA results for each load scenario was captured at locations on the trailer where the strain gauges had been mounted for data acquisition. Thus a comparison was made to determine how the field test data stresses compared to those from the FEA model, and whether the trailer's operational conditions could be considered safe.

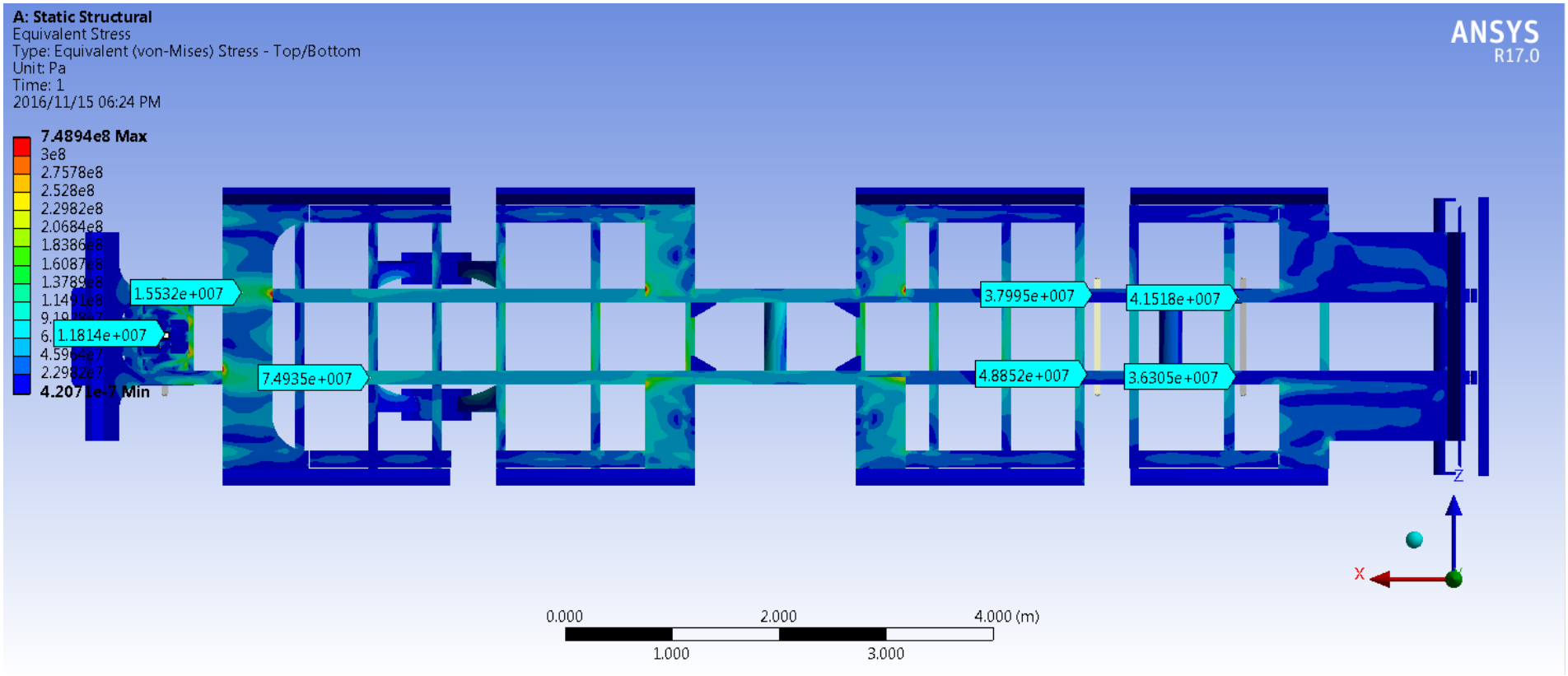

Figure 5.17: Stress points for 2g vertical acceleration load case

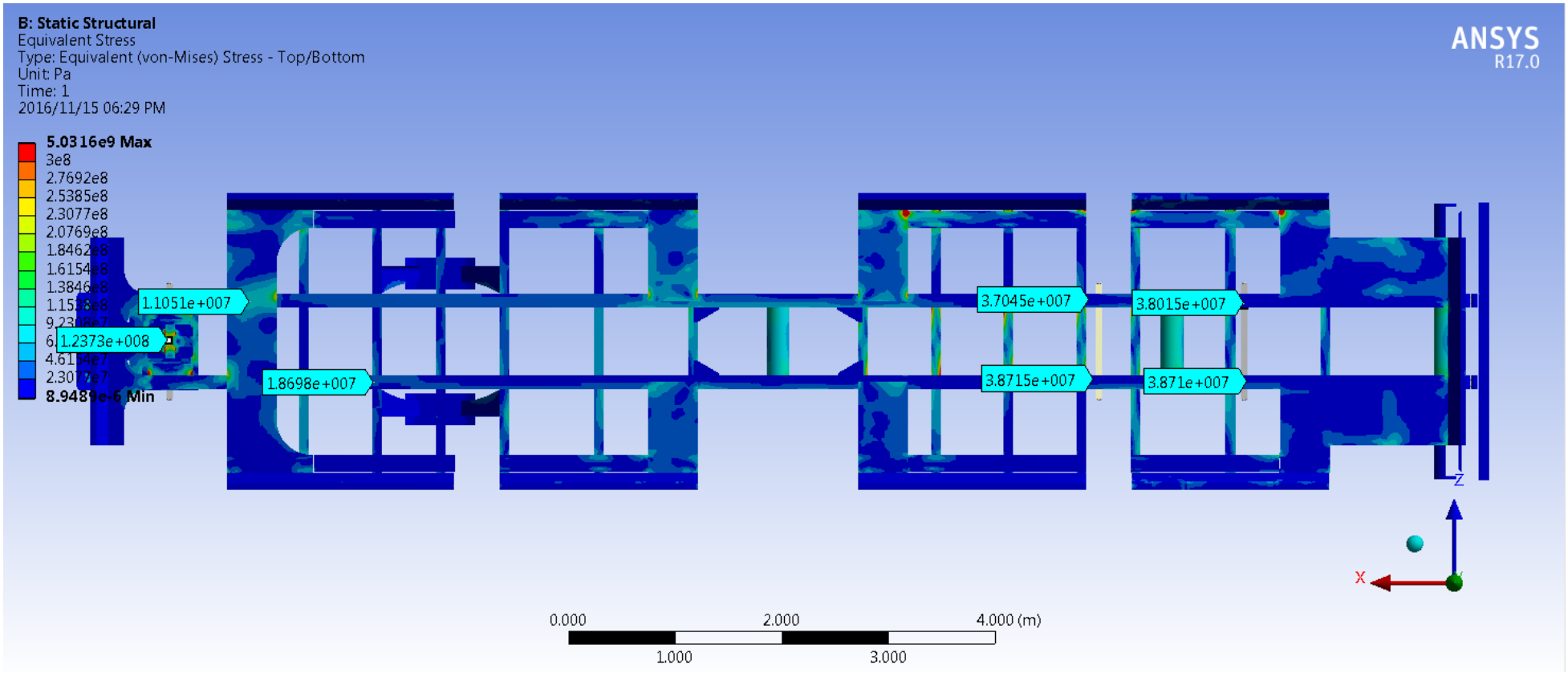

Figure 5.18: Stress points for 1g vertical and 0.25g lateral acceleration load case

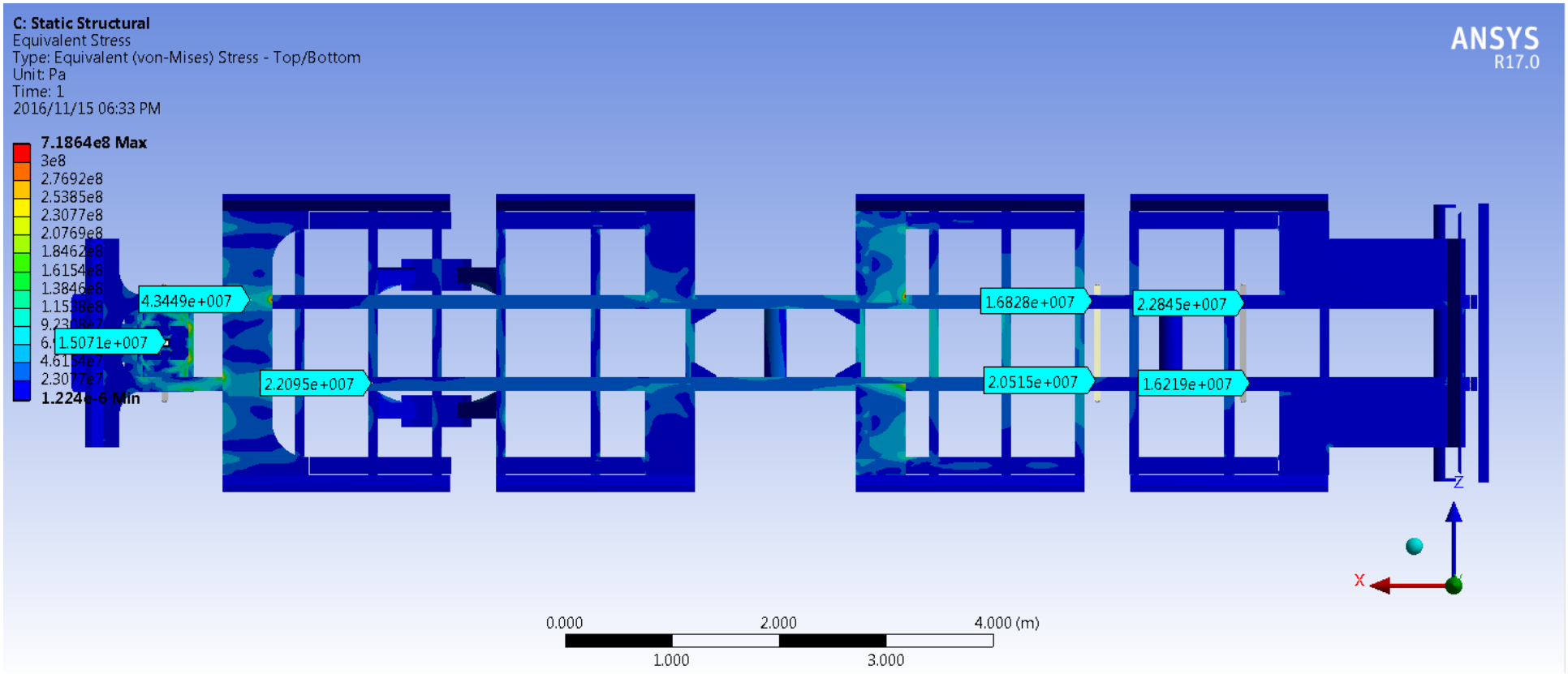

Figure 5.19: Stress points for 1g vertical and 0.8g longitudinal acceleration load case

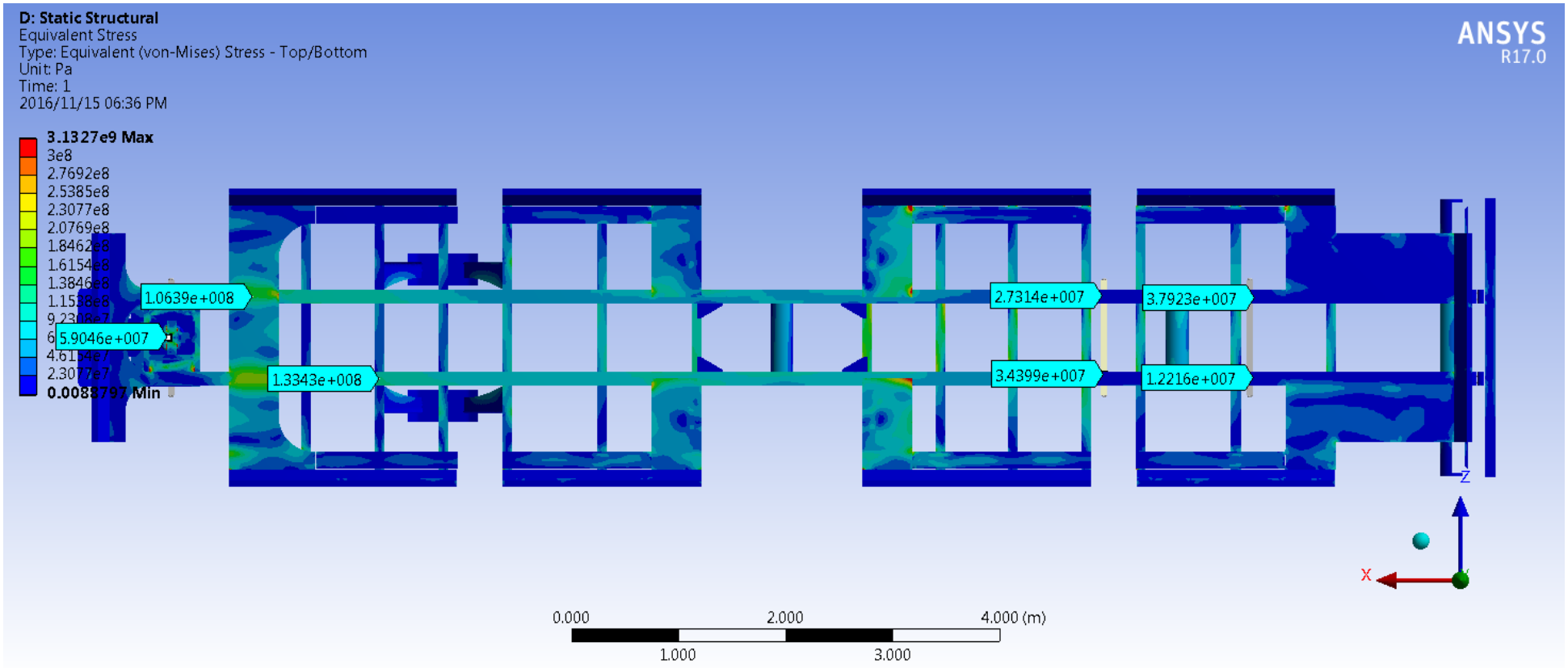

Figure 5.20: Stress points for combined load (2g vertical + 0.8g longitudinal +0.25g lateral) acceleration case

In the field test data results some of the stresses are similar whilst the majority are below that found in the various FEA load cases as shown in Figures 5.17 to 5.20. The field test data mean for each stress was generally lower, confirming that FEA load cases were more likely to occur in the case of an abnormal scenario. The close results of the recorded test stress values compared to the FEA values may be indicative of the high acceleration values that were achieved on the trailer during testing, because of the poor road conditions. The high stress (>300 MPa) found in localised FEA elements caused due to modelling approximations and the right angled connection between mating members [25], [38], [39], [40], [41] are considered safe since significantly lower stresses were found in these regions in the field test data, indicating that there would be no excessive stresses at these points leading to localised failure portrayed in the FEA at similar accelerations. The trailers have been successfully operated for four to five years and they were carefully visually inspected and no cracking, deformation or yielding of members was noticed. There were no failures of any related form reported, proving that the design is safe.

5.3.4 FEA model validation using field test data

The above field test data was used to verify the accuracy of the FEA model and to ensure that there is a close correlation between design and product. This enables refinement in some aspects of the modelling and simulation and thereby in the design. The static FEA analysis required that a similar scenario from the test data be chosen for the validation of the exercise. The un-laden trailer acts on its own mass under Earth's gravity and when a container is loaded, the strain gauge stresses provide a stress value sample which were compared to the FEA model. This is found in the following chapter.

5.3.4.1 Route 3- Loading of 20 foot containers

When the vehicles await container loading from the straddle carriers on Route 3, the vehicles are stationary on a flat surface providing ideal conditions for FEA model validation.

Figure 5.21: Straddle carrier loading first container

Sample 6322 provided the stresses experienced by the trailer with the first container placed stationary on the trailer as shown in Figure 5.21. Table 5.14 shows the comparison.

Name	Bogie Rear 1	Bogie Rear 2	Bogie Front 1	Bogie Front 2	Kingpin	Goose Neck 1	Goose Neck 2
Sample 6322 (MPa)	4.00	5.12	2.06	6.61	27.42	55.07	57.53
BTT FEA stress with 1g acceleration (MPa)	6.96	5.94	2.76	8.62	6.18	10.45	19.71
Percentage error % (sample versus model)	42.53	13.80	25.36	23.32	77.46	426.99	191.88

Table 5.14: Container 1 test data for FEA model verification

For the second container placed stationary behind the first container, sample 20412 provided the stresses experienced by the trailer. Table 5.15 shows the comparison.

Name	Bogie Rear 1	Bogie Rear 2	Bogie Front 1	Bogie Front 2	Kingpin	Goose Neck 1	Goose Neck 2
Sample 20412 (MPa)	18.35	17.70	12.37	14.56	40.94	27.16	27.16
BTT FEA stress with 1g acceleration (MPa)	19.97	19.64	16.15	20.88	10.07	10.53	32.95
Percentage error % (sample versus model)	8.11	9.88	23.41	30.27	306.55	157.93	17.57

Table 5.15: Container 2 test data for FEA model verification

Certain stress values of the sample test data compare within an acceptable range of 1.94-11.32 MPa or 9.88-25% [57] with that from the FEA model at static load (calculated from strain gauges subject to low disturbances [56]). Although the percentage error values is high it was noted that the majority of the field test results are lower than the FEA results providing a safe design [57].

The containers are unlikely to be perfectly evenly loaded onto the trailer which means that a strain gauge on one centre beam (bogie and goose neck) may provide a larger value compared to another at a similar point on the other centre beam. The FEA assumes the load is spread evenly over a given surface area and provides a uniform result regarding the symmetry of the trailer, uneven loading should be a consideration for future FEA models. The kingpin and goose neck sample field test values do not compare well with those of the FEA. This is due to the strain gauge being directly exposed to disturbances and noise from the sub-systems of the straddle carrier as previously explained in Chapter 5.3.3.2. Bogie Rear 1 had an intermittent connection and was omitted from the comparison.

The FEA acceleration values were assessed using the information presented in Chapter 5.3.3.1. This was determined by using maximum absolute acceleration values from the test data routes which include where the trailers were driven with severe turning, acceleration and emergency braking to attain all possible outcomes that might occur during operations. From the field testing data a maximum of 0.199g in the lateral direction and 0.278g in the longitudinal direction were recorded when the trailer was fully laden. Although higher accelerations may have been recorded this was due to the trailer been un-laden. These scenarios present low stresses of no concern when simulated using FEA. Acceptable safety factors of 1.26 and 1.80 from the recommended ranges in studies [28], [49] were incorporated for the lateral and longitudinal accelerations respectively, such that values of 0.25g and 0.5g can be used as the new FEA loading accelerations which also comply with the recognised standards which recommend these loading accelerations as discussed in Chapter 4.10.1. By using the 0.25g lateral acceleration as modelled in Chapter 4.10.2.4 and the 0.5g longitudinal acceleration it would allow better optimised acceleration values used for the redesign in Chapter 6. The vertical 2g used during FEA modelling can be reduced to 1.5g and still incorporate a dynamic design factor of 1.5 from the recommended ranges in Cowling's study [41]. This was determined using the maximum absolute g value of 0.484g from Table 5.7 for Route 3, compared to the 1.5g value now proposed for future FEA design process. In Route 4 (Table 5.8), the peak g values are caused by the un-laden trailer returning to the workshop. Because the trailer was un-laden the stresses were negligible, which was found using FEA and therefore the acceleration data was not included. The laden acceleration data corresponds to accelerations lower than those shown in Table 5.7 as part illustrated in Figure 5.13. Thus, the accelerations proposed above are not influenced. Modifying the future FEA design acceleration values based on the measured data discussed in this chapter will allow more accurate design, potentially leading to cheaper and lighter, yet equally or more robust trailers.

5.4. Testing of the MPT

5.4.1 Preparation of the trailer and test

To initiate the testing, arrangements had to be made with Transnet National Port Authority's (TNPA's) Richard's Bay fleet control staff by briefing them on the project and its requirements. Trailer 90TAP02 with hauler TER 02 was available and used for the test. The strain gauges and accelerometers were fitted as previously explained in Chapter 5.3.1, at locations described in Table 5.16 and Figures 5.22 to 5.24.

Location on Trailer	Sensor
Kingpin (Kp) supporting member	Rosette strain gauge and accelerometer
Goose neck on each side beam	Rosette strain gauge at either alternate bend
Centre of mass (COM) of trailer	Accelerometer
Bogie (rear axle)	Linear and rosette strain gauges on flange and linear gauge on web, Accelerometer

Table 5.16: Sensor allocation to critical areas of the trailer

Figure 5.22: Rosette gauge installed at kingpin supporting structural member. (Direct access to the kingpin was not possible with the top plate of the trailer).

Because of the limited access to the bogie of the trailer, the rear axle could only be fitted with strain gauges. As a result, a comparison was made against the linear and rosette strain gauge (Figure 5.23) by installing them at a similar location on the flange to monitor the strain/stress. This would allow for improved accuracy in the data acquisition, and a better comparison depending on the gauge of concern.

Figure 5.23: Linear and rosette gauges installed at the flange of the centre beam at the rear axle.

Figure 5.24: Final installation of the HBM QuantumX system

The accelerometers were mounted at the kingpin, centre of mass and bogie. All the cabling harnesses were trunked through the trailer and thoroughly checked.

Once the trailer was ready (Figure 5.25), it was necessary to get a well experienced hauler driver and the pair of fully laden 40 ton skips. Loading the skips onto the trailer was accomplished with a forklift. The trailer was then taken to the cargo storage area and the commodity (chromium for the test) was loaded using a wheel loader. Since the cargo does not belong to TNPA, permission had to be obtained from the cargo owners to use their product for the test.

Figure 5.25: The hauler and trailer ready for testing

5.4.2 Field test conditions

The data acquisition was initiated from the instant the hauler and trailer left the workshop area where the trailer was prepared. The relevant acceleration, speed, micro-strain and stress measurements were logged since an un-laden trailer may react more dynamically to road conditions as observed from the BTT test.

The Richard's Bay roads were well maintained and in a generally good condition. Railway tracks and unevenness on certain roads on which the vehicles commuted was found, but were minimal. When the hauler and trailer were ready to leave the workshop, the activity routes in Table 5.17 were taken.

Route	Description of Route
1	Workshop to skip loading area (un-laden)
2	Skip loading area to commodity loading area (loaded with two empty skips)
3	Cargo operations (fully laden)
4	Off-loading of commodity and return to workshop (un-laden)

Table 5.17: Route overview at Richard's Bay Port

On Route 3 sectors were lapped on with severe turning, acceleration and emergency braking to try and attain all the possible outcomes that might occur during operations.

5.4.3 Field test data

5.4.3.1 Acceleration test data

The acceleration was first analysed. The sample rate used was 150Hz. Tables 5.18 to 5.21 provide an overview of the data collected for each of the routes. The data was been filtered to omit periods when the vehicle was stationary and idling with no effective readings. This was done to provide a more effective spectrum of results and to provide more accurate minimum (min), maximum (max), mean, standard deviation (STD) and quartile values. At no point did the hauler and trailer exceed the 30 km/hr limit, this was verified using GPS speed results. X, Y and Z denote accelerations experienced in lateral, longitudinal and vertical directions respectively.

Route 1	**g Values**								
Name	**Kp x**	**Kp y**	**Kp z**	**COM x**	**COM y**	**COM z**	**Bogie x**	**Bogie y**	**Bogie z**
Samples	*129992*	*129992*	*129992*	*125441*	*125441*	*125441*	*125881*	*125881*	*125881*
Min	-0.386	-0.275	-0.530	-0.376	-0.138	-0.467	-0.418	-0.208	-0.026
Max	0.381	0.231	0.703	0.405	0.190	0.619	0.360	0.239	0.013
Mean	0.001	0.020	-0.005	0.008	0.024	-0.016	0.014	-0.003	-0.001
STD	0.020	0.029	0.042	0.021	0.026	0.046	0.020	0.026	0.001
Lower quartile	-0.008	0.003	-0.022	-0.003	0.007	-0.034	0.004	-0.017	-0.002
Inter quartile	0.018	0.035	0.033	0.021	0.034	0.037	0.020	0.028	0.002
Upper quartile	0.010	0.038	0.011	0.018	0.041	0.003	0.023	0.010	-0.00029

Table 5.18: Acceleration values from the workshop to skip loading area

Route 2	g Values								
Name	**Kp x**	**Kp y**	**Kp z**	**COM x**	**COM y**	**COM z**	**Bogie x**	**Bogie y**	**Bogie z**
Samples	*98314*	*98314*	*98314*	*96290*	*96290*	*96290*	*96600*	*96600*	*96600*
Min	-0.195	-0.841	-1.13	-0.158	-0.575	-1.077	-0.228	-0.678	-0.005
Max	0.211	0.820	0.505	0.236	0.566	0.722	0.196	0.635	0.005
Mean	0.010	0.027	-0.014	0.027	0.037	-0.034	0.027	0.019	-0.0006
STD	0.021	0.031	0.045	0.022	0.026	0.050	0.023	0.029	0.0004
Lower quartile	0.00016	0.010	-0.032	0.017	0.022	-0.054	0.016	0.004	-0.0009
Inter quartile	0.018	0.032	0.034	0.019	0.030	0.039	0.023	0.032	0.0006
Upper quartile	0.018	0.042	0.002	0.036	0.052	-0.015	0.039	0.036	-0.0003

Table 5.19: Acceleration values from skip loading area to commodity loading area

Route 3	g Values								
Name	**Kp x**	**Kp y**	**Kp z**	**COM x**	**COM y**	**COM z**	**Bogie x**	**Bogie y**	**Bogie z**
Samples	*374850*	*374850*	*374850*	*374850*	*374850*	*374850*	*374850*	*374850*	*374850*
Min	-0.145	-0.113	-0.434	-0.125	-0.039	-0.286	-0.200	-0.132	-0.071
Max	0.197	0.216	0.388	0.200	0.189	0.274	0.158	0.191	0.011
Mean	0.0187	0.062	-0.008	0.049	0.081	-0.009	-0.003	0.027	-0.001
STD	0.016	0.024	0.053	0.018	0.022	0.038	0.017	0.025	0.0009
Lower quartile	0.008	0.048	-0.025	0.036	0.068	-0.022	-0.011	0.015	-0.001
Inter quartile	0.019	0.027	0.032	0.024	0.026	0.025	0.019	0.026	0.001
Upper quartile	0.027	0.076	0.007	0.060	0.094	0.002	0.008	0.040	-0.004

Table 5.20: Acceleration values of cargo operations

Route 4	g Values								
Name	**Kp x**	**Kp y**	**Kp z**	**COM x**	**COM y**	**COM z**	**Bogie x**	**Bogie y**	**Bogie z**
Samples	*35229*	*35229*	*35229*	*35398*	*35398*	*35398*	*35229*	*35229*	*35229*
Min	-0.175	-0.086	-0.631	-0.144	-0.041	-0.549	-0.311	-0.222	-0.003
Max	0.254	0.365	0.438	0.290	0.239	0.391	0.230	0.205	0.003
Mean	0.028	0.075	-0.034	0.058	0.094	-0.068	0.053	0.031	0.0002
STD	0.022	0.027	0.047	0.022	0.022	0.051	0.023	0.024	0.0004
Lower quartile	0.021	0.058	-0.052	0.049	0.078	-0.087	0.043	0.017	-0.0001
Inter quartile	0.016	0.030	0.035	0.017	0.027	0.037	0.018	0.031	0.0006
Upper quartile	0.037	0.088	-0.018	0.066	0.105	-0.050	0.061	0.048	0.0005

Table 5.21: Acceleration values from off-loading of commodity and return to workshop

The data in Tables 5.18 to 5.21 was arranged in a manner to enable easy assessment of the results and compare various values at the three positions measured on the trailer. The good road conditions at the port show that the acceleration values are low, and maximum acceleration values (Figures 5.26 to 5.28) were found when the empty skips were loaded onto the trailer using a forklift. Because a wheel loader loads the commodity into the skip, a single scoop of commodity is far less than the mass of the skip, which means we do not see any peak acceleration values when the skips are fully laden because the progress to maximum is gradual.

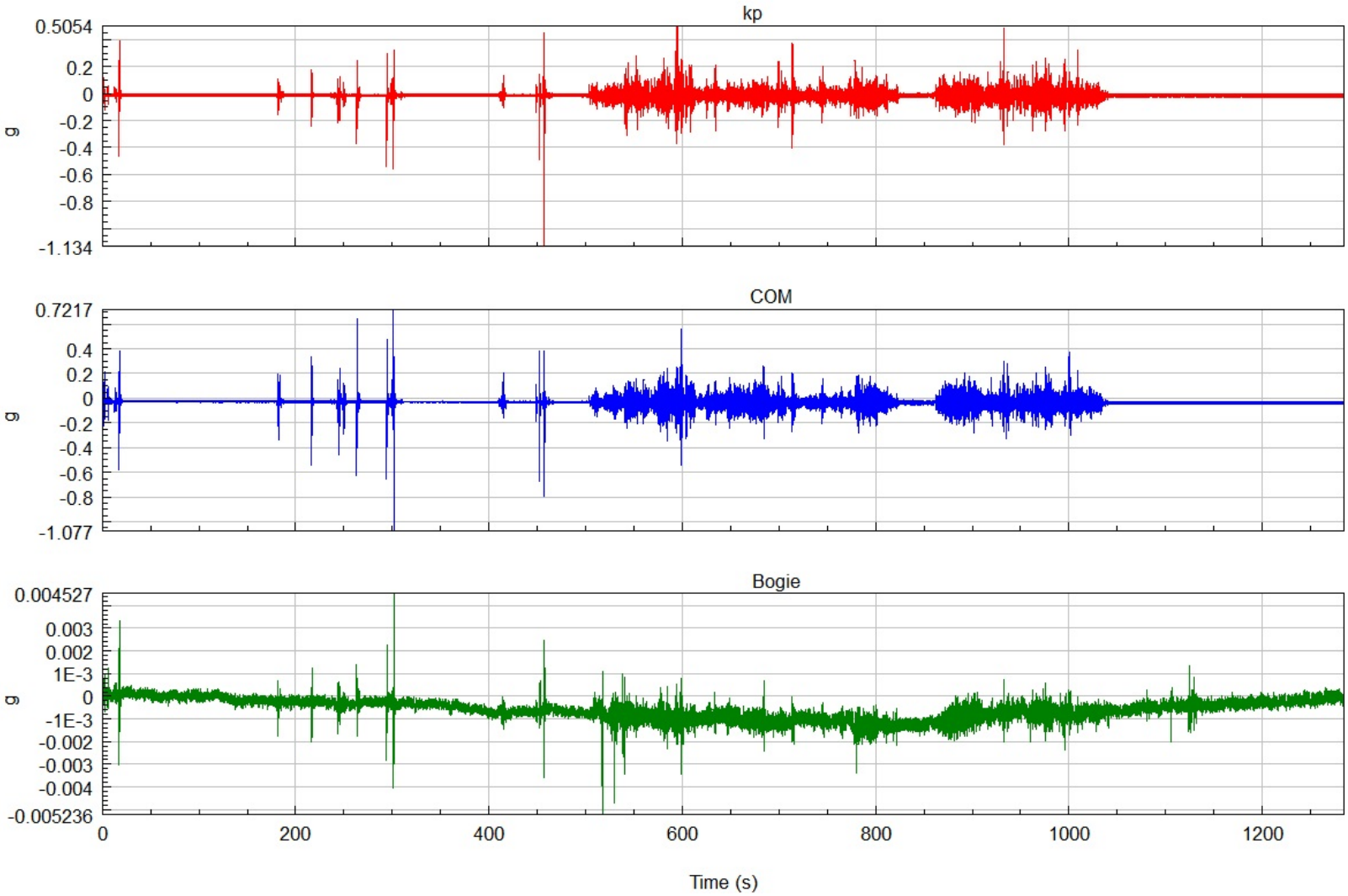

Figure 5.26: Z direction acceleration (g) values for Route 2 (Unfiltered; to show loading spikes whilst stationary)

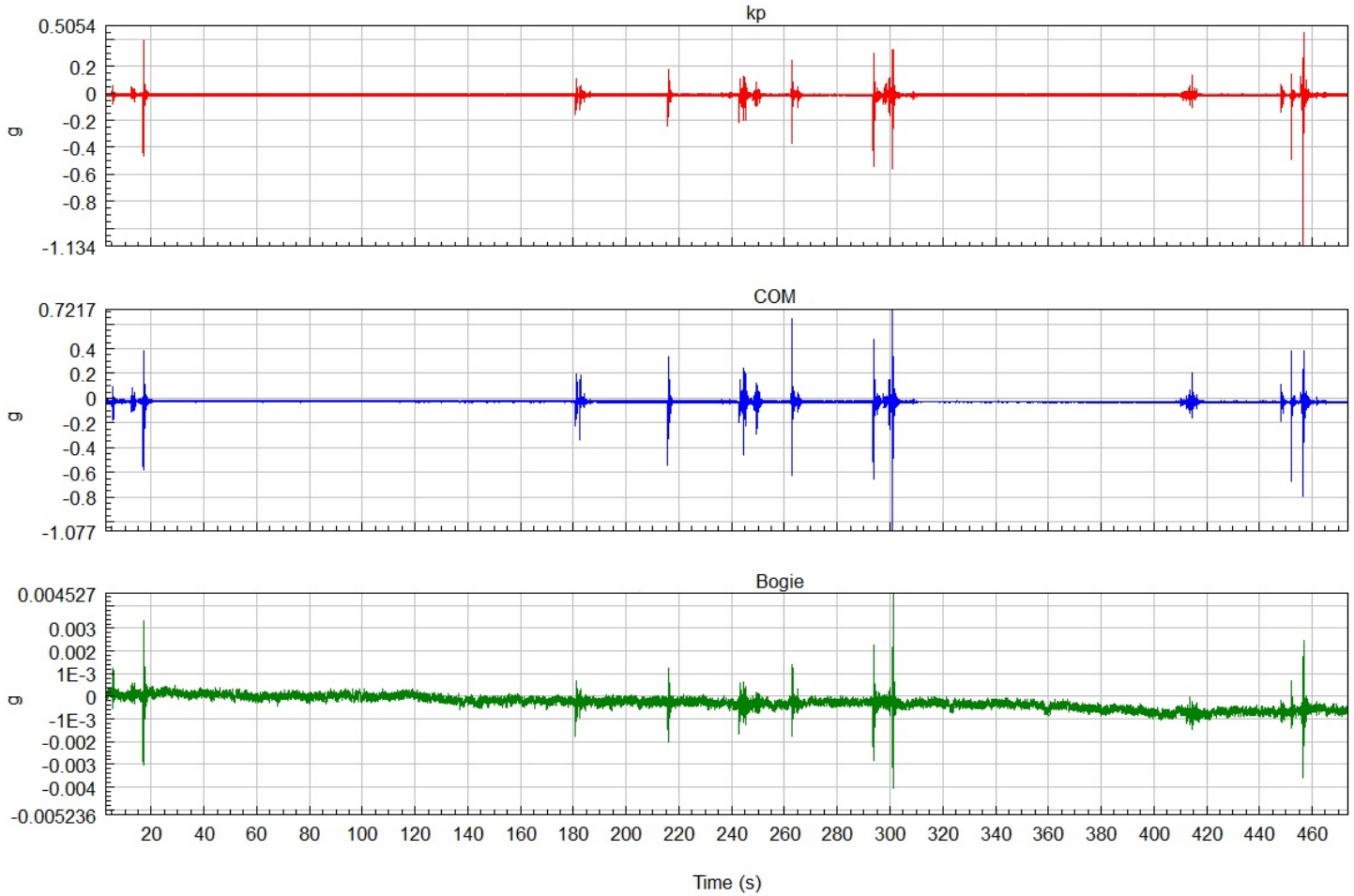

Figure 5.27: Z direction acceleration (g) values for loading of the skips on Route 2

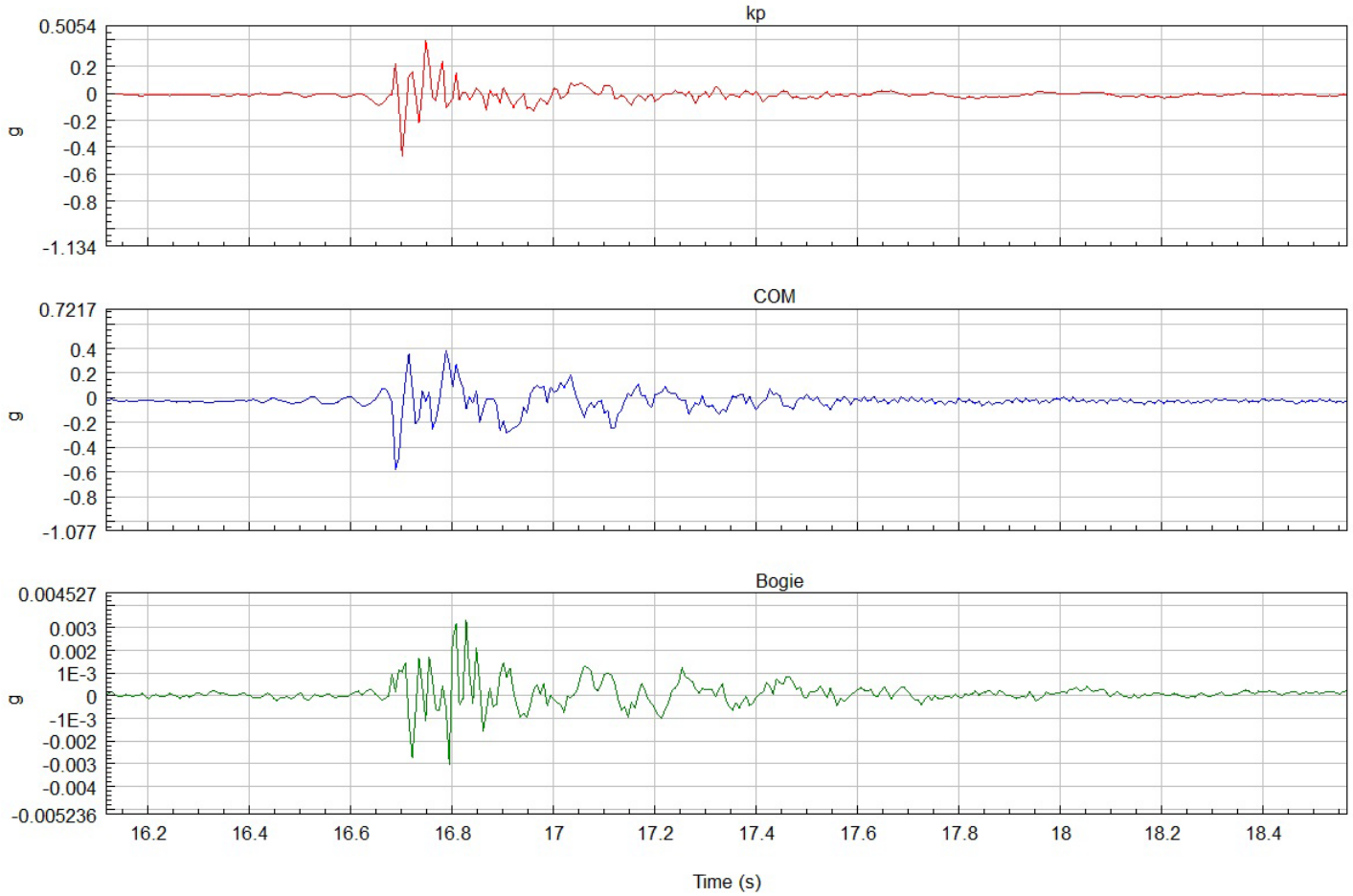

Figure 5.28: Z direction acceleration (g) values for loading of the first skip

During the drive on Route 3 the acceleration values showed maximums of no concern. The smooth road surfaces in Richard's Bay allowed capture of relatively low acceleration values compared to Durban Pier 2. The load translation through the trailer as previously described in Chapter 5.3.3.1 was also consitent as shown in Figure 5.29, and because of the good road conditions there were no abnormal disturbances.

On Route 2 and 3, the bogie experienced low acceleration readings as shown in Figure 5.30 during loading, off-loading and transporting the commodity to the vessels. Two scenarios could explain this; first, the load dampened the trailer structure such that the suspension and experienced very little travel in the vertical direction. Second, the load was too great causing the suspension to be inadequate to carry out its purpose, and "bottom out". However it was observed during the test that the suspension was still functioning as it needed to. The operational routes were found to be in good condition with or without the load, and Route 4 showed similar results when the trailer was off-loaded and made a return trip to the workshop. Figures 5.31 and 5.32 show these scenarios.

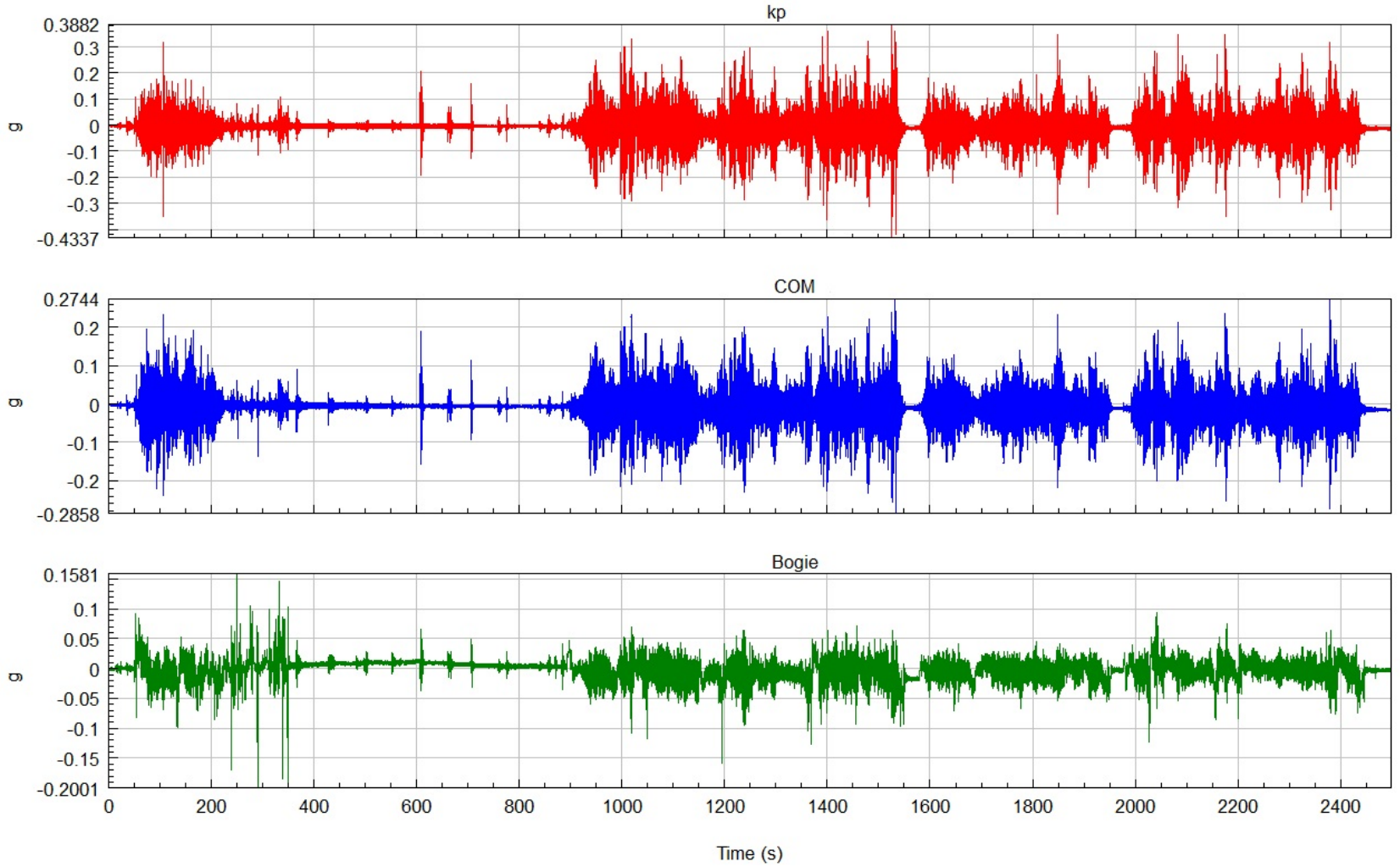

Figure 5.29: Kp z, COM z and Bogie x acceleration test data for Route 3

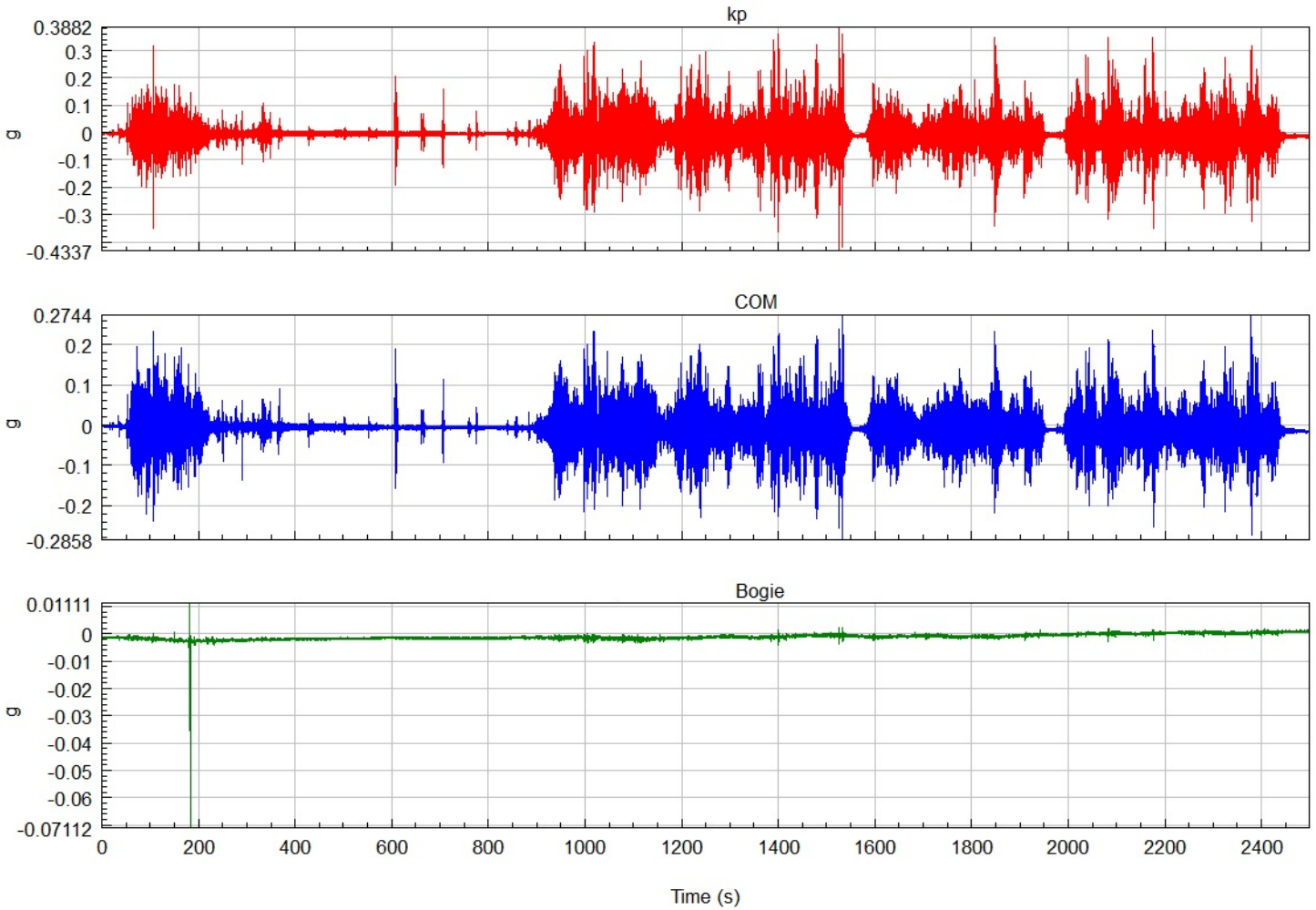

Figure 5.30: Z direction acceleration (g) test data for Route 3

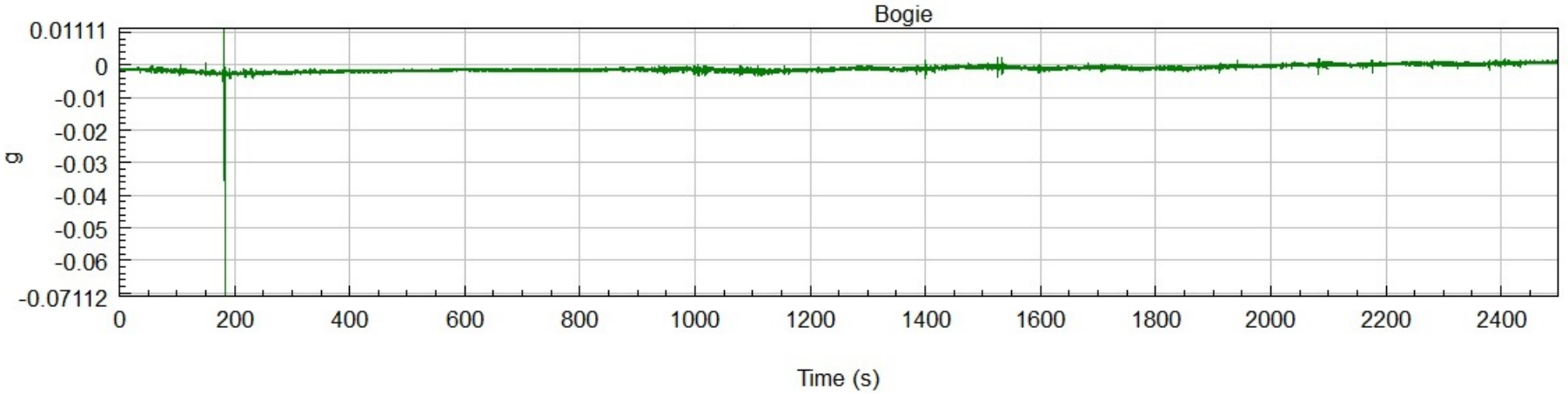

Figure 5.31: Bogie z acceleration test data for Route 3

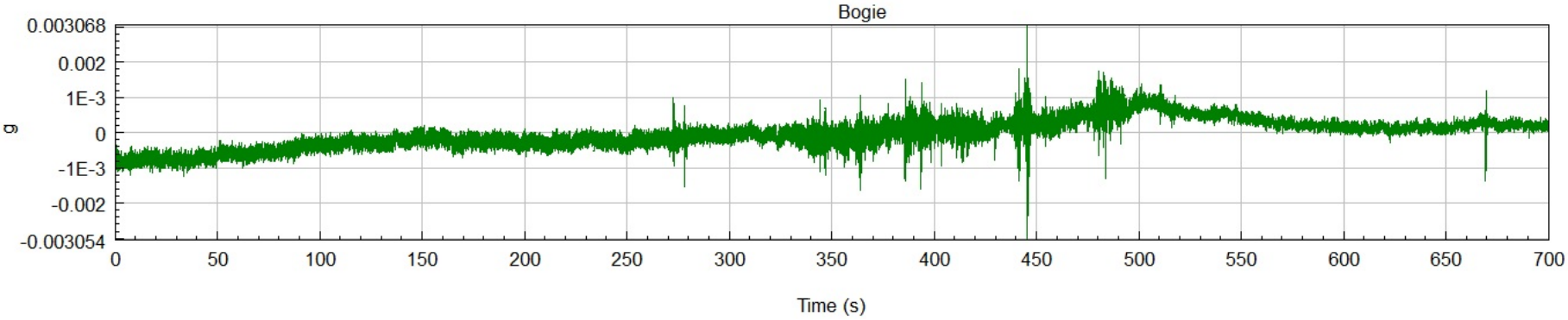

Figure 5.32: Bogie z acceleration test data for Route 4

5.4.3.2 Strain gauge test data

The strain gauges were placed critically along the length of the trailer as shown in Table 5.22, where data could be captured and compared to that obtained from the FEA.

Structural member on Trailer	Gauge type and location
Kingpin supporting member	Rosette strain gauge and accelerometer
Goose Neck 1	Rosette strain gauge at goose neck bend closest to kingpin
Goose Neck 2	Rosette strain gauge at goose neck bend closest to landing legs
Bogie Rear axle 1/ Linear 1	Linear strain gauge on web for rear axle
Bogie Rear axle 2/Linear 2	Linear strain gauge on flange for rear axle
Bogie Rosette	Rosette strain gauge on flange for rear axle next to Bogie Rear axle 2/Linear 2

Table 5.22: MPT strain gauge placements

Route 1	**Stress in MPa**					
Name	**Bogie Rear axle 1/ Linear 1**	**Bogie Rear axle 2/Linear 2**	**Bogie Rosette**	**Kingpin**	**Goose Neck 1**	**Goose Neck 2**
Samples	*206201*	*206201*	*206765*	*209008*	*206765*	*206765*
Min	-6.35	-6.41	0.6656	0.351	2.89	0.40
Max	5.68	19.89	17.10	39.83	174.10	19.38
Mean	0.358	7.11	6.16	6.41	80.68	5.74
STD	1.930	2.39	2.54	3.26	30.26	2.56
Lower quartile	-0.934	-6.25	4.62	4.66	62.30	3.27
Inter quartile	2.900	3.23	3.36	3.66	42.65	4.15
Upper quartile	1.967	-0.016	7.99	8.31	104.95	7.41

Table 5.23: Stress values from the workshop to skip loading area

Route 2	Stress in MPa					
Name	**Bogie Rear axle 1/ Linear 1**	**Bogie Rear axle 2/Linear 2**	**Bogie Rosette**	**Kingpin**	**Goose Neck 1**	**Goose Neck 2**
Samples	*192743*	*192743*	*192743*	*192743*	*192743*	*192743*
Min	-8.83	-4.31	4.251	1.45	22.34	2.28
Max	4.03	18.88	18.24	36.49	539.25	26.55
Mean	-0.73	8.22	9.91	14.20	84.75	9.41
STD	2.40	8.09	1.56	8.55	27.91	3.94
Lower quartile	-2.85	2.47	8.48	5.21	58.51	6.07
Inter quartile	3.11	8.64	2.53	15.33	50.97	7.20
Upper quartile	0.26	11.10	11.01	20.54	109.48	13.27

Table 5.24: Stress values from skip loading area to commodity loading area

Route 3	Stress in MPa					
Name	**Bogie Rear axle 1/Linear 1**	**Bogie Rear axle 2/Linear 2**	**Bogie Rosette**	**Kingpin**	**Goose Neck 1**	**Goose Neck 2**
Samples	*370632*	*370632*	*374850*	*374850*	*374850*	*374850*
Min	-10.27	0.305	0.304	8.944	-207.39	6.613
Max	-16.29	20.69	19.06	71.79	528.52	146.04
Mean	-0.31	8.91	8.30	33.12	11.26	77.24
STD	5.42	2.70	3.24	6.66	116.84	39.58
Lower quartile	-5.08	6.98	5.62	30.02	-49.82	39.98
Inter quartile	8.69	3.59	5.41	6.28	76.97	65.94
Upper quartile	3.60	10.57	11.03	36.30	27.15	105.92

Table 5.25: Stress values for cargo operations

Route 4	Stress in MPa					
Name	**Bogie Rear axle 1/Linear 1**	**Bogie Rear axle 2/Linear 2**	**Bogie Rosette**	**Kingpin**	**Goose Neck 1**	**Goose Neck 2**
Samples	*101756*	*101756*	*105031*	*105031*	*105031*	*105031*
Min	0.97	-5.73	0.7413	33.81	100.29	13.47
Max	13.52	11.75	9.495	48.03	298.33	127.43
Mean	5.34	5.01	4.128	39.88	253.63	45.90
STD	2.36	4.42	2.364	2.850	50.91	43.80
Lower quartile	4.40	-2.17	2.22	37.43	212.19	18.83
Inter quartile	2.05	4.86	4.44	4.20	74.16	90.36
Upper quartile	6.45	2.69	6.66	41.63	286.35	109.20

Table 5.26: Stress values from off-loading of commodity and return to workshop

The stress data in Tables 5.23 to 5.26 was compared in a similar manner to the acceleration data. This was the second trailer to be tested, so certain installation aspects were improved upon.

Unfortunately the bogie channels showed an internal amplifier error when the stress was computed because the gauges did not zero when the trailer was un-laden. However by subtracting this error from the data, it was corrected.

Channel Goose Neck 1 illustrated high stress values which were out of range when compared to channels Goose Neck 2 and Kingpin, which were in the same vicinity. Upon inspection, traces of contaminant was found, which prevented the gauge from being mounted flush, thus creating the disturbances that caused high values. Therefore this data (Goose Neck 1) is not a true representation as the strain gauge sensitivity was compromised by an external contaminant. Goose Neck 2 however still provided sufficient data for analysis, since it was mounted on the same bend of the goose neck, but on the other centre beam.

All of the remaining strain gauges and channels obtained usable data, and were filtered for comparison.

A comparison of the linear and rosette strain gauges was made to determine differences in the results. Using test data from Route 3 as an example, it was clear that both gauges provided a close range of stress results. Although both gauges operate at 150Hz the rosette shows more sensitivity, which can be seen in Figure 5.33. The linear gauge measures uniaxial strain/stress whilst the rosette measures a resultant strain/stress of three directions, so certain extremities are displayed in either gauge results.

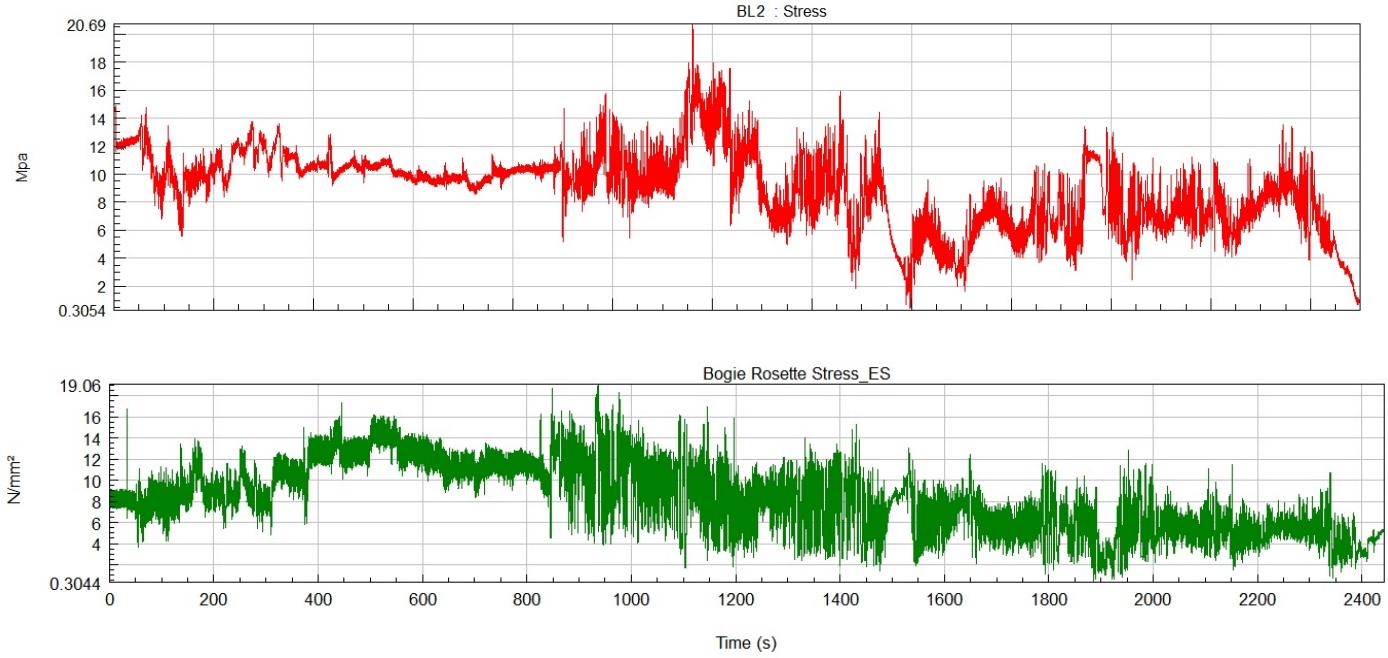

Figure 5.33: Route 3 data of the linear and the rosette strain gauge at similar points on the flange of the trailer

The MPT FEA results for each load scenario was captured at the locations on the trailer where the strain gauges were mounted for data acquisition. This showed how the field test data stresses compared to that of the FEA, and whether the trailer's operational conditions could be considered safe.

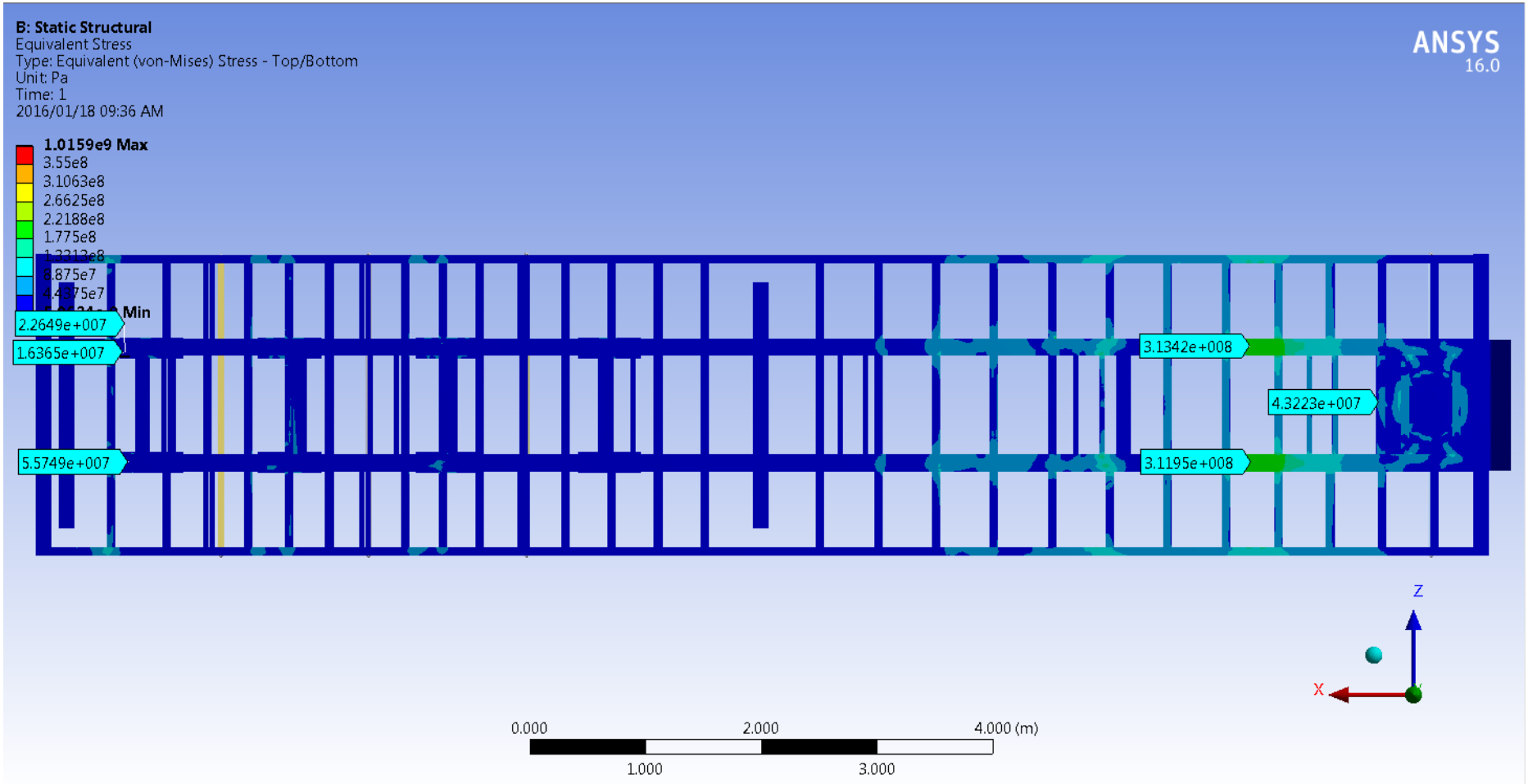

Figure 5.34: Stress points for 2g vertical acceleration load case

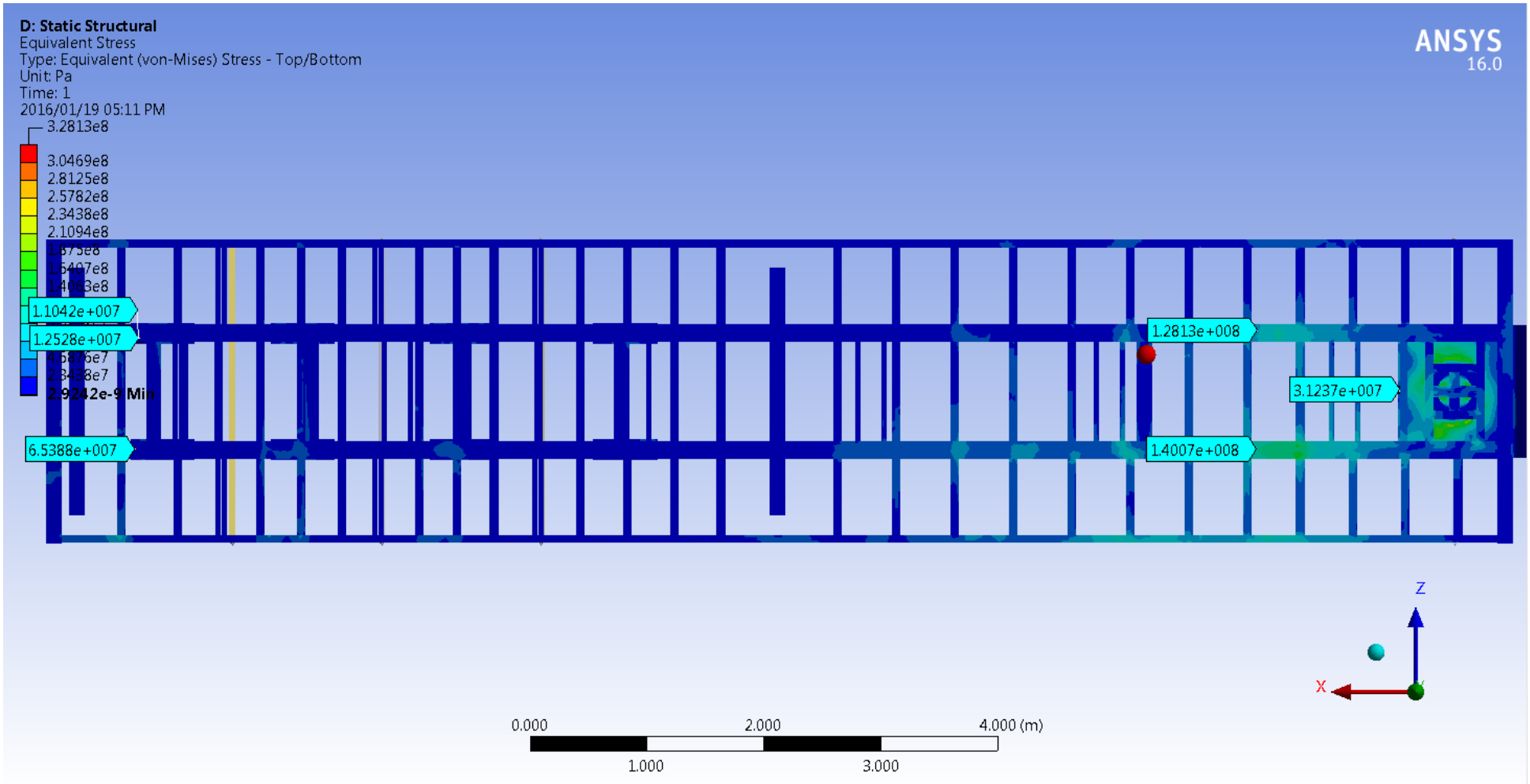

Figure 5.35: Stress points for 1g vertical and 0.25g lateral acceleration load case

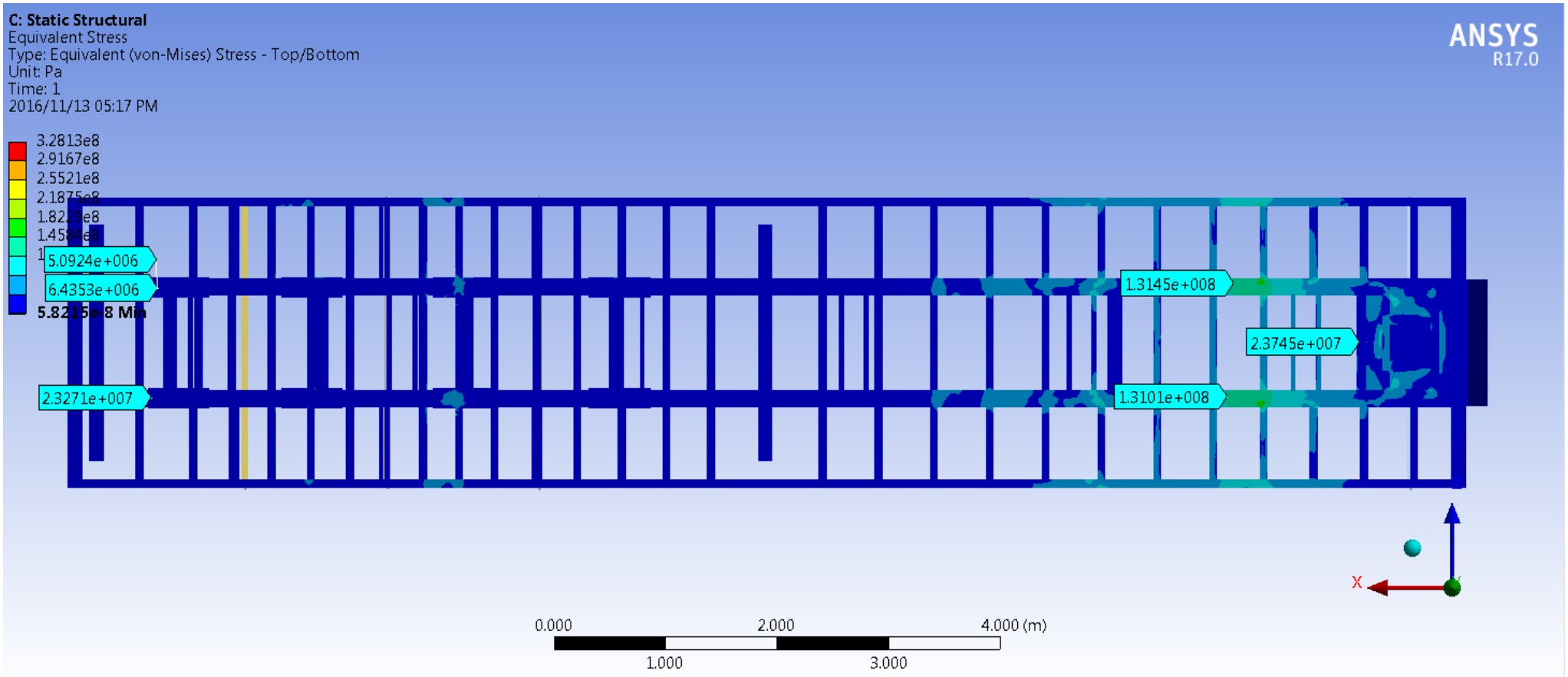

Figure 5.36: Stress points for 1g vertical and 0.8g longitudinal acceleration load case

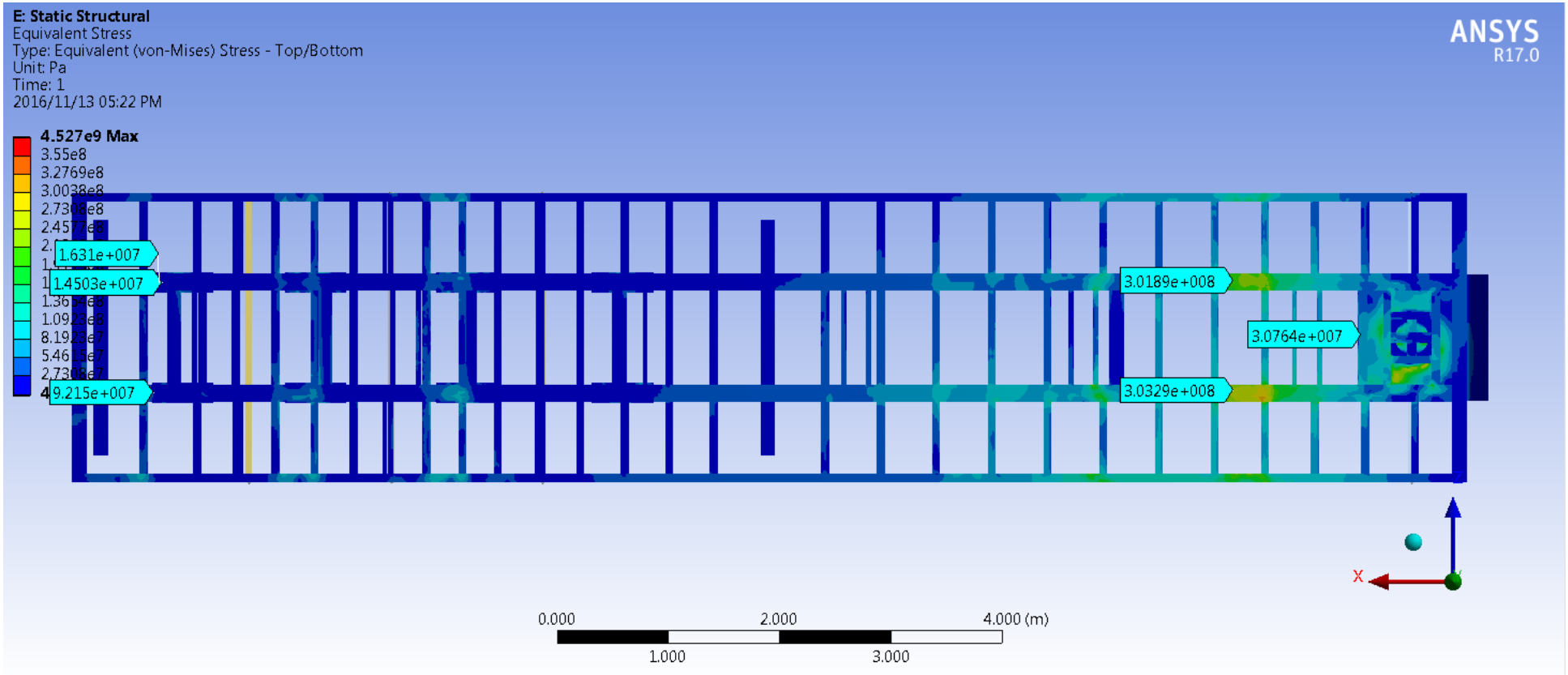

Figure 5.37: Stress points for combined load (2g vertical + 0.8g longitudinal +0.25g lateral) acceleration case

In the field test data results some of the stresses are similar whilst the majority are below that found in the various FEA load cases as shown in Figures 5.34 to 5.37. The field test data mean for each stress was generally lower.

The data was also effected by noise which was caused by external sources [56] as described in Chapter 5.3.3.2. For example on Route 1, the kingpin experienced a mean stress of 6.41 MPa and on Route 4 when the trailer was off-loaded it experienced a mean stress of 39.88 MPa. This was not possible as for both cases the trailer was un-laden. However on Route 4, the wheel loader and forklift were present in the vicinity of the hauler and trailer to off-load the skips and the commodity, and electrostatic and magnetic noise from reciprocating or rotating machines, electric motors, starters, generators, relays and transformers of the various vehicles systems, accumitively provided disturbances yielding the results obtained [56]. The graphs below (Figures 5.38 to 5.41) sequentially shows the events that occured on the kingpin strain gauge and Figure 5.41 shows the disturbance caused by the vehicles which only decreased after leaving the area where other vehicles were off-loading the commodity.

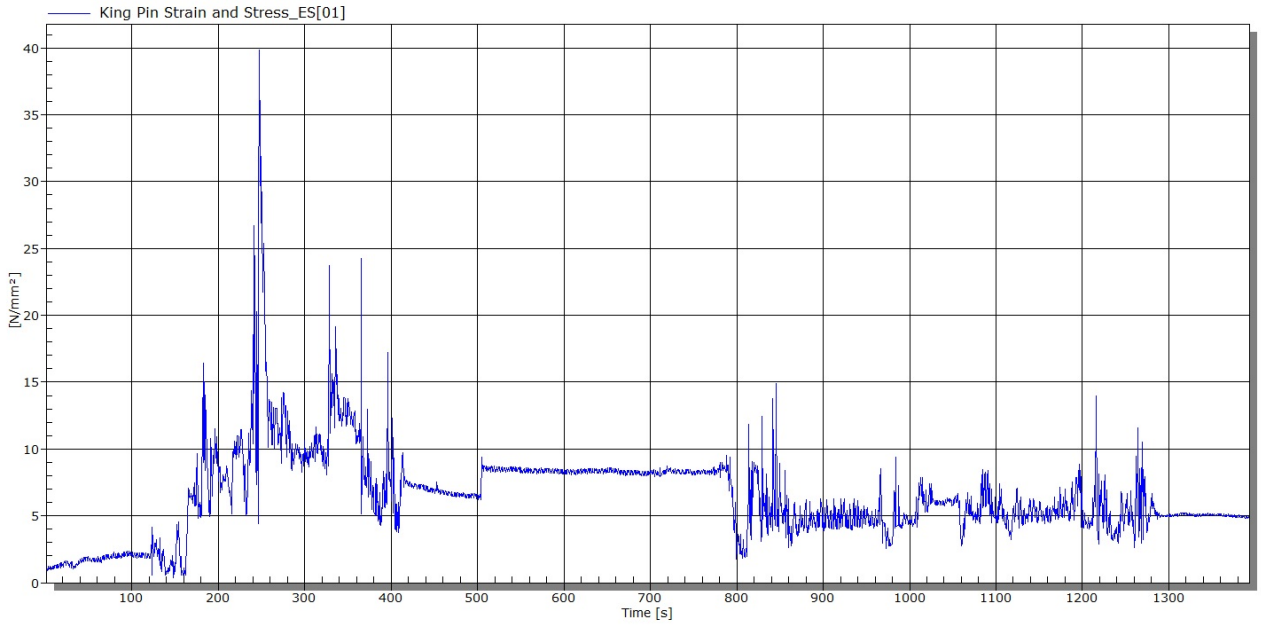

Figure 5.38: Kingpin stress (MPa) for Route 1

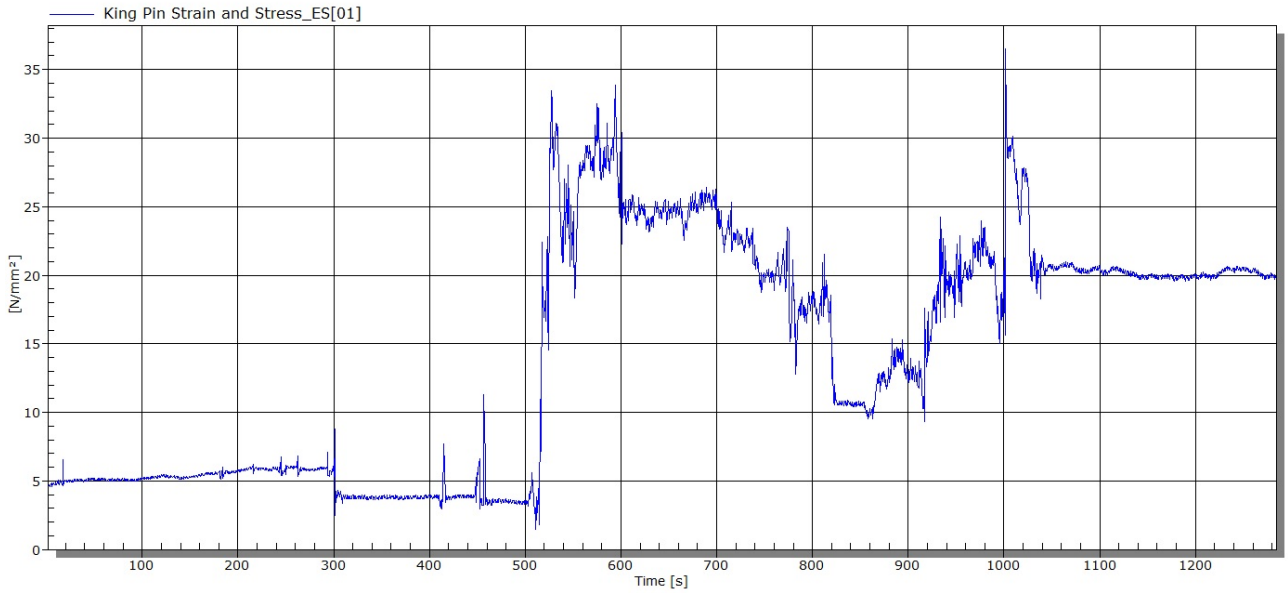

Figure 5.39: Kingpin Stress (MPa) for Route 2

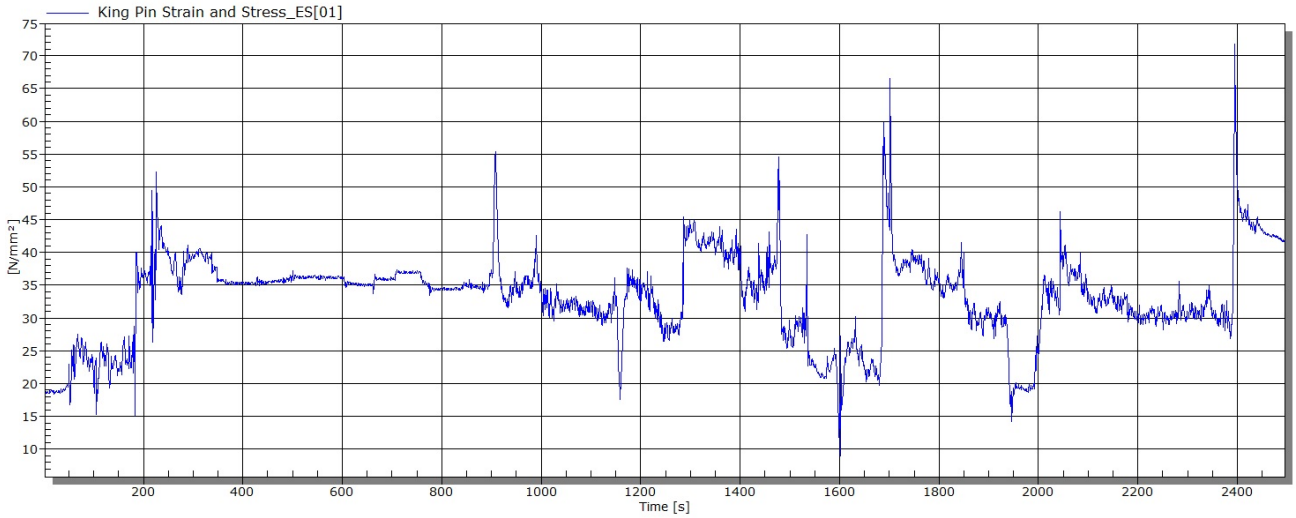

Figure 5.40: Kingpin Stress (MPa) for Route 3

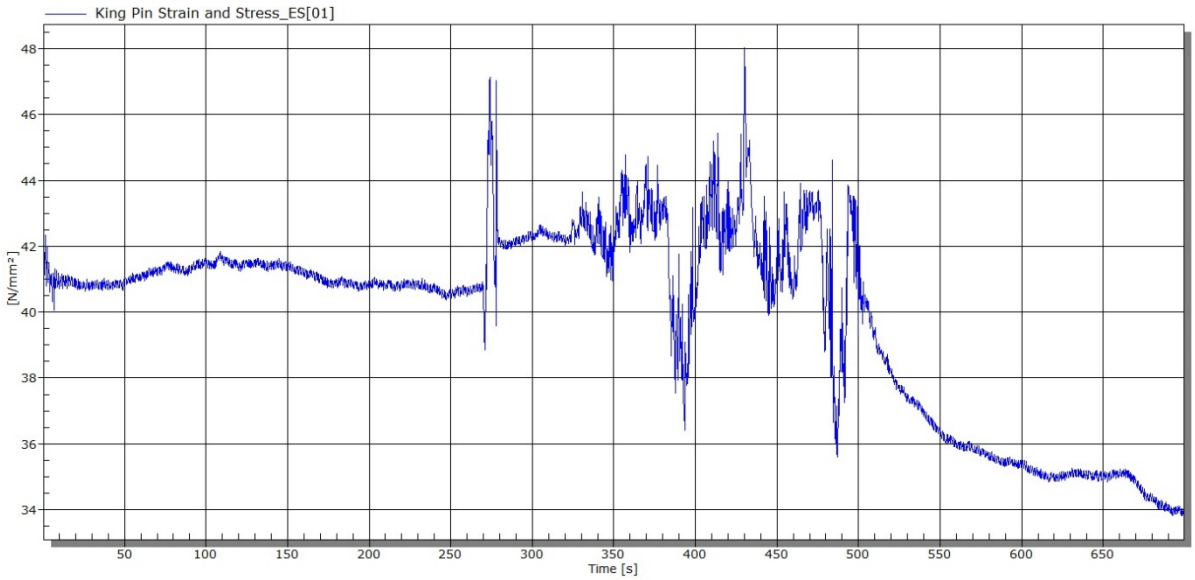

Figure 5.41: Kingpin Stress (MPa) for Route 4

The FEA high stress (>355 MPa) localised elements caused due to where spring elements attach to the centre beams, and right angled connections between mating members, [25], [38], [39], [40], [41] are considered safe since significantly lower stresses were found in these regions in the field test data, indicating that there would be no excessive stresses at these points leading to the localised failure as portrayed in the FEA at similar accelerations. The trailers have been successfully operated for three years and they were carefully visually inspected and no cracking, deformation or yielding of members was noticed. There were no failures of any related form reported, suggesting that the design is safe.

5.4.4 FEA model validation using field test data

The above field test data was used to verify the accuracy of the FEA model and that there is close correlation between design and product. This enables refinement in some aspect of modelling and simulation and thereby in the design.

The static FEA analysis required that a similar scenario from the test data be was chosen for the validation of the exercise. The un-laden trailer acts on its own mass under Earth's gravity and when a skip is loaded the strain gauge stresses provide stress value sample which was compared to the FEA model. This is found in the following chapter.

5.4.4.1 Route 2- Loading of un-laden 40 ton skips

On Route 2 where the vehicles await loading of the skips from the forklift, the vehicles are both stationary and on a flat surface providing ideal conditions for providing samples for the FEA model validation.

Figure 5.42: Example of 40 ton skips loaded onto the MPT

Sample 2519 provided the stresses experienced by the trailer with the first skip placed stationary on the trailer. Table 5.27 shows the comparison.

Name	Bogie Rosette	Bogie Rear Axle 2/Linear 2	Bogie Rear Axle 1/Linear 1	Kingpin	Goose Neck 1	Goose Neck 2
Sample 2519 (MPa)	3.79	3.13	1.34	5.03	97.38	7.77
MPT FEA stress with 1g acceleration (MPa)	3.84	3.72	1.37	6.23	17.83	17.49
Percentage error % (sample versus model)	1.30	15.86	2.19	19.26	446.16	55.57

Table 5.27: Skip 1 test data for FEA model verification

For the second skip placed stationary on the trailer, sample 45177 provided the stresses experienced by the trailer. Table 5.28 shows the comparison.

Name	Bogie Rosette	Bogie Rear Axle 2/Linear 2	Bogie Rear Axle 1/Linear 1	Kingpin	Goose Neck 1	Goose Neck 2
Sample 45177 (MPa)	11.57	10.55	3.56	2.35	48.94	15.68
MPT FEA stress with 1g acceleration (MPa)	12.62	11.84	3.99	3.14	17.26	17.57
Percentage error % (sample versus model)	8.32	10.90	10.78	25.16	183.55	10.76

Table 5.28: Skip 2 test data for FEA model verification

Most of the stress values of the sample test data compare within an acceptable range of 0.05-9.72 MPa or 1.30-25% [57] with that from the FEA model at static load (calculated from strain gauges subject to low disturbances [56]). Although the percentage error values were high it was noted that the majority

were better in comparison compared to the BTT, and the field test results were lower than the FEA results providing a safe design [57].

The first skip was unlikely to be evenly loaded onto the trailer hence the strain gauge on one centre beam (Bogie Rosette, Bogie Linear 2 and Goose Neck 2) provided a larger stress value compared to the other gauge at a similar point on the other centre beam. The FEA assumes the load is spread evenly over the given surface area and provides a more uniform result regarding the symmetry of the trailer, uneven loading should be a consideration for future FEA models. The difference in results should not be taken as a high error rather that the loading is different in actual conditions compared to the FEA simulation. The second skip was loaded more evenly with a single motion using the forklift, and the stress comparison was better. The second skip (Skip 2) was loaded on the rear of the trailer hence giving greater readings on the bogie strain gauges. The kingpin comparison of the field test data and FEA stresses are better compared to that of the BTT, due to the strain gauge being shielded from noise and disturbances from the hauler and other loading vehicles [56]. The MPT has a top plate on the trailer compared to the BTT skeletal frame. Although a difference in results are present, other factors such as the hauler's self-levelling suspension, skips loaded and the king pin self-aligning with the fifth wheel, bring unforeseen strain into the data. Goose Neck 1 was omitted from the comparison because of the contaminant in the gauge.

The FEA acceleration values were assessed using the information from the trailer routes in Chapter 5.4.3.1. This was determined by using maximum absolute acceleration values from the test data routes which include where the trailers were driven with severe turning, acceleration and emergency braking to attain all possible outcomes that might occur during operations. From the field testing data a maximum of 0.20g in the lateral direction and 0.216g in the longitudinal direction was recorded when the trailer was fully laden. Acceptable safety factors of 1.25 and 2.31 from the recommended ranges [28], [49] were incorporated for the lateral and longitudinal accelerations respectively, such that values of 0.25g and 0.5g can be used as the new FEA loading accelerations which comply with the recognised standards which recommend these loading accelerations as discussed in Chapter 4.10.1. By using the 0.25g lateral acceleration as modelled in Chapter 4.10.3.4 and the 0.5g longitudinal acceleration it would allow better optimised acceleration values used for the redesign in Chapter 6. The FEA vertical 2g previously used can be reduced to 1.5g and still incorporate a dynamic design factor of 1.5 from the recommended ranges shown in Cowling's study [41]. This was determined using the maximum absolute g value of 0.434g from Table 5.20 compared to the 1.5g value now proposed for future FEA design process. Table 5.19 which shows acceleration values for Route 2 with the two empty skips, provides acceleration data that exceed that of Table 5.7. However, the mass loads of the two empty skips (4 200 kg each) with those peak accelerations, present low stresses of no concern when simulated using FEA. Thus, the accelerations proposed above are not influenced.

6. Redesign of trailers

6.1 Introduction and loading accelerations

The redesign of the trailers was performed, with the FEA assessment and field testing of the existing designs, as a foundation. The redesign was therefore based on a good understanding of previous designs in the port environment in which the trailers operate. The reference loading conditions for the vertical downwards, longitudinal and lateral acceleration found in Chapter 4.10.1, provides an excellent reference for trailer design and modelling as verified in Chapter 5, using the accelerations obtained from field tests. The Richard's Bay Port yielded more favourable road conditions as shown in Chapter 5.4. The trailers model's redesign was done using the material dimensions reduced for the centre beams in Chapter 4.6 and 4.9. The FEA simulations were performed using the acceleration loading values (1.5g vertical, 0.5g longitudinal and 0.25g lateral accelerations) determined from the field testing results with included safety factors as shown in Chapters 5.3.4 and 5.4.4.

6.1.2 BTT Analysis

6.1.2.1 General finite model

The FEA model from 4.10.2.1 was structurally modified and solved to illustrate the redesign of the trailer with the same loads and constraints. The structural material thickness changes determined as shown in Chapter 4.6 have been performed for the centre beams. The material used in the redesign is S355 steel [55], as the steel used in the original design, namely 300WA has been discontinued.

The global coordinates in the comparisons correspond to X denoting longitudinal, Y denoting vertical and Z denoting lateral directions.

6.1.2.2 BTT – 1.5g vertical downward acceleration

The principle criteria for assessing the results of the FEA model was that the Von-Mises stress should not exceed the yield stress of the material. The loading acceleration of 1.5g has the included dynamic design factor of 1.5 [41] as shown in Chapter 5.3.4.

The 1.5g caseloads are tabulated below:

Force	Magnitude	Location
Gravity	14.72 m/s^2 (g)	Entire model
Container loads	30.48 tons per container	On surface areas of the container which are in contact with the trailer

Table 6.1: Vertical loads and values

The caseload constraints are tabulated below:

Constraint	Location
Translation X	On kingpin
Translation Y	On bottom of springs
Translation Z	On kingpin and suspension

Table 6.2: Load constraints

The analysis complied with the design criteria and the stresses were found to be below the yield stress as shown in Figures 6.1 to 6.6. except for the peak localised stress found on a few elements as previously explained in Chapter 4.10.2.2 [25], [38], [39], [40], [41].The FEA model showed that the trailer will support its full static load mass with a peak allowable stress range of 207 MPa to 230 MPa which allows an acceptable safety factor range of 1.54-1.71 from the range in [28] using material properties [55].

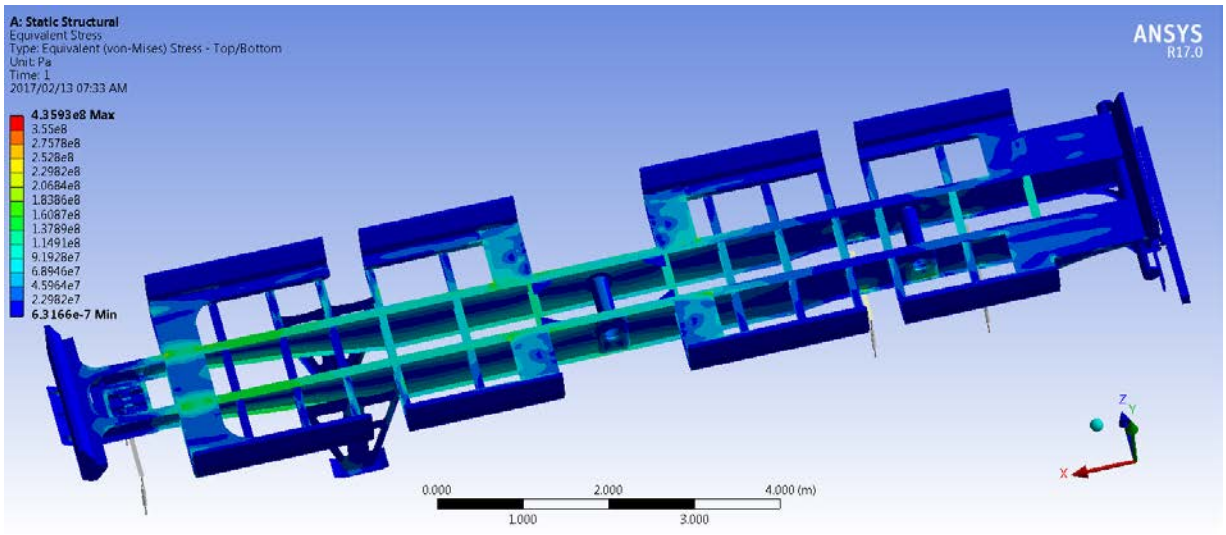

Figure 6.1: Stress plot - top view (Von-Mises)

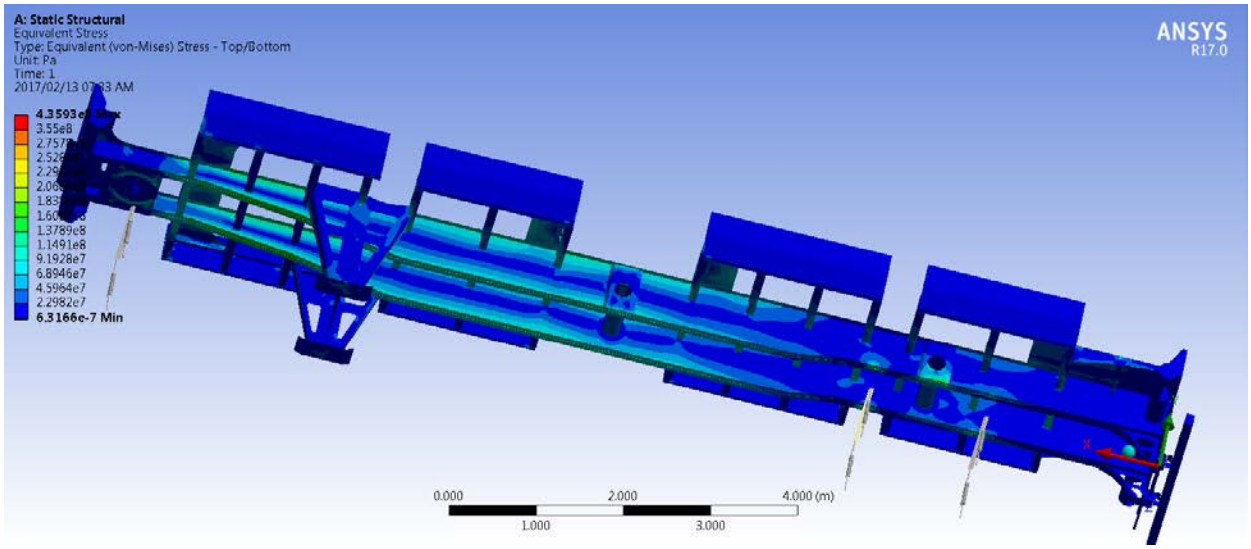

Figure 6.2: Underframe Stress plot (Von-Mises)

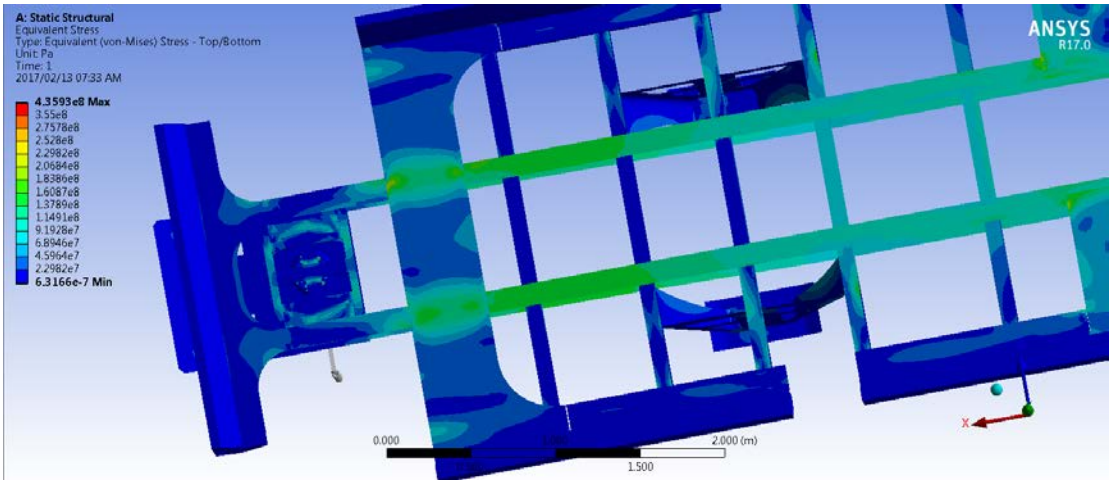

Figure 6.3: Closer view of the kingpin area

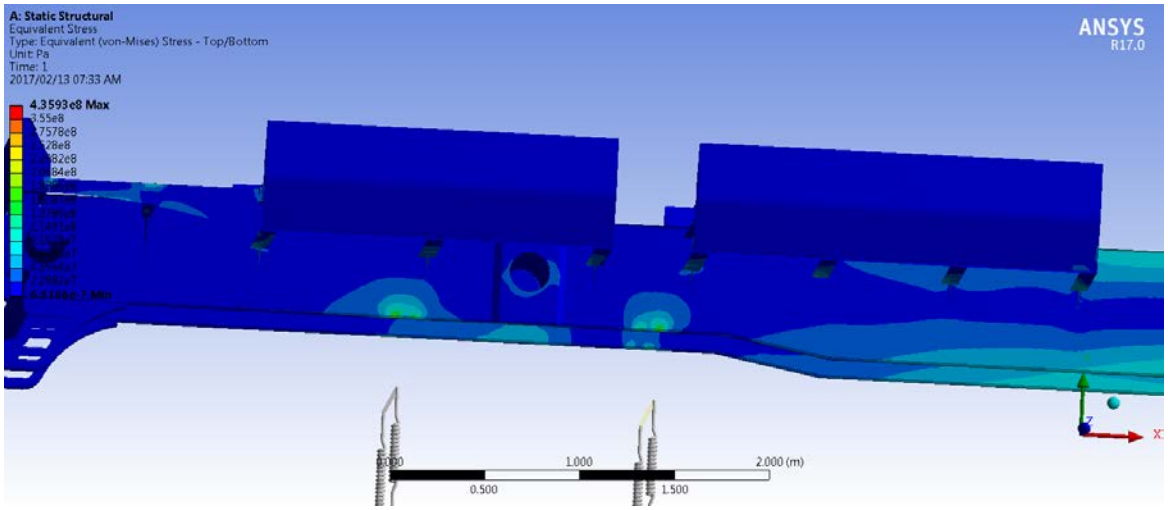

Figure 6.4: Close up Stress plot – bogie/suspension mounting (Von-Mises)

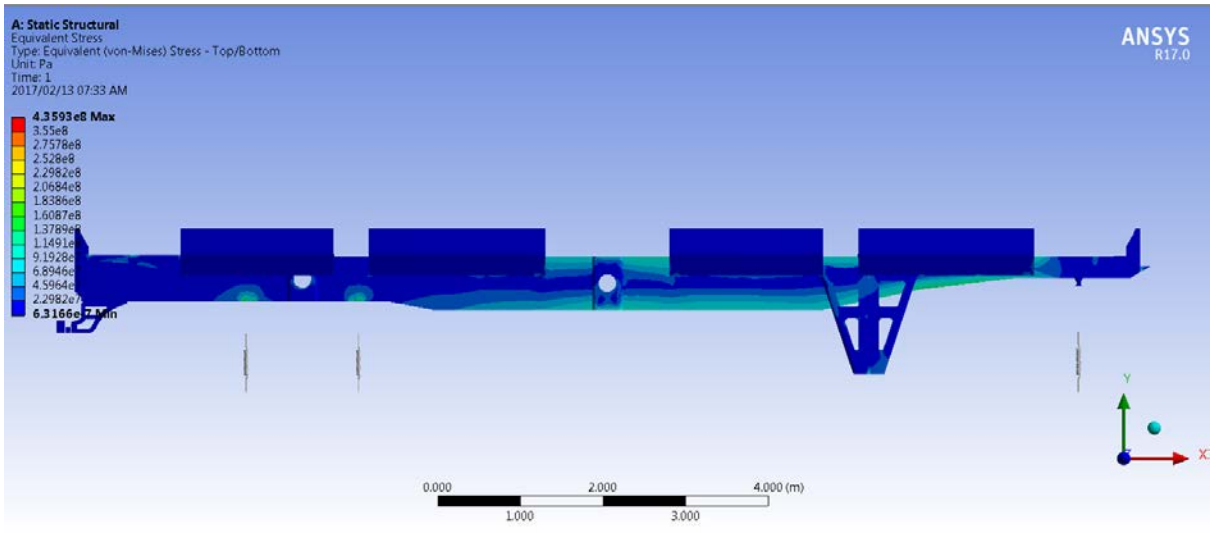

Figure 6.5: Stress plot of main centre beam (Von-Mises)

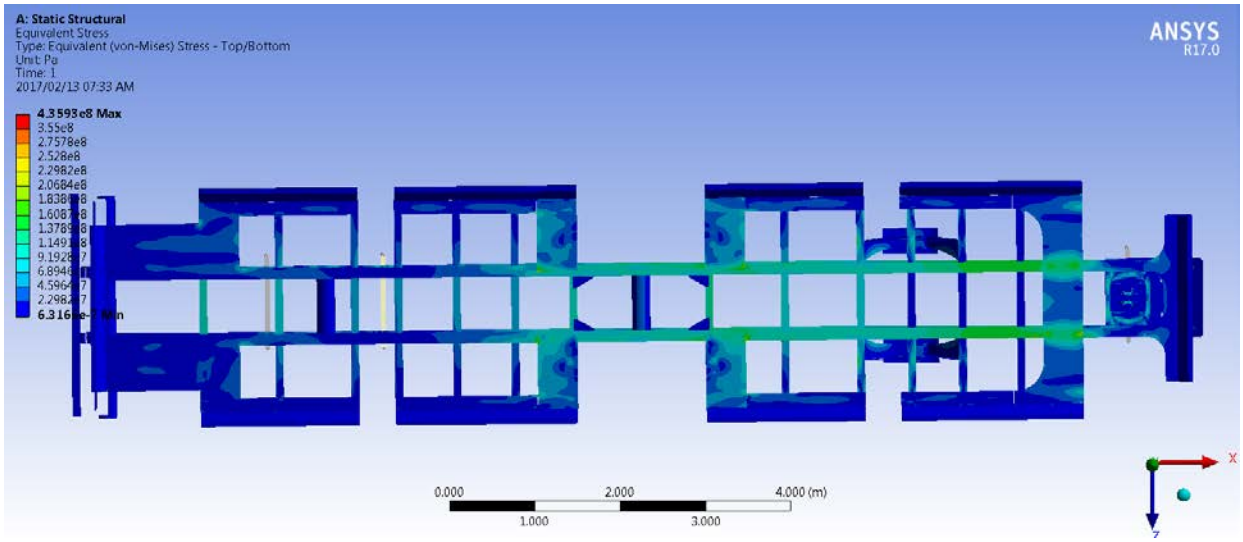

Figure 6.6: Stress plot of top of trailer (Von-Mises)

6.1.2.3 BTT – 0.5g longitudinal acceleration and 1g vertical acceleration

The fully loaded trailer structure must sustain a 0.5g longitudinal and 1g vertical acceleration together with the applied loads. The principle criteria for assessing the results of the FEA model was that the Von-Mises stress should not exceed the yield stress of the material. The 0.5g loading acceleration has the included safety factor of 1.80 [28], [49] as shown in Chapter 5.3.4.

The 0.5g + 1g caseloads are tabulated below:

Force	Magnitude	Location
Gravity (vertical)	-9.81 m/s^2 (g)	Entire model
Container loads	30.48 tons per container	On surface areas of the container which are in contact with the trailer
Longitudinal acceleration	4.905 m/s^2 (0.5 x g)	Entire model

Table 6.3: Vertical and longitudinal loads and values

The caseload constraints are tabulated below:

Constraint	Location
Translation X	On kingpin
Translation Y	On bottom of springs
Translation Z	On kingpin and suspension

Table 6.4: Load constraints

The analysis complied with the design criteria as shown in Figures 6.7 to 6.11 with a peak allowable stress of 219 MPa. The region where spring elements attach to the centre beams, and right angled connections between mating members, has a tendency to produce high stress regions [25], [38], [39], [40], [41]. These localised stress regions also found in Chapter 4.10.2 were investigated on operational trailers at the port in Chapter 5.3.3.2 and none showed damage, cracking or deformation.

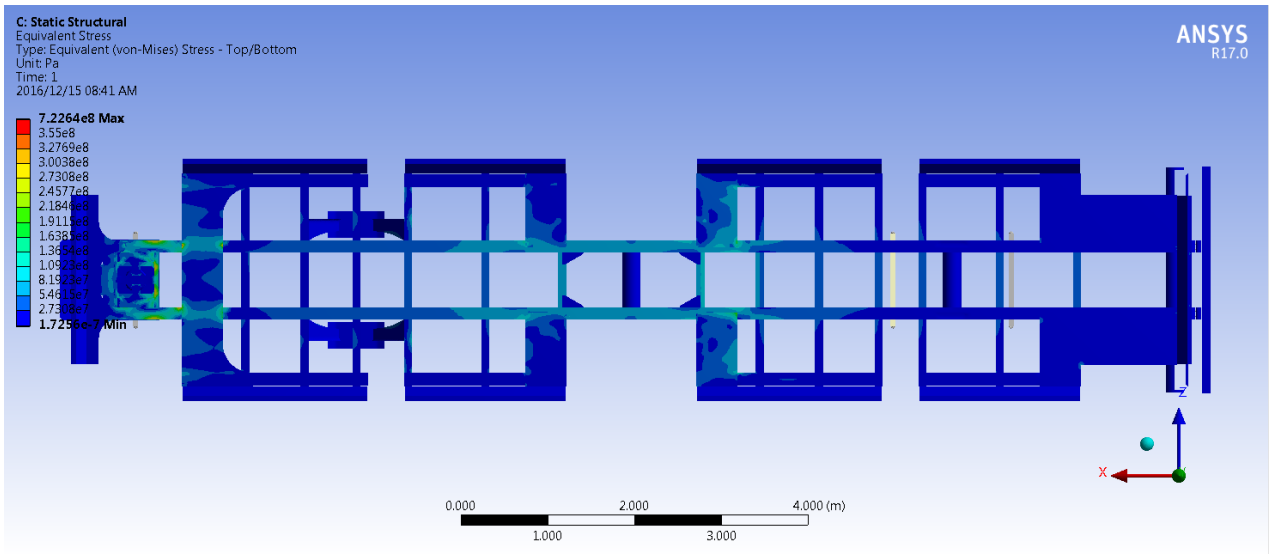

Figure 6.7: Stress plot - top view (Von-Mises)

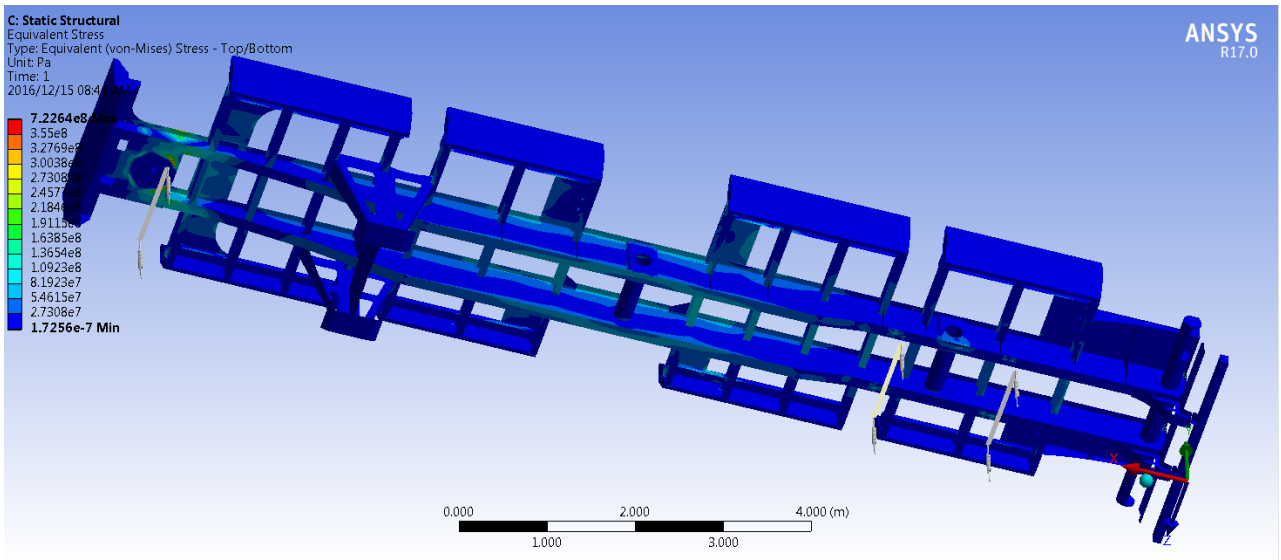

Figure 6.8: Underframe Stress plot - (Von-Mises)

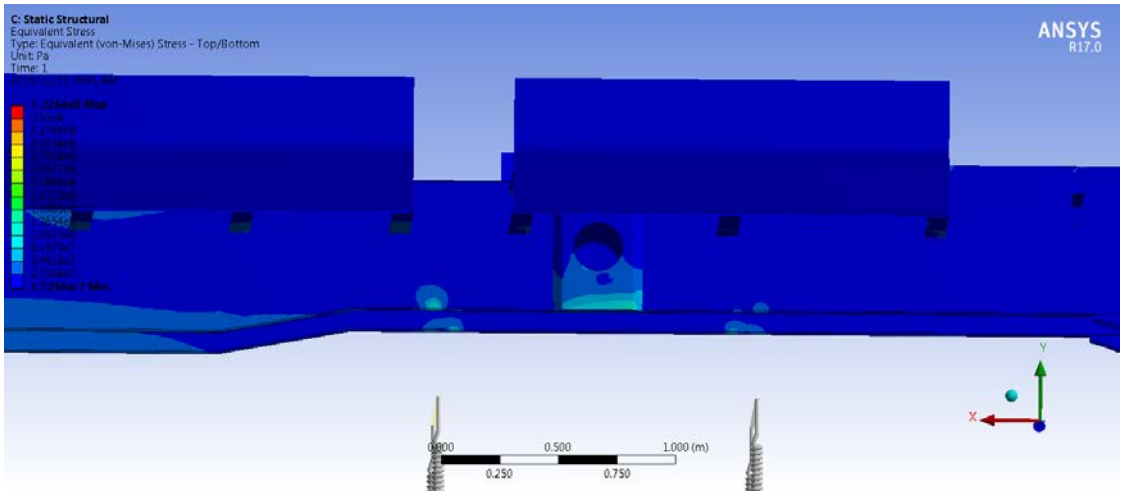

Figure 6.9: Close up Stress plot – bogie/suspension mounting (Von-Mises)

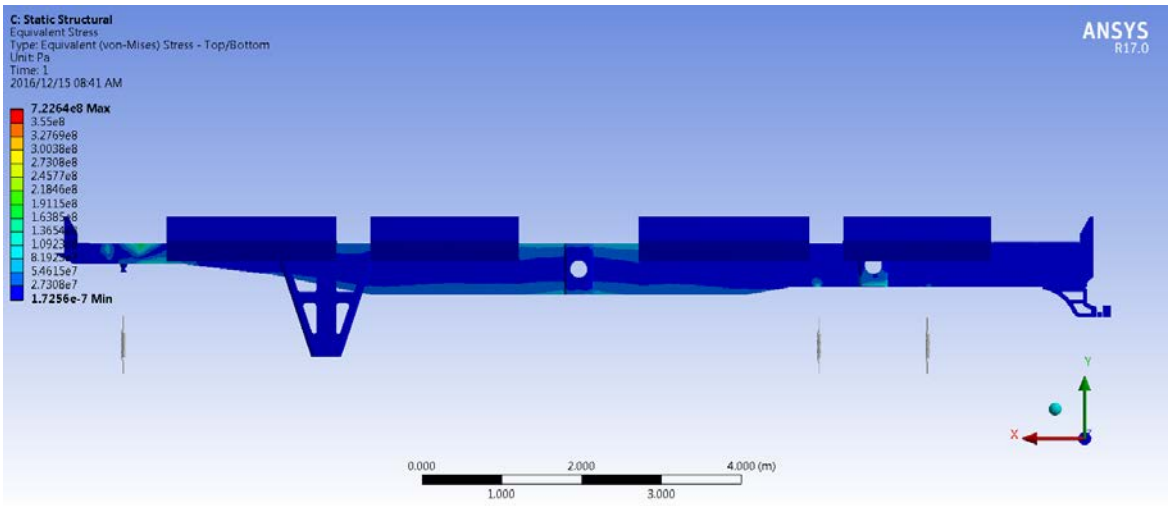

Figure 6.10: Stress plot of main centre beam (Von-Mises)

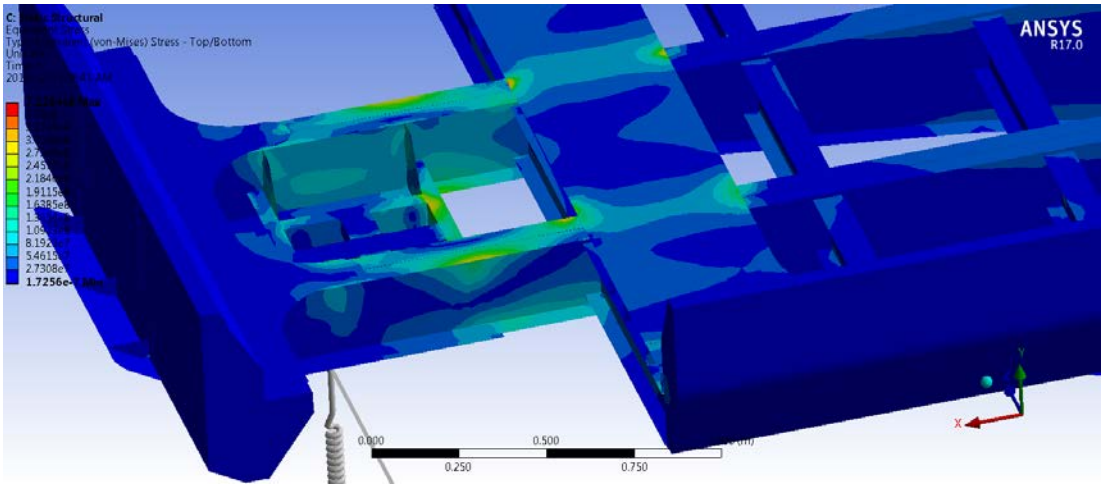

Figure 6.11: Localised stress (>355 MPa) previously found near the kingpin has been alleviated

6.1.2.4 BTT – 0.25g lateral acceleration and 1g vertical acceleration

The fully loaded trailer structure must sustain a 0.25g lateral and 1g vertical acceleration together with the applied loads. The principle criteria for assessing the results of the FEA model was that the Von-Mises stress should not exceed the yield stress of the material. The loading acceleration of 0.25g has the included safety factor of 1.26 [28], [49] included as shown in Chapter 5.3.4.

The 0.25g + 1g caseloads are tabulated below:

Force	Magnitude	Location
Gravity (vertical)	-9.81 m/s^2 (g)	Entire model
Container loads	30.48 tons per container	On surface areas of the container which are in contact with the trailer
Lateral acceleration	2.4525 m/s^2 (0.25 x g)	Entire model

Table 6.5: Vertical and lateral loads and values

The caseload constraints are tabulated below:

Constraint	Location
Translation X	On kingpin
Translation Y	On bottom of springs
Translation Z	On kingpin and suspension

Table 6.6: Load constraints

The analysis complied with the design criteria as shown in Figures 6.12 to 6.16 with a peak allowable stress of 219 MPa except for the localised stress regions found in the FEA [25], [38], [39], [40], [41]. These were investigated on operational trailers at the port in Chapter 5.3.3.2 and none showed damage, cracking or deformation.

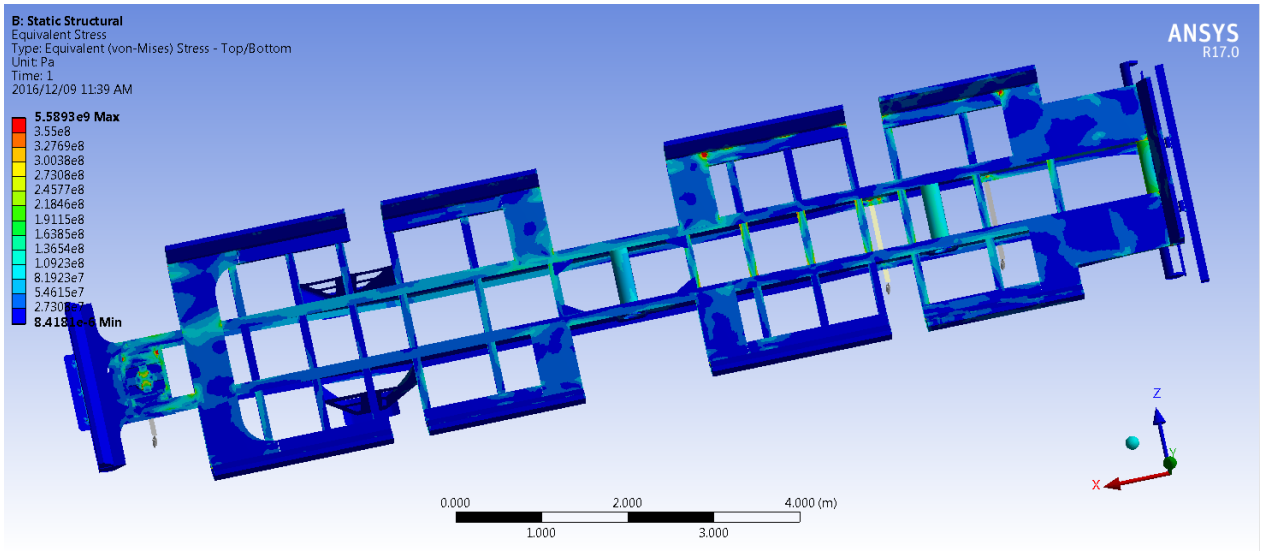

Figure 6.12: Stress plot - top view (Von-Mises)

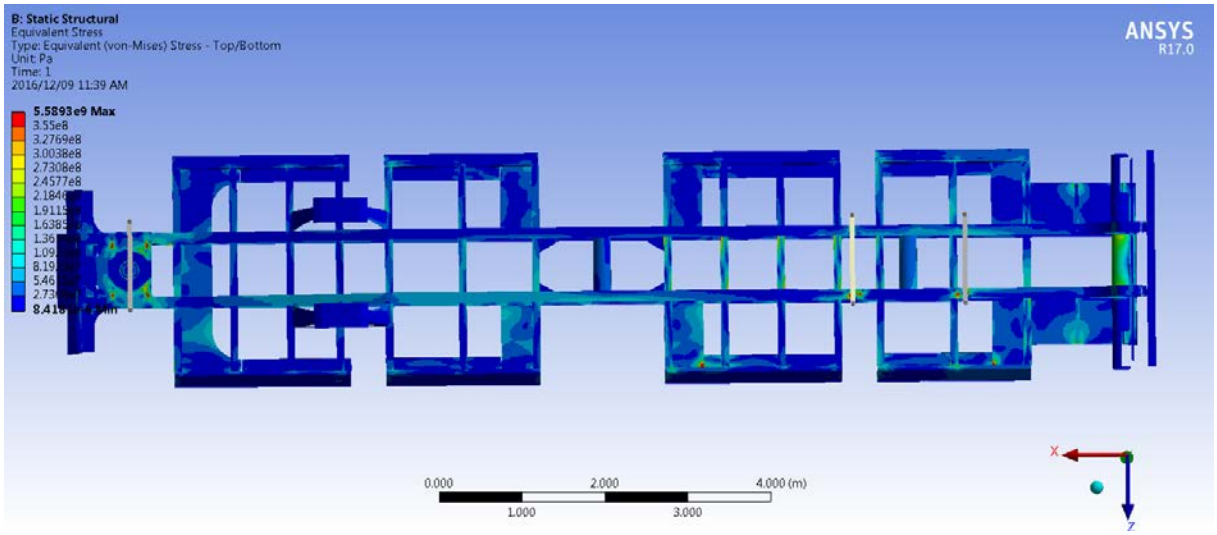

Figure 6.13: Stress plot - bottom view (Von-Mises)

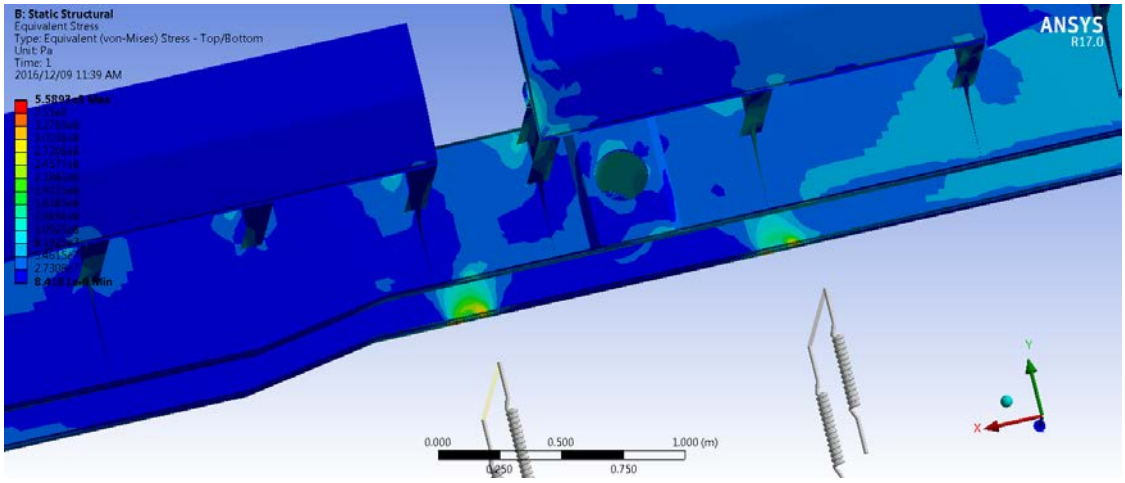

Figure 6.14: Close up Stress plot – bogie/suspension mounting (Von-Mises)

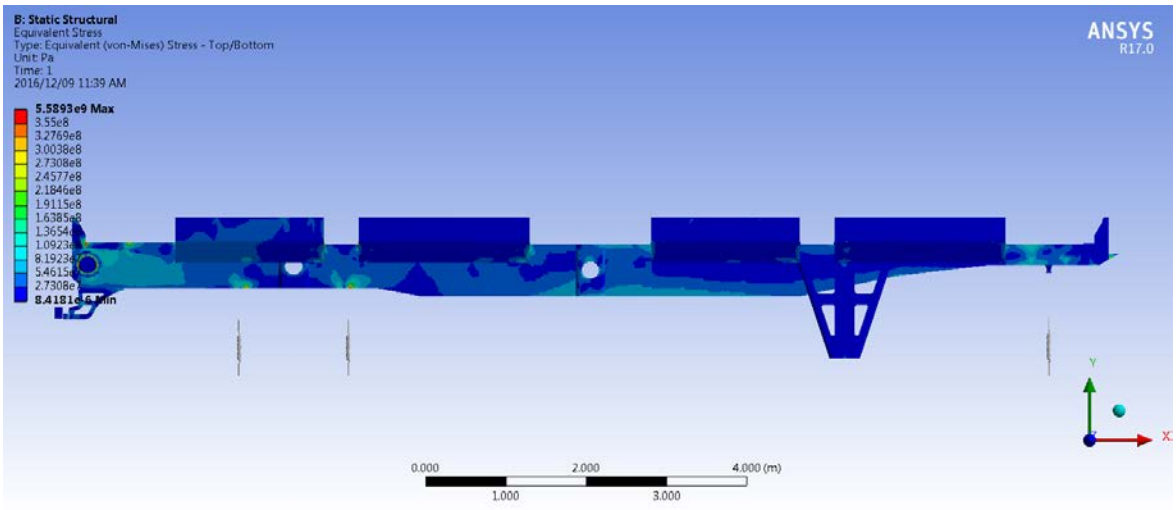

Figure 6.15: Stress plot of main centre beam (Von-Mises)

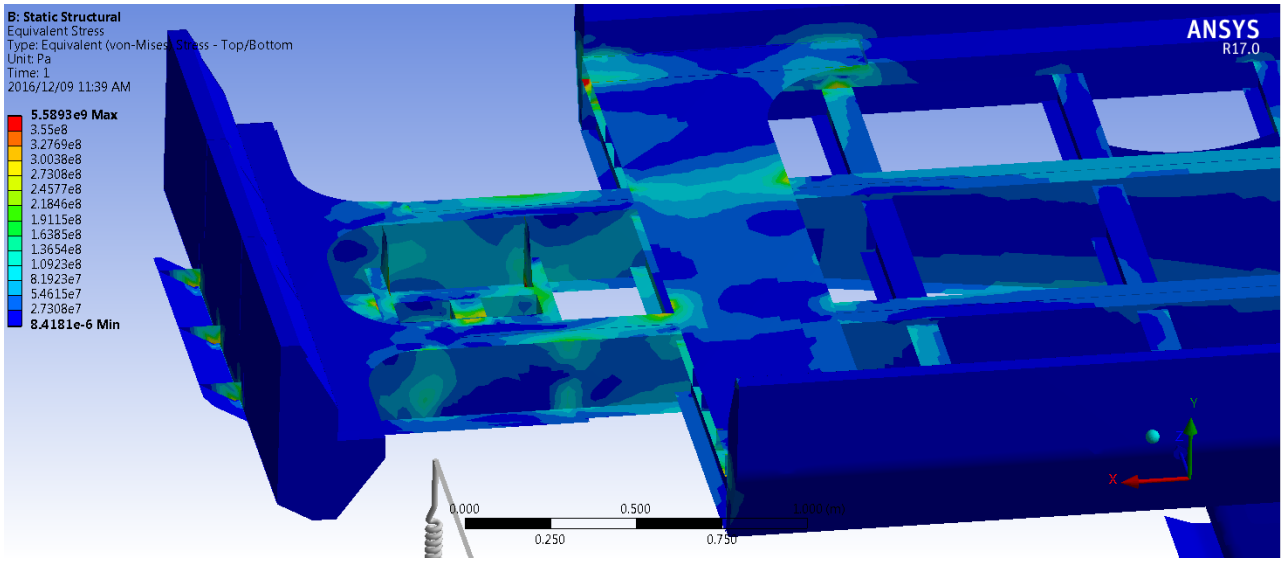

Figure 6.16: Closer view of gussets supporting the skid plate

6.1.2.5 BTT – 1.5g vertical and 0.5g longitudinal and 0.25g lateral acceleration

The fully loaded trailer structure should sustain a 1.5g vertical acceleration, 0.5g longitudinal and 0.25g lateral acceleration together with the applied loads. This loading scenario should allow the total combined cases to be analysed on the structure at once. The principle criteria for assessing the results of the FEA model was that the Von-Mises stress should not exceed the yield stress of the material.

The 1.5g + 0.5g + 0.25g caseloads are tabulated below:

Force	Magnitude	Location
Gravity(vertical)	-14.72 m/s^2 (g)	Entire model
Container loads	30.48 tons per container	On surface areas of the container which are in contact with the trailer
Longitudinal acceleration	4.905 m/s^2 (0.5 x g)	Entire model
Lateral acceleration	2.4525 m/s^2 (0.25 x g)	Entire model

Table 6.7: Vertical, longitudinal and lateral loads and values

The load case constraints are tabulated below:

Constraint	Location
Translation X	On kingpin
Translation Y	On bottom of springs
Translation Z	On kingpin and suspension

Table 6.8: Load constraints

The combined analysis complied with the design criteria as shown in Figures 6.17 to 6.23 with a peak allowable stress of 219 MPa except for the high stress region on the supporting channels for the skid plate in Figures 6.19. It only occurs on a few elements at the area. The region where spring elements attach to the centre beams, and right angled connections between mating members, has a tendency to produce these high stress regions [25], [38], [39], [40], [41] as previously shown in Chapter 4.10.2.5.

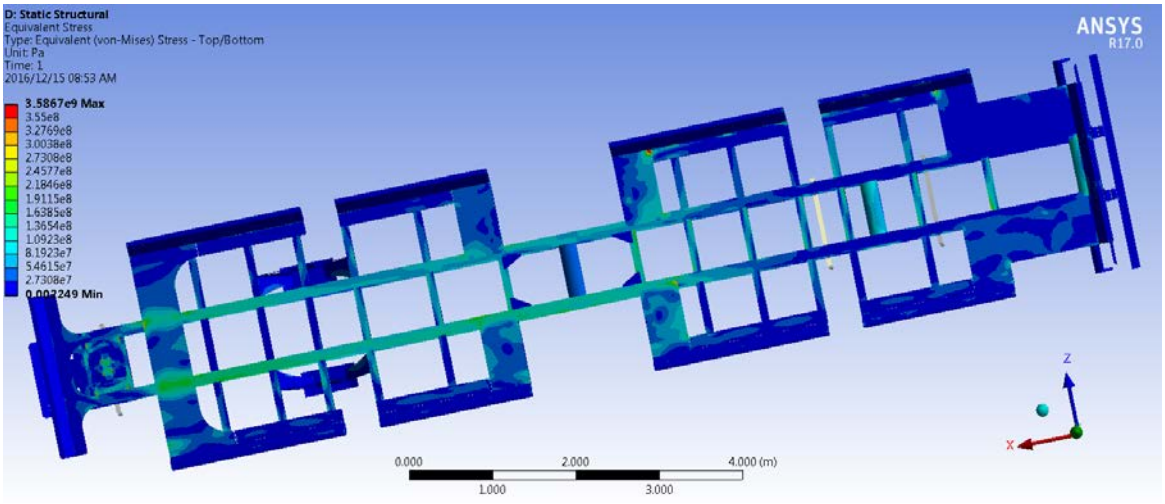

Figure 6.17: Stress plot - top view (Von-Mises)

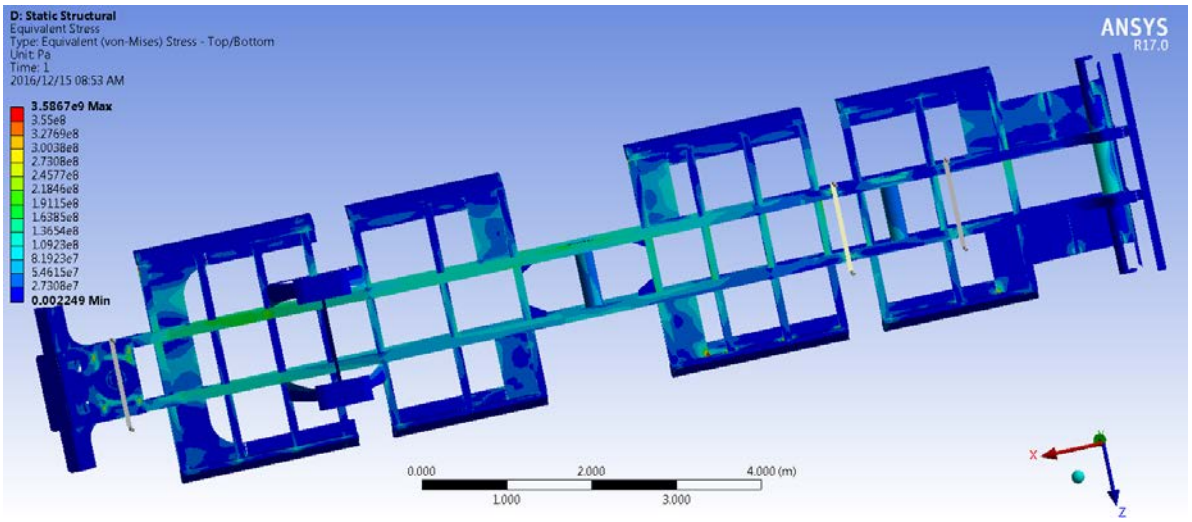

Figure 6.18: Underframe stress plot (Von-Mises)

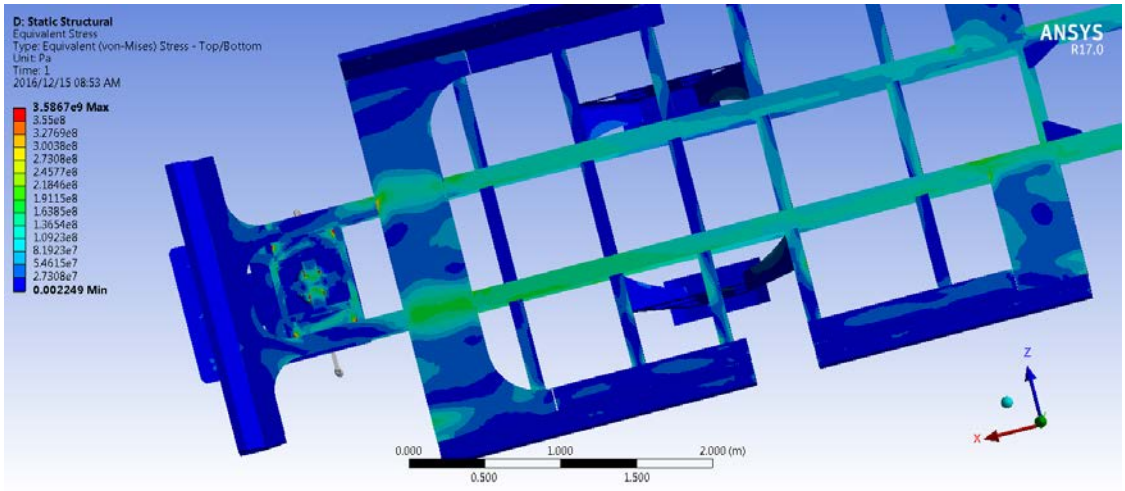

Figure 6.19: High stress region (>355 MPa) found at the supporting channel of the kingpin area

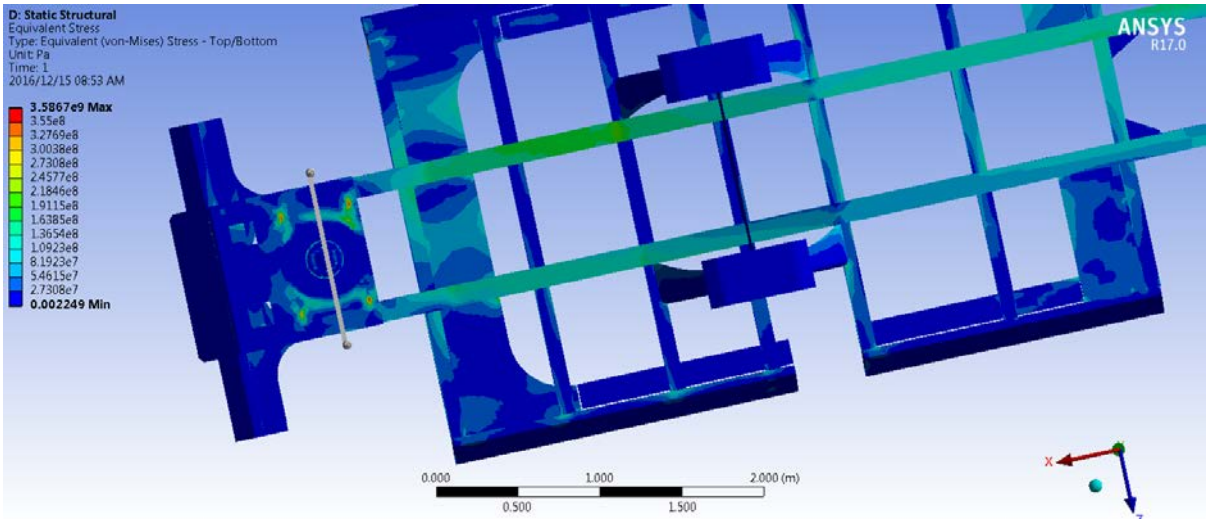

Figure 6.20: Localised stresses (>355 MPa) found on the bottom skid plate

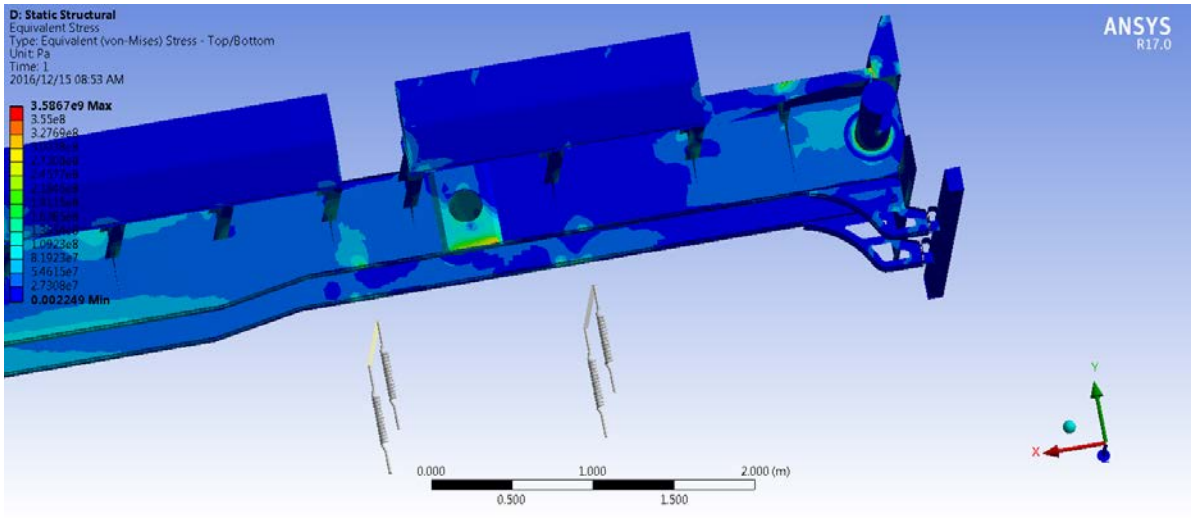

Figure 6.21: Underframe of bogie end stress plot (Von-Mises)

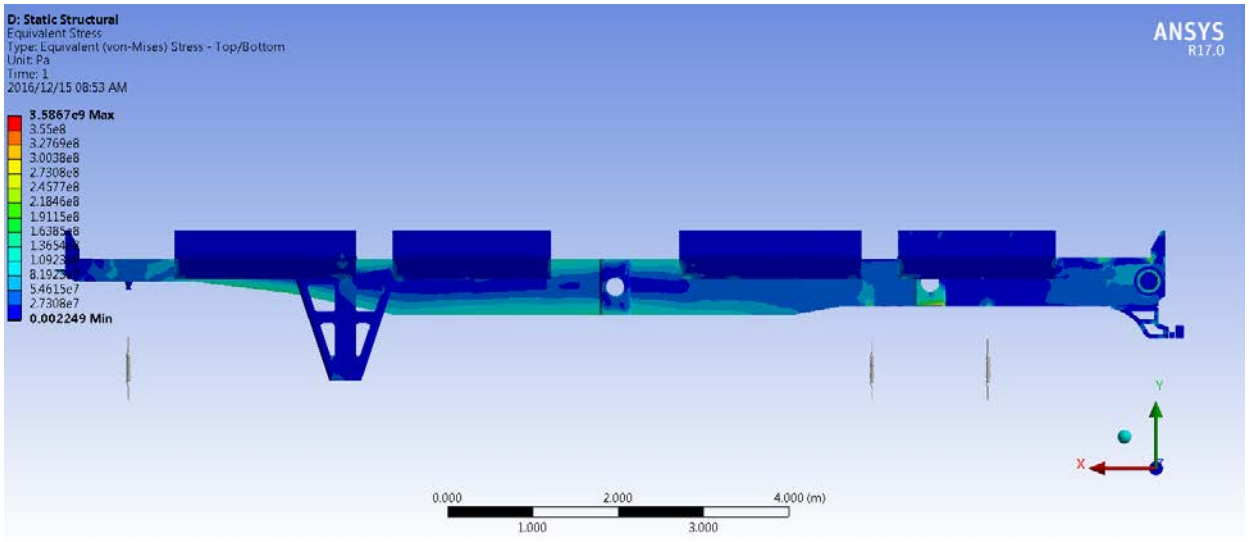

Figure 6.22: Stress plot of main centre beam (Von-Mises)

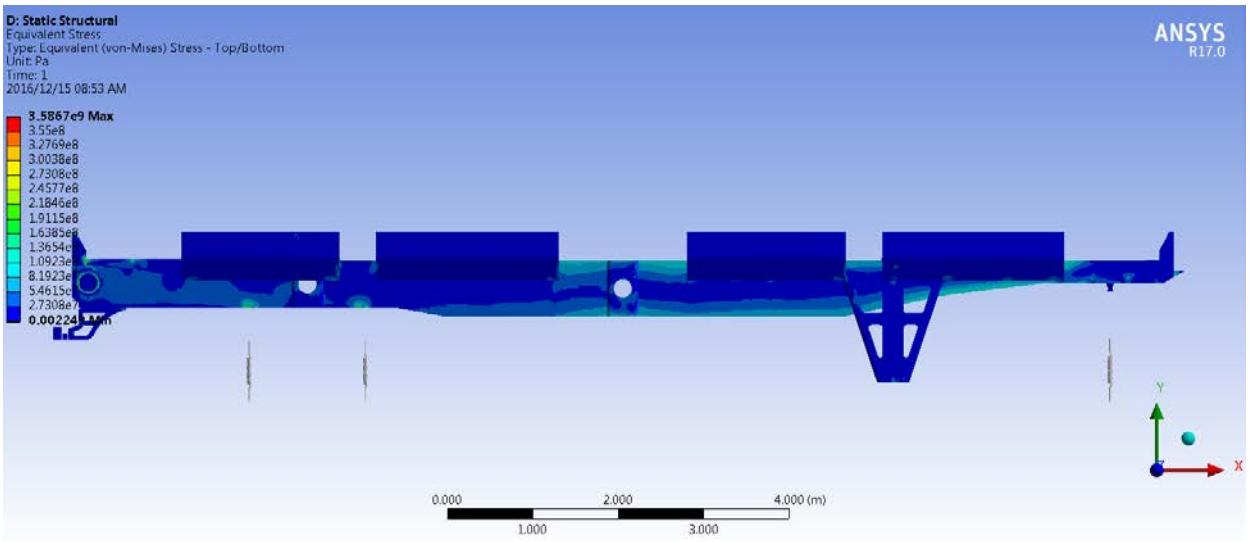

Figure 6.23: Stress plot of main centre beam (Von-Mises)

The final trailer mass is 5769 kg, 610 kg less than the previous design. The current study focused on better optimising the design of the trailers centre beams but other members of the structure can also be better optimised where possible. After non critical material was removed and the thickness of the non-critical structural members were reduced, the FEA was simulated to conform to loading conditions from Chapters 6.1.2.2 to 6.1.2.5. The model in Figure 6.24 and 6.25 with further minimisation of the structure has mass reduced by 775 kg, which means that with the saving of 610 kg on the centre beams, a total of 1385 kg can be saved on material closer to final design.

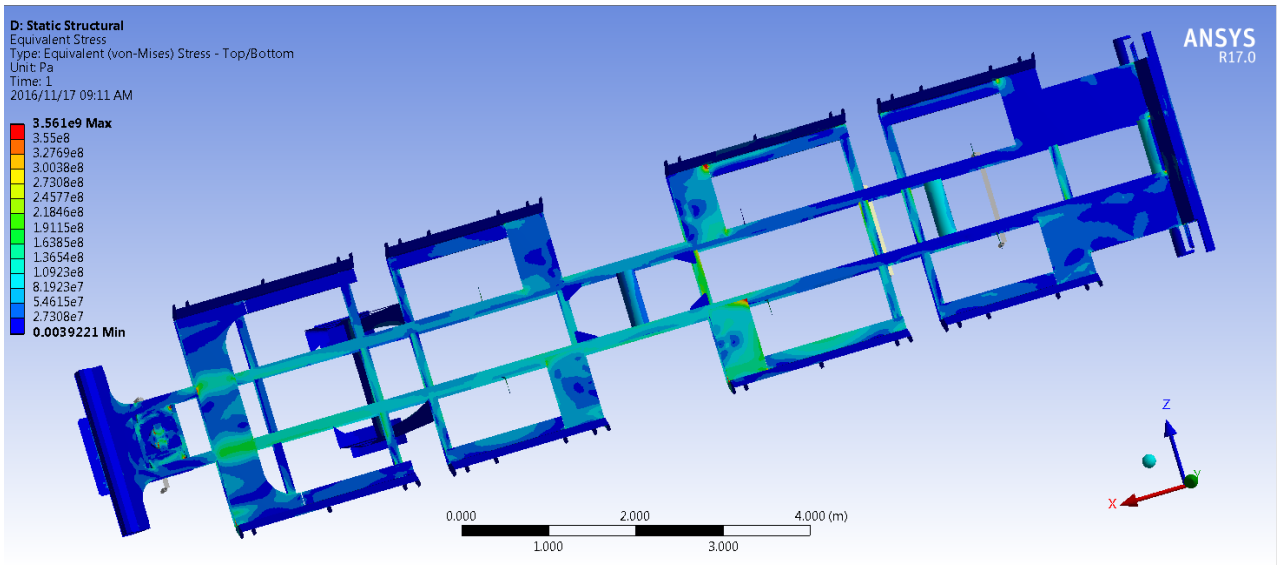

Figure 6.24: Stress plot of redesigned trailer- top view

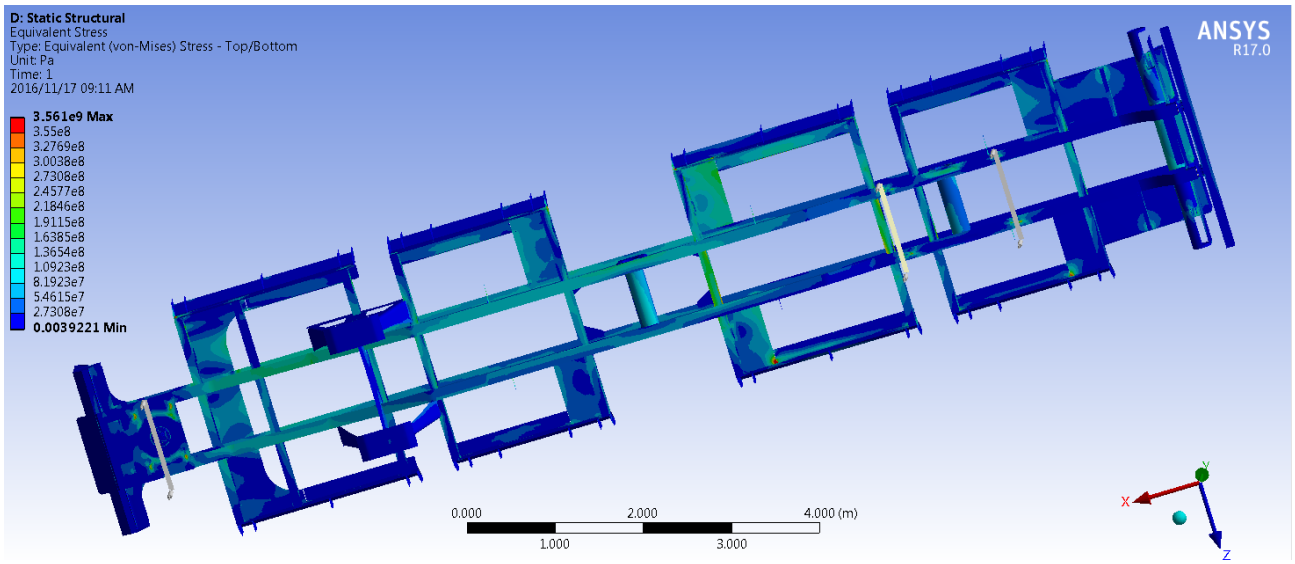

Figure 6.25: Stress plot of redesigned trailer with combined accelerations- bottom view

6.1.3 MPT Analysis

6.1.3.1 General Finite model

The FEA model from Chapter 4.10.3.1 was structurally modified and solved to illustrate the redesign of the trailer. The structural material height and thickness changes shown in Chapter 4.9 were performed for the centre beams, and S355 steel was used as in the existing design. The FEA was simulated to the loading conditions in Chapters 6.1.3.2 to 6.1.3.5 and it was discovered that further optimisation of the model was possible. The following structural changes were also implemented:

a) The centre beams recommended calculated web thickness was 14 mm but upon further FEA investigation, 12 mm was found to be suitable and was used for the FEA model.
b) The web height was decreased from 600 mm to 450 mm to reduce the dimension further. However at the goose neck transition the bottom flange was increased in thickness (25 mm) to overcome high stress experienced in that region by the trailer's centre beams.

The global coordinates in the comparisons correspond to X denoting longitudinal, Y denoting vertical and Z denoting lateral directions.

6.1.3.2 MPT – 1.5g Vertical downward acceleration

The principle criteria for assessing the results of the FEA model was that the Von-Mises stress should not exceed the yield stress of the material. The loading acceleration of 1.5g has the included dynamic design factor of 1.5 [41] as shown in Chapter 5.4.4.

The 1.5g caseloads are tabulated below:

Force	Magnitude	Location
Gravity	14.72 m/s^2 (1.5 x g)	Entire model
Skip loads	44.2 tons per skip	On surface areas of the skip which are in contact with the trailer

Table 6.9: Vertical load cases and values

The caseload constraints are tabulated below:

Constraint	Location
Translation X	On kingpin
Translation Y	On bottom of springs
Translation Z	On kingpin and suspension

Table 6.10: Load constraints

The analysis complied with the design criteria with a peak allowable stress range of 178 MPa to 266 MPa as shown in Figures 6.23 to 6.30 which allows an acceptable safety factor range of 1.33-1.99 from [28] using material properties [55]. The two high stress regions at the goose neck (Figure 6.28) and near the suspension pedestals (Figure 6.30) are eliminated which were present in the original design in Chapter 4.10.3.2. The highest stress value in the stress legend corresponds to a single element near the king pin due to modelling approximations [25], [38], [39], [40], [41].

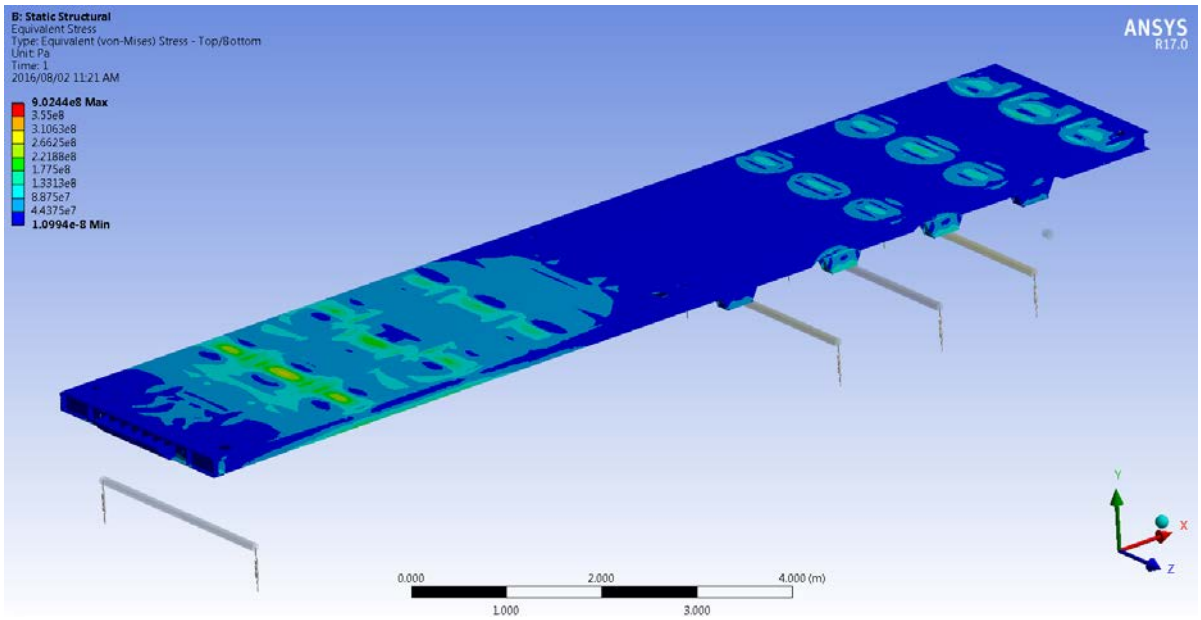

Figure 6.26: Stress plot - top view (Von-Mises)

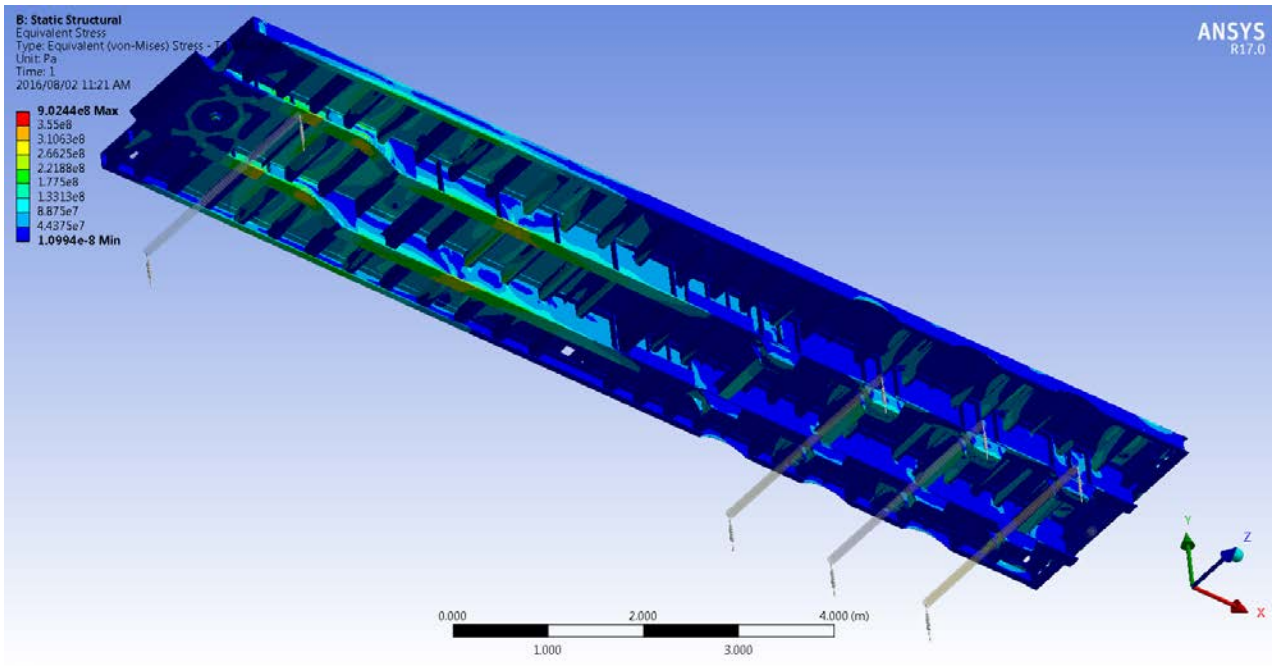

Figure 6.27: Underframe stress plot (Von-Mises)

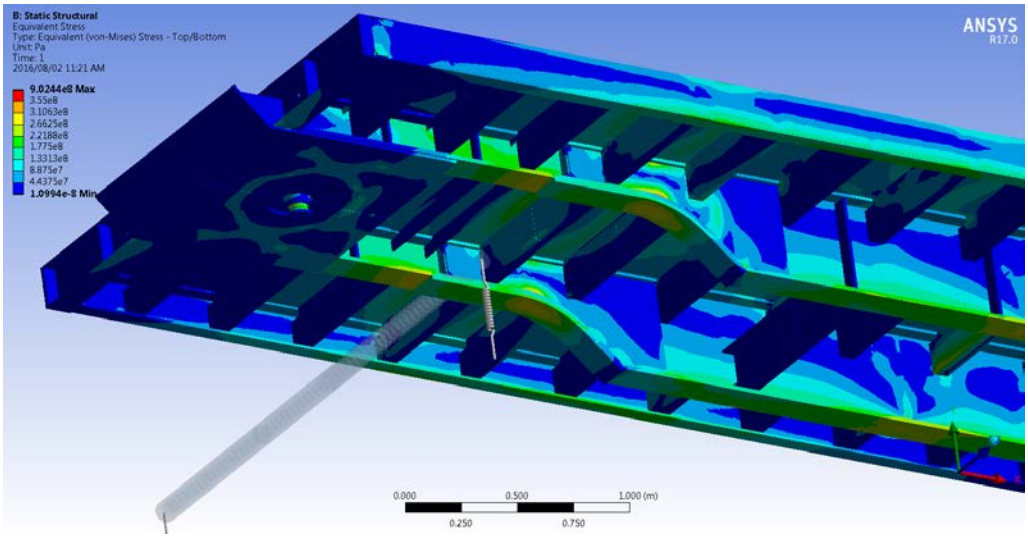

Figure 6.28: View of the bend of the goose neck

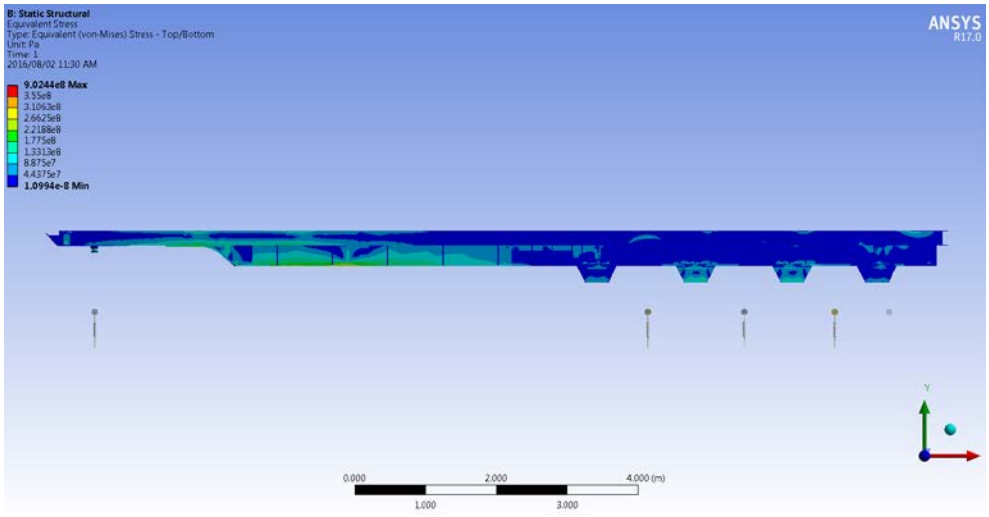

Figure 6.29: Stress plot of main centre beam (Von-Mises)

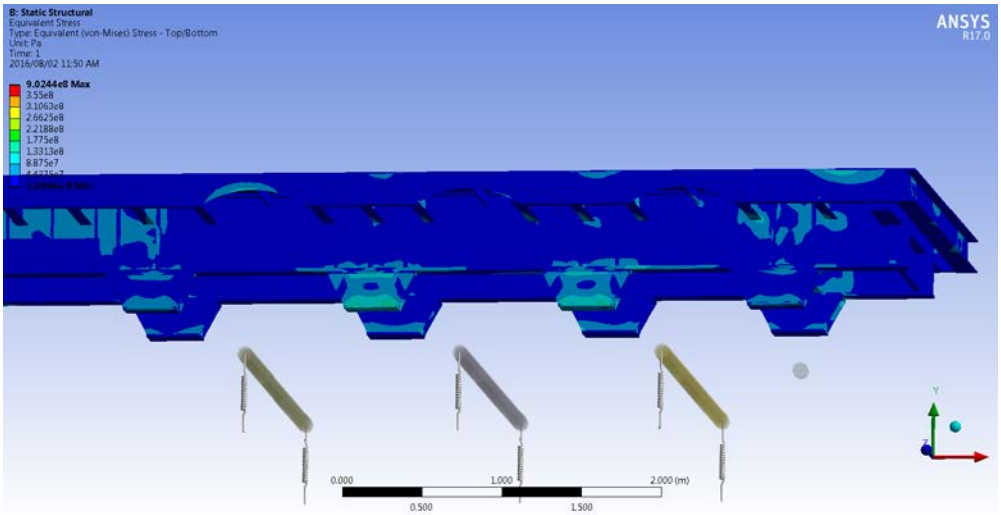

Figure 6.30: Stresses of the main beam and the suspension pedestals

6.1.3.3 MPT – 0.5g longitudinal acceleration and 1g vertical acceleration

The fully loaded trailer structure must sustain a 0.5g longitudinal and a 1g vertical acceleration together with the applied loads. The principle criteria for assessing the results of the FEA model was that the Von-Mises stress should not exceed the yield stress of the material. The loading acceleration of 0.5g has the included safety factor of 2.31 [28], [41], [49] included as shown in Chapter 5.4.4.

The 0.5g + 1g caseloads are tabulated below:

Force	Magnitude	Location
Gravity(vertical)	-9.81 m/s^2 (g)	Entire model
Skip loads	44.2 tons per skip	On surface areas of the skip which are in contact with the trailer
Longitudinal acceleration	4.905 m/s^2 (0.5 x g)	Entire model

Table 6.11: Vertical and longitudinal loads and values

The caseload constraints are tabulated below:

Constraint	Location
Translation X	On kingpin
Translation Y	On bottom of springs
Translation Z	On kingpin and suspension

Table 6.12: Load constraints

The analysis complied with the design criteria and the stresses were found to be below the yield stress as shown in Figures 6.31 to 6.33. The peak allowable stress is 219 MPa. The highest stress value in the stress legend corresponds to a single element near the king pin and is due to modelling approximations [25], [38], [39], [40], [41].

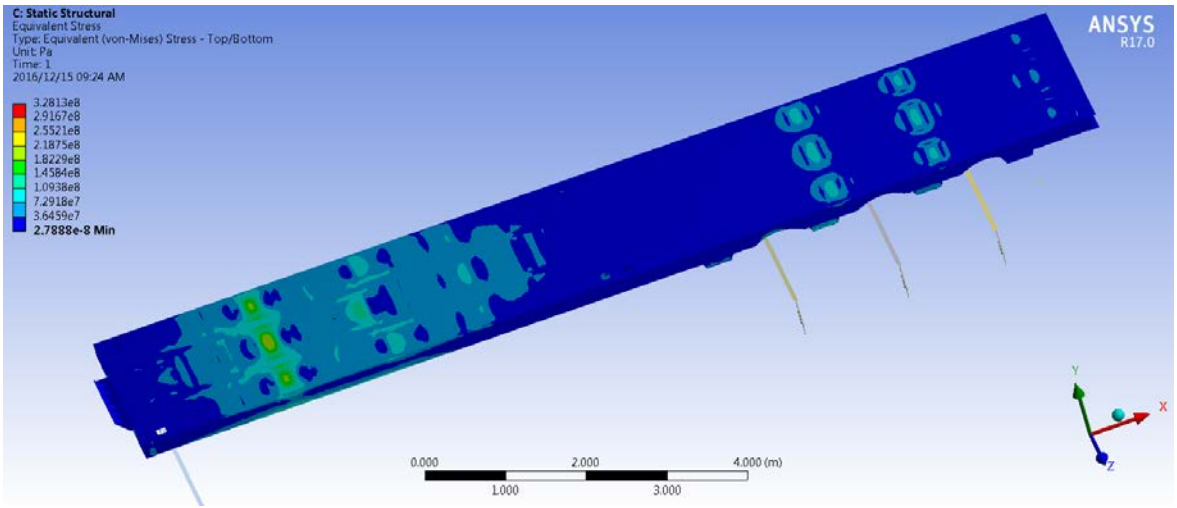

Figure 6.31: Stress plot - top view (Von-Mises)

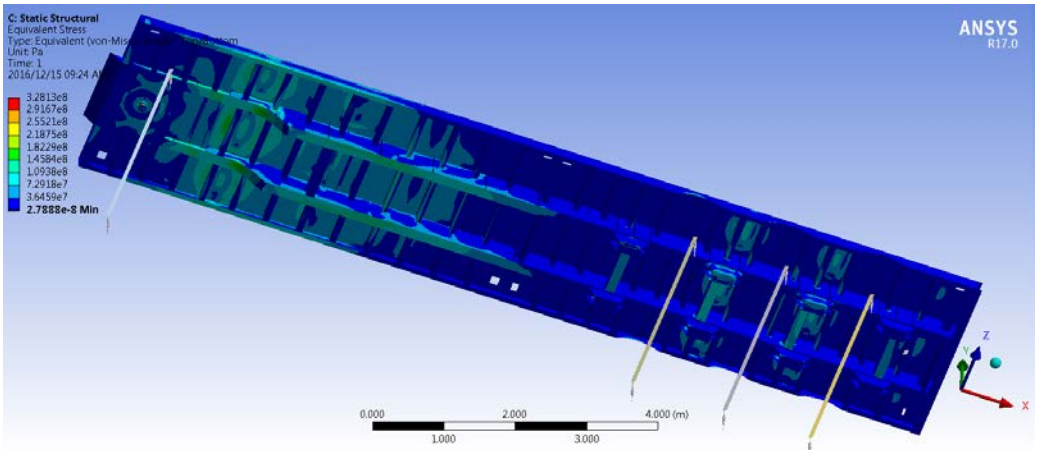

Figure 6.32: Underframe stress plot (Von-Mises)

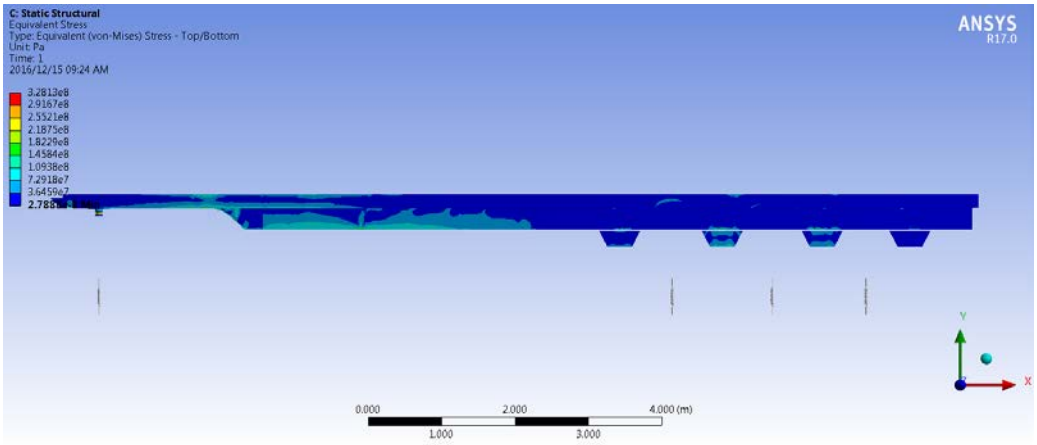

Figure 6.33: Stress plot of main centre beam (Von-Mises)

6.1.3.4 MPT – 0.25g lateral acceleration and 1g vertical acceleration

The fully loaded trailer structure must sustain a 0.25g lateral and a 1g vertical acceleration together with the applied loads. The principle criteria for assessing the results of the FEA model was that the Von-Mises stress should not exceed the yield stress of the material. The loading acceleration of 0.25g has the included safety factor of 1.25 [28], [49] included as shown in Chapter 5.4.4.

The 0.25g + 1g caseloads are tabulated below:

Force	Magnitude	Location
Gravity(vertical)	-9.81 m/s^2 (g)	Entire model
Skip Loads	44.2 tons per skip	On surface areas of the skip which are in contact with the trailer
Lateral acceleration	2.4525 m/s^2 (0.25 x g)	Entire model

Table 6.13: Vertical and lateral loads and values

The caseload constraints are tabulated below:

Constraint	Location
Translation X	On kingpin
Translation Y	On bottom of springs
Translation Z	On kingpin and suspension

Table 6.14: Load constraints

The analysis complied with the design criteria and the stresses were found to be below the yield stress as shown in Figures 6.34 to 6.36. The peak allowable stress is 234 MPa. The highest stress value in the stress legend corresponds to a single element near the king pin and can be omitted because of modelling approximations [25], [38], [39], [40], [41].

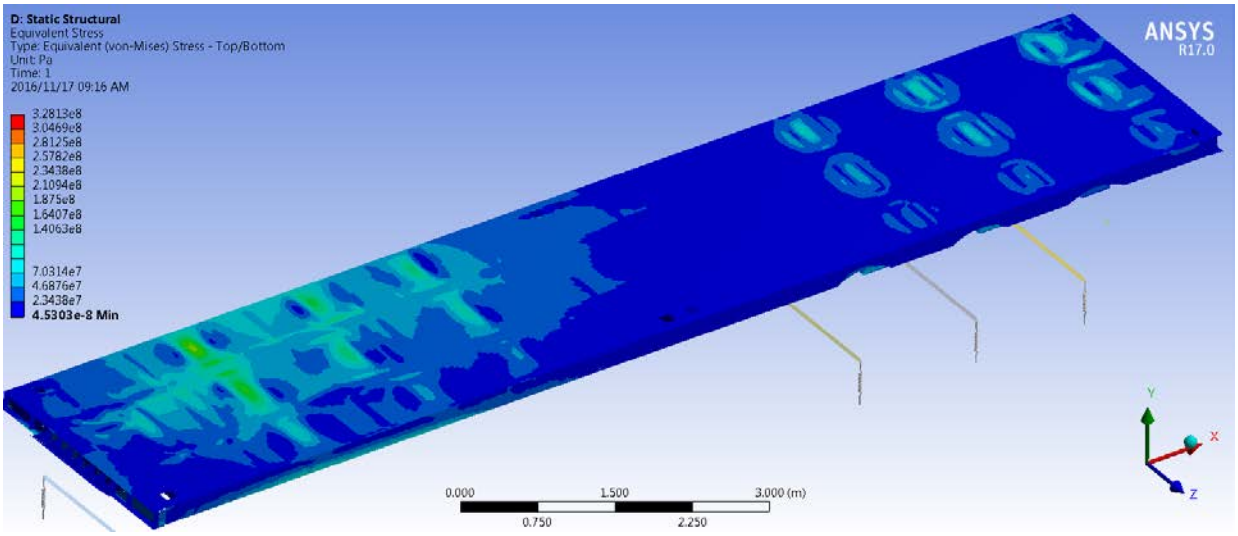

Figure 6.34: Stress plot - top view (Von-Mises)

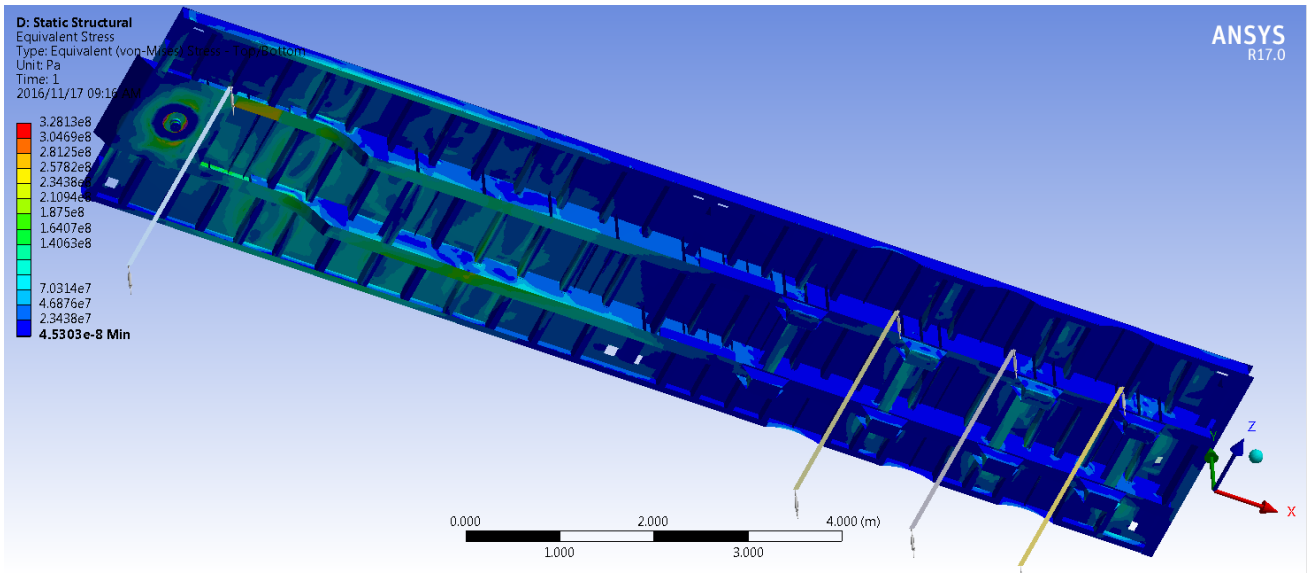

Figure 6.35: Underframe stress plot (Von-Mises)

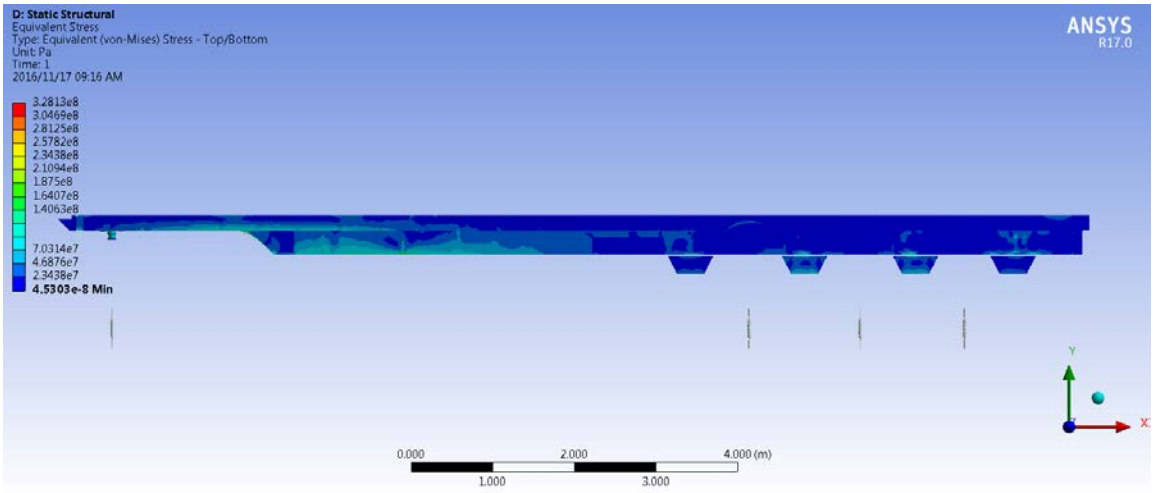

Figure 6.36: Stress plot of main centre beam (Von-Mises)

6.1.3.5 MPT – 1.5g vertical and 0.5g longitudinal and 0.25g lateral acceleration

The fully loaded trailer structure must sustain a 1.5g vertical acceleration, 0.5g longitudinal and 0.25g lateral acceleration together with the applied loads. This loading scenario allows the total combined cases to be analysed on the structure at once. The principle criteria for assessing the results of the FEA model was that the Von-Mises stress should not exceed the yield stress of the material.

The 1.5g + 0.5g + 0.25g caseloads are tabulated below:

Force	Magnitude	Location
Gravity(vertical)	-14.72 m/s^2 (1.5 x g)	Entire model
Skip loads	44.2 tons per skip	On surface areas of the skip which are in contact with the trailer
Longitudinal acceleration	4.905 m/s^2 (0.5 x g)	Entire model
Lateral acceleration	2.4525 m/s^2 (0.25 x g)	Entire model

Table 6.15: Vertical, longitudinal and lateral loads and values

The load case constraints are tabulated below:

Constraint	Location
Translation X	On kingpin
Translation Y	On bottom of springs
Translation Z	On kingpin and suspension

Table 6.16: Load constraints

The analysis complied with the design criteria and the stresses are shown in Figures 6.37 to 6.45 with a peak allowable stress of 219 MPa. Figures 6.37 and 6.40 have been alleviated of high stresses which were present as previously shown in Chapter 4.10.3.5. The high stress points in Figures 6.39 and 6.45 are localised because of modelling approximations. The region where spring elements attach to the centre beams, and right angled connections between mating members, has a tendency to produce high stress regions [25], [38], [39], [40], [41]. The stresses exceed the 355 MPa yield stress however failure is not expected as these localised stress regions also found in Chapter 4.10.3 were investigated on operational trailers at the port in Chapter 5.4.3.2 and none showed damage, cracking or deformation.

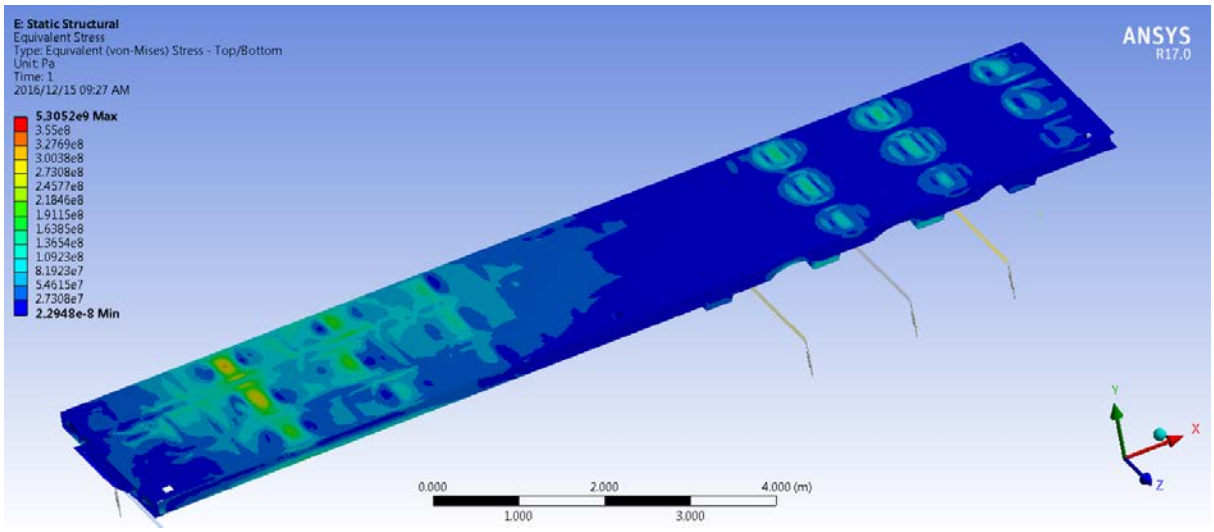

Figure 6.37: Stress plot - top view (Von-Mises)

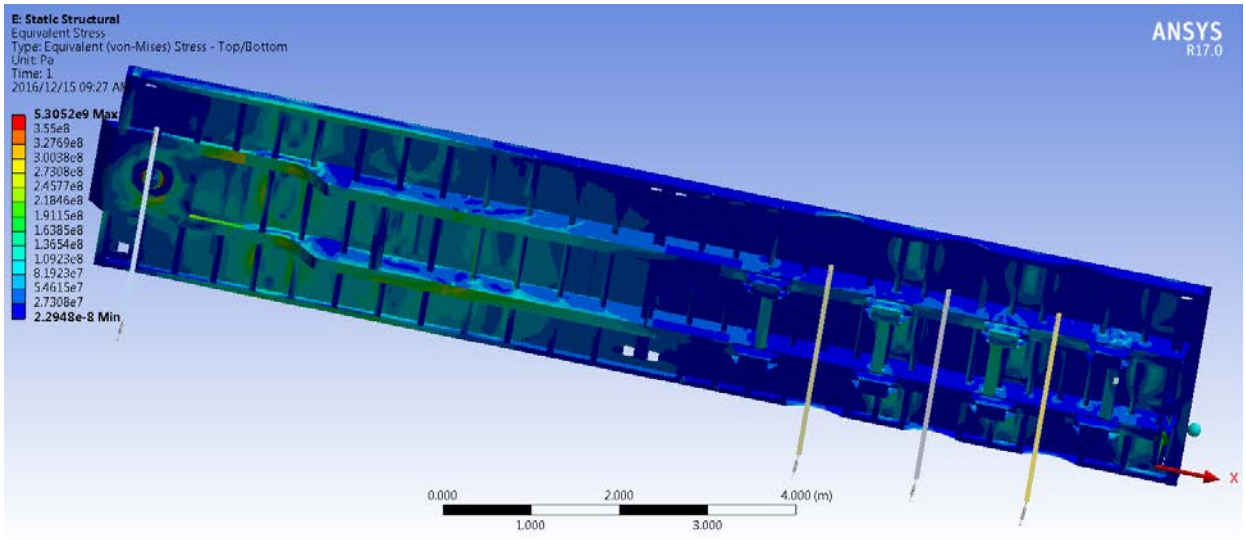

Figure 6.38: Underframe stress plot (Von-Mises)

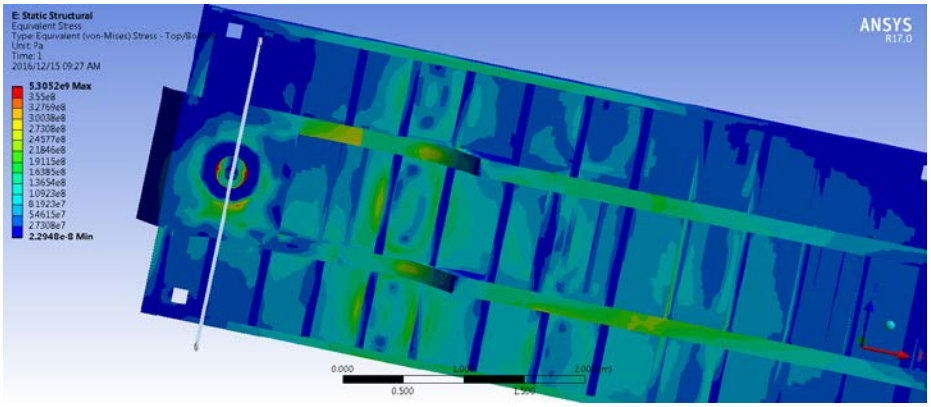

Figure 6.39: High stress region (>355 MPa) found near the kingpin

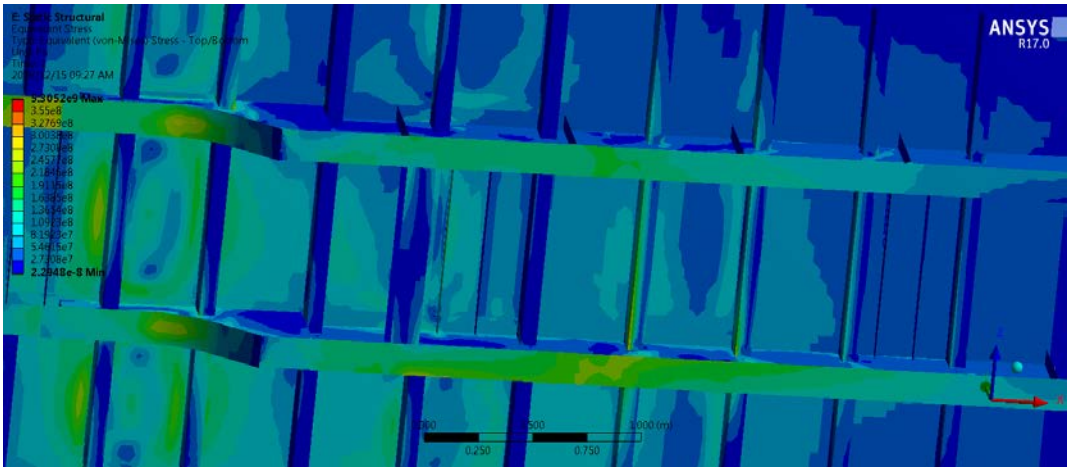

Figure 6.40: High stress region (>355 MPa) found previously on the structural cross member number 10 (using front structural beam as 1) has been alleviated of high stress

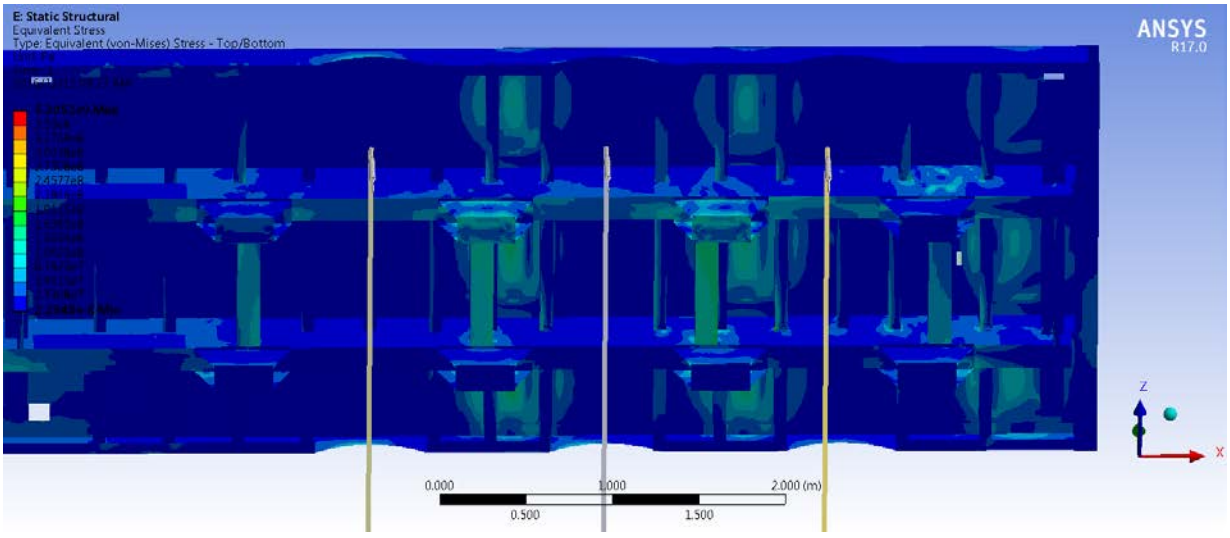

Figure 6.41: Underframe of bogie end stress plot (Von-Mises)

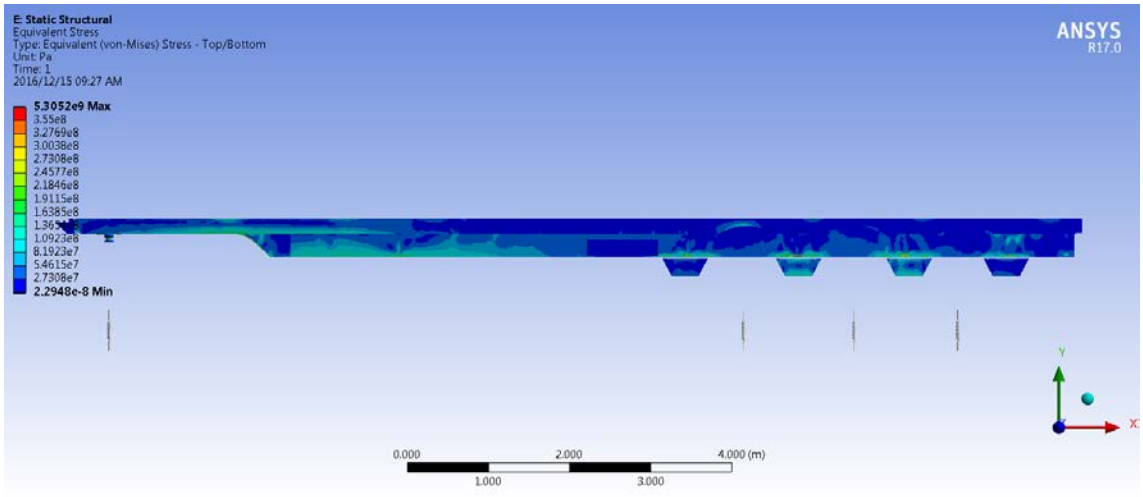

Figure 6.42: Stress plot of main centre beam (Von-Mises)

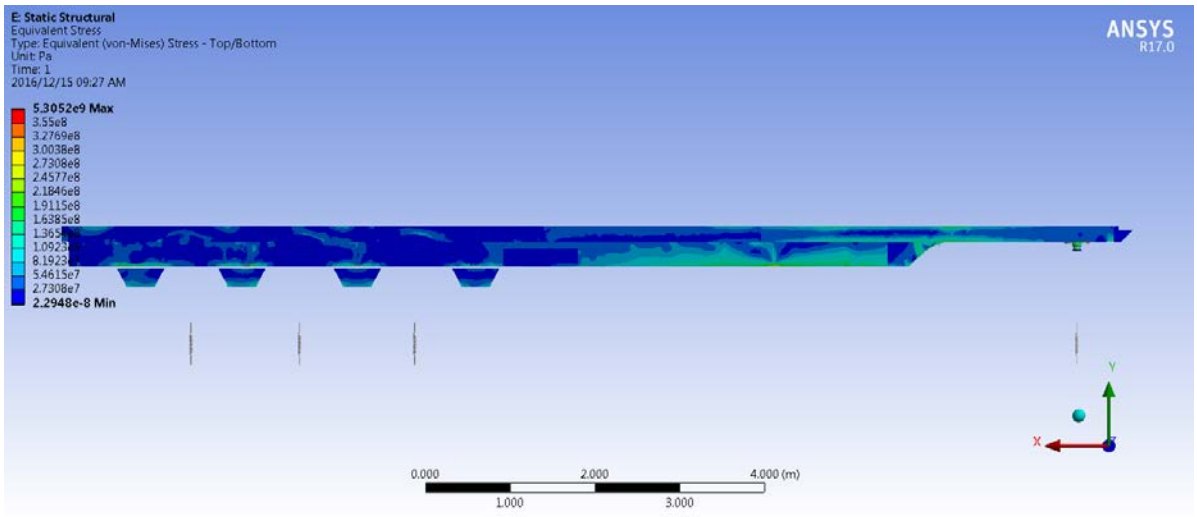

Figure 6.43: Stress plot of main centre beam (Von-Mises)

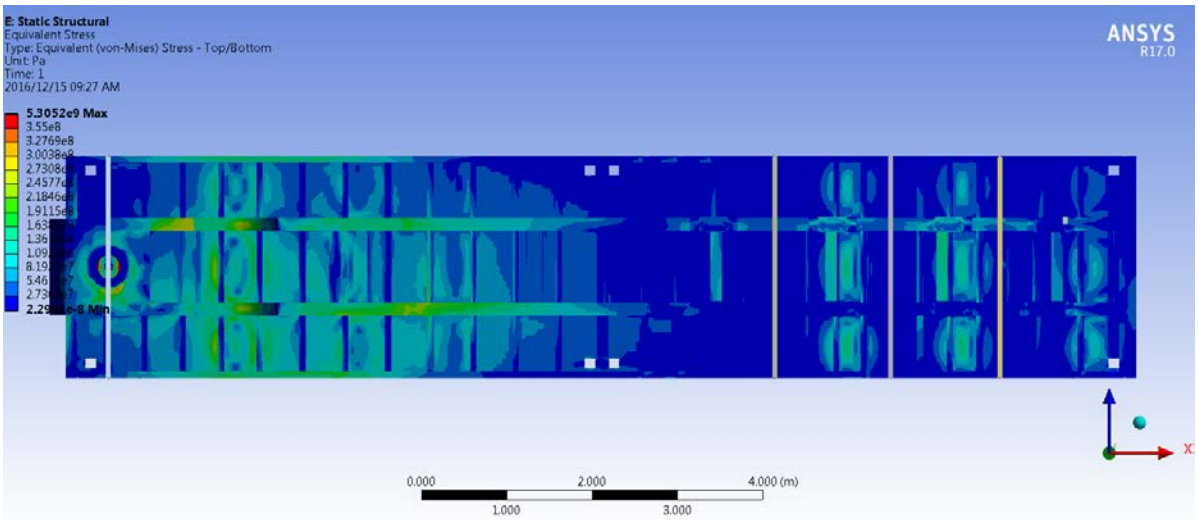

Figure 6.44: Stress plot of main centre beam bottom flange (Von-Mises)

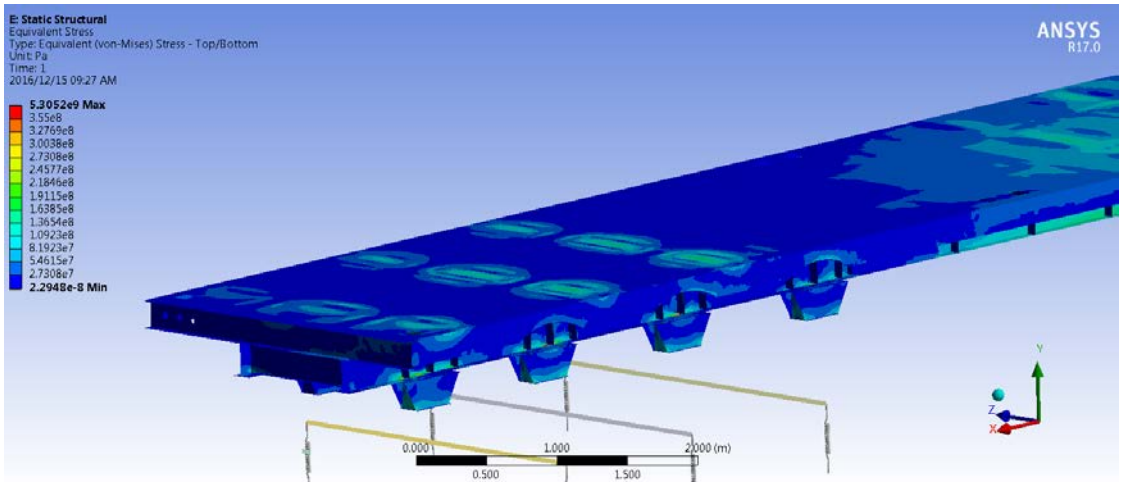

Figure 6.45: High stress region (>355 MPa) previously found on the connection points of the main beam to the suspension pedestals have been reduced

The final trailer mass is 7858 kg, 892 kg less than the previous trailer. The current study focused on better optimising the design of the trailers centre beams, but other members of the trailer's structure can be further optimised where possible. After non critical material was removed and the model conformed to the loading conditions from Chapters 6.1.3.2 to 6.1.3.5, a further 236 kg was omitted, allowing a total possible reduction of 1128 kg, which can be achieved closer to final design as shown in Figures 6.46 and 6.47.

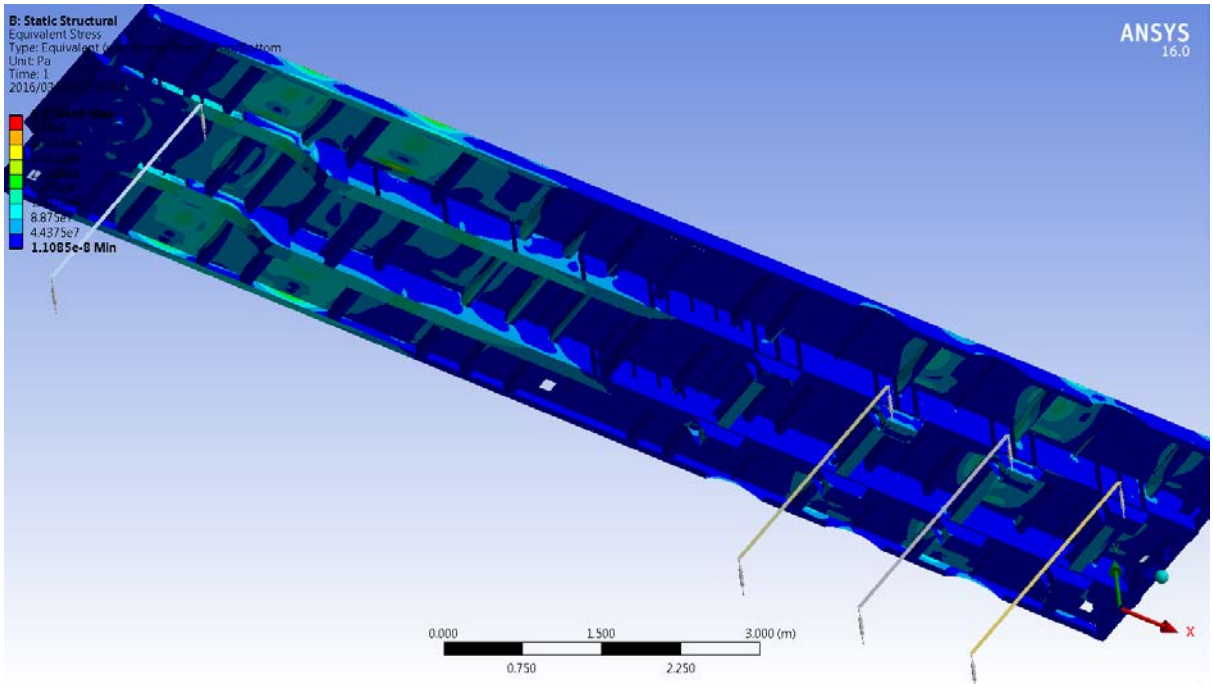

Figure 6.46: Stress plot of redesigned trailer (1.5g vertical acceleration)

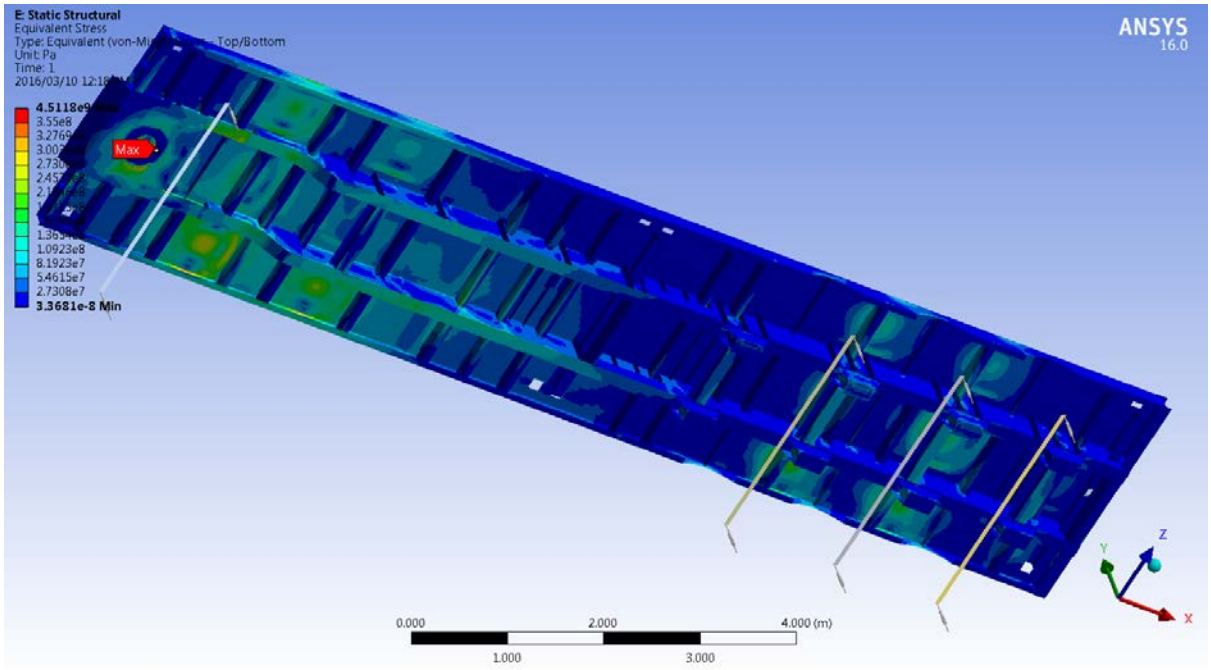

Figure 6.47: Stress plot of redesigned trailer (combined acceleration)

7. Discussion

The analytical assessment of the existing BTT and MPT was used to provide the foundation for a better optimised redesign of the centre beams since relevant geometric features (load and constraint locations) would necessarily remain unchanged. The calculations carried out in Chapters 4.6 and 4.9 supported a reduction in dimensions from the existing designs. This was verified in Chapter 6 via the FEA modelling redesigns. The redesign of the centre beams was predominantly responsible for the mass reduction of the trailers.

In Chapter 4, approximations for the analytical analysis such as the load type of the containers (distributed) and skips (point), the trailer centre of mass and the bogie/suspension as reaction point loads were made so as to simplify the calculations; this was treated similarly in previous studies [15], [41]. These approximations were made to facilitate the analytical calculations, which provided a good basis towards optimisation of the principal structural members.

The Microsoft Excel calculators shown in Figures 4.4 and 4.10 which were setup to determine the kingpin and bogie reaction forces of the trailers', use the respective trailer's total tare mass less the bogie and wheels similarly suggested in previous studies [15], [41]. These masses are 6710 kg for the existing BTT and 9110 kg for the existing MPT from Table 1.2. However, the same Microsoft Excel calculators use the existing trailers total tare mass for calculating the D value of the kingpin as required in equation 4 [51]. The total gross mass of the payloads remains unchanged.

The corresponding global coordinate axis labels for vertical, longitudinal and lateral directions differ for the FEA chapters (Chapters 4 and 6) versus the field testing chapter (Chapter 5). This has been clarified in each relevant chapter prior to giving the associated results. This discrepancy was not deliberate, it originated because the existing trailer CAD models used from TE's mechanical design office had pre-set global coordinates.

The analytically determined reaction forces for the existing trailers' kingpin and bogie were compared to the reaction forces found in the FEA as shown in Chapters 4.10.2.2 and 4.10.3.2. This enabled a simple method for FEA model verification and since these results were within an acceptable limit [37] of each other (1.02% - 3.5%) as shown in Tables 4.18 and 4.31, the analytical method incorporating the stated approximations is shown to provide a useful design foundation. The existing trailer FEA models then also provided a basis for executing modified analyses and iterative redesign. The greasing system, braking system, welding, paint and accessories masses from Tables 4.17 and 4.30 are non-structural components which increase the total mass of the FEA trailer models. These accessories and components which increase the sprung mass were incorporated into the entire trailer FEA model

as distributed mass elements. This brought the FEA model mass up to that of the trailers structure's tare mass as shown in Tables 4.18 and 4.31. The incorporation of these masses aided in narrowing the small differences between the analytical and FEA reaction forces. This addition of the non-structural sprung mass was also necessary to accurately compare the field testing results with the FEA results, per Chapters 5.3.4 and 5.4.4.

The trailers non-structural accessories and components (Table 1.4) that increase the sprung mass account for little mass in comparison to the mass of the trailer structure and the components that make up the un-sprung mass (Tables 4.17 and 4.30). Nearly all the masses not included in the trailer's structural model (rims, tyres, axles and suspension) are un-sprung and thus unnecessary for static FEA of the trailer structure.

The FEA trailer structure was predominantly mid-surfaced which is the most commonly used function to allow plates to be represented with an infinitely thin surface that will be meshed for the FEA model as suggested in studies [19], [23]. In order to reduce computational time, minor details that are unlikely to significantly influence the results were not included in the FEA model. Details such as non-critical locators/brackets for auxiliary equipment were omitted. After the mid-surfacing was performed translation and surface extension were used to join the mating structural plates to each other. Knowledge of manufacturing a trailer assisted the procedure, as it allowed the correct types of bonding contacts to be used, being edge or face type, to the mating structural member. Symmetry functions such as mirroring were used for defining the geometry constraints such as mid-surfacing, edge and face contacts of the steel members. However, at certain points symmetry functions were not used, since force reactions for the axles, and the lateral acceleration loading constraints on the left or right parts of an axle must be able to show results which would not be possible using symmetry. The trailers structure itself is symmetric in design which aided the analysis of FEA results (Chapters 4 and 6) and the comparison of the field testing and FEA results (Chapters 5.3.4 and 5.4.4) [38], [39], [40].

The initial FEA results of the existing BTT were inaccurate because of high stress regions on the trailer originating from incorrect CAD geometry, particularly in the kingpin area as shown in Figure 7.1.

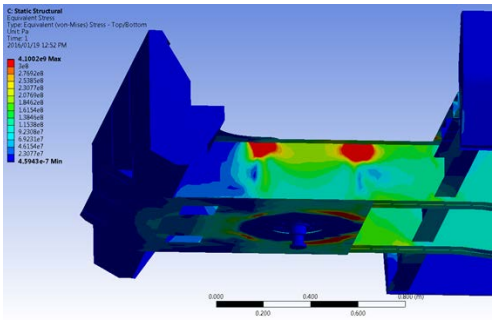

Figure 7.1: High stresses caused on structural components due to omitting and incorrectly bonding connections

The results showed high stress areas which could not be considered localised due to the relatively large region of mesh elements involved. Upon inspection, omitted and incorrectly bonded contacts were also observed between certain structural members. This was a particular problem near the kingpin and goose neck area of the trailer. To remedy the problems, the geometry was correctly updated, mid-surfaced and then manually connected by grouping the components to make sure all the structural members were correctly incorporated. The top plates which are in contact with the point masses were also modelled in the same manner. A main contact which had been mistakenly omitted between the kingpin's mounting, the skid plate and supporting channels of the trailer was included as this aided load transfer from the kingpin to the trailer's structure. To further ensure the contacts were mated to each other, an advanced ANSYS function known as a "pinball region" was used. This user defined region allows the distance to be specified by means of a radius from one contact to the mating contact in a given region so that the connections are correctly bonded even if there are spaces or non-perpendicular profiles between the geometries, for example; to accommodate welding joint preparations. Figure 7.2 illustrates the concept.

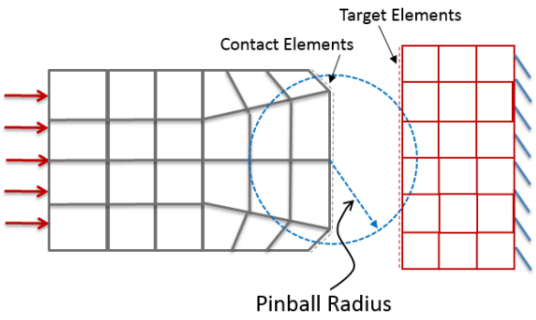

Figure 7.2: Pinball region tool [58]

This function tool was used on supporting gussets and flanges which have detailed welding preparation geometries near the kingpin and goose neck of the trailer.

When meshing an FEA model, a large number of elements can provide a better approximation of the solution, but an excessive number may increase the round-off error (the difference between the approximation of a number and its exact mathematical value) [38], [39], [40]. Therefore, it is

important that the mesh used for this work's models was adequately fine or coarse in the appropriate regions which are specific to the physical system [38], [39], [40]. The models were fully auto meshed using ANSYS, predominantly with quadrilateral shell elements since the stresses of concern need to be as accurate as possible and they provide more contact nodes than triangular elements as shown in studies [19], [23], [38], [39], [40]. At refinement points (bolt holes near the kingpin and areas where the loading conditions and the spring elements applied for axles/suspension), the surrounding mesh was enhanced as suggested and shown in studies [19], [23], [38], [39], [40].

The payloads applied on the trailer are shown in Table 4.2. Point mass loads located at the centre of mass were used in the FEA simulations and were spread over areas where the commodity handling equipment is in contact with the trailer surface. The loads applied in the FEA are a representation using maximum payloads and the contents of a shipping container or skip can thus vary in field conditions.

The localised high stress critical regions found on the trailer models as a result of FEA modelling approximations using the spring elements and the right angled connection between mating members, are considered acceptable for the current work until further research can be undertaken. These localised high stresses are also present in Cowling's FEA results of a cane haulage trailer [41] and further examples are shown on components in studies [25], [38], [39], [40]. The locations of the localised extreme FEA stresses were inspected (by cleaning the localised area down to the steel surface and using a weld inspection magnifying glass) on several operational trailers that had been operating for a minimum of three years. None showed any indication of damage or reported failure.

Some of the translational constraints used in the FEA simulations do not provide an entirely accurate representation of the underlying supporting component. The suspension/bogie, tyres, and hauler's fifth wheel with hydraulic lifting cylinders all provide levels of support, dampening, and movement that cannot be accurately quantified or fully represented by a constraint. Medium to high magnitude localised stress regions will be lower or negated in field conditions partly because of the underlying supporting components interacting with the structure as also described in study [41]. Furthermore, field test data results support and confirm this, via the validation of the static models (Chapters 5.3.4 and 5.4.4).

The Von-Mises stress criteria used to interpret the FEA simulations were compared to the maximum principal, shear and bending stresses to validate the shown stress distributions, yielding and localised stresses of the associated models while performing the simulations [34], [35], [36], [37]. The Von-Mises criteria were found to provide accurate results that could be used for FEA assessment of the trailers with no difference shown, especially for the medium to high and localised stresses which are

critical for assessing the structure. In Chapter 4.10.2.2 the existing BTT FEA model experienced an array of stresses at the kingpin area in the 2g acceleration vertical load case. This area of the trailer model is ideal to show the various stress criteria used to evaluate FEA simulations and why the Von-Mises criteria for assessment is adequate and was selected as the principal assessment criteria (as also found in Chapter 2.2 of the literature review). Figures 7.3 to 7.6 show a comparison of the various stress criteria. The maximum principal stress in Figure 7.4 accurately illustrates yield stresses, however the Von-Mises stress in Figure 7.3 not only accurately exhibits yielding but shows a much more explicit distribution of stress on areas which are not covered in Figure 7.4. Figure 7.6 provides a distribution of stresses which results from bending as illustrated. Although the structure is predominantly stressed in a similar range as the Von-Mises criteria, the critical higher stresses and localised regions are much lower and fewer when compared to Figure 7.3. In Chapter 6 it was noted that certain FEA load cases did not approach or exceed the yield stress of 355 MPa using bending stress criteria, where they did when using Von-Mises criteria.

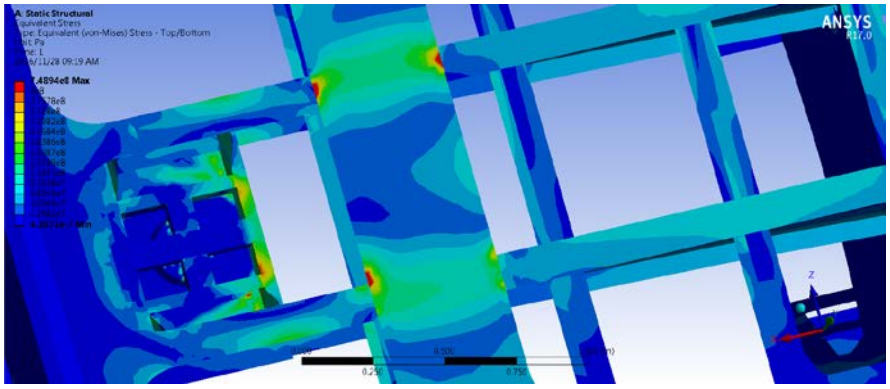

Figure 7.3: Equivalent Von-Mises stress for BTT

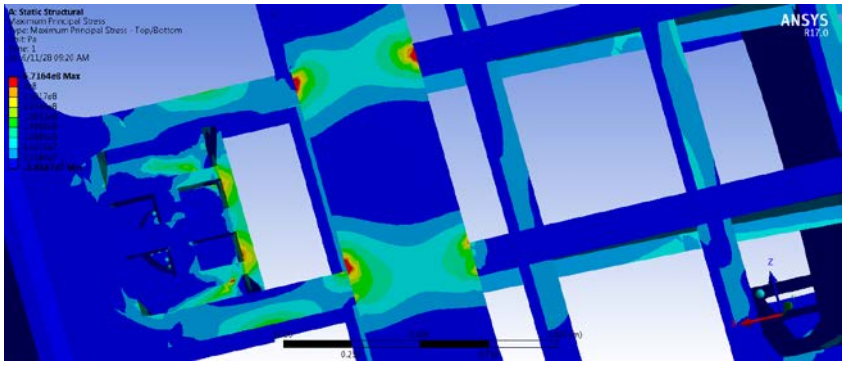

Figure 7.4: Maximum principal stress for BTT

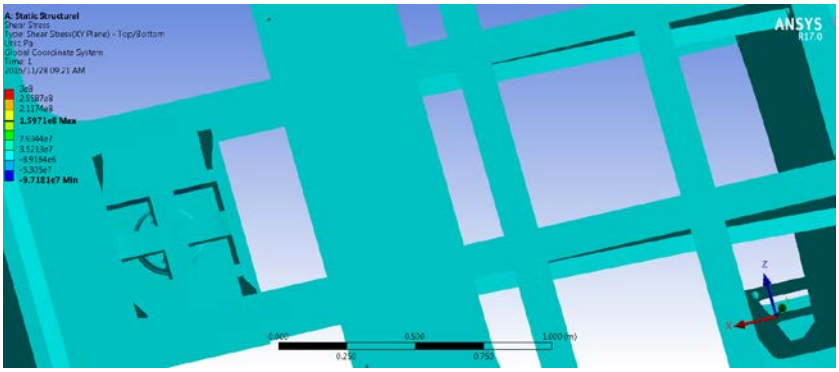

Figure 7.5: Shear stress for BTT

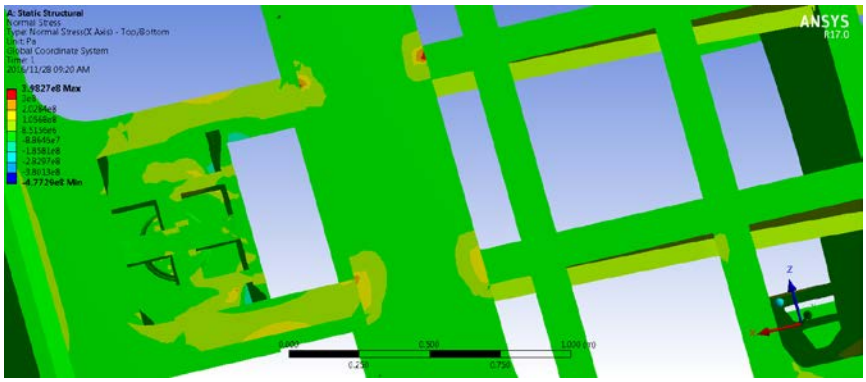

Figure 7.6: Bending stress for BTT

The FEA model techniques applied in Chapter 4 provided a model platform for later trailer redesign and optimisation once the validation of the field test results and FEA results was performed in Chapter 5. The FEA trailers' deflections were assessed by TE's mechanical design office as part of the work against allowable deflections using a recognised standard, as another means for checking structural adequacy. For both the existing trailer and the redesigned trailer FEAs performed, the peak deflections of the trailers was determined to be acceptable according to the standard AS1170.1 [59] which prescribes minimum design loads on structures (as utilised by TE's mechanical design office). The peak deflections for the existing and redesigned trailers were 0.012 m - 0.026 m for the BTT and 0.010 m - 0.020 m for the MPT. The deflections drop closer to final design, due to extra structural members, gussets, supports and bracing which are added where necessary as modifications to support the centre beams at locations for the underlying components, and the trailer's construction, making the structure more rigid [16].

The field testing of the existing trailers was performed to assess the accuracy of the FEA assumptions and model, and therefore the trailer design. The acceleration data acquired reinforced the specifications chosen in Chapter 4.10.1, as shown and discussed in Chapters 5.3.3.1 and 5.4.3.1. The strain gauge data was used to validate two FEA static models in Chapters 5.3.3.2 and 5.4.3.2 by using the stress data from loaded commodity handling equipment.

The laden acceleration field data was within the limits set out in Chapter 4.10.1 on the existing trailers as displayed in Chapters 5.3.3.1 and 5.4.3.1. The poor road conditions of Durban Pier 2 were highlighted in the collected acceleration data with values exceeding the limits in Chapter 4.10.1, when the trailer was un-laden. These peak acceleration values showed the importance of road conditions in vehicle operation. Richard's Bay Port provided more favourable road conditions compared to Durban Pier 2. FEA simulations were performed on un-laden trailers using the accelerations that exceeded the values in Chapter 4.10.1 from both the trailers' field test data. Because the trailers were un-laden, the stresses on the trailers structure were negligible.

Electrostatic and magnetic noise from the sub-systems of the hauler and loading vehicles were all origins of the noise and disturbances [56] experienced by the strain gauges predominantly at the kingpin and goose neck areas of the trailers. This consequently effected the field test data by inducing higher strain/stress values into the data that was logged. Chapters 5.3.3.2, 5.4.3.2, 5.3.4 and 5.4.4 validate this by showing the strain/stress results when other commodity handling equipment was in the trailers' vicinity. Also, the MPT kingpin and goose neck FEA and field test data stress validation results were better than the BTT, which is due to the MPT having a top plate on the trailer which helped shield the strain gauges when the skips were loaded using a forklift. A straddle carrier (Figures 5.9 and 5.21) which is used to load a shipping container on the BTT, surrounds the trailer's skeletal structure, and the strain gauges are thus much more susceptible to noise and related disturbances [56].

The comparison of the field test data with that of the FEA results in Chapters 5.3.4 and 5.4.4 provided BTT stress data within 1.94 MPa - 11.32 MPa and similarly the MPT was within 0.05 MPa - 9.72 MPa. In context it would be advisable to view the stress variation with the acceptable percentage error range of 1.30% - 25.36% [56], [57] as shown in Tables 5.14, 5.15, 5.27 and 5.28 of the actual numerical data. However, it is more relevant to assess the structural stresses relative to the material yield stress.

Field test data from certain strain gauges had to be omitted, due to them having an intermittent electrical connection and contamination as discussed in Chapters 5.3.3.2 and 5.4.3.2 respectively. It proved difficult to create an ideal experimental situation in the operational environment. However, enough usable field test data was obtained to enable comparisons using FEA results, and to safely reduce the FEA model loading accelerations from the specifications in chapter 4.10.1.

The study revealed that it would be better at the prototype stage to fit the strain gauges at certain locations (such as the MPT kingpin; under the top plate, and between the trailers centre beam bottom flange and suspension pedestals) as these areas of the structural members of the trailers would be reached that would not be possible after complete manufacture. Ideally less surface preparation will

be required at prototype stage since the steel surface will not be protected with primer and paint which would benefit the ease of the strain gauge installation.

The field test data had to be filtered using a systematic technique for reasons discussed in Chapters 5.3.3 and 5.4.3:

i. Filtration included omitting irrelevant acceleration data, when the vehicle was idling which would cause overall reduced mean result.
ii. Using a time series calculator to correctly align the data magnitude when the amplifier did not zero, or started at a difficult to use point of origin.
iii. Detecting and omitting peak values, was applied to noise and disturbances that caused illogical values in the stress data range [56]. This data were of such high illogical values that failure would have been imminent should the data be true, which was not the case.

The initial chosen FEA accelerations shown in Chapter 4.10.1 were assessed by using maximum absolute acceleration values from the field test data routes with poor road surfaces and where the trailers were driven with severe turning, acceleration and emergency braking to attain all possible outcomes that might occur during operations. The FEA lateral acceleration value of 0.25g [49] used for the existing trailers was kept the same for the redesigned trailers. The field testing data provided a peak lateral acceleration value of 0.2g for both laden trailers equating to a safety factor of 1.25 [28], [49]. Although the safety factor is on the lower limit of the acceptable ranges as prescribed in studies [28], [49] increasing it will not benefit the design, as it would not then involve a true representation of the cargo payloads as discussed in Chapter 2.3 of the literature review, and Chapter 4.10.1 [49]. The FEA longitudinal acceleration was reduced from the initial 0.8g [54] to 0.5g [49], in light of the peak measured field test longitudinal accelerations (BTT: 0.278g and MPT: 0.216g) which then incorporated an acceptable safety factor from studies [28], [49] for the newly determined longitudinal acceleration value [49]. The field test vertical acceleration data recorded a peak of 0.484g for the BTT and 0.434g for the MPT, both values were rounded off to 0.5g for ease of use. The FEA vertical acceleration was reduced using Cowling's research of dynamic design safety factor [41] from the initial 2g to 1.5g (incorporating earth's gravity with the peak field test 0.5g acceleration). Both the longitudinal and vertical acceleration reductions have been previously discussed in Chapters 5.3.4 and 5.4.4 and shown again in Chapter 6. The redesigned trailers in Chapter 6 were simulated under the newly defined 1.5g vertical acceleration, 0.5g longitudinal acceleration and 0.25g lateral acceleration and both complied as shown in the FEA results. In all FEA load cases in Chapter 6 the peak allowable stress was found using the presented results based on the Von-Mises criteria which was required when evaluating the FEA vertical and combined loading acceleration cases. Together with the material yield stress the safety factors of the designs were determined, these were 1.54 to 1.71 for the BTT and 1.33 to 1.99 for the MPT which is considered ideal in relation to the material properties [55] and to the

prescribed range of 1.25 to 2.5 [28]. The analytical calculations reduced the need for iterations of the redesigned trailers centre beams, however since the MPT met the FEA load case requirements in Chapter 6 comfortably an iterative redesign approach was applied to further reduce the centre beams dimensions as presented in Chapter 6.1.3.1.

To accurately represent the FEA trailers structural models of the redesigned trailers in Chapter 6, distributed mass elements due to the non-structural items were applied to the respective trailers' models. The existing trailer's masses of these items from Tables 4.15 and 4.28 were used. The FEA remodelling of the trailers' centre beams allowed mass reduction of both trailer structures:

i. The redesigned BTT using the calculated centre beam recommendations in Chapter 4.6, and conforming to the newly determined loading accelerations in Chapter 6.1.2, attained a 9.56% decrease in mass from the original BTT.
ii. The redesigned MPT had a decrease in mass of 10.19% from the original MPT. This was achieved using the recommended centre beam calculations in Chapter 4.9 and findings in Chapter 6.1.3.1, whilst conforming to the newly determined loading accelerations in Chapter 6.1.3.

These FEA model mass reductions are based on the material quantity for the trailers' steel structures. Welding, primer, paint, and certain accessories would also be reduced when accurately quantified after manufacture.

8. Conclusion

This work aimed to verify existing TE trailer designs, assess the validity of the currently used specifications in the port environment and propose better optimized, more customised trailer designs.

An analytical calculation design approach was found to be efficient for initially assessing the main centre beams, and useful for early verification of the FEA model. Further, by analysing worst case loading scenarios for each existing trailer and calculating the shear forces and bending moments under peak design loads, appropriate centre beam dimensions could be selected as a foundation for the redesign of the trailers whilst complying with an acceptable safety factor for the application. This approach allowed a dimension reduction before the FEA model was constructed which reduced the need for FEA iterations toward improved optimisation.

The field testing of the existing trailers was performed to assess the accuracy of the FEA assumptions and model, and therefore the trailer design, which showed a favorable reduction of the FEA acceleration values for the laden trailers. The field test data in Chapters 5.3.3.1 and 5.4.3.1 described the relation between road conditions and acceleration values on the trailers and it can be concluded that if roads are regularly and well maintained, the trailers will experience significantly reduced accelerations and stresses. Poor road conditions will not allow for reduced trailer mass structures due to the requirement for the trailers to be designed for extreme load cases.

The initial FEA determined the existing trailers stresses for the loading accelerations selected based on Chapter 4.10.1, and allowed high stress points to be identified for field testing. High stress regions identified in the FEA models of the existing TE trailers were localised due to analytical modelling approximations and the right angled connection between mating members. In Chapters 5.3.3.2 and 5.4.3.2 the strain gauges that logged data in these regions measured strains below the stresses found in the FEA simulations. These localised regions were also carefully visually inspected on numerous trailers which have been operational for a minimum of three years, and none displayed any indication of damage. Methods to more accurately measure the highly localised stresses in the trailers, particularly in a prototype of the new design, will be discussed in the Recommendations chapter.

Methods of field test data acquisition might be improved upon and different options will be discussed in the Recommendations chapter. Filtered data still contains stress values exposed to noise and disturbances which are within an acceptable stress range and thus unfilterable, but deviate from what would be experienced in ideal conditions as explained in Chapters 5.3.3.2, 5.3.4, 5.4.3.2 and 5.4.4.

Chapters 5.3.4 and 5.4.4 compared the field test data with results from the existing FEA models, and were found to be within an acceptable range [56], with the field test results yielding lower stress values than the FEA stress values. The existing FEA models for the trailer designs is now a platform which can be repeatedly used and modified for a range of application-specific designs which may arise. The redesign of the trailers in Chapter 6 was completed based on the new centre beam dimensions determined in Chapters 4.6 and 4.9. The new vertical and longitudinal acceleration values deduced in Chapters 5.3.4 and 5.4.4 from field test data in Chapters 5.3.3.1 and 5.4.3.1 were used when performing those simulations. A mass reduction of 9.56% for the BTT and 10.19% for the MPT was achieved through the redesign of the centre beams. A small further improvement is expected closer to final design phase of the prototype trailers as shown at the end of Chapters 6.1.2.5 and 6.1.3.5 where an iterative design approach is required. The height of the web can be reduced further along the length of the centre beams using the validated FEA models for both trailer types, however the web height constraints which are pre-determined for coupling purposes, and the bogie end of the trailer which needs to be as parallel as possible to the centre axis of the axles, must be taken into consideration.

A long term goal is to create an internal TE specification, particular to TE port conditions and speeds, to be applied across a full range of their trailers during design.

9. Recommendations

The recommendations for future work are as follows:

a) Produce a final detailed design of the redesigned trailers, incorporating all required minor members and accessories, as well as an accurate array of sensors (particularly strain sensors); manufacture a prototype from this design.

b) Continuous monitoring of the prototype trailers' structure, fatigue analysis, welding practices, and material optimisation.

c) A feasibility study should be carried out using other commercial carbon steels for the trailer design. This will be an exercise where manufacturing cost and material saving can be based on the type of steel used. Since no further specialised information will be required, this can be done prior to building the first prototype.

d) Field testing of the trailers and monitoring of the data should continue on new and existing trailers.

e) Road condition improvement shall be highlighted to Durban Pier 2 Port and continuous maintenance should be enforced for fleet safety and reliability.

f) The redefined acceleration values for the FEA loading cases can be further investigated for better optimisation according to the collected field data. However, further collection and assessment is required before implementing this as an official TE design standard. Research into this will be arranged by TE with TPT and TNPA to monitor conditions, and the available data can be optimised per port or standardised pending the outcome of the research.

g) Uneven loading of commodity handling equipment onto the trailers, should be quantified as a consideration for use on future FEA models. Field testing of the commodity handling equipment loaded onto the trailers should be done to determine the various loading scenarios from these structures.

h) Techniques to reduce and omit localised stress points on the FEA models are required to alleviate geometry and connection stresses, and to highlight actual stress data. In all of the FEA models the localised points/regions are a single or few mesh elements, which are not of concern, but a more refined technique would allow them to be better quantified or omitted. This may become critical in the future especially when fatigue FEA analysis is performed.

i) Location points should be placed on the top plate of the MPT to allow the front skip to be loaded in a position that can be consistently controlled for design and stress validation purposes.

j) Sensor fitment will be done prior and during prototype trailers manufacture, instead of post manufacture. This will enable better, more controlled and relevant data acquisition during field testing.

k) The dynamic analysis of the trailer will be investigated to understand its road handling characteristics. This will also allow the web height to be decreased subject to the dynamic handling of the bogie, allowing a better optimised design which may improve lateral loading cases.

l) This work's approach for validating the trailer will be used on other commodity handling equipment (e.g. skips, containers and wagons) as well as on future trailer designs. Equipment's field testing results compared against their FEA results, will allow the loading accelerations and stresses to be validated and improved for a better optimised design. Analytical calculations will provide a good foundation for better optimised main structural members and it will aid reducing the time of the iterative design approach. It is hoped that this will establish new criteria for mechanical vehicle and equipment design at TE.

Appendix A BTT: Reaction forces

$$Taking\ moments \sum M_{king\ pin} = 0$$

$$(Q_{container}\ x\ 6.058)\left(-K + \frac{6.058}{2}\right) + (Q_{container}\ x\ 6.058)\left(A - E + \frac{6.058}{2}\right) - \left(F_{bogie}\ x\ A\right) = 0$$

$$F_{bogie} = \frac{(Q_{container}\ x\ 6.058)\left(-K + \frac{6.058}{2}\right) + (Q_{container}\ x\ 6.058)\left(A - E + \frac{6.058}{2}\right)}{A}$$

$$Taking\ moments \sum M_{bogie} = 0$$

$$(Q_{container}\ x\ 6.058)\left(A + K - \frac{6.058}{2}\right) + (Q_{container}\ x\ 6.058)\left(E - \frac{6.058}{2}\right) - \left(F_{kingpin}\ x\ A\right) = 0$$

$$F\ kingpin = \frac{(Q_{container}\ x\ 6.058)\left(A + K - \frac{6.058}{2}\right) + (Q_{container}\ x\ 6.058)\left(E - \frac{6.058}{2}\right)}{(A)}$$

$F\ kingpin = 232\ 265.26$ and $F_{bogie} = 366\ 946.27\ N$

Shear force and bending moment analysis

The shear force is defined as positive when it tends to rotate the material/beam counter clockwise.

The bending moment is defined as positive when it tends to cause tension at the top of the beam.

$$V1 = -Q_{container} * x1$$

$$M1 = -Q_{container} * \frac{x1^2}{2} \quad (0 < x1 < 0.75)$$

V1 (0) = 0 N and M1 (0) = 0 Nm.

V1 (0.75) = -37 018.53 N and M1 (0.75) = -13 881.95 Nm.

$$V2 = F_{kp} - (Q_{container} * x2)$$

$$M2 = F_{kp} * (x2 - 0.75) - Q_{container} * \frac{x1^2}{2} \ (0.75 \leq x2 < 6.058)$$

V2 (0.75) = 195 246.73 N and M2 (0.75) = -13 881.95 Nm.

V2 (6.058) = -66 745.74 N and M2 (6.058) = 327 159.68 Nm.

Maximum bending moment: $M_{max@3.96}$ (0.75 + 3.96 = 4.71) = 372 289.04 Nm

$$V3 = F_{kp} - (Q_{container})6.058$$

$$M3 = -Q_{container} * 6.058 * \left[(x3 - 6.058) + \frac{6.058}{2}\right] + F_{kp} * (x3 - 0.75) \quad (6.058 \leq x3 < 6.94)$$

V3 (6.058) = -66 745.74 N and M3 (6.058) = 327 159.68 Nm.

V3 (6.94) = -66 745.74 N and M3 (6.94) = 268 289.93 Nm.

$$V4 = -Q_{container} * 6.058 + F_{kp} - Q_{container} * (x4 - 6.94)$$

$$M4 = -Q_{container} * 6.058 * \left[(x4 - 6.058) + \frac{6.058}{2}\right] + F_{kp} * (x4 - 0.75) - Q_{container} * \frac{(x4 - 6.94)^2}{2} \quad (6.94 \leq x4 < 10.15)$$

V4 (6.94) = -66 745.74 N and M4 (6.94) = 268 289.93 Nm.

V4 (10.15) = -225 762.85 N and M4 (10.15) = -201 186.37 Nm.

$$V5 = -Q_{container} * 6.058 + F_{kp} - Q_{container} * (x5 - 6.94) + F_{bogie}$$

$$M5 = -Q_{container} * 6.058 * \left[(x5 - 6.058) + \frac{6.058}{2}\right] + F_{kp} * (x5 - 0.75) - Q_{container} * \frac{(x5 - 6.94)^2}{2} + F_{bogie} * (x5 - 10.4) \quad (10.15 \leq x5 \leq 13)$$

V5 (10.15) = -225 762.85 N and M4 (10.15) = -201 186.37 Nm.

V5 (13) = 0 N and M4 (13) = 0 Nm.

Appendix B MPT: Reaction forces analysis:

$$\sum F\,y = 0: F_{kingpin} + F_{bogie} = W_{trailer} + 2 * W_{skips}$$

$$Taking\ moments \sum M_{kingpin} = 0$$

$$\left(W_{skip}\ x\ (z-w)\right) + \left(W_{skip}\ x\ (z+v)\right) + \left(W_{trailer}\ x\ (z-y)\right) - \left(F_{bogie}\ x\ z\right) = 0$$

$$F_{bogie} = \frac{\left(W_{skip}\ x\ (z-w)\right) + \left(W_{skip}\ x\ (z+v)\right) + \left(W_{trailer}\ x\ (z-y)\right)}{z}$$

$$Taking\ moments \sum M_{bogie} = 0$$

$$\left(W_{skip}\ x\ w\right) - \left(W_{skip}\ x\ v\right) + \left(W_{trailer}\ x\ y\right) - \left(F_{kingpin}\ x\ z\right) = 0$$

$$F_{kingpin} = \frac{\left(\left(W_{skip}\ x\ w\right) - \left(W_{skip}\ x\ v\right) + \left(W_{trailer}\ x\ y\right)\right.}{z}$$

For the analysis in Chapter 4.8, $W_{trailer}$ can be considered 0 to calculate the reaction forces, yielding;

$F_{kingpin} = 263\ 036.17$ N and $F_{bogie} = 604\ 167.83\ N$

Shear force and bending moment analysis:

The shear force is defined as positive when it tends to rotate the material/beam counter clockwise.

The bending moment is defined as positive when it tends to cause tension at the top of the beam.

$$V1 = F_{kp}$$

$$M1 = F_{skip}(x1 - 0.5)\ (0.5 < x1 < 3.5)$$

V1 (0.50) = 263 036.17 N and M1 (0.50) = 0 Nm.

V1 (3.50) = 263 036.17 N and M1 (3.50) = 789 108.51 Nm.

$$V2 = F_{kp} - W_{skip}$$

$$M2 = F_{skip}(x2 - 0.5) - W_{skip}\ (x2 - 3.5) \qquad (3.5 \leq x2 < 9.7)$$

V2 (3.50) = -170 565.83 N and M2 (3.50) = 789 108.51 Nm.

V2 (9.7) = -170 565.83 N and M2 (9.7) = -268 399.64 Nm.

$$V3 = F_{kp} - W_{skip} + F_{bogie}$$

$$M3 = F_{skip}(x3 - 0.5) - W_{skip}\ (x3 - 3.5) + F_{bogie} * (x3 - 9.7) \quad (9.7 \leq x3 < 10.319)$$

V3 (9.7) = 433 602 N and M3 (9.7) = -268 399.64 Nm.

V3 (10.319) = 433 602 N and M3 (10.319) = 0 Nm.

$$V4 = F_{kp} - W_{skip} + F_{bogie} - W_{skip}$$

$$M4 = F_{skip}(x4 - 0.5) - W_{skip}\ (x4 - 3.5) + F_{bogie} * (x4 - 9.7) - W_{skip} * (x4 - 10.319 \quad (10.319 \leq x \leq 13)$$

V4 (10.319) = 0 N and M4 (10.319) = 0 Nm, V4 (13) = 0 N and M4 (13) = 0 Nm.

Appendix C

Chapter 4.6, BTT data:

Trailer length (m)	0-0.75	0.75-6.058	6.058-6.942	6.942-10.15	10.15-13
Shear force/V (N)	-18509.27	97623.37	-33372.87	-112881.43	-70591.71
Bending moment/M (Nm)	-6940.98	186144.52	163579.84	134144.97	-100593.19
Web height	240.00	630.00	630.00	530.00	530.00
Q (m^3)	0.00045320	0.00163880	0.00163880	0.00127680	0.00127680
I (m^4)	0.00009727	0.00071612	0.00071612	0.00049267	0.00049267
y (m)	0.140	0.335	0.335	0.285	0.285
t_{web} (m)	0.008				
Shear stress (Pa)	-10779860.68	27925639.68	-9546472.23	-36567488.95	-22867902.25
Bending stress (Pa)	-9990163.05	87078001.03	76522292.87	77599514.67	-58190647.23
Material yield stress (Pa)	300000000				
Safety factor	27.83	3.45	3.92	3.87	5.16

Table C1: Data per existing centre beam used to generate Figure 4.8 and 4.9

Trailer length (m)	0-0.75	0.75-6.058	6.058-6.942	6.942-10.15	10.15-13
Shear force/V (N)	-18509.27	97623.37	-33372.87	-112881.43	-70591.71
Bending moment/M (Nm)	-6940.98	186144.52	163579.84	134144.97	-100593.19
Web height	240.00	630.00	630.00	530.00	530.00
Q (m^3)	0.00025416	0.00089766	0.00089766	0.00070366	0.00070366
I (m^4)	0.00005418	0.00040487	0.00040487	0.00027880	0.00027880
y (m)	0.132	0.327	0.327	0.277	0.277
t_{web} (m)	0.004				
Shear stress (Pa)	-21707455.83	54110977.68	-18498016.57	-71225269.74	-44541546.41
Bending stress (Pa)	-16910909.04	150341103.45	132116560.01	133279358.07	-99944080.07
Material yield stress (Pa)	355000000				
Safety factor	16.35	2.36	2.69	2.66	3.55

Table C2: Data per redesigned centre beam used to generate Figure 4.8 and 4.9

Chapter 4.9, MPT data:

Trailer length (m)	0-0.5-3.5	0.5-3.5	3.5-9.7	9.7-10.319	10.319-13
Shear force/V (N)	131518.09	131518.09	-85282.92	216801.00	216801.00
Bending moment/M (Nm)	0.00	0.00	394554.26	-134199.82	0.00
Web height	180.00	450.00	800.00	800.00	450.00
Q (m^3)	0.00042960	0.00151500	0.00379000	0.00379000	0.00151500
I (m^4)	0.00006798	0.00045305	0.00169147	0.00169147	0.00045305
y (m)	0.110	0.245	0.420	0.420	0.245
t_{web} (m)	0.016				
Shear stress (Pa)	51948637.49	27487294.28	-11943120.66	30361069.41	45311432.93
Bending stress (Pa)	0.00	0.00	97969880.44	-33322515.61	0.00
Material yield stress (Pa)	355000000				
Safety factor	6.83	12.92	3.62	10.65	7.83

Table C3: Data per existing centre beam used to generate Figure 4.13 and 4.14

Trailer length (m)	0-0.5-3.5	0.5-3.5	3.5-9.7	9.7-10.319	10.319-13
Shear force/V (N)	131518.085	131518.085	-85282.915	216801	216801
Bending moment/M (Nm)	0	0	394554.255	-134199.82	0
Web height	180.00	450.00	600.00	600.00	450.00
Q (m^3)	0.00041340	0.00141375	0.00219000	0.00219000	0.00141375
I (m^4)	0.00006700	0.00043786	0.00082880	0.00082880	0.00043786
y (m)	0.110	0.245	0.320	0.320	0.245
t_{web} (m)	0.014				
Shear stress (Pa)	57959840.71	30331389.53	-16096385.81	40919245.55	49999782.02
Bending stress (Pa)	0.00	0.00	152337550.19	-51814602.32	0.00
Material yield stress (Pa)	355000000				
Safety factor	6.12	11.70	2.33	6.85	7.10

Table C4: Data per redesigned centre beam using Table 4.10 to generate Figure 4.13 and 4.14

References:

[1] Department for Transport, Guide; Freight Best Practice. SMMT. February 2010. The Motor Industry TM, Truck Specification for Best Operational Efficiency. Queens Printer and Controller of HMSO.

[2] Republic of South Africa, Department of Transport, August 2009, 8th Edition, TRH 11- Dimensional and mass limitations and other requirements for abnormal load vehicles.

[3] JOST, 2" and 3 ½" kingpins/ Spare Parts, Pg. 84 and 85. Downloaded from www.jost.co.za , February 2014.

[4] SANS1447-2:2007. South African National Standard. Braking (motor and towed vehicles, designed for low speed or for use off public roads). Part 2: Low speed trailers.

[5] Henred Fruehauf components; manuals, procedures and work instructions PC.PRO.WL14. July 2009.

[6] Go suspension and axles (Pty) Ltd. Communication: Jumbo underslung suspension for port operation. February 2013.

[7] SABS 1046. South African Standard. Lights and light-signalling devices installed on motor vehicles and trailers. Edition 3, 1990.

[8] SANS1376:2006-2008. South African National Standard. Lights for motor vehicles, Part 1, 2 and 3.

[9] SANS1329-3:2007. South African National Standard. Retro-reflective and fluorescent warning signs for road vehicles. Part1, 2, 3 and 4.

[10] SANS1055:2007. South African National Standard. Rear underrun protection devices.

[11] SANS1496:2008. South African National Standard. Wheel flaps fitted to motor vehicles.

[12] SANS3779:2010. South African National Standard. Road vehicles - Vehicle identification number (VIN) - Content and structure.

[13] Republic of South Africa Government Gazette.2010. National Road Traffic Act. Government Gazette 33742. Republic of South Africa. Act 93 of 1996.

[14] Fruehauf Trailer Corporation Trailer/Body Builders. July 1, 1998. Downloaded from http://trailer-bodybuilders.com/archive/fruehauf-proposes-reorganization-plan, March 2014.

[15] Robert Lowdon. 2007. Semi-Trailer Main Beam Design. ENGR 446 Report. Faculty of Engineering: Mechanical Engineering, University of Victoria.

[16] National Code of Practice, Heavy Vehicle Modifications, Chassis Frame Section H. Downloaded from http://wanderlodgegurus.com/database/Theory/Heavy%20Vehicle%20Chassis%20Frame%20National%20Code%20of%20Practice.pdf , September 2014.

[17] Ashif Iqubal, S. M. Oak, R. S.Kharatmal. July - August 2013. Analytical Optimization of Chassis Frame for 40ft Dual-Axle Flatbed Trailer Design. IOSR Journal of Mechanical and Civil Engineering (IOSR-JMCE) e-ISSN: 2278-1684, p-ISSN: 2320-334X, Volume 7, Issue 6, Pg. 76-84.

[18] José Ricardo Lenzi Mariolani, Antonio and Luis Otto. Development of New Underride guards for enhancement between Trucks and Cars. Paper Number 425. State University of Campinas, Brazil.

[19] Tommaso Delpero, Grégoire Lepoittevin, Alberto Sanchez, 01 March 2011, Finite Element Modeling with ANSYS, Centre of Structural Technologies, Swiss Federal Institute of Technology downloaded from www.structures.ethz.ch , July 2014.

[20] Chapter 2 – The Basics of FEA Procedure, FEA Lecture Notes by R. B. Agarwal. Downloaded from http://www.engr.sjsu.edu/ragarwal/ME273/pdf/Chapter%202%20%20The%20Basic%20FEA%20Procedure.pdf, August 2015.

[21] K.Radhakrishna, S.Srinivasa Rao and B.Sudhakara Rao, April 2015, Design and Analysis of Dump Body on Three Wheeled Auto Vehicle, International Journal on Cybernetics & Informatics (IJCI) Vol. 4, No. 2, Pg. 65-73.

[22] K. Fouzan Mohammed and K. Raghavendra, September 2015, Optimization Study on Trailer Arm Chassis by Finite Element Method, International Journal of Research in Engineering and Technology, eISSN: 2319-1163, pISSN: 2321-7308**,** Volume: 04 Issue: 09, Pg. 122-126.

[23] Mehdi Mahmoodi-k, Iraj Davoodabadi, Vinko Višnjić, Amir Afkar, March 2014, Stress and Dynamic Analysis of Optimised Trailer Chassis, Analiza naprezanja i dinamička analiza optimirane šasije prikolice, ISSN 1330-3651(Print), ISSN 1848-6339 (Online), Technical Gazette 21, Pg. 599-608.

[24] Walter J. Paucar Casas, Jun S. Ono Fonseca, Vagner Grison, November 2005, Stuctural Dynamicas of the Chassis of a Light Trailer, 18th International Congress of Mechanical Engineering, Ouro Preto, MG.

[25] Ahmad O. Moaaz and Nouby M. Ghazaly. November 2014. Finite Element Stress Analysis of truck chassis using ANSYS. Review, International Journal of Advances in Engineering & Technology, ISSN: 22311963, Volume 7, Issue 5, Pg. 1386-1391.

[26] David, Joao and Antonio. 20-24 July 2009. Structural optimization of a semi-trailer based on performance and industrial cost. S1216_P0496, 3rd International Conference on Integrity, Reliability and Failure, Porto/Portugal.

[27] Tushar M. Patel, Dr M. G. Bhatt and Harshad K. Patel. March -April 2013. Analysis and validation of Eicher 11.10 chassis frame using ANSYS. International Journal of Emerging Trends & Technology in Computer Science (IJETTCS), ISSN 2278-6856, Volume 2, Issue 2 Pg.85-88.

[28] Ansel C. Ugural, Mechanical Design of Machine Components, Second Edition, Pg. 12-15.

[29] Ojo Kurdi, Roslan Abdul Rahman, July 2010, Finite Element Analysis of road roughness effect on stress distribution of heavy duty truck chassis, International Journal of Technology 1: Pg. 57-64, ISSN 2086-9614

[30] Gajanan S. Datar, Rupa S. Bindu and Durvesh V. Dandekar. 2012. Design and Analysis of 40 Tonne Trailer Used in Heavy Commercial Vehicles. International Journal on Theoretical and Applied Research in Mechanical Engineering (IJTARME), ISSN: 2319 – 3182, Volume 1, Issue 2.

[31] Grzegorz Koszaka, Hubert Dbski and Marek Dziurka, Maciej Kaczor. 2011. Design of a frame to a semi low-loader. Journal of KONES Powertrain and Transport, Vol. 18, No. 2, Pg. 215-223.

[32] Hein Schellens and Ton Peijs. Design of a Multi-Functional Semi-Trailer using Structural Sandwich Panels. Downloaded from http://iccm-central.org/Proceedings/ICCM12proceedings/site/papers/pap1150.pdf , August 2015.

[33] Roslan Abd Rahman, Mohd Nasir Tamin, Ojo Kurdi. December 2008. Stress analysis of heavy duty truck chassis as a preliminary data for its fatigue life prediction using FEM. Jurnal Mekanikal, No. 26, Pg. 76 - 85.

[34] P. David Polly, Finite Element Analysis (FEA), G563 Quantitative Paleontology, Department of Geological Sciences, Indiana University, 2012. Downloaded from http://www.indiana.edu/~g563/Lectures/Finite%20Element%20Analysis.pdf November 2016

[35] Static failure analysis in COSMOSWorks using design check plots, The COSMOS Companion, Volume 106, Intel and Solidworks. Downloaded from www.eng.uwo.ca/designcentre/FEA%20resources/106_FailureAnalysisRefresher.pdf November 2016.

[36] Govind T Sarkar, Yogesh L Yenarkar and Dipak V Bhope, October 2013. Stress analysis of helical gear by finite element method. International journal of mechanical engineering and robotic research, ISSN 2278 – 0149, Vol. 2, No. 4, pg.322-329.

[37] A. Sathyanarayana Achari, R.P.Chaitanya and Srinivas Prabhu, May 2014. A comparison of bending stress and contact stress of a helical gear as calculated by AGMA standards and FEA. International journal of emerging technology and advanced engineering, ISSN 2250-2459, Volume 4, Issue 5, Pg.38-43.

[38] ANSYS, FEA Best Practices, Downloaded from http://innomet.ttu.ee/martin/mer0070/loengud/fea_best_practices.pdf November 2015.

[39] FEA Good Modeling Practices, Downloaded From https://www.ohio.edu/mechanical/design/Resources/FEA_Examples.pdf November 2015.

[40] Paul Kurowski, Avoiding Pitfalls in FEA, November 1994, Machine Design, Pg. 78-86, Downloaded from https://www.engr.colostate.edu/~dga/mech325/handouts/fea_pitfalls.pdf November 2015.

[41] Simon L. Cowling. February 2008. Design optimisation of a cane haulage vehicle. Dissertation for Master of Science in mechanical engineering programme, University of KwaZulu-Natal Downloaded from http://researchspace.ukzn.ac.za/handle/10413/552, November 2016.
[42] James M. Gere, Mechanics of Materials, Sixth Edition, Chapters 1, 5 and 6, Pg. 4, 348 and 429.
[43] Patrick Safarian. Finite Element Analysis Validation Requirements and Methods. The Federal Aviation Administration. Downloaded from http://appliedcax.com/ , January 2016.
[44] Brent William Shoffner. May 2008. Development and validation of a Finite Element Analysis model used to analyse coupling reactions between a tractor's fifthwheel and a semitrailer's kingpin. The Pennsylvania State University, College of Engineering.
[45] Mitchel J. Keil, Upul Attanayake, Pavel Ikonomov and Richard B. Hathaway. July 2012. Developing the Model and Environment for Validation of a Class-8 Truck. Journal of Civil Engineering and Architecture, ISSN 1934-7359, USA, Volume 6, No. 7 (Serial No. 56), Pg. 777–786.
[46] Ebrahim Ebrahimi, Alimohamad Borghei, Morteza Almasi and Hekmat Rabani, 10 May 2010, Design, Fabrication, and Testing of a Hay Bale Trailer, Research Journal of Applied Sciences, Engineering and Technology, ISSN: 2040-7467, Pg. 222-226.
[47] Joop Pauwelussen, Jeroen Visscher, Menno Merts and Karel Kural. An integrated testing and model based design approach for semi-trailer weight reduction. HAN University of Applied Sciences, the Netherlands. Downloaded from http://road-transport-technology.org/ , July 2014.
[48] L.A.W. Horn, J.P. Pauwelussen, R.C. Alderliesten, G.R. ten Ham, D.G. van Rhee, M. van Klink. 2012. Semitrailer chassis design against fatigue on the basis of field test data. HAN University of Applied Sciences, The Netherlands. Heavy Vehicle Transport Technology symposium, Stockholm. Downloaded from http://road-transport-technology.org/ , July 2014.
[49] Chris Winkler, Tom Gillespie and Steve Karamihas. 8-11 September 2014. UMTRI: The Mechanics of Heavy-Duty Truck Systems. The South African Road Federation, The Council for Scientific and Industrial Research, The University of Witwatersrand. Valverde, Muldersdrift, Gauteng, South Africa.
[50] Steinecker Containerhandel, Technical specification for steel dry cargo container, complying with ISO 668 and ISO 1496-1. Downloaded from http://steinecker-container.de/container/Container2/Spez-Container/Spez_high%20cube20.pdf March 2014.
[51] SAF Holland Group, fifth wheel fact book, Pg. 8. Downloaded from http://www.safbenelux.nl/files_content/SAF-HOLLAND_Fifth_Wheel_Fact_Book_en-DE.pdf November 2015.
[52] https://en.wikipedia.org/wiki/I-beam , July 2014.
[53] Tanker Talk, ADR explained, February 2012, GRW quarterly magazine, Pg.4-5, Downloaded from http://www.grw.co.za/files/tanker-talk/tanker-talk-feb-2012.pdf November 2016.
[54] P Andersson, S Soker-Petersen and J Jagelcak. HVTT12, Differences in cargo securing regulations. How could we achieve harmonization? Centre of excellence for systems and services of

intelligent transport II, ITMS 26220120050. Downloaded from http://road-transport-technology.org/Proceedings/HVTT%2012/Differences%20in%20cargo%20securing%20regulations.%20How%20could%20we%20achieve%20harmonization%20-%20Andersson.pdf November 2016.

[55] Macsteel, An abbreviated guide to Structural steel standard SANS 50025 / EN 10025:2004. Downloaded from http://www.macsteel.co.za/ February 2014.

[56] Vishay Precision Group, Micro-Measurements. Strain gages and instruments. Tech Note TN-501-2, Noise Control in Strain Gage Measurements. Document Number: 11051. Revision: 09 July 2013.

[57] Mohammed Imran and Dr. Mohamed Haneef, May 2015, Comparative studies on curved beam under different loading conditions using strain gauges and ANSYS, International Journal of Engineering Research & Technology, ISSN: 2278-0181, Vol. 4 Issue 05, Pg. 104-107.

[58] http://www.padtinc.com/blog/the-focus/be-a-pinball-wizard-with-contact-regions-in-ansys-mechanical November 2016.

[59] AS1170.1-1981. Standards association of Australia Loading Code. Minimum design loads on structures-dead and live loads. Part 1.